Myocardial changes in patients with end-stage heart failure during continuous flow left ventricular assist device support

Sjoukje I. Lok

Myocardial changes in patients with end-stage heart failure during continuous flow left ventricular assist device support

Veranderingen in het myocard van patienten met eind-stadium hartfalen tijdens behandeling met een steunhart

(met een samenvatting in het Nederlands)

Proefschrift

ter verkrijging van de graad van doctor aan de Universiteit Utrecht op gezag van de rector magnificus, prof.dr. G.J. van der Zwaan, ingevolge het besluit van het college voor promoties in het openbaar te verdedigen op donderdag 5 december 2013 des middags te 4.15 uur

door

Sjoukje Irene Lok

geboren op 5 januari 1981 te Groningen

Promotor:	Prof. dr. P.A.F.M. Doevendans
Co-promotoren:	Dr. N. de Jonge
	Dr. R.A. de Weger

CONTENTS

CHAPTER 1

General introduction

General aspects of heart failure

Definition

Heart failure (HF) is considered as an abnormality of cardiac structure or function leading to failure of the heart to deliver oxygen at a rate commensurate with the requirements of the metabolizing tissues, despite normal filling pressures (or only at the expense of increased filling pressures). The diagnosis of HF can be difficult, especially in the early stages, since many of the symptoms of HF are non-specific [1].

Pathophysiology

The concept of the pathophysiology of HF is constantly evolving. Once considered as a straightforward problem of left ventricular pump dysfunction, it is now understood that HF is a highly complex clinical syndrome, not only related to the heart itself, but also manifested by many extra-cardiac features, including neuroendocrine activation and cytokine release [2].

Index event

The onset of HF begins with a preceding index event. Patients often go through a period of latent left ventricular dysfunction before the onset of overt signs and symptoms of HF. Myocardial infarction, acute myocarditis, systemic hypertension, valvular insufficiency and a genetic abnormality can lead to the development of HF. Often, the genesis of the index event is unknown, clinically silent or poorly understood [2]. The maladaptive changes that occur in surviving cardiomyocytes and in the extracellular matrix (ECM) after the index event, lead to changes in the size, shape and function of the heart, a process termed remodeling, with subsequent dilatation and impaired contractility [3] (*Figure 1*).

Remodeling

Cellular remodeling is observed in the form of changes in cardiomyocyte size and shape, molecular modifications, compromised excitation-contraction coupling, myofilament function, cell survival signalling, bioenergetics and the cellular metabolic state. In addition, remodeling of the ECM is crucial for deforming the ventricles and alters the composition of fibrous and vascular elements in the myocardium. Left ventricular dysfunction is accompanied by activation of the sympathetic nervous system (SNS) and renin-angiotensin-aldosterone system (RAAS) [4]. Increased RAAS and SNS are initially compensatory, but over time pathologic, accounting for the clinical manifestation of the syndrome of HF.
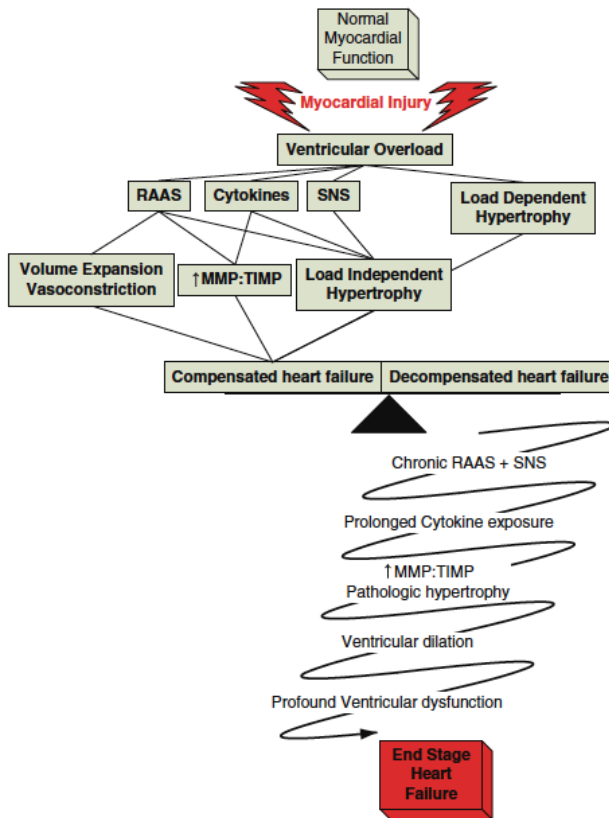
Figure 1: Index event leading to the development of end-stage heart failure
RAAS, renin-angiotensin-aldosterone-system; SNS, sympathetic nervous system; MMP, matrix metalloproteinases; TIMP, tissue inhibitors of matrix metalloproteinases.
Source: Buttler CR, Jugdutt BI. The paradox of left ventricular assist device unloading and myocardial recovery in end-stage dilated cardiomyopathy: implications for heart failure in the elderly. Heart Fail Rev, 2012.
Reproduced with permission.

Treatment of heart failure

Most patients with HF initially respond favourably to pharmacological and electrophysiological treatment. However, 5% to 10 % of all HF patients do not improve or experience frequent recurrence of symptoms despite optimal therapy [5]. Such patients often have symptoms at rest or on minimal exertion, such as profound fatigue, cardiac cachexia and typically require repeated and prolonged hospitalization for intensive management. In the most advanced phase of HF, heart transplantation (HTx) and mechanical support are the only established treatments for improving the quality of life and survival chances [6].

Heart transplantation

HTx is a life-saving therapy for patients with end-stage HF not amenable to conventional medication or surgery. Patients should be considered for HTx if they experience severe symptoms of HF, intractable angina or rhythm disturbances, without any alternative form of treatment available and with poor prognosis [7]. The absolute contra-indications are irreversible pulmonary hypertension or elevated pulmonary vascular resistance, systemic infection, malignancy or history of malignancy with probability of recurrence, inability to comply with complex medical regimen, severe peripheral or cerebrovascular disease, irreversible dysfunction of another organ, including diseases that may limit prognosis after HTx, which can increase perioperative risk or decrease survival post-HTx [7]. According to the latest 29th HTx report of the registry of the International Society for Heart and Lung Transplantation (ISHLT), the median survival after HTx, or the time at which 50% remain alive, is 10 years [8]. Survivors of the first year post-transplant have a 63% and a 27% chance of being alive 10 and 20 years after HTx, respectively [8]. Nevertheless, only a fraction of the HTx candidates will actually benefit from transplantation, as the number of available donor hearts is severely limited.

Left ventricular assist devices

The inadequacy of pharmacological and electrophysiological treatment to favourably impact outcome in advanced HF, coupled with the limited supply of transplantable hearts, have driven development and clinical application of mechanical circulatory support. While mechanical support is commonly used to describe left ventricular assist devices (LVADs), it also includes right ventricular assist devices and biventricular assist devices. Rather than replacing the human heart completely, LVADs supplement the cardiac output of the native but weakened heart.

There are three generations of LVADs, with different technical aspects of the pump (*Figure 2*). First-generation devices are pulsatile-flow LVADs (pf-LVADs) that provide blood flow in a fashion analogous to that in the native heart (*Figure 2A*). In pf-LVADs, blood returns from the lungs to the left side of the heart, exits the apex and crosses an inflow valve into the prosthetic pumping chamber. It is then actively pumped through an outflow valve into the ascending aorta. Such pumps are limited by size and durability, since pulsatility results in the mechanical wear of the device, especially the valves. A common used pf-LVAD is the HeartMate (HM) XVE, one of the devices used in studies presented in this thesis. The second-generation continuous-flow LVADs (cf-LVADs) have small rotating impellers that propel blood forward. These devices have a greater durability and a smaller

size than pf-LVADs (*Figure 2B*). According to literature, more than 95% of implants are currently cf-LVADs [9]. The HM II is a well-known example of the cf-LVAD, which is the pump used in most of the studies described in the thesis. Finally, third generation LVADs use bearing-free designs to minimize device wear. Power delivery still requires percutaneous, rather than transcutaneous, energy sources (*Figure 2C*). The HeartWare is a classic example of third generation LVADs.
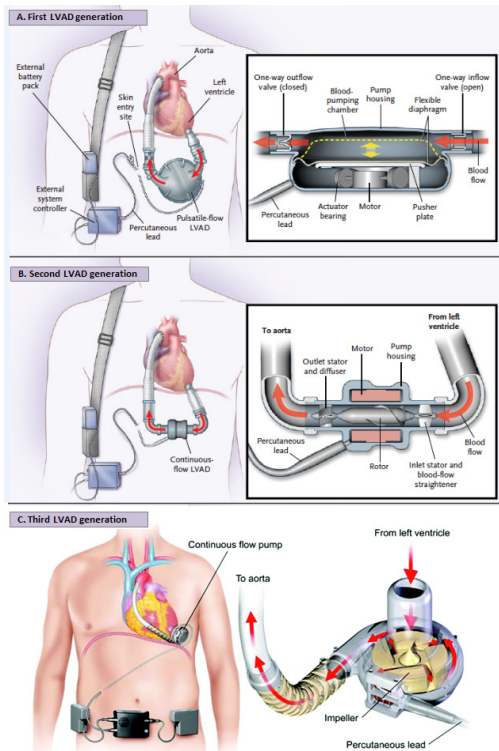
Figure 2: Overview of different left ventricular assist device (LVAD) generations
First-generation pulsatile flow LVAD (*A*); Second-generation continuous flow LVAD (*B*); Third-generation LVADs (HeartWare) (*C*).
Source: Slaughter MS *et al*. Advanced heart failure treated with continuous-flow left ventricular assist devices. N Engl J Med, 2009.
Reproduced with permission.

INTERMACS

The Interagency Registry for Mechanically Assisted Circulatory Support (INTERMACS) database is a registry for patients supported by Food and Drug Administration (FDA)-approved mechanical circulatory support devices. The INTERMACS database now includes more than 6800 patients from 145 participating hospitals [9]. After the first annual INTERMACS report [10], there was broad input from the committee regarding the existing limitations for clinical characterization of device recipients. It has been agreed upon that common used New York Heart Association (NYHA) symptoms did not offer

adequate description to allow optimal patient selection for HTx or mechanical support [11]. Consequently, the INTERMACS investigators developed a classification scheme to prospectively classify advanced HF patients based on severity of illness at the time of device implant (*Table 1*). These classifications, or so-called profiles, facilitate communication with colleagues, adjustment for pre-operative risk and clarification of target populations for future devices. Seven profiles have been defined for the INTERMACS strategy [11].

Table 1: Classification of heart failure

INTERMACS[1]	INTERMACS[1]
Level 1	Critical cardiogenic shock ("crashing and burning")
Level 2	Progressive decline on inotropic support
Level 3	Stable, but inotropic dependent
Level 4	Resting symptoms home on oral therapy
Level 5	Exertion intolerant
Level 6	Exertion limited
Level 7	Advanced NYHA[2] III

[1]INTERMACS, Interagency Registry for Mechanically Assisted Circulatory Support
[2]NYHA, New York Heart Association

According to the latest annual INTERMACS report, the proportion of patients at the time of implant that were in cardiogenic shock (level 1) or demonstrated progressive cardiac decompensation (level 2) has decreased from 64% before 2011 to 54% in 2012 [9]. During the first half of 2012, 13% of patients had HF symptoms at rest (level 4) and only about 5% of the patients were in less ill profiles. The current survival is approximately 80% at 1 year and 70% at 2 years. Patients in INTERMACS levels I and 2 had a 5-8% lower 1-year survival rate compared with other INTERMACS levels [9].

These results have led to an increasing acceptance of LVAD therapy as a suitable therapeutic option for patients with advanced HF. These data have also led to the possible equivalence or superiority of cf-LVADs over optimal medical therapy in treating earlier-stage, less ill HF patients who are currently not indicated for LVAD support. The REVIVE-IT (Randomized Evaluation of VAD Intervention before Inotropic Therapy) is a prospective, randomized, controlled trial designed to compare the use of cf-LVADs with optimal medical management in HF patients with NYHA Class III. The primary endpoint is a composite measure of survival, freedom from disabling stroke, and improvement in functional outcomes, as

measured by the six-minute walk test. The study started in 2011 and it is estimated that the full cohort of 200 patients have been enrolled by the end of 2013. If this trial indicates that LVAD therapy can provide not only superior survival chances, but also significantly better functional improvement and quality of life, it will probably lead to an increase in LVAD therapy.

Various indications of LVAD support

There are various indications of LVAD support, as depicted in *Table 2* and described in more detail in the present paragraph.

Table 2: Implant strategy and target population for LVAD support

Strategy	Patient population
Bridge to transplantation (BTT)	Patients listed for heart transplantation (HTx) that would not survive or would develop progressive end-organ dysfunction from low cardiac output before a donor heart becomes available.
Destination therapy (DT)	Patients who need long-term support, but are ineligible for HTx.
Bridge to candidacy (BTC)	Patients not currently listed for HTx, but who do not have an absolute or permanent contraindication to HTx. This includes patients whose potential for recovery remains unclear.
Bridge to recovery (BTR)	Patients who require temporary circulatory support, during which time the heart is expected to recover from an acute injury and LVAD support is removed without need for HTx.

In 1994, the FDA approved LVADs as bridge to transplantation (BTT) in order to reduce mortality and improve quality of life for end-stage HF patients, while on the waiting list for HTx. LVAD support normalizes hemodynamics and improves end-organ dysfunction and exercise tolerance, allowing patients to be sent home with a low incidence of major adverse events [12,13]. The proportion of BTT patients has increased tremendously and exceeded 30% of transplanted patients in 2009. In our institute, nowadays, 65% of the transplanted patients have been supported with a LVAD prior to HTx.

The recognition that LVADs intended as a BTT delivered durable support to some patients who were not transplanted, provided rationale for the Randomized Evaluation of Mechanical Assistance for the Treatment of Congestive Heart Failure (REMATCH) trial [15]. This trial, demonstrated an improved survival and quality of life in pf-LVAD supported patients compared with medically treated patients. The 1-year survival was 52% in the LVAD group and 25% in the optimal medical therapy group, whereas 2-year survival was

23% and 8% respectively [15]. These data led to the FDA approval of the pf-LVAD HM XVE as an alternative for HTx (Destination Therapy; DT) in November 2002. A randomized multicentre trial was conducted to compare the survival and quality of life between pf-LVAD and cf-LVAD as DT. The primary end-point was survival, at 2 years, free from disabling stroke and reoperation for device repair or replacement. A total of 46% of the patients supported with a cf-LVAD reached primary end-point versus 11% in the pf-LVAD supported group. Moreover, a reduction in complications that led to better quality of life and functional capacity for cf-LVAD supported patients was demonstrated [16]. Since the approval of the cf-LVAD HM II for DT in January 2010, there has been a 10-fold increase in approved LVADs implanted for lifelong support in transplant-ineligible patients (*Figure 3*). According to the latest annual INTERMACS report, more than 40% of implants in 2012 have been designed as DT [9]. However, several issues have been raised regarding the use of LVADs as DT. It remains to be determined whether the reported survival rates in the studies can be achieved in daily practice. The current device for DT was approved, based on 68% survival at 1 year, and 58% survival at 2 years [15]. However, similar 1- and 2-year survival rates have not been reported yet [17]. Furthermore, LVAD support as DT is an expensive therapy. A recent article provided a cost-effectiveness analysis of cf-LVADs as DT for the Dutch context [18], resulting in an incremental cost-effectiveness ratio of €94,100 per "life-years gained" and €107,600 per "quality adjusted life years". Since LVADs are currently considered not cost-effective as DT, their use is currently not approved in the Netherlands. More evidence is needed regarding the selection and management of patients receiving expensive LVADs as DT.

LVADs can also be used as a bridge to candidacy (BTC) in patients with potentially reversible or relative contraindications to HTx. The latest INTERMACS report demonstrated that in 2012 (first 6 months), 33% of all LVAD implants were BTC, making this one of the most listed indication at the time of LVAD implantation [9].

Finally, LVADs can function as "bridge to recovery" (BTR). LVADs provide volume and pressure unloading of the left ventricle, reversing the compensatory responses of the overloaded myocardium and resulting in partial "reverse remodeling" of the tissue [19-22] (*Figure 4*). Clinical experience with LVAD support has shown that a subset of patients could be weaned from the device after restoration of basic cardiac function [23-25]. Achieving substantial and sustained myocardial recovery during LVAD support is one of the most desirable goals in the treatment of heart disease since it could reduce or postpone the need for HTx. Unfortunately, weaned patients sometimes progress again to HF, a process that is termed recurrent remodeling [26].
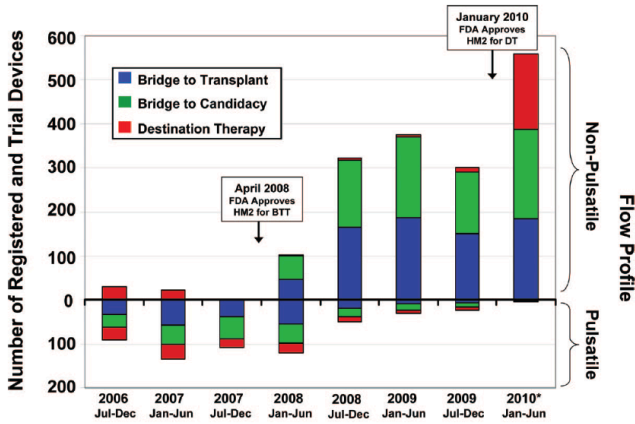
Figure 3: The use of LVADs worldwide from 2006 to 2010
This figure shows the utilization of pulsatile versus non-pulsatile devices, and intended strategy of bridge to transplant (BTT), bridge to transplant candidacy (BTC), and destination therapy (DT).
Source: Stewart GC, Stevenson LW. Keeping left ventricular assist device acceleration on track. Circulation, 2011. Reproduced with permission.
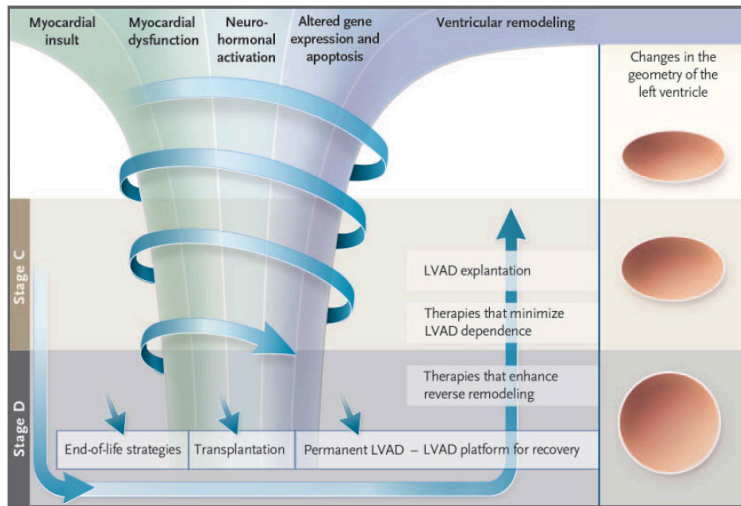
Figure 4. Pathophysiological mechanisms and treatment options for end-stage heart failure (HF) patients
An insult initiates the progression toward cardiac remodeling and subsequently symptomatic HF. End-stage HF patients require heart transplantation or LVAD support. LVADs lead to reverse remodeling. In a minority of patients, LVAD support results in myocardial recovery with subsequent explantation of the device.
Source: Renlund DG, Kfoury AG. When the failing, end-stage heart is not end-stage. N Engl J Med, 2006. Reproduced with permission.

Reverse remodeling

LVADs were primarily designed for pumping blood to restore normal cardiac output and blood pressure. Hence, there are important secondary effects of the LVAD that may have been unanticipated by early LVAD designers, but their importance is now widely recognized. LVADs provide profound left ventricular pressure and volume unloading, reductions in right ventricular afterload and subsequent pulmonary vascular resistance. Moreover, by normalizing blood pressure and cardiac output, LVAD support improves organ perfusion, which results in improved autonomic function and normalization of the neurohormonal and cytokine milieu. Near normalization of this milieu is achieved by LVADs, sometimes leading to cardiac recovery with subsequent explantation of the device [27].

Effects of different LVAD flow patterns on reverse remodeling

cf-LVADs have the advantages of smaller size, better durability, higher energy efficiency and less surgical trauma compared with pf-LVAD support. Concern exists regarding the effects of chronic, diminished-pulsatile flow of cf-LVADs on cardiovascular architecture, end-organ perfusion and long-term outcome. From a hemodynamic perspective, cf-LVADs unload the left ventricle constantly throughout the cardiac cycle, whereas pulsatile devices unload the ventricle only during a selected portion of this cycle. Current studies are comparing the physiologic effects of both devices (*Figure 5*). Two retrospective reviews suggested that end-organ function and clinical outcomes may be equivalent and perhaps superior during cf-LVAD compared with pf-LVAD support [28,29]. Moreover, studies demonstrated that cf-LVADs were similarly effective or even better in transplant rates and post-transplant outcome, and showing fewer LVAD-related complications when compared with pf-LVADs [16]. Despite these potential advantages of cf-LVAD support, volume unloading seems more pronounced in pf-LVAD supported patients [30-33], which may be translated into more favorable outcomes in terms of BTR [34]. cf-LVADs often run at a lower level of support than pf-LVADs to avoid septum shift, eliminate suction events, maintain moderate pulsatility and allow for periodic opening of the aortic valve. The observations of augmented unloading in pf-LVADs may therefore be due to a higher level of support, which might imply that left ventricular unloading is more dependent on operational settings than device type.

To summarize, it is not known which LVAD design is superior in achieving myocardial recovery: pf- or cf-LVAD.

Myocardial recovery with subsequent LVAD explantation

Despite the frequent synonymous use of the terms myocardial recovery and reverse

remodeling to describe the reversal of various aspects of the HF phenotype following medical and device therapy, these terms describe different phenomena. Although the mechanical unloading and normalization of the neurohormonal milieu provided by LVADs routinely results in reverse remodeling, only a small subset of patients can be weaned from LVAD therapy. This has been referred to as myocardial recovery. According to the latest annual INTERMACS report, BTR occurred in only 1.0% of the LVAD supported patients [9]. Many groups have looked at centre-specific rates of BTR, both retrospectively [26,35-37] and prospectively [24,38,39]. Overall, low rates of BTR have been reported, with a relatively high incidence of early HF recurrence [35]. Birks *et al* who utilized concomitant medical therapy during LVAD support, reports the highest rate of successful BTR published to date (73%) [24]. This area of myocardial recovery from chronic HF is an exciting and developing field. There are many controversial areas, such as whether chronic HF can reverse, if the recovery is sustainable and whether predictors of myocardial recovery can be established (*Figure 6*).

Maladaptive responses of cf-LVAD support

Some remodeling responses to mechanical unloading may be maladaptive. The most prominent examples are the concept of fibrosis, myocardial atrophy and aortic valve pathology.

Fibrosis

Fibrosis is recognized as a major component of cardiac remodeling in HF [40]. After cardiac injury, inflammatory cells migrate into the tissue through the vascular system. On arrival, they begin to secrete large amounts of both Transforming Growth Factor- β1 (TFG-β1), interleukin-1β (IL-1β) and endothelin-1 (ET-1). This in turns, releases transcription of the gene encoding α-smooth muscle actin (α-SMA), which stimulates the transformation from fibroblasts into myofibroblasts [41]. Myofibroblasts are not part of normal cardiac tissue and appear only after cardiac injury. They produce extracellular matrix (ECM) components, mainly pro-collagen precursors, which are converted to mature collagen by preoteolytic reactions [42]. Collagen (mainly type I and III) maintains the shape and the size of the heart, provides cardiac tensile strength, actively transduces the force during systole and is the main determinant of diastolic stiffness [43,44]. Breakdown of collagen is caused by certain proteases, mainly matrix metalloproteinases (MMPs). Endogenous inhibitors, known as tissue inhibitors of matrix metalloproteinases (TIMP), bind to MMPs, thereby preventing the enzymatic cleavage activity [45]. The disequilibrium between MMP and TIMP expression plays an important role in cardiac remodeling. Fibrosis occurs as the result of
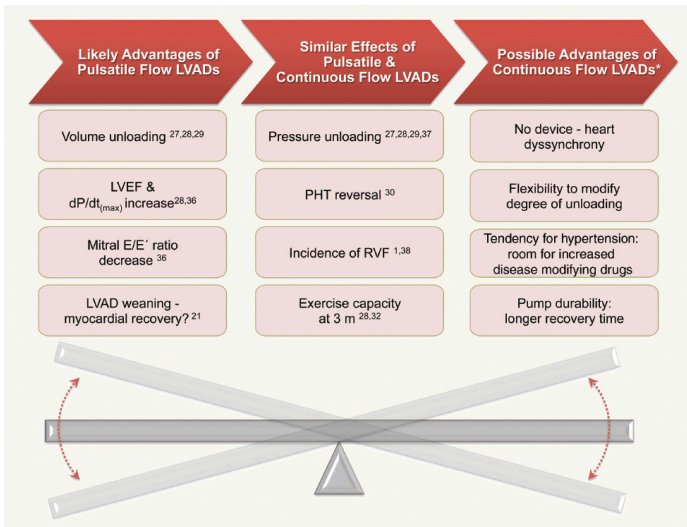
Figure 5: Differences and similar effects of pulsatile flow LVADs and continuous flow LVADs
Source: Bridge to recovery: understanding the disconnect between clinical and biological outcomes. Drakos SG, *et al*. Circulation, 2012.
Reproduced with permission.
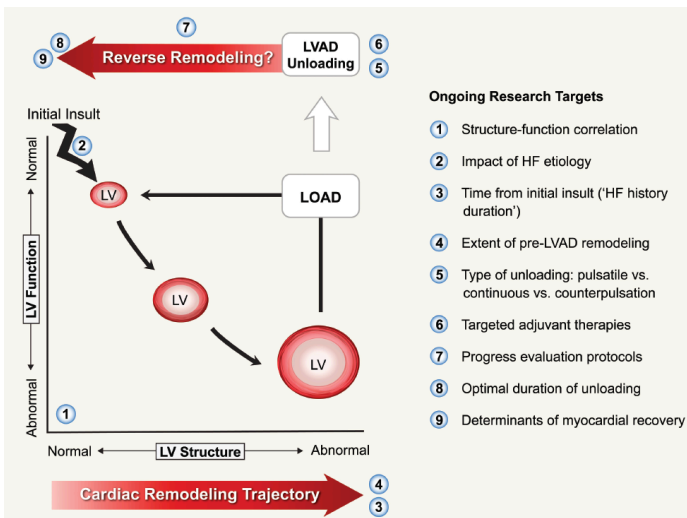
Figure 6: LVAD unloading and cardiac reverse remodeling: unresolved issues and future directions
Research targets have been placed in the figure corresponding to their potential relationship in the continuum of the cardiac remodeling. LV, left ventricle/ventricular; HF, heart failure.
Source: Bridge to recovery: understanding the disconnect between clinical and biological outcomes. Drakos SG, *et al*. Circulation, 2012.
Reproduced with permission.

the unbalance between the enhanced syntheses of collagen and unchanged (or reduced) collagen degradation by MMPs. The net effect of cardiac fibrosis is exaggerated mechanical stiffness, disorganized contraction caused by cardiomyocyte separation and worsening tissue hypoxia [46].

The response of collagen concentration during LVAD support remains controversial. Some studies have found a reduction in collagen during LVAD support [30,31,36], whereas most studies showed an increase [47-54]. An explanation for this discordance might be different staining of myocardial tissue sections, the measurement of collagen content (interstitial, perivascular and/or microscopic fibrosis), the type of LVAD unloading and the duration of LVAD support [20]. Collagen deposition leads to an increase in myocardial stiffness, which could be a contributing factor to the rare occurrence of full recovery, with subsequent LVAD removal and post-explant HF recurrence.

Biomarkers might be used to require additional information about the amount of myocardial fibrosis in LVAD supported patients. In clinical practice, circulating biomarkers are being used to improve diagnosis, prognosis and therapy in HF [40,55,66]. Natriuretic peptides (NPs), such as Brain Natriuretic Peptide (BNP), exert natriuretic and anti-fibrotic effects [57]. NPs are advocated by the guidelines of the European Society of Cardiology as a diagnostic and prognostic tool for HF [1]. Several physiological conditions can cause alternated NP-levels and may complicate the clinical interpretation. NP-levels increase with age, female gender and renal failure, but may be reduced in obese patients [58]. Hence, there is need for novel markers. Several fibrotic markers, such as Osteopontin (OPN), Galectin-3 (Gal-3), Transforming Growth Factor (TGF)-β and Growth Differentiation Factor (GDF)-15, are being tested and introduced into clinical practice.

Myocardial atrophy

During LVAD support, atrophy of cardiac tissue has been observed [59-62]. Muscle atrophy is an energy-requiring process, with mechanisms that are just now being discovered [60]. The Ubiquitin Proteasome System (UPS) seems to play an important role. The UPS degrades 90% of proteins, ensuring that damaged proteins are degraded in the proteasome (*Figure 7*) [63].

Marked accumulation of ubiquitinated proteins in cardiomyocytes of human failing hearts suggest impaired ubiquitin proteasome system in HF [64-66]. Wohlschlager *et al* demonstrated that LVAD unloading reverses the depressed UPS activity [65]. This was recently confirmed by Predmore *et al*, who demonstrated that markedly reduced proteolytic activities in failing human hearts could be partially restored after LV unloading [67]. Activated UPS catalyses

degradation of muscle proteins, especially myofibrillar components (*Figure 8*) [68]. It can be hypothesized that activated UPS may represent overcompensation, because of the lack of opposing hypertrophic stimuli after chronic unloading [60,69]. Activated UPS ultimately leads to protein degradation with subsequent muscle atrophy of LVAD supported hearts.

Atrophy is a reversible process, since the cellular integrity is preserved. Because the atrophic myocardium may not be able to sufficient contractile force, a period of training to reload the ventricle seems to be required for successful weaning from LVAD support [61]. Clinical data seem to support this assumption. Hetzer *et al* used a LVAD weaning protocol that included three weeks of a lower pump rate mode to load the ventricles before LVAD explantation [70]. In their series, LVAD removal was performed in 30% of the patients of whom 68% had long-term cardiac recovery. Along training the ventricle, medical adjuvant treatment (see next paragraph) during prolonged LVAD support might be of interest in preventing atrophy, thereby enhancing BTR.
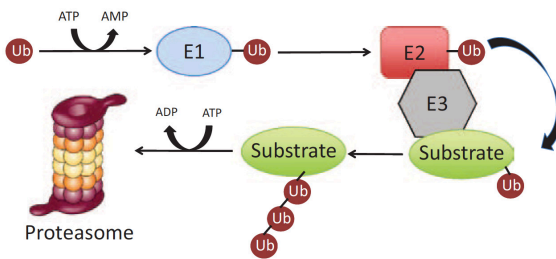
Figure 7: The Ubiquitin Proteasome System (UPS)

Degradation of proteins by the UPS involves covalent binding of multiple ubiquitin molecules to the target protein, catalysed by E1, E2, and E3 enzymes, and subsequent degradation of this protein by proteasome.

Source: Pagan J, *et al*. Role of the Ubiquitin Proteasome System in the heart. Circ Res, 2013.

Reproduced with permission.
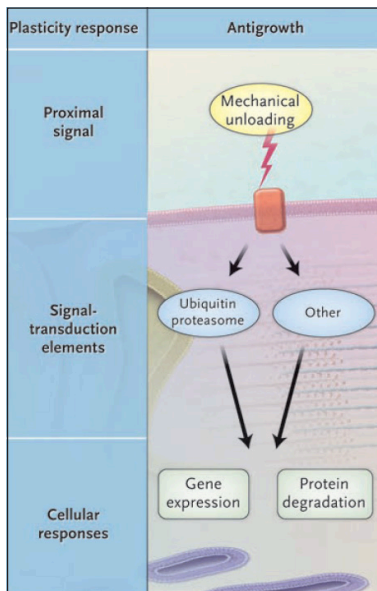
Figure 8: The onset of cardiac atrophy during LVAD support

LVAD support is associated with improved Ubiquitin proteasome (UPS) activity with subsequent protein degradation.

Source: Hill JA, Olson EN. Cardiac plasticity. Hill *et al*. N Engl J Med, 2008.

Reproduced with permission.

Aortic valve pathology

Because of underlying heart disease and poor ventricular function, the pump speed required for adequate circulatory support is often much higher than the pump speed enabling aortic valve opening. As a result, there is continuous backward pressure exerted on the aortic valve resulting in an increase mechanical stress, with subsequent aortic valve remodeling. Our study group has demonstrated that aortic valve regurgitation occurs often after cf-LVAD implantation and may appear during diastole, continuously or solely during systole [71]. Aortic insufficiency impairs the function of the LVAD, increases the risk of thromboembolic events and is of great concern in potential BTR patients. Moreover, our study group demonstrated that, in addition to aortic insufficiency, aortic fusion may occur during cf-LVAD support [72]. Aortic fusion seems to be a non-inflammatory process, in which the aortic valve commissures stick to each other, leading to prominent changes of the aortic valve morphology. Promoting regular aortic valve opening seems to be the best option in order to prevent aortic valve commissural fusion and LVAD-related aortic insufficiency. Intermittently lowering the pump speed, which allows opening of the aortic valve during systole, may prevent aortic valve fusion. Such physiological pump control should therefore be integrated in future devices.

Adjuvant medical therapy during LVAD support

In order to promote the incidence and durability of recovery, Birks *et al* reported successful pf-LVAD [24] and cf-LVAD [25] explantation in a subset of patients with non-ischemic dilated cardiomyopathy (DCM) that received Clenbuterol, a β2-adrenergic-receptor agonist, along with standard medical therapy. In the first prospective study of Birks *et al*, 15 patients with a DCM requiring pf-LVAD support were included [24]. Patients received the Harefield protocol; a two-stage drug regimen. The first stage consisted of treatment with four drugs (beta-blocker, angiotensin converting enzyme (ACE) inhibitor, angiotensin II (AT-II) receptor blocker, aldosterone antagonist) with the maximum titrated doses. This stage was continued until stable left ventricular recovery was achieved (defined by a constant left ventricular size for at least 2 weeks, according to echocardiographic assessment). The second stage of pharmacologic therapy consisted of treatment with a β2-adrenergic-receptor agonist (Clenbuterol) until LVAD explantation. A total of 11 (73%) patients could be successfully weaned from LVAD support. After 4 years of follow-up, the mean ejection fraction improved from 12% pre-LVAD to 64% post-LVAD explantation. Birks *et al* repeated the Harefield Protocol in cf-LVAD supported patients [25]. A total of 12 out of 20 patients (60%) were successfully explanted with a 83% survival at 3 years and a mean ejection fraction

of 58%. However, the apparent success of Clenbuterol needs to be tempered, since the results could not be replicated. George *et al* failed to show any significant improvement in ventricular function after high-dose Clenbuterol in a small case series of LVAD patients [73], although most patients had ischemic HF and traditional HF medication was not emphasized in the same way as in the Harefield Protocol.

Another recent study investigated the potential effects of Ivabradine as adjuvant medical therapy during LVAD support in a HF induced rat model [74]. The effects of Ivabradine were compared with beta-blockade therapy (metoprolol). Ivabradine is an If-inhibitor, which acts specifically on the pacemaker activity of the sinoatrial node. In this study, Ivabradine reversed myocardial fibrosis and enhanced the restoration of deranged E–C coupling, but did not prevent LVAD induced myocardial atrophy.

Conclusion

LVAD support is considered as a life-saving treatment with a relatively good surival rate in end-stage HF patients. Since pf-LVADs have been replaced by cf-LVADs, evaluation of the survival and complications of cf-LVAD support is of interest and is one of the subjects of the present thesis.

An intruiging finding is that LVAD support can lead to reverse remodeling of myocardial tissue [27]. One of the aims of this thesis is to explore reverse remodeling during cf-LVAD support and to identify novel biomarkers associated with reverse remodeling.

Clinical experience with LVAD support has shown that a subset of patients could be weaned from the device after restoration of basic cardiac function (Bridge to Recovery, BTR). Current experience suggest that only a minority of LVAD supported patients demonstrate substantial and sustained cardiac recovery. In this thesis we try to understand why this recovery is neither complete nor permanent, especially when the heart is re-exposed to hemodynamic stress.

Reverse remodeling is not a ubiquitous process [27]. Important examples of myocardial or ventricular properties that do not regress towards normal during LVAD support include atrophy, abnormal extracellular matrix metabolism, myocardial stiffening and partial recovery of genes involved with metabolism. As fibrosis is thought to play an important role in the chance of successful recovery, one of the aims of the present thesis is to establish the amount of fibrosis and cardiomyocyte size during cf-LVAD support and to relate this to novel fibrotic markers in Bridge to Transplantation (BTT) and BTR patients. In literature, broad surveys of myocardial gene expression using gene chip technology reveal that expression of only a small percentage of abnormally expressed genes normalizes during

LVAD support [75]. Therefore, another aim of this thesis is to explore the post-transcriptional regulation by microRNAs (miRs) during LVAD support.

Aims

The aims of this thesis are:

1. To evaluate the survival of patients with end-stage heart failure (HF) during support with a continuous flow left ventricular assists device (cf-LVAD; HeartMate II; HM II) as Bridge to Transplantation (BTT) in the University Medical Center Utrecht (UMC-U).
2. To analyse the adverse events during cf-LVAD support in the UMC-U.
3. To establish histopathological and immunohistochemical changes in the myocardium of cf-LVAD supported patients as BTT and Bridge to Recovery (BTR).
4. To detect and identify protein changes in the myocardium and plasma of cf-LVAD supported patients. Proteins that are differentially expressed pre- and post cf-LVAD will be examined by mass spectrometry.
5. To analyse mRNA expression (by Q-PCR) and circulating levels (by ELISA) of pro-fibrotic biomarkers in end-stage HF patients during cf-LVAD support as BTT and BTR.
6. To investigate cardiac microRNAs (miRs) expression patterns in the myocardium and plasma of end-stage HF patients during pulsatile flow LVAD (pf-LVAD) and cf-LVAD support.

References

1. McMurray JJV, Adamopoulos S, Anker SD, Auricchio A, Böhm M, Dickstein K, et al, ESC Committee for Practice Guidelines. ESC Guidelines for the diagnosis and treatment of acute and chronic heart failure 2012: The Task Force for the Diagnosis and Treatment of Acute and Chronic Heart Failure 2012 of the European Society of Cardiology. Developed in collaboration with the Heart Failure Association (HFA) of the ESC. Eur. Heart J. 2012; 33:1787–1847.

2. Francis GS. Pathophysiology of chronic heart failure. Am. J. Med. 2001; 110 Suppl 7A:37S–46S.

3. McMurray JJV. Clinical practice. Systolic heart failure. N. Engl. J. Med. 2010; 362:228–238.

4. Francis GS, Goldsmith SR, Levine TB, Olivari MT, Cohn JN. The neurohumoral axis in congestive heart failure. Ann. Intern. Med. 1984; 101:370–377.

5. WRITING COMMITTEE MEMBERS, Yancy CW, Jessup M, Bozkurt B, Butler J, Casey DE et al. 2013 ACCF/AHA Guideline for the Management of Heart Failure: A Report of the American College of CardiologyFoundation/American Heart Association Task Force on Practice Guidelines. Circulation. 2013; 128:e240-e319.

6. Francis GS, Greenberg BH, Hsu DT, Jaski BE, Jessup M, LeWinter MM, et al, ACCF/AHA/ACP Task Force. ACCF/AHA/ACP/HFSA/ISHLT 2010 clinical competence statement on management of patients with advanced heart failure and cardiac transplant: a report of the ACCF/AHA/ACP Task Force on Clinical Competence and Training. J. Am. Coll. Cardiol. 2010; 56:424–453.

7. De Jonge N, Kirkels JH, Klöpping C, Lahpor JR, Caliskan K, Maat APWM, et al. Guidelines for heart transplantation. Neth Heart J. 2008; 16:79–87.

8. Stehlik J, Edwards LB, Kucheryavaya AY, Benden C, Christie JD, Dipchand AI, et al, International Society of Heart and Lung Transplantation. The Registry of the International Society for Heart and Lung Transplantation: 29th official adult heart transplant report--2012. J Heart Lung Transplant. 2012; 31:1052–1064.

9. Kirklin JK, Naftel DC, Kormos RL, Stevenson LW, Pagani FD, Miller MA, et al. Fifth INTERMACS annual report: risk factor analysis from more than 6,000 mechanical circulatory support patients. J Heart Lung Transplant. 2013; 32:141–156.

10. Kirklin JK, Naftel DC, Stevenson LW, Kormos RL, Pagani FD, Miller MA, et al. INTERMACS database for durable devices for circulatory support: first annual report. J Heart Lung Transplant. 2008; 27:1065–1072.

11. Stevenson LW, Pagani FD, Young JB, Jessup M, Miller L, Kormos RL, et al. INTERMACS profiles of advanced heart failure: the current picture. J Heart Lung Transplant. 2009; 28:535–541.

12. Levin HR, Oz MC, Chen JM, Packer M, Rose EA, Burkhoff D. Reversal of chronic ventricular dilation in patients with end-stage cardiomyopathy by prolonged mechanical unloading. Circulation. 1995; 91:2717–2720.

13. Frazier OH, Rose EA, Macmanus Q, Burton NA, Lefrak EA, Poirier VL, et al. Multicenter clinical evaluation of the HeartMate 1000 IP left ventricular assist device. Ann. Thorac. Surg. 1992; 53:1080–1090.

14. Stehlik J, Edwards LB, Kucheryavaya AY, Benden C, Christie JD, Dobbels F, et al. The Registry of the International Society for Heart and Lung Transplantation: Twenty-eighth Adult Heart Transplant Report--2011. J Heart Lung Transplant. 2011; 30:1078–1094.

15. Rose EA, Gelijns AC, Moskowitz AJ, Heitjan DF, Stevenson LW, Dembitsky W, et al, Randomized Evaluation of Mechanical Assistance for the Treatment of Congestive Heart Failure (REMATCH) Study Group. Long-term use of a left ventricular assist device for end-stage heart failure. N. Engl. J. Med. 2001; 345:1435–1443.

16. Slaughter MS, Rogers JG, Milano CA, Russell SD, Conte JV, Feldman D, et al, HeartMate II Investigators. Advanced heart failure treated with continuous-flow left ventricular assist device. N. Engl. J. Med. 2009; 361:2241–2251.

17. Stewart GC, Stevenson LW. Keeping left ventricular assist device acceleration on track. Circulation. 2011; 123:1559–68; discussion 1568.

18. Neyt M, Van den Bruel A, Smit Y, de Jonge N, Erasmus M, Van Dijk D, et al. Cost-effectiveness of continuous-flow left ventricular assist devices. Int J Technol Assess Health Care. 2013; 29:254–260.

19. Wohlschlaeger J, Schmitz KJ, Schmid C, Schmid KW, Keul P, Takeda A, et al. Reverse remodeling following insertion of left ventricular assist devices (LVAD): a review of the morphological and molecular changes. Cardiovasc. Res. 2005; 68:376–386.

20. Bruggink AH, van Oosterhout MFM, de Jonge N, Ivangh B, van Kuik J, et al. Reverse remodeling of the myocardial extracellular matrix after prolonged left ventricular assist device support follows a biphasic pattern. J Heart Lung Transplant. 2006; 25:1091–1098.

21. Ambardekar AV, Buttrick PM. Reverse remodeling with left ventricular assist devices: a review of clinical, cellular, and molecular effects. Circ Heart Fail. 2011; 4:224–233.

22. Birks EJ, George RS. Molecular changes occurring during reverse remodelling following left ventricular assist device support. J Cardiovasc Transl Res. 2010; 3:635–642.

23. Oosterom L, De Jonge N, Kirkels J, Klöpping C, Lahpor J. Left ventricular assist device as a bridge to recovery in a young woman admitted with peripartum cardiomyopathy. Neth Heart J. 2008; 16:426–428.

24. Birks EJ, Tansley PD, Hardy J, George RS, Bowles CT, Burke M, et al. Left ventricular assist device and drug therapy for the reversal of heart failure. N. Engl. J. Med. 2006; 355:1873–1884.

25. Birks EJ, George RS, Hedger M, Bahrami T, Wilton P, Bowles CT, et al. Reversal of severe heart failure with a continuous-flow left ventricular assist device and pharmacological therapy: a prospective study. Circulation. 2011; 123:381–390.

26. Farrar DJ, Holman WR, McBride LR, Kormos RL, Icenogle TB, Hendry PJ, et al. Long-term follow-up of Thoratec ventricular assist device bridge-to-recovery patients successfully removed from support after recovery of ventricular function. J Heart Lung Transplant. 2002; 21:516–521.

27. Burkhoff D, Klotz S, Mancini DM. LVAD-induced reverse remodeling: basic and clinical implications for myocardial recovery. J Card Fail. 2006; 12:227–239.

28. Radovancevic B, Vrtovec B, de Kort E, Radovancevic R, Gregoric ID, Frazier OH. End-organ function in patients on long-term circulatory support with continuous- or pulsatile-flow assist devices. J Heart Lung Transplant. 2007; 26:815–818.

29. Feller ED, Sorensen EN, Haddad M, Pierson RN, Johnson FL, Brown JM, et al. Clinical outcomes are similar in pulsatile and nonpulsatile left ventricular assist device recipients. Ann. Thorac. Surg. 2007; 83:1082–1088.

30. Thohan V, Stetson SJ, Nagueh SF, Rivas-Gotz C, Koerner MM, Lafuente JA, et al. Cellular and hemodynamics responses of failing myocardium to continuous flow mechanical circulatory support using the DeBakey-Noon left ventricular assist device: a comparative analysis with pulsatile-type devices. J Heart Lung Transplant. 2005; 24:566–575.

31. Kato TS, Chokshi A, Singh P, Khawaja T, Cheema F, Akashi H, et al. Effects of continuous-flow versus pulsatile-flow left ventricular assist devices on myocardial unloading and remodeling. Circ Heart Fail. 2011; 4:546–553.

32. Haft J, Armstrong W, Dyke DB, Aaronson KD, Koelling TM, Farrar DJ, et al. Hemodynamic and exercise performance with pulsatile and continuous-flow left ventricular assist devices. Circulation. 2007; 116:I8–15.

33. Klotz S, Deng MC, Stypmann J, Roetker J, Wilhelm MJ, Hammel D, et al. Left ventricular pressure and volume unloading during pulsatile versus nonpulsatile left ventricular assist device support. Ann. Thorac. Surg. 2004; 77:143–9; discussion 149–50.

34. Krabatsch T, Schweiger M, Dandel M, Stepanenko A, Drews T, Potapov E, et al. Is bridge to recovery more likely with pulsatile left ventricular assist devices than with nonpulsatile-flow systems? Ann. Thorac. Surg. 2011; 91:1335–1340.

35. Dandel M, Weng Y, Siniawski H, Potapov E, Lehmkuhl HB, Hetzer R. Long-term results in patients with idiopathic dilated cardiomyopathy after weaning from left ventricular assist devices. Circulation. 2005; 112:I37–45.

36. Bruckner BA, Stetson SJ, Perez-Verdia A, Youker KA, Radovancevic B, Connelly JH, et al. Regression of fibrosis and hypertrophy in failing myocardium following mechanical circulatory support. J Heart Lung Transplant. 2001; 20:457–464.

37. Simon MA, Kormos RL, Murali S, Nair P, Heffernan M, Gorcsan J, et al. Myocardial recovery using ventricular assist devices: prevalence, clinical characteristics, and outcomes. Circulation, 2005; 112:I32–I36.

38. Müller J, Wallukat G, Weng YG, Dandel M, Spiegelsberger S, Semrau S, et al. Weaning from mechanical cardiac support in patients with idiopathic dilated cardiomyopathy. Circulation. 1997; 96:542–549.

39. Maybaum S, Mancini D, Xydas S, Starling RC, Aaronson K, Pagani FD, et al, LVAD Working Group. Cardiac improvement during mechanical circulatory support: a prospective multicenter study of the LVAD Working Group. Circulation. 2007; 115:2497-2505.

1

40.   de Jong S, van Veen TAB, de Bakker JMT, Vos MA, van Rijen HVM. Biomarkers of myocardial fibrosis. J. Cardiovasc. Pharmacol. 2011; 57:522–535.

41.   Baum J, Duffy HS. Fibroblasts and myofibroblasts: what are we talking about? J. Cardiovasc. Pharmacol. 2011; 57:376–379.

42.   van den Borne SWM, Díez J, Blankesteijn WM, Verjans J, Hofstra L, Narula J. Myocardial remodeling after infarction: the role of myofibroblasts. Nat Rev Cardiol. 2010; 7:30–37.

43.   Weber KT, Sun Y, Tyagi SC, Cleutjens JP. Collagen network of the myocardium: function, structural remodeling and regulatory mechanisms. J Mol Cell Cardiol. 1994; 26:279–292.

44.   Swynghedauw B. Molecular mechanisms of myocardial remodeling. Physiol. Rev. 1999; 79:215–262.

45.   Visse R, Nagase H. Matrix metalloproteinases and tissue inhibitors of metalloproteinases: structure, function, and biochemistry. Circ. Res. 2003; 92:827–839.

46.   Kapur NK. Transforming growth factor-β: governing the transition from inflammation to fibrosis in heart failure with preserved left ventricular function. Circ Heart Fail. 2011; 4:5–7.

47.   Klotz S, Foronjy RF, Dickstein ML, Gu A, Garrelds IM, Danser AHJ, et al. Mechanical unloading during left ventricular assist device support increases left ventricular collagen cross-linking and myocardial stiffness. Circulation. 2005; 112:364–374.

48.   Barbone A, Holmes JW, Heerdt PM, The AH, Naka Y, Joshi N, et al. Comparison of right and left ventricular responses to left ventricular assist device support in patients with severe heart failure: a primary role of mechanical unloading underlying reverse remodeling. Circulation. 2001; 104:670–675.

49.   Madigan JD, Barbone A, Choudhri AF, Morales DL, Cai B, Oz MC, et al. Time course of reverse remodeling of the left ventricle during support with a left ventricular assist device. J. Thorac. Cardiovasc. Surg. 2001; 121:902–908.

50.   Matsumiya G, Monta O, Fukushima N, Sawa Y, Funatsu T, Toda K, et al. Who would be a candidate for bridge to recovery during prolonged mechanical left ventricular support in idiopathic dilated cardiomyopathy? J. Thorac. Cardiovasc. Surg. 2005; 130:699–704.

51.   McCarthy PM, Nakatani S, Vargo R, Kottke-Marchant K, Harasaki H, James KB, et al. Structural and left ventricular histologic changes after implantable LVAD insertion. Ann. Thorac. Surg. 1995; 59:609–613.

52.   Nakatani S, McCarthy PM, Kottke-Marchant K, Harasaki H, James KB, Savage RM, et al. Left ventricular echocardiographic and histologic changes: impact of chronic unloading by an implantable ventricular assist device. J. Am. Coll. Cardiol. 1996; 27:894–901.

53.   Drakos SG, Kfoury AG, Hammond EH, Reid BB, Revelo MP, Rasmusson BY, et al. Impact of mechanical unloading on microvasculature and associated central remodeling features of the failing human heart. J. Am. Coll. Cardiol. 2010; 56:382–391.

54.   Klotz S, Danser AHJ, Foronjy RF, Oz MC, Wang J, Mancini D, et al. The impact of angiotensin-converting enzyme inhibitor therapy on the extracellular collagen matrix during left ventricular assist device support in patients with end-stage heart failure. J. Am. Coll. Cardiol. 2007; 49:1166–1174.

55. Braunwald E. Biomarkers in heart failure. N. Engl. J. Med. 2008; 358:2148–2159.

56. Ahmad T, Fiuzat M, Felker GM, O'Connor C. Novel biomarkers in chronic heart failure. Nat Rev Cardiol. 2012; 9:347–359.

57. Kapoun AM, Liang F, O'Young G, Damm DL, Quon D, White RT, et al. B-type natriuretic peptide exerts broad functional opposition to transforming growth factor-beta in primary human cardiac fibroblasts: fibrosis, myofibroblast conversion, proliferation, and inflammation. Circ. Res. 2004; 94:453–461.

58. McMurray JJV, Adamopoulos S, Anker SD, Auricchio A, Böhm M, Dickstein K, et al, ESC Committee for Practice Guidelines. ESC guidelines for the diagnosis and treatment of acute and chronic heart failure 2012: The Task Force for the Diagnosis and Treatment of Acute and Chronic Heart Failure 2012 of the European Society of Cardiology. Developed in collaboration with the Heart Failure Association (HFA) of the ESC. Eur. J. Heart Fail. 2012; 14:803–869.

59. Kinoshita M, Takano H, Taenaka Y, Mori H, Takaichi S, Noda H, et al. Cardiac disuse atrophy during LVAD pumping. ASAIO Trans. 1988; 34:208–212.

60. Hill JA, Olson EN. Cardiac plasticity. N. Engl. J. Med. 2008; 358:1370–1380.

61. Schena S, Kurimoto Y, Fukada J, Tack I, Ruiz P, Pang M, et al. Effects of ventricular unloading on apoptosis and atrophy of cardiac myocytes. J. Surg. Res. 2004; 120:119–126.

62. Cao DJ, Jiang N, Blagg A, Johnstone JL, Gondalia R, Oh M, et al. Mechanical unloading activates FoxO3 to trigger Bnip3-dependent cardiomyocyte atrophy. J Am Heart Assoc. 2013; 2:e000016.

63. Pagan J, Seto T, Pagano M, Cittadini A. Role of the ubiquitin proteasome system in the heart. Circ. Res. 2013; 112:1046–1058.

64. Weekes J, Morrison K, Mullen A, Wait R, Barton P, Dunn MJ. Hyperubiquitination of proteins in dilated cardiomyopathy. Proteomics. 2003; 3:208–216.

65. Wohlschlaeger J, Sixt SU, Stoeppler T, Schmitz KJ, Levkau B, Tsagakis K, et al. Ventricular unloading is associated with increased 20s proteasome protein expression in the myocardium. J Heart Lung Transplant. 2010; 29:125–132.

66. Kostin S, Pool L, Elsässer A, Hein S, Drexler HCA, Arnon E, et al. Myocytes die by multiple mechanisms in failing human hearts. Circ. Res. 2003; 92:715–724.

67. Predmore JM, Wang P, Davis F, Bartolone S, Westfall MV, Dyke DB, et al. Ubiquitin proteasome dysfunction in human hypertrophic and dilated cardiomyopathies. Circulation. 2010; 121:997–1004.

68. Lecker SH, Goldberg AL, Mitch WE. Protein degradation by the ubiquitin-proteasome pathway in normal and disease states. J. Am. Soc. Nephrol. 2006; 17:1807–1819.

69. Herrmann J, Ciechanover A, Lerman LO, Lerman A. The ubiquitin-proteasome system in cardiovascular diseases-a hypothesis extended. Cardiovasc. Res. 2004; 61:11–21.

70. Hetzer R, Müller JH, Weng Y, Meyer R, Dandel M. Bridging-to-recovery. Ann. Thorac. Surg. 2001; 71:S109–13– discussion S114–5.

71. Martina J, de Jonge N, Sukkel E, Lahpor J. Left ventricular assist device-related systolic aortic regurgitation. Circulation. 2011; 124:487–488.

1

72. Martina JR, Schipper MEI, de Jonge N, Ramjankhan F, de Weger RA, Lahpor JR, et al. Analysis of aortic valve commissural fusion after support with continuous-flow left ventricular assist device. Interact Cardiovasc Thorac Surg. 2013; 17: 616-624.

73. George I, Xydas S, Mancini DM, Lamanca J, DiTullio M, Marboe CC, et al. Effect of Clenbuterol on cardiac and skeletal muscle function during left ventricular assist device support. J Heart Lung Transplant. 2006; 25:1084–1090.

74. Navaratnarajah M, Ibrahim M, Siedlecka U, van Doorn C, Shah A, Gandhi A, et al. Influence of ivabradine on reverse remodelling during mechanical unloading. Cardiovasc. Res. 2013; 97:230–239.

75. Margulies KB, Matiwala S, Cornejo C, Olsen H, Craven WA, Bednarik D. Mixed messages: transcription patterns in failing and recovering human myocardium. Circ. Res. 2005; 96:592–599.
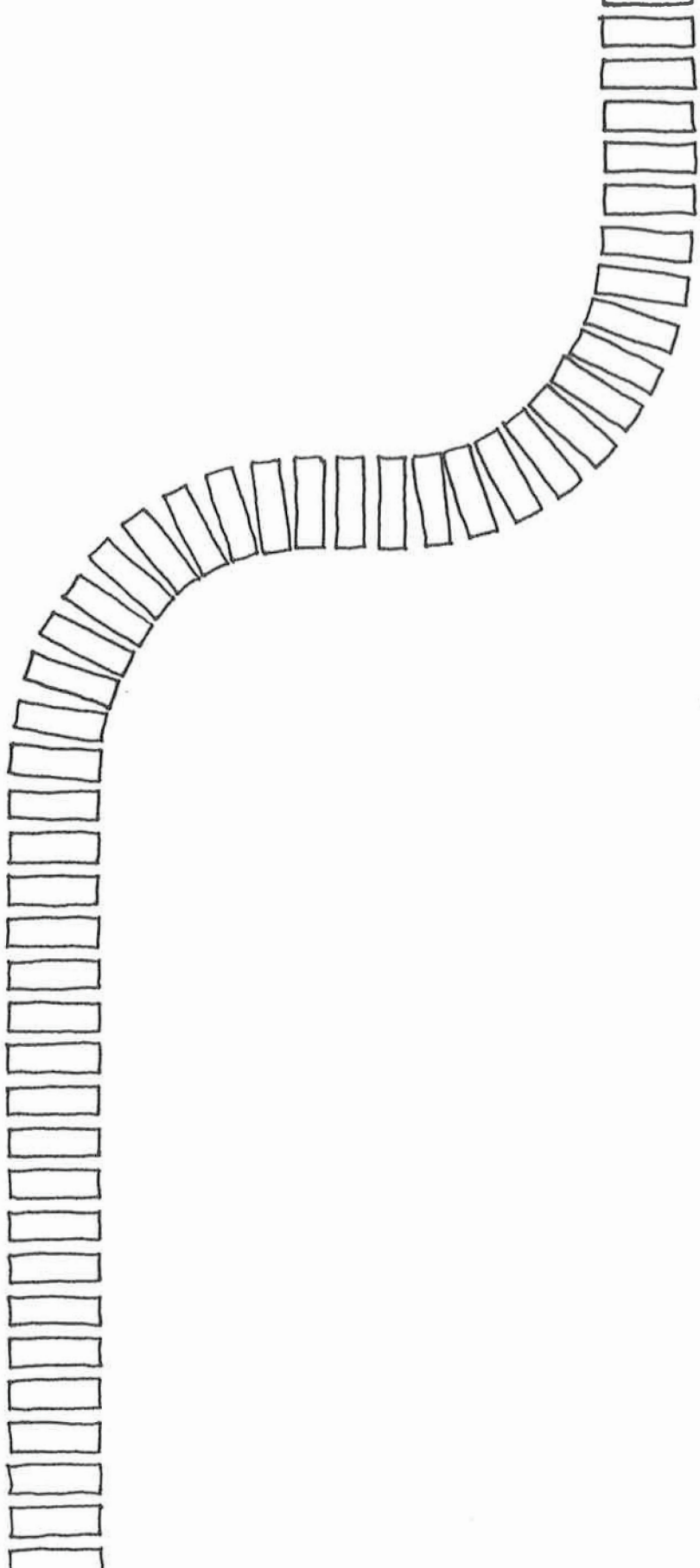
CHAPTER 2

Single-centre experience of 85 patients with continuous flow left ventricular assist device: clinical practice and outcome after extended support

Sjoukje I. Lok[1, ξ], Jerson R. Martina[2, ξ], Tim Hesselink[1], Ben F.M. Rodermans[3], Nelienke Hulstein[2]; Bjorn Winkens[4], Corinne Klöpping[1], J. Hans Kirkels[1], Pieter A. Doevendans[1], Faiz Ramjankhan[2], Roel A. de Weger[5], Nicolaas de Jonge[1], Jaap R. Lahpor[2]

[1] Department of Cardiology, University Medical Center, Utrecht
[2] Department of Cardiothoracic Surgery, University Medical Center Utrecht
[3] Department of Medical Technology, University Medical Center Utrecht
[4] Department of Methodology and Statistics, University of Maastricht
[5] Department of Pathology, University Medical Center, Utrecht

ξ: Both authors contributed equally to this work

Abstract

Background: We evaluated our single-centre clinical experience with the HeartMate II (HM II) left ventricular assist device (LVAD) as bridge to transplantation (BTT) in end-stage heart failure (HF) patients.

Methods: Survival rates, echocardiographic parameters, laboratory values and adverse events of 85 consecutive patients supported with a HM II were evaluated.

Results: Overall, mean age was 45±13 years, 62 (73%) were male and non-ischemic dilated cardiomyopathy was present in 60 (71%) patients. The median duration of mechanical support was 387 days (IQR 150-600), with a range of 1 to 1835 days. The 6 months, 1-, 2-, 3- and 4-year survival rates during HM II LVAD support were 85, 81, 76, 76 and 68%, respectively. Echocardiographic parameters demonstrated effective left ventricular unloading, while laboratory results reflected adequate organ perfusion. However, HM II support was associated with adverse events, such as infections in 42 patients (49%; 0.67 events/patient-year), cardiac arrhythmia in 44 patients (52%; 0.86 events/patient-year), bleeding complications in 32 patients (38%; 0.43 events/patient-year) and neurological dysfunction in 17 patients (20%; 0.19 events/patient-year).

Conclusion: In view of the increasing shortage of donor hearts, HM II LVAD support may be considered a life-saving treatment in end-stage HF patients, with good survival. However, it is still associated with some serious adverse events, of which neurologic complications are the most critical.

Introduction

Heart transplantation (HTx) has been the most successful treatment of end-stage heart failure (HF), however, its use is hampered by a progressive shortage of donor hearts. The use of left ventricular assist devices (LVADs) as a bridge to transplantation (BTT) has shown favourable long-term results. The first generation of LVADs consisted of large pulsatile flow LVADs (pf-LVADs) with limited mechanical durability. The second generation, continuous flow LVADs (cf-LVAD), have demonstrated improved durability, long-term survival and exercise capacity [1-4]. More recently, cf-LVADs have also been considered as an alternative for HTx, so called destination therapy (DT). While results with cf-LVADs have consistently improved over time, several questions remain with regard to timing of device implantation, patient selection, management and timing of HTx and DT. Adverse events, including bleeding, infection and stroke, also continue to pose challenges. This study describes a single-centre experience with the HeartMate II (HM II; Thoratec, Pleasanton, CA, USA) LVAD support as BTT over a 5-year period.

Materials and methods

Patient selection
From March 2006 until December 2011, 85 patients received a HM II as a BTT at the University Medical Center in Utrecht in the Netherlands. Throughout this study period, much experience has been obtained with long-term support using cf-LVADs in our centre. Patients were categorized according to the Interagency Registry for Mechanically Assisted Circulatory Support (INTERMACS), which is based on severity of illness at the time of device implantation [5].

HeartMate-II LVAD
The HM II, a cf-LVAD, has a titanium axial-flow pump with an inlet cannula that is placed in the left ventricular apex and an outlet cannula in the ascending aorta. It has a percutaneous lead that connects the pump to an external system driver and power source. The pump generates up to 10 L/min of flow at a mean pressure difference of 100 mm Hg [6]. Implantation is done through a median sternotomy using extracorporeal circulation on the beating heart and the device is placed in a small pre-peritoneal pocket.

Anticoagulation therapy

The post-operative anticoagulation regimen included warfarin, heparin and acetylsalicyl acid. Assuming no bleeding, heparin was started 24 hours after surgery. A heparin ratio of 2 was aimed, which means that the APTT value was targeted twice as normal. Heparin was only considered if: 1) Total drain production during the first 3 consecutive hours post-implant did not exceed 100 ml, 2) pro-thrombin time was less than 18 seconds and 3) activated partial tromboplastin time was less than 40 seconds. Heparin was stopped when INR>1.5. From March 2006 until August 2009, warfarin was titrated to an INR of 2-2.5, seven days after implant. With this anticoagulation regimen, reported incidence of bleeding events in literature was substantial, leading to a recommended reduction in INR range [7.] Therefore, our INR target was adapted to a range of 1.5-2 from August 2009 until December 2011. In case of major bleeding, all anticoagulation was temporarily stopped and continued on an individual basis after the bleeding episode.

Patient and device management

All patients were seen on scheduled visits 1 week after discharge and 1, 3, 6, and 12 months in our out-patient department, every 3 months thereafter, and more often when indicated. Echocardiographic analyses were performed at 3, 6 and 12 months after implantation. Baseline and follow-up data were collected prospectively, including patient characteristics, blood chemistry analysis, hematologic findings and neurological status.

Definition of adverse events

Each event was scored and defined according to the INTERMACS definitions [5] with the following adjustments;

Major infection was characterized as a clinical infection accompanied by pain, fever, drainage and/or leucocytosis with a positive culture from the infected site or organ, which was treated by anti-microbial agents. The general categories of infections were sepsis, pocket, driveline and non-device related infections.

Haemolysis was defined as elevated levels of LDH (>1500 U/L) and bilirubin (>21 μmol/L), low haptoglobin (<30 mg/dl) in combination with increased fatigue, muscle ache and dark urine, occurring after the first 72 hours post-implant.

Right HF was classified as symptoms and signs of persistent right ventricular dysfunction requiring right ventricular assist device (RVAD) implantation and/or inhaled nitric oxide ≥48 hrs and/or inotropic therapy for a duration of more than 14 days at any time after LVAD implantation or LVAD replacement [8].

Statistical analysis

Categorical data are presented by number (%) and continuous data by median (interquartile range; IQR, i.e. 25th-75th percentile) or by estimated mean ± standard error, where appropriate. The laboratory and echocardiography parameters were analysed with linear mixed models, where data were checked for normality using histograms and log-transformed if data were positively skewed. The estimated means and confidence interval were presented on the original scale. Survival was analysed based on Kaplan-Meier with patients censored for device explantation (recovery), or HTx. Adverse events are presented both as percentages of all patients as well as events/patient year (e/pt-y). A p-value < 0.05 was considered as statistically significant. All analyses were done with SPSS 20.0 software (SPSS Inc, Chicago, IL).

Results

Baseline characteristics

Baseline characteristics are presented in *Table 1*. Prior to HM II implantation, 21 patients (25%) were in critical cardiogenic shock (INTERMACS profile-I) and 64 patients (75%) experienced progressive hemodynamic deterioration (INTERMACS profile-II). The mean age was 45±13 years (range 17-69). Sixty-two patients (73%) were male. The etiology of HF was non-ischemic dilated cardiomyopathy in 60 patients (71 %), ischemic cardiomyopathy in 24 patients (28%) and hypertrophic cardiomyopathy in 1 patient (1%). The median duration of support was 387 days (IQR 150-600), with a range of 1 to 1835 days.

Outcome

On December 31st 2011, 17 patients (20%) had died, 32 (38%) were still ongoing (LVAD duration 543 ± 411 days; range 33-1835), 3 (4%) had recovered with subsequent device explantation and 33 (39%) were transplanted (LVAD duration 566 ± 386 days; range 85-1393).

The 6-months, 1, 2, 3 and 4-year actuarial survival during HM II support were 85, 81, 76, 76 and 68%, respectively (*Figure 1*). Of the 17 non-survivors, 10 died perioperatively (≤30 days after HM II implantation) due to major bleeding (n=2), pneumonia (n=2), ischemic CVA (n=1), haemorrhagic CVA (n=1), sepsis (n=1), irreversible multi-organ failure (n=2) and right HF (n=1). Late mortality (>30 days) occurred in 7 patients due to pump thrombosis (n=2), right HF (n=1), recurrent myocarditis (n=1), ischemic CVA (n=2)

and severe encephalopathy due to MELAS syndrome (n=1). After HM II implantation, 73 patients (86%) were discharged after a mean hospital stay of 40 ± 24 days. Rehospitalisation occurred 84 times in 39 patients. The mean rehospitalisation period was 14 days (range 1–177).

Table 1: Baseline characteristics of 85 patients with end-stage heart failure (HF) prior to continuous flow LVAD (cf-LVAD) support

Variable	Number
Inclusion periode	March 2006 to December 2011
Mean age (years) ± SD	45 ± 13 (range 17-69)
Male/Female	62 (73%) / 23 (27%)
INTERMACS level	
I	21 (25%)
II	64 (75%)
HF duration (days)	1413 ± 1790 (range 1-7386)
Etiology	
Ischemic	24 (28%)
Non-ischemic	60 (71%)
DCM	
HCM	1 (1%)
Diabetes mellitus	8 (9%)
Hypertension	5 (6%)
ICD	49 (58%)

HF, heart failure; ICD, implantable cardioverter defibrillator; DCM, dilated cardiomyopathy; HCM, hypertrophic cardiomyopathy.

Echocardiographic data

Echocardiographic data at baseline pump speed are presented in *Figure 2*. The left ventricular end-diastolic dimension (LVEDD) and the left ventricular end-systolic dimension (LVESD) decreased significantly after 3 months of mechanical support (overall trend for both p<0.0001) and the LVESD further decreased significantly after 12 months compared to 3 months (p=0.037).
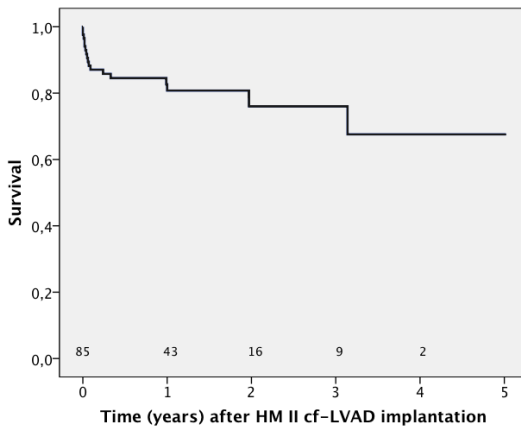
Figure 1: Actuarial survival (Kaplan-Meier analysis) of 85 patients during continuous flow LVAD (cf-LVAD) support as bridge to transplantation (BTT) in our centre
The 6-months, 1, 2, 3, and 4-year actuarial survival during HM II support were 85, 81, 76, 76 and 68% respectively.
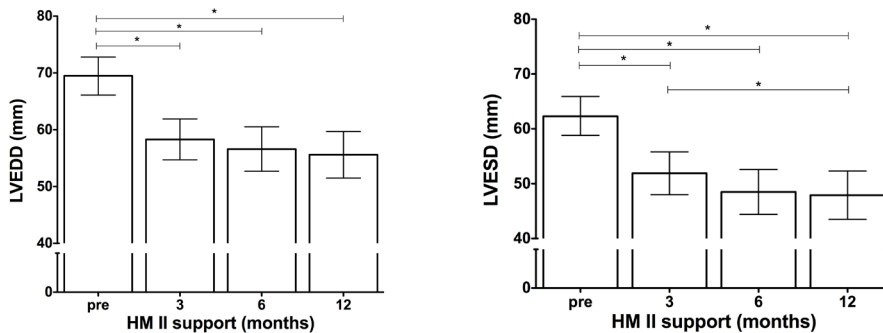
Figure 2: Echocardiography during continuous flow LVAD (cf-LVAD) support
Left ventricular end-diastolic dimension (LVEDD) and left ventricular end-systolic dimension (LVESD) decreased significantly during cf-LVAD support.
The asterisk (*) represents p<0.05.

Laboratory parameters

Serum markers of end-organ function before HM II implantation and after 3, 6, and 12 months of follow-up are shown in *Figure 3*. Mainly, BNP decreased rapidly after implantation. Kidney (creatinine and urea), hepatic (AST, ALT and GGT) and inflammatory markers (leukocytes, CRP) improved for up to 1-year post-implant.
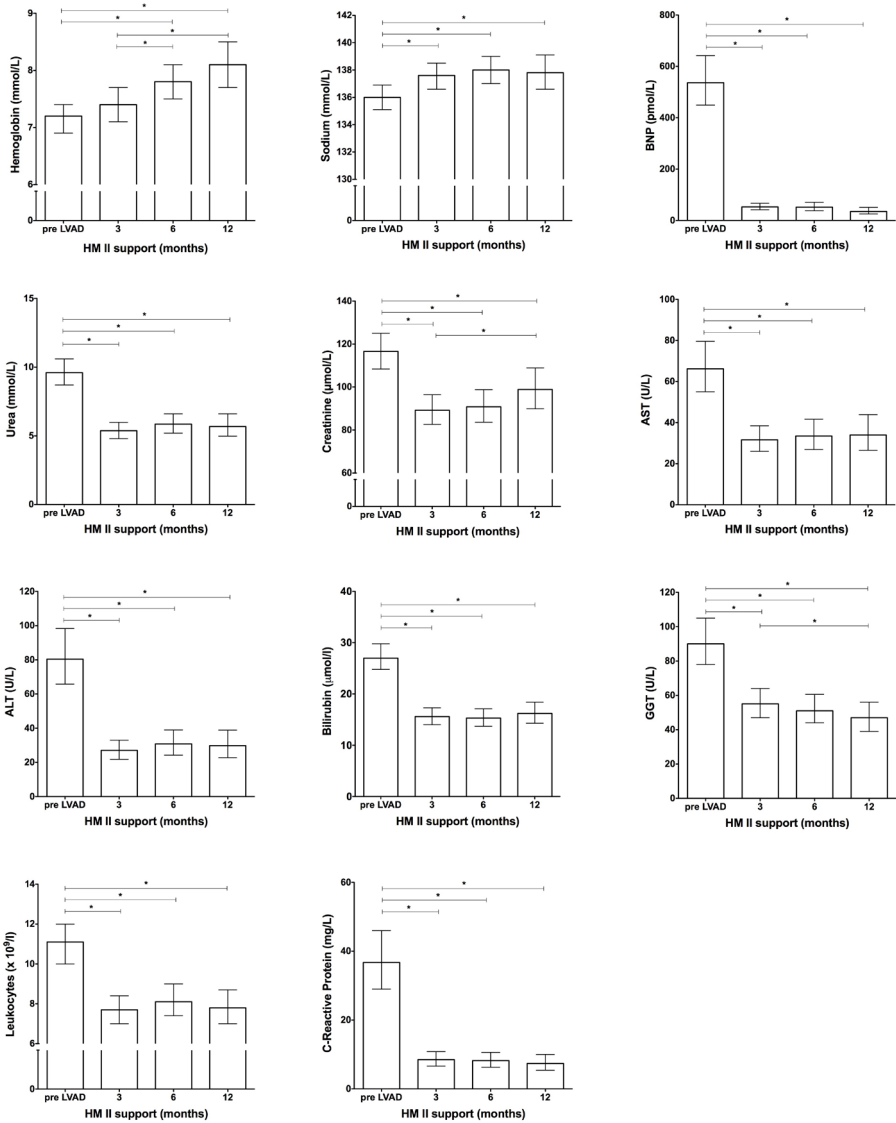
Figure 3: Change in laboratory parameters during continuous flow LVAD (cf-LVAD) support
Haemoglobin and sodium levels increased significantly during cf-LVAD support. Brain Natriuretic Peptide (BNP) decreased significantly rapidly after cf-LVAD implantation and remained stable thereafter. Kidney (creatinine and urea), hepatic (AST, ALT and GGT) and inflammatory markers (leukocytes, CRP) improved for up to 1-year post-implant. The asterisk (*) represents p<0.05.

Adverse events

Adverse events of the 85 BTT patients are presented in *Table 2*. There were 310 adverse events during a cumulative support time of 109.1 years (2.8 events/patient-year; e/pt-y). In total, 73 major infections occurred in 42 patients (49%; 0.67 e/pt-y), 22% of them were non-device related infections and sepsis. Driveline infections occurred 14 times in 12 patients (0.13 e/pt-y) and 4 pocket infections were diagnosed in 4 patients (0.04 e/pt-y). In particular, 7 patients with driveline and/or pocket infection received permanent antibiotic prophylaxes until HTx.

Cardiac arrhythmias occurred 94 times in 44 patients (52%; 0.86 e/pt-y). In 1 patient, ventricular tachycardia remained untreatable while the patient was hemodynamically compromised, despite HM II support. As a result, the patient had to be rehospitalised for several months and eventually underwent emergency HTx.

A total of 47 major bleeding events were identified in 32 patients (38%; 0.43 e/pt-y), mostly early post-operative and often related to surgery (<30 days after implantation). Late bleeding, in particular, gastro-intestinal (GI) bleeding developed 5 times in 4 patients (5%; 0.05 e/pt-y, onset GI bleeding after HM II implantation 211 ± 180 days).

Twenty-seven right HF events occurred in 27 patients (32%; 0.25 e/pt-y), of which 25 within the first 30 days after implantation. In case of right HF, patients were treated with a phosphodiesterase-3 inhibitor and nitric oxide. Yet, 4 patients required a RVAD. Of these, RVAD explantation was possible in 2 patients after 12 and 7 days respectively. The other 2 patients died during RVAD support, due to right HF and severe encephalopathy, respectively.

Furthermore, 21 neurological events (8 TIAs, 9 ischemic CVAs and 4 haemorrhagic CVAs) occurred in 17 patients (20%; 0.19 e/pt-y). Mean interval until first neurological event was 213 ± 316 days. Of the 13 CVAs, 4 were fatal, 6 resulted in minor limitations and 3 in major limitations of daily life activities.

Haemolysis was noted in 16 patients (21 episodes; 19%; 0.19 events/patient-year), often after 30 days post-implantation.

Device malfunction was the result of driveline fractures in 4 patients (5%; 0.04 e/p-y). One of these fractured drivelines was repaired, while the other three were irreparable and pump replacement was necessary. Pump thrombosis occurred in 7 patients (8%; 0.06 e/pt-y). Four of these patients needed a pump replacement, 2 patients died and 1 patient died of a recurrent myocarditis with pump thrombosis as secondary finding. Other adverse events were peri-operative renal failure requiring continuous veno-venous hemofiltration

Table 2: Adverse events during continuous flow LVAD (cf-LVAD) support (n=85)

Adverse Event	Overall (support duration 109,1 Patient-Yrs)			0-30 Days (support duration 6,3 Patient-Yrs)			>30 Days (support duration 102,6 Patient-Yrs)		
	Patients with event, n(%)	No. Of events	Event Rate*	Patients with event	No. Of events	Event Rate*	Patients with event	No. Of events	Event Rate*
Major bleedings	32 (38)	47	0,43	26	36	5,71	11	11	0,11
Major infections	42 (49)	73	0,67	24	30	4,76	22	43	0,42
Non-device	19 (22)	21	0,19	13	13	2,06	7	8	0,08
Driveline	12 (14)	14	0,13	6	6	0,95	7	8	0,08
Pocket	4 (5)	4	0,04	1	1	0,16	3	3	0,03
Sepsis	23 (27)	34	0,31	10	10	1,59	15	24	0,23
Cardiac arrhythmias	44 (52)	94	0,86	37	42	6,67	14	52	0,51
SVT	12 (14)	13	0,12	11	11	1,75	2	2	0,02
VT/VF	34 (40)	81	0,74	26	31	4,92	12	50	0,49
Neurologic dysfunction	17 (20)	21	0,19	8	9	1,43	10	12	0,12
TIA	7 (8)	8	0,07	3	4	0,63	4	4	0,04
Ischemic CVA	9 (11)	9	0,08	3	3	0,48	6	6	0,06
Hemorrhagic CVA	4 (5)	4	0,04	2	2	0,32	2	2	0,02
Device malfunctions	11 (13)	11	0,10	1	1	0,16	10	10	0,10
Non-pump	4 (5)	4	0,04	0	0	0,00	4	4	0,04
Pump thrombosis	7 (8)	7	0,06	1	1	0,16	6	6	0,06
Hemolysis	16 (19)	21	0,19	4	4	0,63	12	17	0,17
Renal failure	9 (11)	9	0,08	9	9	1,43	0	0	0,00
Venous thrombotic events	7 (8)	7	0,06	7	7	1,11	0	0	0,00
Right HF	27 (32)	27	0,25	25	25	3,97	2	2	0,02

*Events/patient-years; GI, gastrointestinal; SVT, supraventricular tachycardia; VT, ventricular tachycardia; CVA, cerebrovascular accident; HF, heart failure

(CVVH) in 9 patients (11%; 0.08 e/pt-y) and 7 venous thrombotic events a result of central venous catheters (including 3 pulmonary embolism) in 7 patients (8%; 0.06 e/pt-y).

Discussion

The discrepancy between the limited availability of donor hearts and the increasing number of end-stage HF patients has led to an increased use of LVADs as a BTT. Over the last 6 years, there has been a transition from pf-LVADs to cf-LVADs. Compared to our earlier limited experience with pf-LVADs [9], cf-LVADs provide circulatory support for longer periods of time. This study evaluated the outcome of 85 patients supported with a single type of cf-LVAD. Our 1- and 2-year actuarial survival rates during HM II as BTT were 83% and 76% respectively, consistent with other recent publications [10,12]. In the present study, most common adverse events during HM II support were cardiac arrhythmias (mainly ventricular arrhythmias) and peri-operative bleeding. The incidence of infections was substantial with 0.67 e/p-y, but did not lead to mortality and was similar to that reported by other centers [10,12].

In our cohort, thromboembolic complications resulted in limitations of daily live activities or were a cause of death. Pump thrombosis occurred in 8% of patients (0.06 e/p-y) and required pump exchange. These incidences imply that the anticoagulation regimen remains a challenge, and requires precise evaluation and follow-up to limit associated complications. Remarkably, GI-bleedings were less frequent in our cohort compared to other experiences [13,14]. It has been suggested that GI-bleedings during HM II support are related to the decrease in pulsatility induced by the cf-LVAD with minimal opening of the aortic valve. This may induce angiodysplasia of the GI tract, arteriovenous malformations and eventually cause bleeding, especially in combination with anticoagulants, platelet inhibitors and acquired von Willebrand syndrome [13]. Our policy is setting the pump speed to maintain some degree of pulsatility. Our low incidence of GI-bleeding may also be generally associated with a younger patient cohort, the possible differences in anticoagulation regimens and the use of standard proton-pump inhibitors in this patient cohort.

It is well known that patient selection and timing of implantation remain important issues in optimizing the results after device implantation. In contrast to reported HM II trials including selected patients, our series present the results of a consecutive cohort of patients referred to our center. In this study, 25% of the patients who received a device were classified as INTERMACS profile-I and 75% as INTERMACS profile-II, reflecting a population with

severe HF. Yet, medium-term survival was comparable with other reported results from cohorts mostly based on less-sick patients (INTERMACS profiles III and IV) [5].

This analysis represents a single-centre experience of 85 end-stage HF patients with long-term HM II support used explicitly as BTT. Despite the fact that HTx remains the only curative therapy for end-stage HF, HM II LVAD therapy provides an off-the-shelf live-saving solution for critically ill patients who have no chance of surviving the increasing waiting periods required for a donor heart to become available. Yet, there is a price to pay in terms of risk of serious adverse events during support. Therefore, emphasis should be focused on minimizing adverse events while improving survival and quality of life while on HM II support. It is important to explore treatment options to achieve the optimal anticoagulation regimen, improve the management of ventricular arrhythmias and diminish device-related infections and haemolysis.

References

1. Miller LW, Pagani FD, Russell SD, John R, Boyle AJ, Aaronson KD, Conte JV, Naka Y, Mancini D, Delgado RM, MacGillivray TE, Farrar DJ, Frazier OH, HeartMate II Clinical Investigators: Use of a continuous-flow device in patients awaiting heart transplantation. N Engl J Med 2007, 357:885–896.

2. Slaughter MS, Rogers JG, Milano CA, Russell SD, Conte JV, Feldman D, Sun B, Tatooles AJ, Delgado RM, Long JW, Wozniak TC, Ghumman W, Farrar DJ, Frazier OH, HeartMate II Investigators: Advanced heart failure treated with continuous-flow left ventricular assist device. N Engl J Med 2009, 361:2241–2251.

3. Pruijsten RV, Lok SI, Kirkels HH, Klöpping C, Lahpor JR, de Jonge N: Functional and hemodynamic recovery after implantation of continuous-flow left ventricular assist devices in comparison with pulsatile left ventricular assist devices in patients with end-stage heart failure. Eur J Heart Fail 2012, 14:319–325.

4. Strüber M, Sander K, Lahpor J, Ahn H, Litzler P-Y, Drakos SG, Musumeci F, Schlensak C, Friedrich I, Gustafsson R, Oertel F, Leprince P: HeartMate II left ventricular assist device; early European experience. Eur J Cardiothorac Surg 2008, 34:289–294.

5. Kirklin JK, Naftel DC, Kormos RL, Stevenson LW, Pagani FD, Miller MA, Baldwin JT, Young JB: The Fourth INTERMACS Annual Report: 4,000 implants and counting. J Heart Lung Transplant 2012, 31:117–126.

6. Griffith BP, Kormos RL, Borovetz HS, Litwak K, Antaki JF, Poirier VL, Butler KC: HeartMate II left ventricular assist system: from concept to first clinical use. Ann Thorac Surg 2001, 71:S116–20– discussion S114–6.

7. Boyle AJ, Russell SD, Teuteberg JJ, Slaughter MS, Moazami N, Pagani FD, Frazier OH, Heatley G, Farrar DJ, John R: Low thromboembolism and pump thrombosis with the HeartMate II left ventricular assist device: analysis of outpatient anti-coagulation. J Heart Lung Transplant 2009, 28:881–887.

8. Dang NC, Topkara VK, Mercando M, Kay J, Kruger KH, Aboodi MS, Oz MC, Naka Y: Right heart failure after left ventricular assist device implantation in patients with chronic congestive heart failure. J Heart Lung Transplant 2006, 25:1–6.

9. Oosterom L, De Jonge N, Kirkels J, Klöpping C, Lahpor J: Left ventricular assist device as a bridge to recovery in a young woman admitted with peripartum cardiomyopathy. Neth Heart J 2008, 16:426–428.

10. Lahpor J, Khaghani A, Hetzer R, Pavie A, Friedrich I, Sander K, Strüber M: European results with a continuous-flow ventricular assist device for advanced heart-failure patients. Eur J Cardiothorac Surg 2010, 37:357–361.

2

11. Starling RC, Naka Y, Boyle AJ, Gonzalez-Stawinski G, John R, Jorde U, Russell SD, Conte JV, Aaronson KD, McGee EC, Cotts WG, DeNofrio D, Pham DT, Farrar DJ, Pagani FD: Results of the post-U.S. Food and Drug Administration-approval study with a continuous flow left ventricular assist device as a bridge to heart transplantation: a prospective study using the INTERMACS (Interagency Registry for Mechanically Assisted Circulatory Support). J Am Coll Cardiol 2011, 57:1890–1898.

12. John R, Naka Y, Smedira NG, Starling R, Jorde U, Eckman P, Farrar DJ, Pagani FD: Continuous flow left ventricular assist device outcomes in commercial use compared with the prior clinical trial. Ann Thorac Surg 2011, 92:1406–13– discussion 1413.

13. Stern DR, Kazam J, Edwards P, Maybaum S, Bello RA, D'Alessandro DA, Goldstein DJ: Increased incidence of gastrointestinal bleeding following implantation of the HeartMate II LVAD. J Card Surg 2010, 25:352–356.

14. Morgan JA, Paone G, Nemeh HW, Henry SE, Patel R, Vavra J, Williams CT, Lanfear DE, Tita C, Brewer RJ: Gastrointestinal bleeding with the HeartMate II left ventricular assist device. J Heart Lung Transplant 2012, 31:715–718.
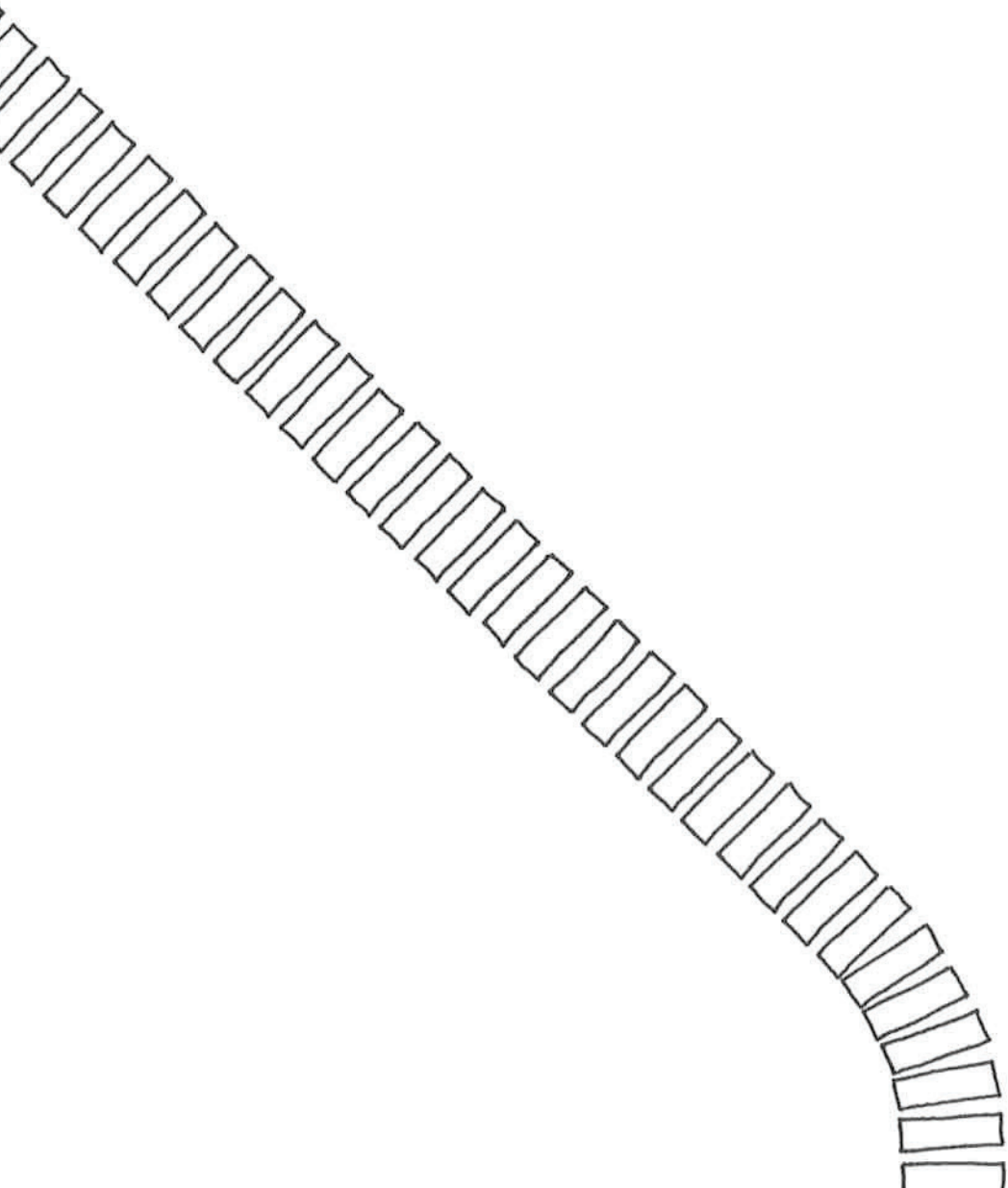
CHAPTER 3

Myocardial fibrosis and pro-fibrotic markers in end-stage heart failure patients during continuous flow LVAD support

Sjoukje I. Lok[1], Fay M.A. Nous[2], Joyce van Kuik[2], Petra van der Weide[2], Erica Siera[2], Hans Kemperman[3], Andre Huisman[2], Bjorn Winkens[4], Pieter A. Doevendans[1], Jaap R. Lahpor[5], J. Hans Kirkels[1], Corinne Klöpping[1], Roel A. de Weger[2], Nicolaas de Jonge[1]

[1] Department of Cardiology, University Medical Center Utrecht
[2] Department of Pathology, University Medical Center Utrecht
[3] Department of Clinical Chemistry and Hematology, University Medical Center Utrecht
[4] Department of Methodology and Statistics, University of Maastricht
[5] Department of Cardiothoracic Surgery, University Medical Center Utrecht

Abstract

Aim: During support with a left ventricular assist device (LVAD), partial reverse remodeling takes place in which fibrosis plays an important role. In this study, we analyzed the histological changes and expression of fibrotic markers in patients with advanced heart failure during continuous flow LVAD (cf-LVAD) support.

Methods: Myocardial tissue at time of LVAD implantation (pre-LVAD) was compared with tissue from the explanted left ventricle (post-LVAD). Interstitial fibrosis and cardiomyocyte size were analyzed pre- and post LVAD. Plasma was obtained from 30 patients before and during LVAD support. Plasma levels, cardiac mRNA and protein expression of Brain-Natriuretic Peptide (BNP), Galectin-3 (Gal-3), Connective Tissue Growth Factor (CTGF), Osteopontin (OPN) and Transforming Growth Factor β-1 (TGFβ-1) were determined.

Results: Fibrosis increased during cf-LVAD unloading (p<0.05). Cardiomyocytes elongated (p<0.05), whereas cross-sectional area did not change. BNP, Gal-3, CTGF and OPN were significantly elevated pre-LVAD in comparison to controls. BNP decreased significantly after 1 month of cf-LVAD support (p<0.001) to near-normal levels. Pro-fibrotic markers remained elevated in comparison to controls.

Conclusion: cf-LVAD support is associated with lengthening of cardiomyocytes, without alterations in diameter size. Remarkably, myocardial fibrosis increased as well as circulating pro-fibrotic markers. Whether the morphological changes are a direct effect of reduced pulsatility during cf-LVAD support or due to heart failure progression, requires further investigation.

Introduction

Left Ventricular Assist Devices (LVADs) are being used as bridge to transplantation (BTT) [1-3] in end-stage heart failure (HF) patients and provide volume and pressure unloading of the left ventricle, resulting in partial reverse remodeling of the heart [4-8]. Achieving sustained myocardial recovery, allowing LVAD removal (bridge to recovery; BTR), is one of the most desirable goals as this could reduce the need for heart transplantation (HTx). The mechanisms of reverse remodeling remain poorly understood. A lot of knowledge has emerged from studies of pulsatile flow LVADs (pf-LVADs), but currently these devices have been replaced by continuous flow LVADs (cf-LVADs). Differences in left ventricular unloading with cf-LVADs suggest that our experience of BTR with pf-LVADs might no longer apply. In addition, the lack of validated biomarkers for recovery aggravates uncertainties about ideal timing for LVAD explantation [9]. As fibrosis is thought to play an important role in the chance of successful recovery [10], the purpose of this study was to establish the amount of fibrosis and cardiomyocyte size during cf-LVAD support and to relate this to novel fibrotic markers, such as Galectin-3 (Gal-3), Connective Tissue Growth Factor (CTGF), Osteopontin (OPN) and Transforming Growth Factor β-1 (TGFβ-1), and Brain Natriuretic Peptide (BNP) in BTT and BTR patients.

Methods and materials

Patient characteristics

Thirty patients with a non-ischemic dilated cardiomyopathy (DCM) supported with a cf-LVAD (HeartMate II, Thoratec, CA, USA) as BTT (n=25) and BTR (n=5) were included. In the BTR group, 2 pf-LVADs and 3 cf-LVADs were used. Plasma was collected before LVAD implantation, 1, 3 and 6 months after implantation and prior to HTx or explantation. Control plasma was gathered from 10 healthy individuals. Of the 25 BTT patients, 17 underwent HTx. Myocardial tissue at time of LVAD implantation (pre-LVAD; apical core) was collected and compared with tissue from the explanted left ventricle (post-LVAD), outside the suture area of the inflow cannula. Control myocardial tissue was obtained from 3 donor hearts declined for HTx because of non-cardiac reasons. Written informed consent was obtained from all LVAD patients.

Cardiomyocyte size and fibrosis

Myocardial tissue was fixed in 10 % formalin and embedded in paraffin. After staining, the slides (5 μm; size: ± 1x1 cm) were analyzed at 40x magnification using an Aperio XT slide scanner (Aperio, Vista, CA, USA) and measured with Aperio Image Scope. Cardiomyocyte length was measured between the intercalated discs after staining the specimens with N-Cadherin. To determine the diameter of the cardiomyocytes, specimens were stained with Modified Azan and point-to-point perpendicular lines were drawn across the cross-sectional area of the cell at the level of the nucleus. Results were expressed as the average size of 200 cardiomyocytes per slide. For the evaluation of fibrosis, sections were stained with Masson Trichrome and 15 random fields were selected. Automated image analysis was done using a colour deconvolution algorithm [11] and myocardial fibrosis was calculated with the use of Image J (National Institute of Health, Bethesda, USA), a commonly used technique [12]. Any field containing large scar area was excluded so that quantification reflected interstitial fibrosis only. Three independent researchers performed the measurements. The percentage of fibrosis was expressed as the average ratio of the total fibrotic area divided by the total myocardial area of the whole slide. Comparison between groups was performed within the same staining procedure.

Biomarkers

Plasma levels

Gal-3, CTGF, OPN and TGFβ-1 were analyzed in EDTA plasma by ELISA according the description of the manufacturer: Gal-3, BG Medicine Inc., Waltham, USA; CTGF, FibroGen Inc., San Francisco, USA; OPN, Assay Design Inc., Ann Arbor, USA; TGFβ-1, eBioscience, San Diego, USA. BNP was analyzed on a DxI 800 immunochemistry system (Beckman Coulter, Brea, California).

mRNA

mRNA expression of all biomarkers was determined by Q-PCR on the LightCycler 480 (Roche Diagnostics BV, Almere, the Netherlands) as described previously [13]. Total RNA was isolated out of 20 slides of 10 μm frozen myocardial tissue using miRNeasy Mini Kit (Qiagen, Inc., Austin, USA). Copy DNA (cDNA) was synthesized with the use of superscript III, oligo-dT and random primers (Invitrogen, Oslo, Norway).

Immunohistochemistry (IHC) of Gal-3, OPN and CTGF

Formalin fixed, paraffin-embedded myocardial tissue samples were cut at 5-μm thickness.

Endogenous peroxidase was blocked with H_2O_2 for 30 min. Sections were pre-treated with either citrate (Gal-3 and CTGF) or pepsin (OPN) and incubated with primary antibody diluted in PBS/1% BSA for 1 hr. For CTGF, slides were incubated with primary antibody in PBS/3% BSA overnight (4°C), followed by a washing step in PBS/Tween-20. PowerVision poly-anti-rabbit IgG (Immunovision Technologies, Duiven, the Netherlands), PowerVision poly-anti-mouse IgG (Immunovision Technologies) and RagPo polyclonal rabbit-anti-goat IgG (Dako, Heverlee, Belgium) were used as secondary antibodies for OPN, Gal-3 and CTGF, respectively. The slides were developed with DAB solution for 10 min. For CTGF, three step IHC was carried out. As a tertiary antibody, 150 µL of peroxidase labeled anti-rabbit BrightVision IgG (ImmunoLogic, Duiven, the Netherlands) was used for 30 min. After a 5 min washing step of PBS, the slides were developed with 200 µL NovaRed solution for 10 min. The nuclei were counterstained with Mayer's Haematoxylin.

Statistical analysis

Categorical data are presented by number (%) and continuous data by median (interquartile range IQR, i.e. 25th - 75th percentile) or by mean ± standard error, where appropriate. Mann-Whitney U-tests and Fisher's exact tests were performed to compare differences between BTT and BTR patients, and between patients and healthy controls. The pre- and post-LVAD differences were evaluated with the Wilcoxon signed-rank test. The inter-observer variability is indicated by the interclass correlation coefficient. Plasma data were evaluated using a random intercept model that adjusts for within-subject correlation between repeated measurements. A p-value of<0.05 was considered as statistically significant. All analyses were performed using SPSS, version 18 (SPSS Inc., Chicago, Illinois).

Results

Clinical setting

Demographics

Patient demographics are shown in *Table 1*. All patients presented initially with NYHA IV functional class despite optimal medical therapy, including intravenous inotropic therapy (*Table 2*). Mean duration of mechanical support (BTT 279 days, BTR 343 days) was not significantly different between groups. None of the BTR patients were supported with a biventricular pacemaker or ICD prior to LVAD implantation, whereas in the group of BTT patients this percentage was 64 % (p<0.01). In the BTR group, patients had a shorter HF

duration, more often diagnosed with peripartum cardiomyopathy and had a higher heart rate before implantation compared to BTT patients.

Prior to LVAD implantation, only 9 (36%) and 15 (60%) patients received beta-blockade and ACE-inhibition, respectively (*Table 2*). Beta-blockers and ACE-inhibitors often had to be stopped because of deterioration of hemodynamics and after initiation of inotropic therapy. After LVAD implantation, ~50% of the patients were treated with ACE-inhibition and the majority of the patients (~70%) received aldosterone antagonists (*Table 2*).

Table 1: Baseline characteristics of patients with end-stage dilated cardiomyopathy (DCM) prior to continuous flow LVAD support (cf-LVAD) as a Bridge to Transplantation (BTT) and Bridge to Recovery (BTR)

Characteristic[a]	BTT (n=25)	BTR (n=5)	p-value
Age, years	46 (31-54)	37 (28-53)	0.44
Male	18 (72%)	2 (40%)	0.30
Duration of HF, days	1754 (416-2301)	42 (16-101)	0.01
Body Mass Index, kg/m2	23.0 (20.3-26.2)	24.0 (22.8-31.0)	0.56
NYHA[b] classification IV	25 (100%)	5 (100%)	1.00
bvPM/ICD[c]	16 (64%)	0 (0%)	0.01
Non-ischemic DCM	25 (100%)	4 (80%)	0.17
Etiology of non-ischemic DCM			
Idiopathic	9 (36%)	1 (20%)	1.00
Familial[d]	11 (44%)	0 (0%)	0.27
Myocarditis	3 (12%)	1 (20%)	0.47
Peripartum	0 (0%)	2 (40%)	0.02
Toxic (drugs/medication)	2 (8%)	0 (0%)	1.00
cf-LVAD support	25 (100%)	3 (60%)	0.02
Days of LVAD support[e]	279 (193-505)	343 (120-363)	0.90

[a] Categorical data are presented as number (%) and continuous data as median (25% - 75% percentile).

[b] NYHA; New York Heart Association.

[c] bvPM/ICD; biventricular pacemaker/implantable cardioverter defibrillator.

[d] Familial DCM is defined if the patient has one or more family members who are diagnosed with idiopathic DCM and/or has a first-degree relative with an unexplained sudden death under the age of 35 years.

[e] Days of LVAD support are based on the patients who already underwent heart transplantation.

[f] Mann-Whitney U- and Fisher's exact tests were used to check for differences in continuous and categorical variables.

Table 2: Medication use before and during continuous flow LVAD (cf-LVAD) support as Bridge to Transplantation (BTT)

	pre-LVAD (n=25)	1 month (n=25)	3 month (n=25)	6 months (n=23)
Inotropic	22 (88%)	–	–	–
Amiodarone	12 (48%)	17 (68%)	17 (68%)	16 (70%)
ACE[1]-inhibitor/ARB[2]	15 (60%)	13 (52%)	14 (56%)	10 (43%)
Beta-blocker	9 (36%)	1 (4%)	3 (12%)	3 (13%)
Digoxin	5 (2%)	2 (8%)	1 (4%)	1 (4%)
Diuretic	23 (92%)	15 (60%)	11 (44%)	10 (43%)
Aldosterone antagonist	21 (84%)	17 (68%)	18 (72%)	15 (65%)

[1] ACE; Angiotensin Converting Enzyme

[2] Angiotensin Receptor Blockers
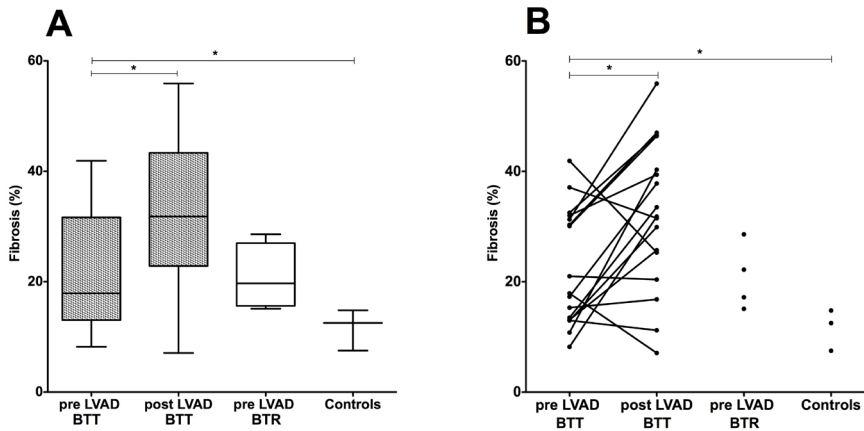
Figure 1: Changes in endomyocardial fibrosis before and after LVAD support as Bridge to Transplantation (BTT) and Bridge to Recovery (BTR)

Total fibrosis presented as whiskers with minimum and maximum (*A*) and individual fibrosis (*B*) in pre-LVAD BTT, post-LVAD BTT, pre-LVAD BTR and in controls.

Prior to LVAD implantation, interstitial fibrosis was significantly higher ($p < 0.05$) than in healthy controls and increased significantly ($p < 0.05$) during LVAD support. There was some individual variation (*B*). In the majority of BTT patients (n=11), interstitial fibrosis increased during LVAD support, in 3 patients it remained stable and in 3 patients the amount of fibrosis decreased. BTT (n=17), BTR (n=4), controls (n=3). The asterisk represents $p < 0.05$.

Morphology

Change in fibrosis during cf-LVAD support

Biopsies from patients with end-stage HF prior to cf-LVAD implantation showed 18% fibrosis (± IQR 13-32), whereas healthy controls demonstrated 13% (± IQR 8-15; p<0.05). After cf-LVAD support, fibrosis increased from 18% to 32% (± IQR 23-43; p<0.05), with some individual variation (*Figure 1A-B*). The inter-observer variability was 0.937, indicating a high inter-observer reliability. In *Figure 2*, representative examples of the myocardium of pre cf-LVAD (*A*), post cf-LVAD (*B*) and healthy controls (*C*) are shown with arrowheads pointing to interstitial fibrosis. *Figure 3* represents the change in fibrosis in relation to the length of support, suggesting that the change is not related to cf-LVAD duration.
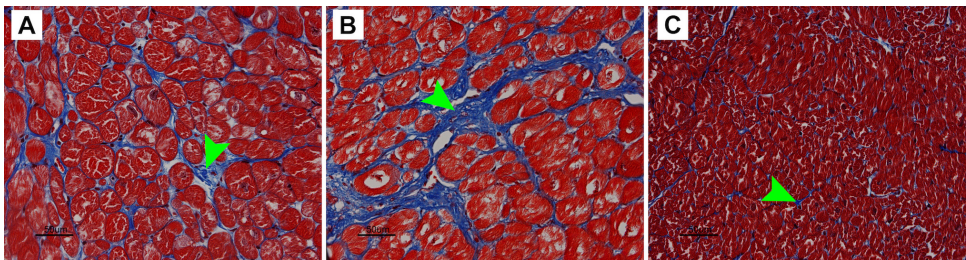
Figure 2: Representative examples of myocardial fibrosis.
Pre continuous flow LVAD (cf-LVAD) support (*A*), post cf-LVAD (*B*) and healthy controls (*C*). The images clearly show the increase in fibrosis (green arrowheads) between pre- and post-LVAD myocardium and the unchanged cross-sectional area of the cardiomyocytes. Note the significant smaller cross-sectional area in control. Scale bar = 50 μm.
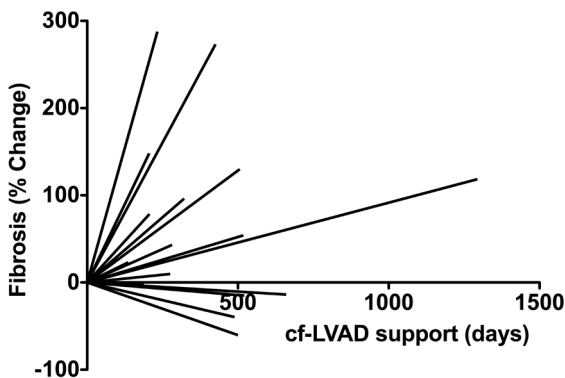
Figure 3: The percentage change in fibrosis during continuous flow LVAD (cf-LVAD) support.
The change of fibrosis is independent of cf-LVAD duration (days; n=17). The amount of fibrosis pre-LVAD is set at 0. The asterisk (*) represents p<0.05.

Change in cardiomyocyte size during cf-LVAD support.

The cross-sectional area of the cardiomyocytes prior to cf-LVAD in the BTT group was 649 μm2 ± 71 (mean ± SEM) and decreased slightly to 588 μm2 ± 71 (p=0.33). In the BTR group, cross-sectional area was a bit smaller than in BTT patients (581 μm2 ± 95; p=0.87). In controls, the cross-sectional area was significantly smaller (242 μm2 ± 59; p<0.01; *Figure 4A*).

The length of the cardiomyocytes before cf-LVAD implantation in the BTT group was 74 μm ± 3.5, significantly longer than controls (53 μm ± 5.9; p<0.05; *Figure 4B*). After cf-LVAD support, cardiomyocyte length increased significantly (p<0.05) to 82 μm ± 2.7. There was no relation between the length of cardiomyocytes and the duration of cf-LVAD support (data not shown).
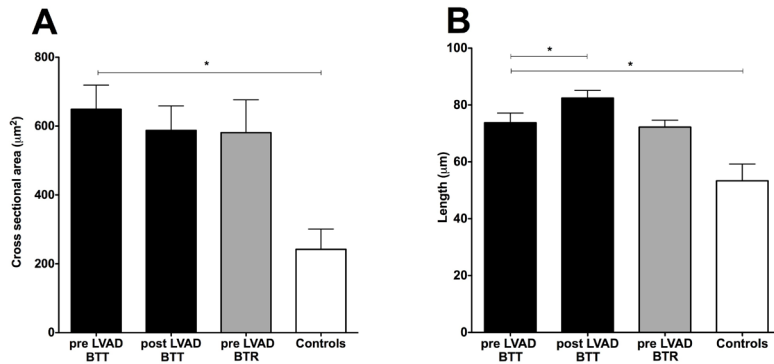
Figure 4: Changes in cardiomyocyte size during LVAD support.
Cross sectional area *(A)* did not change whereas cardiomyocytes significantly elongated *(B)* during LVAD support in Bridge to Transplantation (BTT) patients (n=14). Cardiomyocytes of Bridge to Recovery (BTR) patients (n=4) showed similar sizes as BTT prior implantation and control cardiomyocytes (n=3) were significantly smaller. Data are presented as mean ± standard error. The asterisk (*) represents p<0.05.

Biomarkers

B-type Natriuretic peptide

Plasma (*Figure 5A*): BNP was severely elevated in patients with end-stage HF before cf-LVAD (1925 pg/ml ± 163; mean ± SEM), but decreased rapidly after implantation to almost normal levels (p<0.001) and remained stable thereafter. BNP levels in BTR patients did not differ from BTT patients (overall trend between groups p=0.93).

mRNA (*Figure 6B*): mRNA of BNP in myocardial tissue decreased significantly during cf-LVAD support, but remained higher compared to controls (relative quantity; pre 1.7 ± 0.5; post 0.5 ± 0.14; mean ± SEM; p=0.01).

Galectin-3

Plasma (*Figure 5B*): Patients before cf-LVAD support demonstrated substantially elevated Gal-3 levels (35.5 ± 3.7 ng/ml) in comparison to controls (p<0.001), that temporarily decreased after implantation (21.2 ± 3.7 ng/ml; p<0.001), but rose again prior to HTx (32.1 ± 3.9 ng/ml; p<0.05 versus 6 months of cf-LVAD support). Although Gal-3 levels seemed lower in BTR patients, this difference was not statistically significant (overall trend between groups p=0.43).

mRNA (*Figure 6B*): mRNA levels were significantly elevated prior to and after LVAD implantation compared to controls (relative quantity; pre 1.2 ± 0.18; post 1.2 ± 0.16).

IHC (*Figure 7A-B*): Gal-3 stained weak to moderate in the cardiomyocytes and did not change during mechanical support. Capillaries and stromal cells stained stronger pre-LVAD compared to post-LVAD (arrowheads). Inflammatory cells, when present, stained even more intense.

Connective Tissue Growth Factor

Plasma (*Figure 5C*): In HF patients, the CTGF concentration was significantly higher (23.6 ± 2.7 ng/ml) compared to controls (13.1 ± 1.1 ng/ml; p=0.02) and remained stable during cf-LVAD support. There was no difference in CTGF in the BTR patients compared to the BTT group (overall trend between groups p=0.18).

mRNA (*Figure 6C*): mRNA levels in cardiac tissue were elevated in comparison to controls, but, like the plasma levels, did not change significantly during mechanical support.

IHC (*Figure 7C-D*): CTGF staining of cardiomyocytes decreased during cf-LVAD support. The majority of stromal cells were negative (arrowheads).

Osteopontin

Plasma (*Figure 5D*): In HF patients, the OPN concentration prior to cf-LVAD implantation was severely elevated (99.5 ± 11.8 ng/ml) compared to controls (26.7 ± 3.7). Directly after implantation, OPN increased even further, but tended to decrease and at the time of HTx it was back on its pre-implantation level. There was no significant difference between BTR and BTT patients (overall trend between groups p=0.52).

mRNA (*Figure 6D*): The mRNA of OPN in cardiac tissue pre-LVAD decreased significantly (relative quantity; pre 0.14 ± 0.07, post 0.02 ± 0.004; p<0.01) and reached control level.

IHC (*Figure 7E-F*): OPN showed a moderate staining in the cardiomyocytes pre- and post-LVAD. Endothelial tissue and stromal cells were negative for OPN (arrowheads). In post-LVAD, the extracellular matrix stained strongly.

Transforming Growth Factor β-1

Plasma: TGFβ-1 levels in HF patients were lower than in controls and a large inter-individual variation was seen. Plasma levels of TGFβ-1 did not alter during mechanical support (data not shown). Circulating TGFβ-1 was not analyzed in the BTR patients.

mRNA (*Figure 6E*): During LVAD support, there was a significant increase in TGFβ-1 mRNA (relative quantity; pre: 0.10 ± 0.008, post: 0.19 ± 0.03; p<0.001).
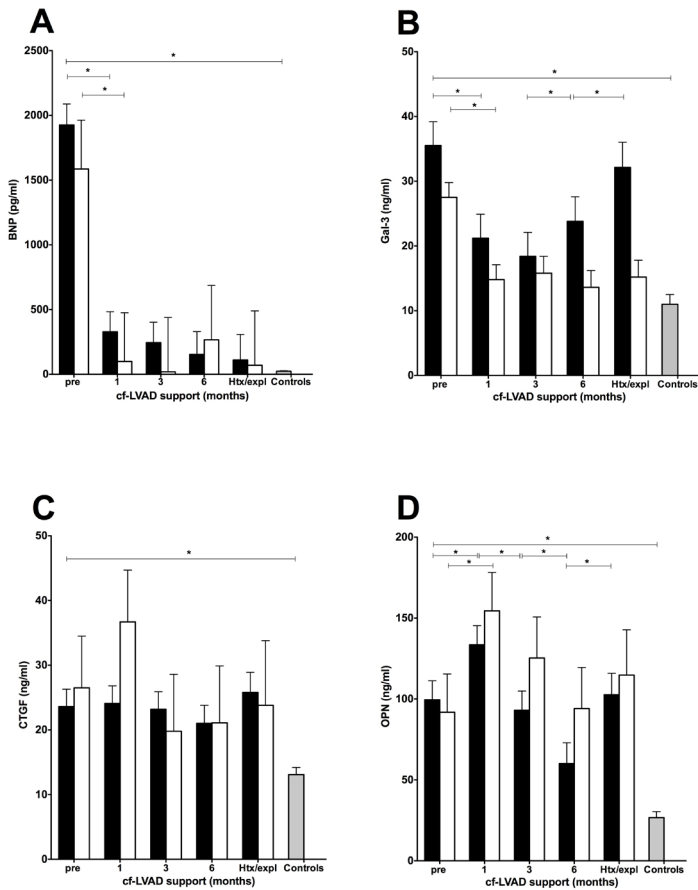
Figure 5: Circulating biomarkers during continuous flow LVAD (cf-LVAD) support
Brain Natriuretic Peptide (BNP, *A*); Galectin-3 (Gal-3, *B*); Connective Tissue Growth Factor (CTGF, *C*) and Osteopontin (OPN, *D*) before, 1, 3 and 6 months after LVAD implantation and prior heart transplantation (HTx) or explantation. The white bars indicate the group of Bridge to Recovery (BTR) patients (n=5) and the black bars the group of Bridge to Transplantation (BTT) patients (n=25). Data is presented as mean ± standard error. The asterisk (*) represents p<0.05.
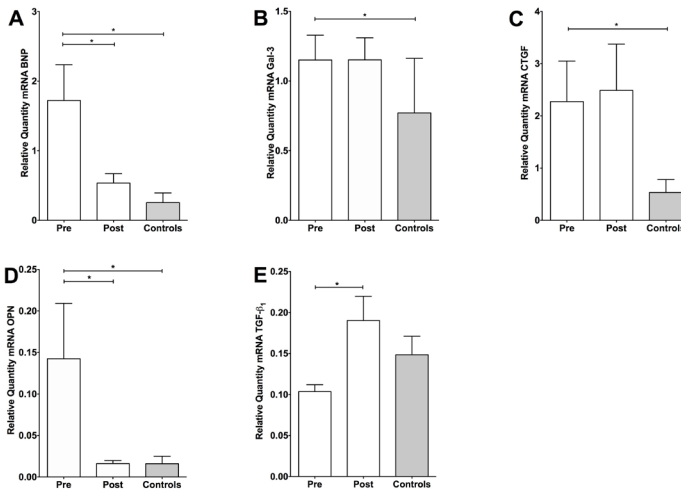
Figure 6: Cardiac mRNA of biomarkers before and after continuous flow LVAD (cf-LVAD) implantation

Expression of Brain Natriuretic Peptide (BNP, *A*); Galectin-3 (Gal-3, *B*); Connective Tissue Growth Factor (CTGF, *C)* and Osteopontin (OPN, *D*) Transforming Growth Factor beta-1 (TGFβ-1, *E)* before and after cf-LVAD implantation in Bridge to Transplantation (BTT) patients (n=15). BNP and OPN mRNA decreased, Gal-3 and CTGF mRNA remained stable and only TGFβ-1 mRNA increased after cf-LVAD support. Except for TGFβ-1 mRNA, all levels were high in heart failure patients compared to controls. Data is presented as mean ± standard error. The asterisk (*) represents p<0.05.
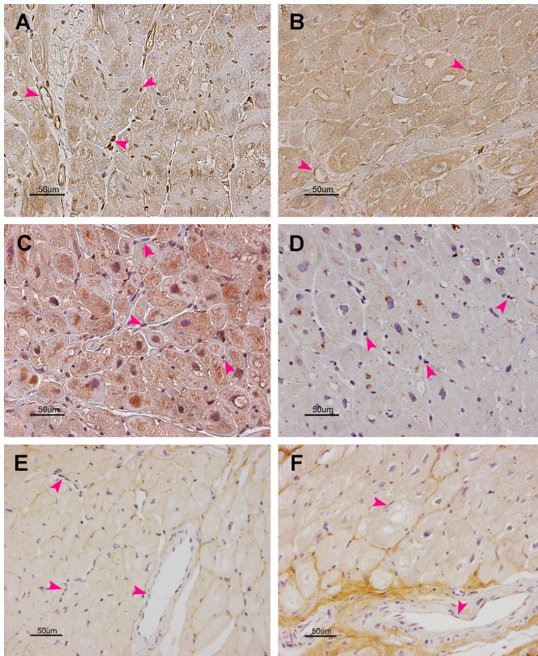
Figure 7: Immunohistochemical staining of fibrotic markers in the myocardium pre- and post-continuous flow LVAD (cf-LVAD) support

Galectin-3 (Gal-3, pre, *A*; post, *B*) expression in the cardiomyocytes did not change during mechanical support. The staining of capillaries and stromal cells stained more intense pre-LVAD compared to post-LVAD (pink arrowheads). Connective Tissue Growth Factor staining (CTGF, pre, *C*; post, *D*) of cardiomyocytes decreased post-LVAD and the majority of stromal cells were negative (pink arrowheads). Osteopontin (OPN, pre, *E*; post, *F*) showed a moderate staining in the cardiomyocytes pre- and post-LVAD. Endothelial tissue and stromal cells were negative for OPN (pink arrowheads). In post-LVAD, the extracellular matrix stained strongly. Staining was performed on 15 pre- and post cf-LVAD tissue samples. Scale bar = 50 μm.

Discussion

This study presents a comprehensive analysis of myocardial fibrosis and plasma levels and cardiac mRNA of several fibrotic markers in patients with end-stage HF during cf-LVAD support. The principle findings are that cf-LVAD support is associated with an overall increase in myocardial fibrosis and lengthening of cardiomyocytes, accompanied by increased plasma levels of pro-fibrotic markers. No difference in expression of fibrotic markers could be detected between recovered and non-recovered patients, although only few patients could be weaned from the device. Our data could not answer whether the increase in fibrosis is a direct effect of reduced pulsatility during cf-LVAD support or due to HF progression and warrants further investigation.

Cardiomyocyte size and fibrosis

As has been reported previously, pf-LVAD support results in partial reverse remodeling of the heart, characterized by a substantial decrease in cardiomyocyte diameter and length [12,14,15]. However, in our study with cf-LVAD patients, the diameter of the cardiomyocytes did not change and the length increased. This difference in response of cardiomyocyte size between devices might be consistent with less ventricular unloading during cf-LVAD support [16,17], although the almost complete normalization of BNP in our study does not seem to support that. It might be that cardiomyocyte size in cf-LVAD patients is influenced by the physiological consequences of long-term continuous flow on the peripheral vasculature [9].

In the present study, BTR patients demonstrated less hypertrophy and fibrosis prior implantation compared to the BTT group, although not significantly. This is consistent with literature, showing that the severity of cardiac fibrosis and cardiomyocyte size at time of LVAD implantation predicts the degree of improvement in cardiac function and recovery during mechanical support [10,18]. With regard to the change in myocardial fibrosis during mechanical support, discrepant results are reported in literature [12,16,19]. We previously demonstrated a biphasic reaction of the fibrotic response after pf-LVAD implantation [20], which was not observed in the present study with cf-LVAD patients. The response of collagen concentration during LVAD support remains controversial. Some studies have found a reduction in collagen during LVAD support [16,19,21], whereas most studies showed an increase [12,18,22-28], which is in agreement with the present study. Differences in techniques or concomitant medication could account for some of these discrepancies in total collagen measurement. In our study, a large microscopic field was examined, scar tissue was excluded and three independent investigators performed the measurements with a strong

inter-observer correlation coefficient, thereby minimizing the effects of the heterogeneous nature of fibrosis.

Clinical data have shown that treatment with angiotensin converting enzyme (ACE) inhibitors and aldosterone antagonists reduce myocardial collagen turnover in patients with HF [29]. The individual variation, which we noted in the alterations of fibrosis, appeared not to be due to the use of pharmacologic therapy and/or to the time of cf-LVAD support. The use of ACE-inhibitors and aldosterone antagonists are in essence not changed before and after LVAD therapy. Before LVAD therapy, 88% of the patients were treated with intravenous inotropic therapy. After LVAD this treatment was stopped in all. Six months after LVAD-implantation, 13% of our patients received beta-blockers. It seems unlikely that the overall increase in myocardial fibrosis is caused by the low incidence of beta-blockade in combination with persistent activity of the sympathetic system in our cohort. The LVAD implantation resulted in a complete reversal of HF as assessed by the clinical improvement and the sustained normalization of BNP accompanied by decreased sympathetic activity.

Biomarkers

Plasma biomarkers to predict myocardial recovery during mechanical support are needed in order to assess the feasibility and ideal timing for LVAD explantation [30]. As fibrosis is thought to play an important role in successful recovery, levels of circulating fibrotic biomarkers (BNP, Gal-3, CTGF, OPN and TGFβ-1) were evaluated. Moreover, cardiac mRNA of all biomarkers was analyzed by Q-PCR and protein expression by IHC.

BNP, a well known HF marker, is related to wall stress of the left ventricle and also has a direct effect on cardiac fibroblasts to inhibit fibrotic responses [31]. Plasma and mRNA of BNP decrease during mechanical support [16,32-35], as was confirmed in our study. This decrease confirms the impressive effects of LVAD support on the decompensated state. In this regard, BNP seems not suitable as a load-independent predictive marker of myocardial function in patients on cf-LVAD support.

Gal-3 promotes cardiac fibroblast proliferation and collagen deposition [36] and high levels are associated with an increased risk for new-onset HF in apparently healthy subjects [37]. Moreover, Gal-3 can predict long-term mortality in acute and chronic HF [38,39]. In a study by Milting *et al*, Gal-3 plasma levels were significantly increased in HF patients and appeared to be a biomarker predictive of survival during LVAD support [33]. In a more recent study of the same research group, it was shown that plasma Gal-3 concentration was an univariate, but not an independent risk factor for death on device after LVAD implantation [40]. In our study, and in agreement with literature, circulating Gal-3 was significantly elevated in advanced

HF patients compared to healthy individuals. During cf-LVAD support, a temporarily decline of Gal-3 levels was noted, followed by an increase to pre-LVAD levels after longer periods of support, accompanied by an increase in myocardial fibrosis.

CTGF, a downstream modulator of the TGFβ pathway, promotes fibroblast proliferation and modulates the activity of growth factors in the extracellular matrix, thereby promoting myocardial fibrosis [41]. Plasma levels of CTGF were upregulated in patients with chronic HF [41,42], which was confirmed in our study. During cf-LVAD support, circulating levels of CTGF as well as myocardial mRNA remained stable. Nevertheless, the expression of CTGF by IHC showed a diminished expression in cardiomyocytes post-LVAD compared to pre-LVAD.

OPN is required for the differentiation and activation of myofibroblasts in response to TGFβ-1 [43]. In this study, directly after implantation OPN increased, later on tended to decrease, but at the time of HTx it was back on its pre-implantation level. The initial increase might be explained by the surgical procedure of cf-LVAD implantation, whereas the final increase might be related to the pro-fibrotic response during mechanical support. The decrease in mRNA and stable protein expression of OPN in this study was consistent with our previous work, where we examined OPN levels in pf-LVAD supported patients [44]. Lack of parallel changes in mRNA and plasma levels of OPN might be explained by post-transcriptional regulators within the myocardium.

TGFβ-1 is a pro-fibrotic cytokine that stimulates the production of extracellular matrix proteins in the heart [45]. TGFβ-1 mRNA increased significantly during cf-LVAD support whereas circulating TGFβ-1 remained stable, but was lower in comparison to controls. This may indicate that the increase in myocardial TGFβ-1 stimulates fibrosis, but the myocardial levels are not reflected in the circulation. The increase in mRNA expression of TGFβ-1 is in contrast to a previous study by Felkin *et al*, that did not detect changes during mechanical support [45]. Since TGFβ-1 showed variation between individuals and circulating levels did not alter, circulating TGFβ-1 does not seem to be a suitable marker for reverse remodeling during cf-LVAD support.

From this study it seems plausible that the increase in myocardial fibrosis after cf-LVAD implantation might be the result of the increase in Gal-3, the persisting high levels of CTGF and the increase in myocardial levels of TGFβ-1. The recurrence of high levels of OPN at the end of cf-LVAD support might be additive.

Conclusion

In contrast to pf-LVAD studies, we demonstrate lengthening of cardiomyocytes and an increase in fibrosis during cf-LVAD support, together with the persistence of several pro-fibrotic circulating markers. At this moment, it is not clear whether this pro-fibrotic response is caused by the lesser degree of ventricular unloading by the cf-LVAD, the potential pathophysiological alterations induced by chronic less pulsatile support or due to HF itself. In our study, the complete normalization of BNP levels suggests that lesser unloading by cf-LVADs does not seem to be an explanation. Whatever the cause, it may have substantial impact on the chance of successful recovery in these patients.

Limitations

We acknowledge a number of limitations to this study. Of the total number of patients with LVAD as BTT (n=25), a minority (n=3) had a relatively short history of HF duration (between 50-100 days). Excluding these three patients, however, did not influence the outcome. Also, since the duration of LVAD support is variable until HTx, we corrected for this time difference for circulating biomarkers by linear mixed model with time as continuous variable and similar results were found. Due to ethical reasons, myocardial tissue of a control group consisting of end-stage HF patients without LVAD support is unavailable. Hence, it is not possible to determine whether the increase in fibrosis is a manifestation of further progression of cardiac remodeling or a direct result of lesser degree of ventricular unloading during cf-LVAD support. In addition, the small number of BTR patients constitutes a major limitation. Moreover, 2 of these patients were supported with a pf-LVAD, whereas the rest of our patients received a cf-LVAD as bridge to HTx. Consequently, it is difficult to draw significant conclusions between BTT and the BTR groups. Finally, histological analysis is restricted to the left ventricle only, due to the location of the inflow cannula.

References

1. Lahpor J, Khaghani A, Hetzer R, Pavie A, Friedrich I, Sander K, et al. European results with a continuous-flow ventricular assist device for advanced heart-failure patients. Eur J Cardiothorac Surg. 2010 Feb;37(2):357–61.

2. Slaughter MS, Rogers JG, Milano CA, Russell SD, Conte JV, Feldman D, et al. Advanced heart failure treated with continuous-flow left ventricular assist device. N. Engl. J. Med. 2009 Dec 3;361(23):2241–51.

3. Miller LW, Pagani FD, Russell SD, John R, Boyle AJ, Aaronson KD, et al. Use of a continuous-flow device in patients awaiting heart transplantation. N. Engl. J. Med. 2007 Aug 30;357(9):885–96.

4. Wohlschlaeger J, Schmitz KJ, Schmid C, Schmid KW, Keul P, Takeda A, et al. Reverse remodeling following insertion of left ventricular assist devices (LVAD): a review of the morphological and molecular changes. Cardiovasc. Res. 2005 Dec 1;68(3):376–86.

5. Soppa GKR, Barton PJR, Terracciano CMN, Yacoub MH. Left ventricular assist device-induced molecular changes in the failing myocardium. Curr Opin Cardiol. 2008 May;23(3):206–18.

6. Ambardekar AV, Buttrick PM. Reverse remodeling with left ventricular assist devices: a review of clinical, cellular, and molecular effects. Circ Heart Fail. 2011 Mar;4(2):224–33.

7. Birks EJ, George RS. Molecular changes occurring during reverse remodelling following left ventricular assist device support. J Cardiovasc Transl Res. 2010 Dec;3(6):635–42.

8. Drakos SG, Terrovitis JV, Anastasiou-Nana MI, Nanas JN. Reverse remodeling during long-term mechanical unloading of the left ventricle. J Mol Cell Cardiol. 2007 Sep;43(3):231–42.

9. Margulies KB, Rame JE. Adaptations to pulsatile versus nonpulsatile ventricular assist device support. Circ Heart Fail. 2011 Sep;4(5):535–7.

10. Saito S, Matsumiya G, Sakaguchi T, Miyagawa S, Yamauchi T, Kuratani T, et al. Cardiac fibrosis and cellular hypertrophy decrease the degree of reverse remodeling and improvement in cardiac function during left ventricular assist. J Heart Lung Transplant. 2010 Jun;29(6):672–9.

11. Ruifrok AC, Johnston DA. Quantification of histochemical staining by color deconvolution. Anal. Quant. Cytol. Histol. 2001 Aug;23(4):291–9.

12. Drakos SG, Kfoury AG, Hammond EH, Reid BB, Revelo MP, Rasmusson BY, et al. Impact of mechanical unloading on microvasculature and associated central remodeling features of the failing human heart. J. Am. Coll. Cardiol. 2010 Jul 27;56(5):382–91.

13. Lok SI, Winkens B, Goldschmeding R, van Geffen AJP, Nous FMA, van Kuik J, et al. Circulating Growth Differentiation Factor-15 correlates with myocardial fibrosis in patients with non-ischemic dilated cardiomyopathy and decreases rapidly after left ventricular assist device support. Eur. J. Heart Fail. 2012 Nov;14(11):1249–56.

14. de Jonge N, van Wichen DF, Schipper MEI, Lahpor JR, Gmelig-Meyling FHJ, Robles de Medina EO, et al. Left ventricular assist device in end-stage heart failure: persistence of structural myocyte damage after unloading. An immunohistochemical analysis of the contractile myofilaments. J. Am. Coll. Cardiol. 2002 Mar 20;39(6):963–9.

3

15. Maybaum S, Mancini D, Xydas S, Starling RC, Aaronson K, Pagani FD, et al. Cardiac improvement during mechanical circulatory support: a prospective multicenter study of the LVAD Working Group. Circulation. 2007 May pp. 2497–505.

16. Kato TS, Chokshi A, Singh P, Khawaja T, Cheema F, Akashi H, et al. Effects of continuous-flow versus pulsatile-flow left ventricular assist devices on myocardial unloading and remodeling. Circ Heart Fail. 2011 Sep 1;4(5):546–53.

17. Klotz S, Deng MC, Stypmann J, Roetker J, Wilhelm MJ, Hammel D, et al. Left ventricular pressure and volume unloading during pulsatile versus nonpulsatile left ventricular assist device support. Ann. Thorac. Surg. 2004 Jan;77(1):143–9; discussion149–50.

18. Matsumiya G, Monta O, Fukushima N, Sawa Y, Funatsu T, Toda K, et al. Who would be a candidate for bridge to recovery during prolonged mechanical left ventricular support in idiopathic dilated cardiomyopathy? J. Thorac. Cardiovasc. Surg. 2005 Sep;130(3):699–704.

19. Thohan V, Stetson SJ, Nagueh SF, Rivas-Gotz C, Koerner MM, Lafuente JA, et al. Cellular and hemodynamics responses of failing myocardium to continuous flow mechanical circulatory support using the DeBakey-Noon left ventricular assist device: a comparative analysis with pulsatile-type devices. J Heart Lung Transplant. 2005 May;24(5):566–75.

20. Bruggink AH, van Oosterhout MFM, de Jonge N, Ivangh B, van Kuik J, Voorbij RHAM, et al. Reverse remodeling of the myocardial extracellular matrix after prolonged left ventricular assist device support follows a biphasic pattern. J Heart Lung Transplant. 2006 Sep;25(9):1091–8.

21. Bruckner BA, Stetson SJ, Perez-Verdia A, Youker KA, Radovancevic B, Connelly JH, et al. Regression of fibrosis and hypertrophy in failing myocardium following mechanical circulatory support. J Heart Lung Transplant. 2001 Apr;20(4):457–64.

22. Klotz S, Foronjy RF, Dickstein ML, Gu A, Garrelds IM, Danser AHJ, et al. Mechanical unloading during left ventricular assist device support increases left ventricular collagen cross-linking and myocardial stiffness. Circulation. 2005 Jul 19;112(3):364–74.

23. Barbone A, Holmes JW, Heerdt PM, The AH, Naka Y, Joshi N, et al. Comparison of right and left ventricular responses to left ventricular assist device support in patients with severe heart failure: a primary role of mechanical unloading underlying reverse remodeling. Circulation. 2001 Aug 7;104(6):670–5.

24. Madigan JD, Barbone A, Choudhri AF, Morales DL, Cai B, Oz MC, et al. Time course of reverse remodeling of the left ventricle during support with a left ventricular assist device. J. Thorac. Cardiovasc. Surg. 2001 May;121(5):902–8.

25. McCarthy PM, Nakatani S, Vargo R, Kottke-Marchant K, Harasaki H, James KB, et al. Structural and left ventricular histologic changes after implantable LVAD insertion. Ann. Thorac. Surg. 1995 Mar;59(3):609–13.

26. Nakatani S, McCarthy PM, Kottke-Marchant K, Harasaki H, James KB, Savage RM, et al. Left ventricular echocardiographic and histologic changes: impact of chronic unloading by an implantable ventricular assist device. J. Am. Coll. Cardiol. 1996 Mar 15;27(4):894–901.

27.   McGowan BS, Scott CB, Mu A, McCormick RJ, Thomas DP, Margulies KB. Unloading-induced remodeling in the normal and hypertrophic left ventricle. Am. J. Physiol. Heart Circ. Physiol. 2003 Jun;284(6):H2061–8.

28.   Klotz S, Danser AHJ, Foronjy RF, Oz MC, Wang J, Mancini D, et al. The impact of angiotensin-converting enzyme inhibitor therapy on the extracellular collagen matrix during left ventricular assist device support in patients with end-stage heart failure. J. Am. Coll. Cardiol. 2007 Mar 20;49(11):1166–74.

29.   MacFadyen RJ, Barr CS, Struthers AD. Aldosterone blockade reduces vascular collagen turnover, improves heart rate variability and reduces early morning rise in heart rate in heart failure patients. Cardiovasc. Res. 1997 Jul;35(1):30–4.

30.   Kramer F, Milting H. Novel biomarkers in human terminal heart failure and under mechanical circulatory support. Biomarkers. 2011 Jul;16 Suppl 1:S31–41.

31.   Huntley BK, Ichiki T, Sangaralingham SJ, Chen HH, Burnett JC. B-type natriuretic peptide and extracellular matrix protein interactions in human cardiac fibroblasts. J. Cell. Physiol. 2010 Oct;225(1):251–5.

32.   Kemperman H, den Berg van M, Kirkels H, de Jonge N. B-type natriuretic peptide (BNP) and N-terminal proBNP in patients with end-stage heart failure supported by a left ventricular assist device. Clin. Chem. 2004 Sep;50(9):1670–2.

33.   Milting H, Ellinghaus P, Seewald M, Cakar H, Bohms B, Kassner A, et al. Plasma biomarkers of myocardial fibrosis and remodeling in terminal heart failure patients supported by mechanical circulatory support devices. J Heart Lung Transplant. 2008 Jun;27(6):589–96.

34.   Sareyyupoglu B, Boilson BA, Durham LA, McGregor CGA, Daly RC, Redfield MM, et al. B-type natriuretic peptide levels and continuous-flow left ventricular assist devices. ASAIO J. 2010 Oct;56(6):527–31.

35.   Bruggink AH, de Jonge N, van Oosterhout MFM, van Wichen DF, de Koning E, Lahpor JR, et al. Brain natriuretic peptide is produced both by cardiomyocytes and cells infiltrating the heart in patients with severe heart failure supported by a left ventricular assist device. J Heart Lung Transplant. 2006 Feb;25(2):174–80.

36.   Sharma UC, Pokharel S, van Brakel TJ, van Berlo JH, Cleutjens JPM, Schroen B, et al. Galectin-3 marks activated macrophages in failure-prone hypertrophied hearts and contributes to cardiac dysfunction. Circulation. 2004 Nov 9;110(19):3121–8.

37.   Ho JE, Liu C, Lyass A, Courchesne P, Pencina MJ, Vasan RS, et al. Galectin-3, a marker of cardiac fibrosis, predicts incident heart failure in the community. J. Am. Coll. Cardiol. 2012 Oct 2;60(14):1249–56.

38.   Lok DJA, van der Meer P, la Porte de PWB-A, Lipsic E, Van Wijngaarden J, Hillege HL, et al. Prognostic value of galectin-3, a novel marker of fibrosis, in patients with chronic heart failure: data from the DEAL-HF study. Clin Res Cardiol. 2010 May;99(5):323–8.

39.   Shah RV, Chen-Tournoux AA, Picard MH, van Kimmenade RRJ, Januzzi JL. Galectin-3, cardiac structure and function, and long-term mortality in patients with acutely decompensated heart failure. Eur. J. Heart Fail. 2010 Aug;12(8):826–32.

3

40. Erkilet G, Özpeker C, Böthig D, Kramer F, Röfe D, Bohms B, et al. The biomarker plasma galectin-3 in advanced heart failure and survival with mechanical circulatory support devices. J Heart Lung Transplant. 2013 Feb;32(2):221–30.

41. Daniels A, van Bilsen M, Goldschmeding R, van der Vusse GJ, van Nieuwenhoven FA. Connective Tissue Growth Factor and cardiac fibrosis. Acta Physiol (Oxf). 2009 Mar;195(3):321–38.

42. Koitabashi N, Arai M, Niwano K, Watanabe A, Endoh M, Suguta M, et al. Plasma connective Tissue Growth Factor is a novel potential biomarker of cardiac dysfunction in patients with chronic heart failure. Eur. J. Heart Fail. 2008 Apr;10(4):373–9.

43. Lenga Y, Koh A, Perera AS, McCulloch CA, Sodek J, Zohar R. Osteopontin expression is required for myofibroblast differentiation. Circ. Res. 2008 Feb 15;102(3):319–27.

44. Schipper MEI, Scheenstra MR, van Kuik J, van Wichen DF, van der Weide P, Dullens HFJ, et al. Osteopontin: a potential biomarker for heart failure and reverse remodeling after left ventricular assist device support. J Heart Lung Transplant. 2011 Jul;30(7):805–10.

45. Felkin LE, Lara-Pezzi E, George R, Yacoub MH, Birks EJ, Barton PJR. Expression of extracellular matrix genes during myocardial recovery from heart failure after left ventricular assist device support. J Heart Lung Transplant. 2009 Feb;28(2):117–22.
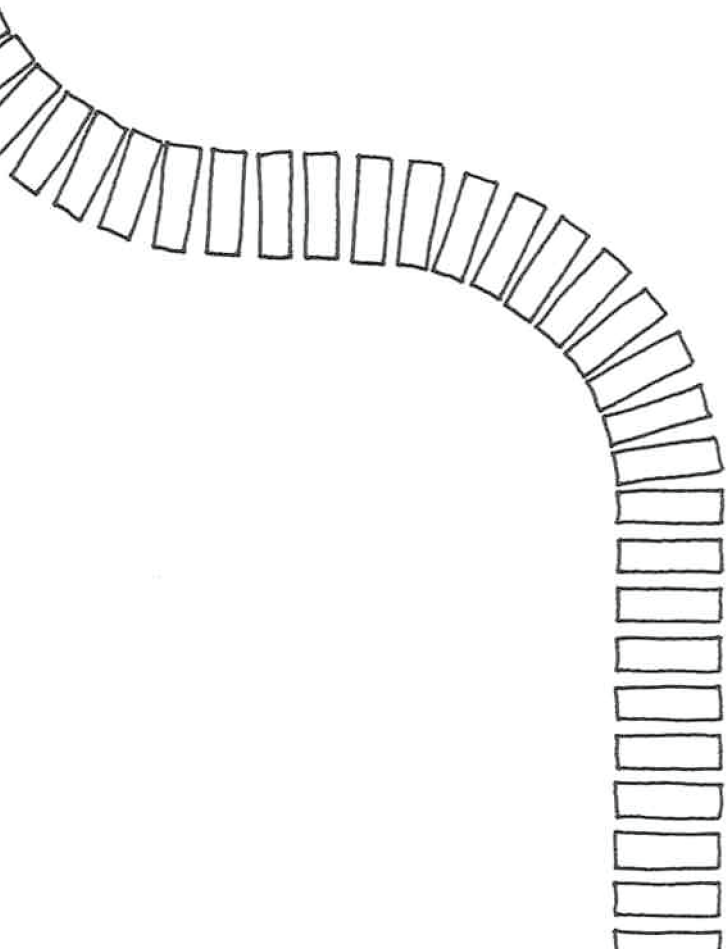
CHAPTER 4

Circulating Growth Differentiation Factor-15 correlates with myocardial fibrosis in patients with non-ischemic dilated cardiomyopathy and decreases rapidly after LVAD support

Sjoukje I. Lok[1], Bjorn Winkens[2], Roel Goldschmeding[3], Ankie J.P. van Geffen[3], Fay M.A. Nous[3], Joyce van Kuik[3], Petra van der Weide[3], Corinne Klöpping[1], J. Hans Kirkels[1], Jaap R. Lahpor[4], Pieter A. Doevendans[1], Nicolaas de Jonge[1], Roel A. de Weger[3]

[1] Department of Cardiology, University Medical Centre Utrecht
[2] Department of Methodology and Statistics, University of Maastricht
[3] Department of Pathology, University Medical Centre Utrecht
[4] Department of Cardiothoracic Surgery, University Medical Centre

Abstract

Aims: Growth Differentiation Factor-15 (GDF-15) is a stress-responsive cytokine and is emerging as a biomarker of cardiac remodelling. Left ventricular assist devices (LVADs) provide unloading of the left ventricle, resulting in partial reverse remodelling. Our aim was to study GDF-15 in patients with a non-ischemic dilated cardiomyopathy (DCM) during LVAD support.

Methods and results: We analysed circulating GDF-15 in 30 patients before and 1, 3, and 6 months after LVAD implantation and before heart transplantation (Htx) or explantation. In addition, mRNA and protein expression of GDF-15 were evaluated in myocardial tissue obtained prior to and after LVAD support. Circulating GDF-15 was significantly higher before LVAD implantation as compared with healthy controls (p<0.001). After 1 month of mechanical support, GDF-15 levels were significantly decreased compared with pre-implantation levels (p<0.001) and remained stable thereafter. Circulating GDF-15 was significantly correlated with kidney function and the severity of myocardial fibrosis. Interestingly, GDF-15 mRNA and protein expression in the myocardium were hardly detectable.

Conclusion: High circulating levels of GDF-15 in patients with end-stage non-ischemic DCM correlate with myocardial fibrosis and kidney function and decline strongly after 1 month of mechanical unloading, remaining stable thereafter. However, cardiac mRNA and protein expression of GDF-15 are very low, suggesting that the heart is not an important source of GDF-15 production in these patients.

Introduction

The incidence of end-stage heart failure (HF) is steadily rising and the need for heart transplantation (HTx) continues to exceed donor organ availability [1]. Left ventricular assist devices (LVADs) were introduced as a bridge to transplantation (BTT) in order to reduce mortality and improve quality of life while awaiting HTx [2,3]. LVADs provide volume and pressure unloading of the left ventricle, reversing the compensatory responses of the overloaded heart resulting in partial reverse remodelling [4]. Achieving sustained myocardial recovery, allowing LVAD removal (bridge to recovery; BTR), is one of the most desirable goals, as for these patients the LVAD could postpone and reduce the need for HTx. Clearly, the ability to identify BTR patients, with for instance biomarkers, will reduce the need for donor hearts. The current era of genomics, proteomics, and metabolomics has led to the discovery of an immense number of novel candidate biomarkers. The American Heart Association emphasized the critical appraisal of novel markers to determine their clinical utility [5]. Recently, Growth Differentiation Factor (GDF)-15 has come under increasing scrutiny as a biomarker in patients with acute and chronic cardiovascular disease [6,12]. GDF-15 will be up-regulated in response to various stimuli including HF [7,11,13], oxidative stress [14], pressure overload [15], and atherosclerosis [6]. GDF-15 is a member of theTransforming Growth Factor-β (TGF-β) cytokine superfamily. Cardiac effects of TGFβ-1 have been extensively studied. TGFβ-1 influences cardiac remodelling by induction of fibrosis, apoptosis, and enhancement of hypertrophic responsiveness of cardiomyocytes [16]. A recent study demonstrated a correlation of circulating GDF-15 with the severity of pulmonary fibrosis [17], indicating that GDF-15 is involved in the process of fibrosis.

In the present study, we investigated whether circulating GDF-15 in patients with severe non-ischemic dilated cardiomyopathy (DCM) is correlated with myocardial fibrosis, and whether GDF-15 is a suitable marker to identify potential BTR patients. In addition, expression of GDF-15 mRNA and protein in myocardial tissue was investigated pre- and post-LVAD support to investigate if the heart was the source of GDF-15 in end-stage DCM.

Methods

Patient characteristics

Thirty patients with end-stage HF supported with an LVAD were included in this study. Of these, the majority (25 patients) were diagnosed with a non-ischemic, non-valvular DCM and supported with a continuous flow LVAD (cf-LVAD; HeartMate II, Thoratec, Pleasanton, CA, USA) as BTT. In addition, we examined five patients from whom the LVAD could eventually be explanted (BTR). Of the 5 BTR patients, 2 were supported with a pulsatile flow LVAD (pf-LVAD; HeartMate I, Thoratec.)and three with a cf-LVAD (HeartMate II, Thoratec). Plasma was collected before LVAD implantation and 1, 3, and 6 months after implantation, and prior to HTx or explantation. Control plasma was gathered from 10 healthy individuals.

Of the 25 BTT patients, 16 had already undergone HTx. Myocardial tissue was collected from the apical part of the left ventricle at the time of LVAD implantation and compared with tissue from the explanted left ventricle outside the suture area of the inflow cannula at the time of HTx. Control myocardial tissue was obtained from three donor hearts declined for HTx because of non-cardiac reasons. To analyse GDF-15 expression in non-myocardial tissues, redundant autopsy samples from multiple organs of patients who died of a non-cardiac cause were obtained from the human tissue bank at the University Medical Center in Utrecht.

All LVAD patients gave written informed consent for the use of their tissues for research purposes. Anonymous use of redundant tissue for research purposes is part of the standard treatment agreement with patients in our hospital [18].

Plasma Growth Differentiation Factor-15

Circulating GDF-15 was measured in EDTA plasma by enzyme-linked immunosorbent assay (ELISA), according to the instructions of the manufacturer (R&D Systems Inc., Minneapolis, USA). In short, the assay diluents were added in a 96-well plate coated with antibody (mouse monoclonal GDF-15 anti-human). Standards, controls, and samples were added in duplicate and incubated on the shaker. After the first washing step, the conjugate was added, followed by incubation on the shaker. The next washing step was followed by the addition of the substrate solution and incubation on a shaker plate. The stop solution was added and wells were read on a microplate reader.

Growth Differentiation Factor-15 mRNA

Total RNA was isolated from 20 slides of 10 μm frozen tissue using an miRNeasy Mini Kit (Qiagen, Inc., Austin, TX, USA). cDNA was synthesized with the use of superscript III, oligo-(dT) and random primers (Invitrogen, Oslo, Norway). The Q-PCR mix consisted of 6.25 μL of mastermix, 0.625 μL of primer/probe Taqman Gene Expression Assay (Life Technologies, Bleiswijk, The Netherlands), and 3.13 μL of milliQ. The expression of the endogenous control glyceraldehyde 3-phosphate dehydrogenase (GAPDH) was measured for each sample. Each primer/probe combination was also measured in placental cDNA, which was used as the calibrator (positive control). Thermal c ycling comprised a 10 min denaturation step at 95°C, followed by 40 cycles of 15 s at 95°C and 1 min at 60°C. GDF-15 mRNA expression was determined on the LightCycler 480 (Roche Diagnostics BV, Almere, The Netherlands). Data was quantified with the comparative quantification cycle (Cq) method. Relative quantity (RQ) were defined as $2^{-\Delta\Delta Cq}$, in which $\Delta Cq = Cq$ (target)-Cq (endogenous control), $\Delta\Delta Cq = \Delta Cq$ (sample)– ΔCq (calibrator). Cq values >35 were defined as negative.

4

Protein expression of Growth Differentiation Factor-15 by immunohistochemistry

Formalin-fixed and paraffin-embedded tissue, 5 μm thick sections were cut and dried overnight in a 56°C stove. The sections were deparaffinized and rehydrated with an alcohol series from 100% to 70%. The endogenous peroxidase was blocked with H_2O_2 for 30 min. Sections were treated with an Antigen Retrieval Solution (ARS) of EDTA. After a wash in phosphate-buffered saline (PBS)/Tween-20, slides were incubated with 100 μL of primary antibody diluted in PBS/1% bovine serum albumin (BSA) (GDF-15 rabbit anti-human 1:80, Sigma-Aldrich, Inc., St. Louis, MO, USA) for 1 h. After a washing step in PBS/Tween-20, a secondary antibody of PowerVision poly-Anti-Rabbit IgG (Immunovision Technologies, Duiven, The Netherlands) was used. After two washing steps of PBS/Tween-20 and PBS, the slides were developed with 3-diaminobenzidine (DAB) solution for 10 min. The nuclei were counterstained with Mayer's haematoxylin for 30 sec.

Myocardial fibrosis analysis

Myocardial tissue was obtained from the apical core before cf-LVAD implantation and in the explanted hearts. In addition, fibrosis was examined in donor hearts declined for HTx, to measure the degree of fibrosis in normal hearts. The specimens were fixed in 10% formalin, embedded in paraffin and sectioned at a thickness of 5 μm. Specimens were stained with an automatic staining system (DakoCytomation Artisan, Glostrup, Denmark) with Masson

Trichome, digitalized and analysed at x 40 magnification. The percentage of fibrosis was calculated with the use of Image J (Bethesda, MD, USA), as the average ratio of the fibrosis area divided by the total area of 15 random sections. Any field containing a large scar area was excluded so that quantification reflected interstitial and perivascular fibrosis only.

Statistics

Categorical data are presented by number (%) and continuous data by median (interquartile range IQR, i.e. 25th - 75th percentile) or by estimated mean ± SE, where appropriate. The longitudinal trend of GDF-15 (from pre-LVAD until 6 months after LVAD implantation) was evaluated using the mixed model analysis with a random intercept to account for the correlation between repeated measurements within the same person. Pre-HTx/explantation values were not included in this analysis since the time until Htx/explantation varies greatly. Due to the small number of BTR patients and controls, comparisons between BTT and BTR patients prior to implantation and between BTT and controls were performed using Mann Whitney U-test for continuous variables and Fisher's exact test for categorical variables. Associations between GDF-15 and laboratory parameters and myocardial fibrosis were tested using Pearson or Spearman correlation, where appropriate. A p value ≤0.05 is considered significant. All analyses were performed using SPSS, version 18 (SPSS, Inc., Chicago, IL, USA).

Results

Baseline characteristics

Baseline characteristics of the BTT and BTR patients are presented in *Table 1*. The BTT patients had a median age of 46 (IQR 31-54) years, 72% (n=18) were male with a median HF duration of 1754 days (IQR 415-2301) and LVAD duration of 279 (IQR 193-505) days. The BTR group consisted of patients with a median age of 37 (IQR 28-53) years, 40% (n=2) were male and 80% (n=4) were diagnosed with DCM. The median duration of HF was significantly shorter in the BTR group (42 days, IQR 16-101). Sixty percent (n=3) of the BTR patients were supported with a cf-LVAD, and the LVAD duration was 343 (IQR 120-363) days.

Table 1

Baseline characteristics of Bridge to Transplantation (BTT) vs Bridge to Recovery (BTR) patients, prior to pulsatile flow (pf-LVAD) and continuous flow LVAD (cf-LVAD) implantation.

Patient characteristics[a]	BTT (n=25)	BTR (n=5)	p-value
Age, years	46 (31 - 54)	37 (28 - 53)	0.44
Male, %	18 (72%)	2 (40%)	0.30
Body Mass Index, kg/m2	23.0 (20.3 - 26.2)	24.0 (22.8 - 31.0)	0.56
Diabetes Mellitus, %	2 (8%)	0 (0%)	1.00
Hypertension, %	0 (0%)	1 (20%)	0.17
Hyperlipidaemia, %	3 (12%)	0 (0%)	1.00
CVA/TIA, %	6 (24%)	0 (0%)	0.55
NYHA classification IV, %	25 (100%)	5 (100%)	1.00
Duration of HF prior to LVAD (days)	1754 (415-2301)	42 (16-101)	0.01
Etiology of HF, %			
Ischemic Heart Disease (IHD)	0 (0%)	1 (20 %)	
DCM	25 (100%)	4 (80%)	
Idiopathic	9 (36%)	1 (20%)	1.00
Familial[b]	11 (44%)	0 (0%)	0.27
Myocarditis	3 (12%)	1 (20%)	0.47
Peripartum	0 (0%)	2 (40%)	0.02
Toxic (drugs/medication)	2 (8%)	0 (0%)	1.00
bvPM[c]/ICD, %	16 (64%)	0 (0%)	0.01
LVAD support			0.02
cf-LVAD	25 (100 %)	3 (60%)	
pf-LVAD	0 (0 %)	2 (40 %)	
Days of LVAD support	279 (193 - 505)	343 (120 - 363)	0.90
Laboratory parameters			
Hemoglobin (Hb), mmol/L	7.2 (6.5 - 8.1)	7.5 (5.8 -7.6)	0.63
C-Reactive Protein (CRP), mg/L	21.0 (11.8 - 46.3)	35 (13.5 - 49.8)	0.67
Urea, mmol/L	9.6 (7.5 - 13.1)	7.4 (4.4 - 14.2)	0.28
Creatinine, µmol/L	116.0 (106.5 - 146.0)	114.0 (75 - 152.5)	0.45

[a] Categorical data are presented as number (%) and continuous data as median (25% - 75% percentile).

[b] Familial DCM is defined when the patient has one or more family members diagnosed with idiopathic DCM or a first-degree relative with an unexplained sudden death under the age of 35 years

[c] bvPM= biventricular pacemaker

[d] Mann-Whitney U- and Fisher's exact tests were used to check for differences in continuous and categorical variables

4

Plasma Growth Differentiation Factor-15 (GDF-15)

A significantly higher GDF-15 level was found in BTT patients prior to cf-LVAD as compared with healthy controls (p<0.001; 7.1 ± 0.6 ng/ml vs. 0.5 ng/ml ± 0.1; *Figure 1A*) and a large individual variation was found (*Figure 1B*). There was a rapid decline after 1 month of mechanical support (p<0.001), GDF-15 levels remained stable thereafter but did not reach the control level (GDF-15 at 6 months vs. controls p=0.03; *Figure 1A*). This longitudinal trend in circulating GDF-15 was not significantly different between the BTT and BTR group (overall trend p=0.62). *Figure 2* represents the fraction of BTT patients with elevated circulating GDF-15 levels in relation to the upper reference limit in apparently healthy elderly individuals, i.e. <1.2 ng/ml, as previously defined [7]. Prior to cf-LVAD implantation, in only one patient (4.3%) of the total patient population, the GDF-15 level was within the normal range. The percentage of patients with normal range GDF-15 increased to 38, 68, and 75% after 1, 3, and 6 months of support, respectively.
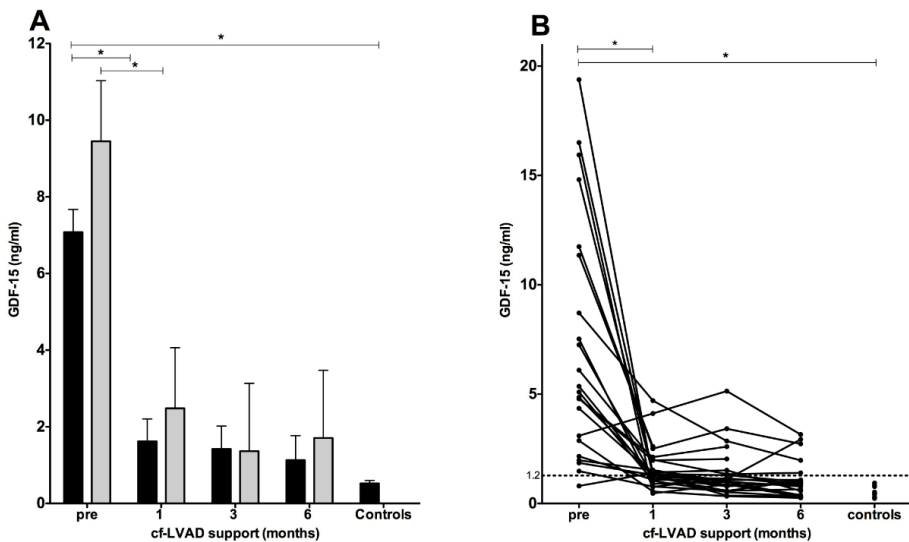
Figure 1: Circulating Growth Differentiation Factor-15 (GDF-15) during continuous flow left ventricular assist device (cf-LVAD) support

Plasma levels of GDF-15 were significantly increased prior to cf-LVAD support as compared to controls (Bridge to Transplantation; BTT p<0.001). After one month of support, there was a significant decrease in GDF-15 and remained stable thereafter (BTT p<0.001). The longitudinal trend in circulating GDF-15 was not significantly different between the BTT (black bars) and Bridge to Recovery (BTR) group (grey bars; overall trend p=0.62). Figure 1B presents the large individual variation in BTT patients of circulating GDF-15 prior to cf-LVAD implantation. The dotted line indicates the upper limit of circulating GDF-15 in healthy individuals. The asterisk (*) represents p<0.05.

A range of standard laboratory values obtained prior to cf-LVAD was examined for individual associations with plasma GDF-15 levels in BTT patients. *Table 2* indicates that urea, creatinine and aspartate transaminase (AST) were significantly correlated with circulating levels of GDF-15 prior to LVAD support. In addition, the change in GDF-15 between pre-LVAD levels and 6 months after implantation was significantly correlated with the change in AST (r=0.51, p=0.037), but not with change in urea (r=0.42, p=0.094) and creatinine (r=0.47, p=0.055). However, there was one extreme outlier. After exclusion of this outlier (*Figure 3*), the difference was still significant for change in creatinine (r=0.77, p=0.001) and AST (r=0.77, p=0.001), but not for the change in urea (r=0.39, p=0.134).
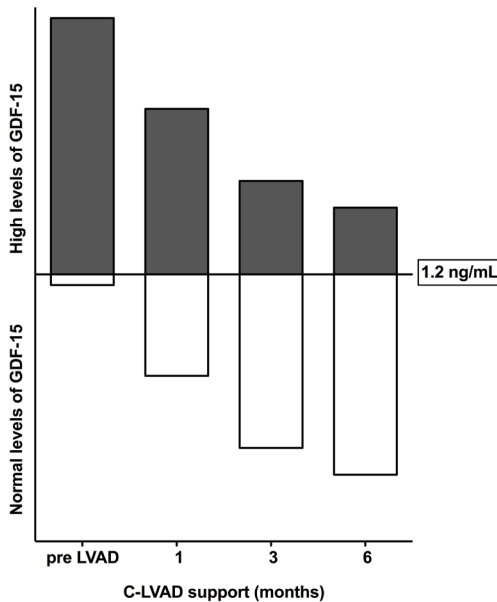
Figure 2: Plasma levels of Growth Differentiation Factor 15 (GDF-15) during continuous flow LVAD (cf-LVAD) support

The proportion of elevated circulating GDF-15 in patients with non-ischemic dilated cardiomyopathy before cf-LVAD implantation, in relation to the upper reference limit in apparently healthy elderly individuals (1.2 ng/ml). Prior to cf-LVAD implantation, 96% of heart failure patients had elevated plasma levels of GDF-15, whereas after 6 months of support, this percentage was only 25%.

Table 2: Correlation with circulating Growth Differentiation Factor-15 (GDF-15)
Laboratory parameters prior to continuous flow LVAD (cf-LVAD) support. Urea, creatinine and aspartate transaminase (AST) were significantly correlated with circulating GDF-15 in end-stage dilated cardiomyopathy patients before cf-LVAD implantation.

Laboratory parameters	p-value	Correlation (r)
Urea, mmol/L	0.02	0.49
Creatinine, μmol/L	0.02	0.50
AST[1],U/L	0.02	0.50
ALT[1],U/L	0.34	0.22
LD[1],U/L	0.09	0.36
Bilirubin, μmol/L	0.33	0.21
GGT, U/L	0.75	-0.07
Alkaline phosphatase, U/L	0.47	-0.16
CRP, mg/L	0.38	0.20
Leukocytes, *10^9/L	0.81	0.05
BNP[1], pmol/L	0.10	0.35

[1]Spearman correlation was used.

AST, aspartate transaminase; ALT, alanine transaminase; LD, lactate dehydrogenase;

GGT, gamma glutamyl transferase; CRP, C-reactive protein.
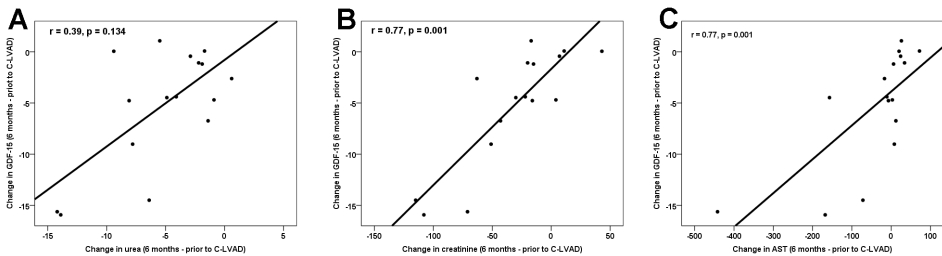
Figure 3: Correlation of Growth Differentiation Factor 15 (GDF-15) during continuous flow LVAD (cf-LVAD)
Correlation of change in urea (*A*), creatinine (*B*) and aspartate transaminase (AST; *C*) with the change in GDF-15 prior to cf-LVAD implantation versus 6 months after implantation. One outlier was excluded. Change in creatinine and aspartate transaminase (AST) were significantly correlated to the change in GDF-15 after 6 months of LVAD implantation.

Growth Differentiation Factor-15 mRNA

Expression of GDF-15 mRNA was assessed by Q-PCR in cDNA prepared from heart tissue of 16 DCM patients before and after LVAD support. GDF-15 expression was present in the calibrator samples (placental mRNA), confirming that the Q-PCR assay works properly. However, cardiac GDF-15 mRNA in all preparations was below the detection level, implying very low GDF-15 mRNA in dilated hearts.

Protein expression of Growth Differentiation Factor-15

Heart tissue: Immunohistochemistry revealed no GDF-15 staining on paraffin tissue of 16 DCM patients before and after cf-LVAD (*Figure 4*).

Other organs: Liver, spleen, lymph node, and striated muscle did not show staining of GDF-15. However, in kidney and pancreas, a moderate staining was observed. Placenta tissue showed strong GDF-15 staining (*Figure 4*).
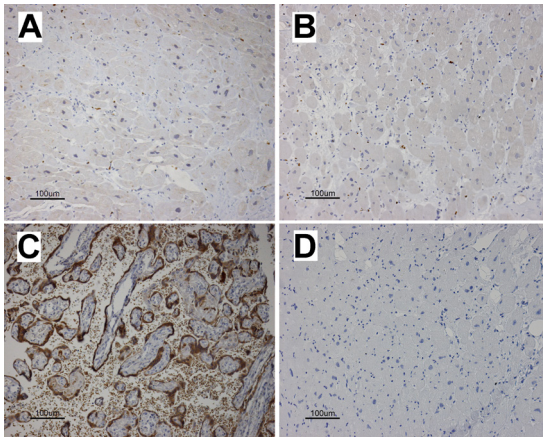
Figure 4: Protein expression of Growth Differentiation Factor-15 (GDF-15).
A. Heart tissue of a patient with dilated cardiomyopathy (DCM) prior to continuous flow left ventricular assist device (cf-LVAD).
B. Heart tissue of the same patient post cf-LVAD.
C. Positive control (placenta).
D. Negative control (heart tissue without primary antibody of a patient with DCM).
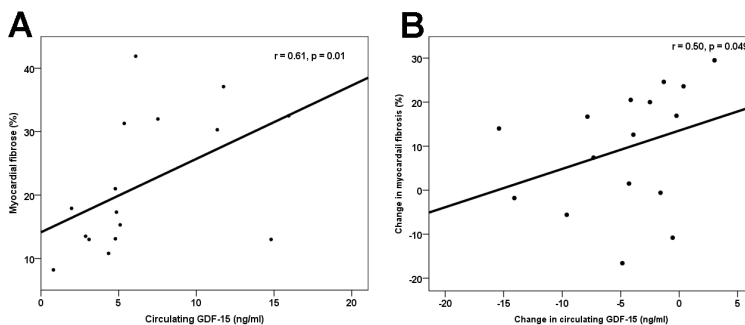
Figure 5: Correlation of circulating Growth Differentiation Factor-15 (GDF-15) with myocardial fibrosis
Circulating GDF-15 was significantly correlated to the amount of myocardial fibrosis in patients with non-ischemic dilated cardiomyopathy prior to continuous flow left ventricular assist device (cf-LVAD) implantation (*A*) and in the time-period until heart transplantation (*B*).

Myocardial fibrosis

The median percentage of fibrosis in biopsies from patients with end-stage HF prior to cf-LVAD implantation was 17.6 % (IQR 13.0-17.7), significantly higher (p<0.05) than in healthy controls (12.5 %, IQR 7.5-14.8). Circulating GDF-15 was significantly correlated to the amount of myocardial fibrosis in end-stage HF patients prior to LVAD implantation (r=0.61, p=0.01; *Figure 5A*). Moreover, the median change in fibrosis while on LVAD support was 13.3 (IQR -1.2 to 20.2) and the median change of GDF-15 was -4.0 (IQR -7.6 to -0.9) in BTT patients. The alteration in circulating GDF-15 correlated significantly with the increase in myocardial fibrosis (r=0.50, p<0.05; *Figure 5B*).

Discussion

The three most important observations in this study are that i) elevated levels of circulating GDF-15 decrease rapidly to near normal values within 1 month of cf-LVAD support, ii) circulating GDF-15 levels appear to correlate with the degree of myocardial fibrosis and iii) GDF-15 mRNA and protein expression were hardly detectable in dilated hearts, indicating that the myocardium is not an important source of GDF-15 in these patients. Furthermore, we confirmed that plasma creatinine, urea and aspartate transaminase (AST) are significantly correlated with circulating GDF-15, consistent with the literature [11,19-21]. Since there was no difference in levels of circulating GDF-15 between BTT and BTR patients at any time point, it is unlikely that GDF-15 can identify those patients that will demonstrate substantial recovery.

We showed that 96% of the end-stage HF patients had elevated GDF-15 levels prior to cf-LVAD implantation and that this percentage decreased to 25% after 6 months of mechanical unloading. Impaired cardiac output in patients with end-stage HF leads to an increase in oxidative stress [22], subsequently promoting high levels of circulating GDF-15 [14]. We hypothesize that, after restoration of low cardiac output by LVADs, these effects will be abolished. To the best of our knowledge, this is the first study demonstrating, that hemodynamic restoration by LVAD support leads to a reduction of GDF-15 in HF patients. Circulating levels of GDF-15 are associated with prognosis in patients with cardiovascular diseases, especially coronary artery disease [6,8-10,12,23]. GDF-15 seems to be an independent predictor of mortality and recurrent events beyond established clinical and biochemical markers in patients with stable [24] and unstable angina pectoris [8,10,25]. Patients with non-ST-

elevation myocardial infarction (NSTEMI) and elevated GDF-15 levels benefit from early revascularization, whereas patients with lower levels of GDF-15 did not [9]. Paradoxically, accumulating evidence suggests that GDF-15 may protect against cardiac injury due to its anti-apoptotic [23,26] and anti-inflammatory effects by repressing polymorphonuclear leucocyte recruitment into infarcted areas in mice [27].

The role of GDF-15 in patients with chronic HF has been less-extensively examined. An independent correlation between GDF-15 and prognosis has been demonstrated in patients with HF with a reduced ejection fraction (HFrEF) [7,11,13]. GDF-15 was related to outcome that was or was not attributed to ischemic heart disease [7,11]. In patients with HF and a preserved ejection fraction (HFpEF), circulating GDF-15 was elevated and was associated with impairment in exercise capacity [28,29]. Also, GDF-15 could predict mortality and morbidity after cardiac resynchronization therapy [30].

Still, the role of GDF-15 in chronic HF patients remains unclear. The only human organs known to express GDF-15 under physiological conditions are the placenta and the prostate [31,32]. An increase in GDF-15 expression has been described in cardiomyocytes exposed to ischemia [7] and increased wall stress [27]. Consistently, expression of GDF-15 was increased in dilated hearts of mice [33]. However, in our study, we did not detect appreciable cardiac mRNA and protein expression of GDF-15 in severe non-ischemic HFrEF patients. Yet, we detected a significant correlation between levels of circulating GDF-15 and the amount of myocardial fibrosis. Previously, such a relationship with fibrosis was found in the lungs of patients with systemic sclerosis [17], but until now, this was not established in the heart.

Limitations

The small number of BTR patients constitutes a major limitation. Moreover, 2 of these patients were supported with a pf-LVAD, whereas the rest of our patients received a cf-LVAD as bridge to HTx. Hence, it is difficult to draw significant conclusions comparing BTT and the BTR groups. Moreover, the present study found an association of GDF-15 with fibrosis. However, the duration of LVAD support is variable until HTx, which is not taken into account into the analysis.

Conclusion

Elevated levels of circulating GDF-15 declined rapidly during LVAD support and were significantly correlated with myocardial fibrosis. Interestingly, GDF-15 mRNA and protein expression was hardly detectable in severe decompensated non-ischemic hearts.

References

1. Writing Group Members, Roger VL, Go AS, Lloyd-Jones DM, Benjamin EJ, Berry JD, Borden WB, Bravata DM, Dai S, Ford ES, Fox CS, Fullerton HJ, Gillespie C, Hailpern SM, Heit JA, Howard VJ, Kissela BM, Kittner SJ, Lackland DT, Lichtman JH, Lisabeth LD, Makuc DM, Marcus GM, Marelli A, Matchar DB, Moy CS, Mozaffarian D, Mussolino ME, Nichol G, Paynter NP, et al. Executive Summary: Heart Disease and Stroke Statistics--2012 Update: A Report From the American Heart Association. Circulation. 2012 Jan. 3;125(1):188–197.

2. Dickstein K, Cohen-Solal A, Filippatos G, McMurray JJV, Ponikowski P, Poole-Wilson PA, Strömberg A, van Veldhuisen DJ, Atar D, Hoes AW, Keren A, Mebazaa A, Nieminen M, Priori SG, Swedberg K, ESC Committee for Practice Guidelines (CPG). ESC Guidelines for the diagnosis and treatment of acute and chronic heart failure 2008: the Task Force for the Diagnosis and Treatment of Acute and Chronic Heart Failure 2008 of the European Society of Cardiology. Developed in collaboration with the Heart Failure Association of the ESC (HFA) and endorsed by the European Society of Intensive Care Medicine (ESICM). Eur. Heart J. 2008. p. 2388–2442.

3. Lahpor JR. State of the art: implantable ventricular assist devices. Curr Opin Organ Transplant. 2009 Oct.;14(5):554–559.

4. Birks EJ, George RS. Molecular changes occurring during reverse remodelling following left ventricular assist device support. J Cardiovasc Transl Res. 2010 Dec.;3(6):635–642.

5. Hlatky MA, Greenland P, Arnett DK, Ballantyne CM, Criqui MH, Elkind MSV, Go AS, Harrell FE, Hong Y, Howard BV, Howard VJ, Hsue PY, Kramer CM, McConnell JP, Normand S-LT, O'Donnell CJ, Smith SC, Wilson PWF, American Heart Association Expert Panel on Subclinical Atherosclerotic Diseases and Emerging Risk Factors and the Stroke Council. Criteria for evaluation of novel markers of cardiovascular risk: a scientific statement from the American Heart Association. Circulation. 2009 May 5;119(17):2408–2416.

6. Brown DA, Breit SN, Buring J, Fairlie WD, Bauskin AR, Liu T, Ridker PM. Concentration in plasma of macrophage inhibitory cytokine-1 and risk of cardiovascular events in women: a nested case-control study. Lancet. 2002 Jun. 22;359(9324):2159–2163.

7. Kempf T, Haehling von S, Peter T, Allhoff T, Cicoira M, Doehner W, Ponikowski P, Filippatos GS, Rozentryt P, Drexler H, Anker SD, Wollert KC. Prognostic utility of Growth Differentiation Factor-15 in patients with chronic heart failure. J. Am. Coll. Cardiol. 2007 Sep. 11;50(11):1054–1060.

8. Kempf T, Björklund E, Olofsson S, Lindahl B, Allhoff T, Peter T, Tongers J, Wollert KC, Wallentin L. Growth-differentiation factor-15 improves risk stratification in ST-segment elevation myocardial infarction. Eur. Heart J. 2007 Dec.;28(23):2858–2865.

9. Wollert KC, Kempf T, Lagerqvist B, Lindahl B, Olofsson S, Allhoff T, Peter T, Siegbahn A, Venge P, Drexler H, Wallentin L. Growth Differentiation Factor 15 for risk stratification and selection of an invasive treatment strategy in non ST-elevation acute coronary syndrome. Circulation. 2007 Oct. 2;116(14):1540–1548.

10. Wollert KC, Kempf T, Peter T, Olofsson S, James S, Johnston N, Lindahl B, Horn-Wichmann R, Brabant G, Simoons ML, Armstrong PW, Califf RM, Drexler H, Wallentin L. Prognostic value of growth-differentiation factor-15 in patients with non-ST-elevation acute coronary syndrome. Circulation. 2007 Feb. 27;115(8):962–971.

11. Anand IS, Kempf T, Rector TS, Tapken H, Allhoff T, Jantzen F, Kuskowski M, Cohn JN, Drexler H, Wollert KC. Serial measurement of growth-differentiation factor-15 in heart failure: relation to disease severity and prognosis in the Valsartan Heart Failure Trial. Circulation. 2010 Oct. 5;122(14):1387–1395.

12. Eggers KM, Kempf T, Lagerqvist B, Lindahl B, Olofsson S, Jantzen F, Peter T, Allhoff T, Siegbahn A, Venge P, Wollert KC, Wallentin L. Growth-differentiation factor-15 for long-term risk prediction in patients stabilized after an episode of non-ST-segment-elevation acute coronary syndrome. Circ Cardiovasc Genet. 2010 Feb.;3(1):88–96.

13. Kempf T, Horn-Wichmann R, Brabant G, Peter T, Allhoff T, Klein G, Drexler H, Johnston N, Wallentin L, Wollert KC. Circulating concentrations of growth-differentiation factor 15 in apparently healthy elderly individuals and patients with chronic heart failure as assessed by a new immunoradiometric sandwich assay. Clin. Chem. 2007 Feb.;53(2):284–291.

14. Han E-S, Muller FL, Pérez VI, Qi W, Liang H, Xi L, Fu C, Doyle E, Hickey M, Cornell J, Epstein CJ, Roberts LJ, Van Remmen H, Richardson A. The in vivo gene expression signature of oxidative stress. Physiol. Genomics. 2008 Jun. 12;34(1):112–126.

15. Xu J, Kimball TR, Lorenz JN, Brown DA, Bauskin AR, Klevitsky R, Hewett TE, Breit SN, Molkentin JD. GDF15/MIC-1 functions as a protective and antihypertrophic factor released from the myocardium in association with SMAD protein activation. Circ. Res. 2006 Feb. 17;98(3):342–350.

16. Huntgeburth M, Tiemann K, Shahverdyan R, Schlüter K-D, Schreckenberg R, Gross M-L, Mödersheim S, Caglayan E, Müller-Ehmsen J, Ghanem A, Vantler M, Zimmermann WH, Böhm M, Rosenkranz S. Transforming Growth Factor β(1) Oppositely Regulates the Hypertrophic and Contractile Response to β-Adrenergic Stimulation in the Heart. PLoS ONE. 2011;6(11):e26628.

17. Yanaba K, Asano Y, Tada Y, Sugaya M, Kadono T, Sato S. Clinical significance of serum Growth Differentiation Factor-15 levels in systemic sclerosis: association with disease severity. Mod Rheumatol. 2012 Sep;22(5):668-75.

18. van Diest PJ. No consent should be needed for using leftover body material for scientific purposes. For. BMJ. 2002 Sep. 21;325(7365):648–651.

19. Frankenstein L, Remppis A, Frankenstein J, Hess G, Zdunek D, Gut S, Slottje K, Katus HA, Zugck C. Reference change values and determinants of variability of NT-proANP and GDF15 in stable chronic heart failure. Basic Res. Cardiol. 2009 Nov.;104(6):731–738.

20. Lajer M, Jorsal A, Tarnow L, Parving H-H, Rossing P. Plasma Growth Differentiation Factor-15 independently predicts all-cause and cardiovascular mortality as well as deterioration of kidney function in type 1 diabetic patients with nephropathy. Diabetes Care. 2010 Jul.;33(7):1567–1572.

4

21.   Wang F, Guo Y, Yu H, Zheng L, Mi L, Gao W. Growth Differentiation Factor 15 in different stages of heart failure: potential screening implications. Biomarkers. 2010 Dec.;15(8):671–676.

22.   Giordano FJ. Oxygen, oxidative stress, hypoxia, and heart failure. J. Clin. Invest. 2005 Mar.;115(3):500–508.

23.   Kempf T, Eden M, Strelau J, Naguib M, Willenbockel C, Tongers J, Heineke J, Kotlarz D, Xu J, Molkentin JD, Niessen HW, Drexler H, Wollert KC. The transforming growth factor-beta superfamily member growth-differentiation factor-15 protects the heart from ischemia/reperfusion injury. Circ. Res. 2006 Feb. 17;98(3):351–360.

24.   Schnabel RB, Schulz A, Messow CM, Lubos E, Wild PS, Zeller T, Sinning CR, Rupprecht HJ, Bickel C, Peetz D, Cambien F, Kempf T, Wollert KC, Benjamin EJ, Lackner KJ, Münzel TF, Tiret L, Vasan RS, Blankenberg S. Multiple marker approach to risk stratification in patients with stable coronary artery disease. Eur. Heart J. 2010 Dec.;31(24):3024–3031.

25.   Bonaca MP, Morrow DA, Braunwald E, Cannon CP, Jiang S, Breher S, Sabatine MS, Kempf T, Wallentin L, Wollert KC. Growth Differentiation Factor-15 and risk of recurrent events in patients stabilized after acute coronary syndrome: observations from PROVE IT-TIMI 22. Arterioscler. Thromb. Vasc. Biol. 2011 Jan.;31(1):203–210.

26.   Heger J, Schiegnitz E, Waldthausen von D, Anwar MM, Piper HM, Euler G. Growth Differentiation Factor 15 acts anti-apoptotic and pro-hypertrophic in adult cardiomyocytes. J. Cell. Physiol. 2010 Jul.;224(1):120–126.

27.   Kempf T, Zarbock A, Widera C, Butz S, Stadtmann A, Rossaint J, Bolomini-Vittori M, Korf-Klingebiel M, Napp LC, Hansen B, Kanwischer A, Bavendiek U, Beutel G, Hapke M, Sauer MG, Laudanna C, Hogg N, Vestweber D, Wollert KC. GDF-15 is an inhibitor of leukocyte integrin activation required for survival after myocardial infarction in mice. Nat. Med. 2011 May;17(5):581–588.

28.   Stahrenberg R, Edelmann F, Mende M, Kockskämper A, Düngen H-D, Lüers C, Binder L, Herrmann-Lingen C, Gelbrich G, Hasenfuss G, Pieske B, Wachter R. The novel biomarker Growth Differentiation Factor 15 in heart failure with normal ejection fraction. Eur. J. Heart Fail. 2010 Dec.;12(12):1309–1316.

29.   Dinh W, Füth R, Lankisch M, Hess G, Zdunek D, Scheffold T, Kramer F, Klein RM, Barroso MC, Nickl W. Growth-differentiation factor-15: a novel biomarker in patients with diastolic dysfunction? Arq. Bras. Cardiol. 2011 Jul.;97(1):65–75.

30.   Foley PWX, Stegemann B, Ng K, Ramachandran S, Proudler A, Frenneaux MP, Ng LL, Leyva F. Growth Differentiation Factor-15 predicts mortality and morbidity after cardiac resynchronization therapy. Eur. Heart J. 2009 Nov.;30(22):2749–2757.

31.   Lawton LN, Bonaldo MF, Jelenc PC, Qiu L, Baumes SA, Marcelino RA, de Jesus GM, Wellington S, Knowles JA, Warburton D, Brown S, Soares MB. Identification of a novel member of the TGF-beta superfamily highly expressed in human placenta. Gene. 1997 Dec. 5;203(1):17–26.

32. Paralkar VM, Vail AL, Grasser WA, Brown TA, Xu H, Vukicevic S, Ke HZ, Qi H, Owen TA, Thompson DD. Cloning and characterization of a novel member of the transforming growth factor-beta/bone morphogenetic protein family. J Biol Chem. 1998 May 29;273(22):13760–13767.

33. Harding P, Yang X-P, Yang J, Shesely E, He Q, LaPointe MC. Gene expression profiling of dilated cardiomyopathy in older male EP4 knockout mice. Am. J. Physiol. Heart Circ. Physiol. 2010 Feb.;298(2):H623–32.

4
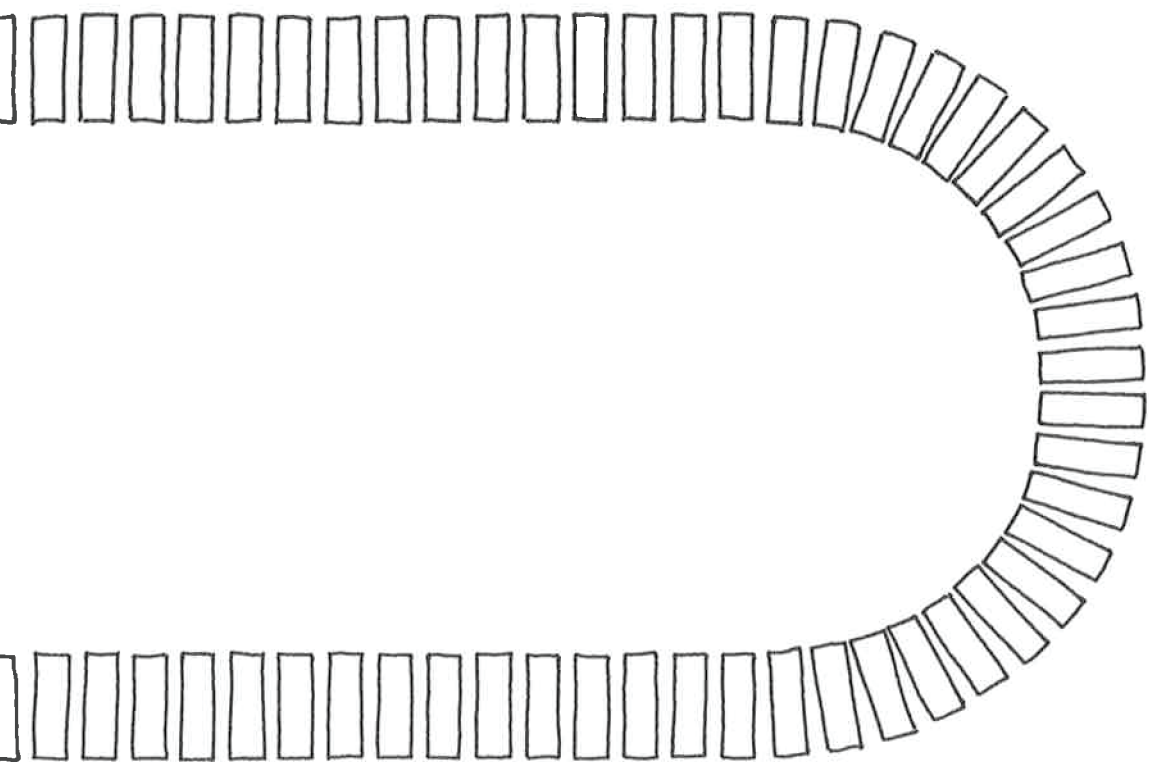
CHAPTER 5

Alterations of myocardial haptoglobin expression are suggestive for diminished inflammatory activity and persistent hemolysis during mechanical circulatory support

Sjoukje I. Lok[1], Ankie J. van Geffen[2], Niels Bovenschen[2], Bjorn Winkens[3], Pieter A. Doevendans[1], Erica Siera[2], Hub F.J. Dullens[2], Jaap R. Lahpor[4], Roel A. de Weger[2], Nicolaas de Jonge[1]

[1] Department of Cardiology, University Medical Centre Utrecht
[2] Department of Pathology, University Medical Center, Utrecht
[3] Department of Methodology and Statistics, University of Maastricht
[4] Department of Cardiothoracic Surgery, University Medical Center Utrecht

Abstract

Background: Alterations in tissue and plasma concentrations of various proteins, like osteopontin, integrins and haptoglobin (HPTG), have been related to various stages of heart failure (HF). Mechanical unloading by left ventricular assist devices (LVADs) result in partial reverse remodeling, paralleled by changes in protein levels both in plasma and tissue. The aim of this study was to analyze changes in localization, production, tissue content and plasma levels of HPTG in continuous flow LVAD (cf-LVAD) supported patients.

Methods and results: Analysis of pooled pre- versus post cf-LVAD myocardial tissue samples by proteomics indicated that HPTG showed the most profound reduction after mechanical circulatory support. This was accompanied by a significant decrease ($p < 0.001$) in plasma HPTG to levels below that of healthy controls ($p = 0.002$). Immunohistochemistry showed that HPTG was mainly localized in endothelial and stromal cells in the heart tissue before cf-LVAD support. After cf-LVAD support, hardly any HPTG could be detected. The low level of HPTG mRNA expression in the heart did not alter significantly during support.

Conclusion: Considering the low level of HPTG mRNA in heart tissue, local production seemed negligible. In the myocardium, the endothelial, stromal and inflammatory cells stained strongly for HPTG pre-LVAD and the intensity decreased dramatically post-LVAD. Therefore, the strong expression of HPTG in stromal and inflammatory cells in the heart in patients with end-stage HF is due to uptake from the circulation. During mechanical support, signs of HF decline, accompanied by decreased levels of cytokines and inflammatory markers and low HTPG levels. The decline in HTPG can also be explained by persistent hemolysis during support.

Introduction

The number of end-stage heart failure (HF) patients increases and their quality of life and expected survival rates are poor, despite optimal medical treatment. Left ventricular assist devices (LVADs) were introduced as bridge to transplantation (BTT) in patients with advanced HF [1,2]. LVADs offer the opportunity to induce significant improvement to the structure and function of the heart, being referred to as reverse remodeling [3-5]. Reverse remodeling is a highly complex process and is incompletely understood. Recently, we reported that protein levels change in myocardial tissue during pulsatile flow LVAD (pf-LVAD) support [6]. However, since pf-LVAD support has been replaced by continuous flow LVADs (cf-LVADs) and the physiology of both devices differ, we performed proteomics in pooled heart tissue of end-stage HF patients supported with a cf-LVAD. Haptoglobin (HPTG) showed to be the protein with the most profound decrease post-LVAD compared with pre-LVAD tissue. To reveal the significance of the observed changes in HPTG levels, the changes in circulating and myocardial HPTG, as well as the localization, were analyzed in individual HF patients, before, during and after cf-LVAD support.

Materials and methods

Study population
A total of 37 patients were included in this study. All were diagnosed with end-stage HF and supported with a continuous flow LVAD (cf-LVAD; HeartMate II, Thoratec, CA, USA) as BTT. Plasma was obtained before and 1, 3 and 6 months after LVAD implantation and before heart transplantation (HTx). Control plasma was obtained from 12 healthy individuals. Of the 37 patients, 20 already underwent HTx. Myocardial tissue was collected from the apical part of the left ventricle at time of LVAD implantation (pre-LVAD) and compared with tissue from the explanted left ventricle outside the suture area of the inflow cannula at time of HTx (post-LVAD). Control myocardial tissue was obtained from 3 donor hearts declined for HTx because of non-cardiac reasons. All patients have given written informed consent for the use of their tissues for research purposes.

2D-DIGE of myocardial tissue
With the use of fluorescent 2-dimensional difference gel electrophoresis (2D-DIGE), a comparative analysis was made of protein expression in myocardial tissue prior to and

after cf-LVAD implantation of 8 patients and 4 controls. For the 2D-DIGE, tissue samples were mixed with 50 mMTris (pH 7.4), 150 mMNaCl, and 1% NP-40, incubated for 30 min at 4°C. Lysates were cleared by centrifugation at 14,000 rpm for 10 min. Pre- and post-LVAD samples (75 μg) were labeled with 400 pmol of Cy3 or Cy5, and a 1:1 mixture of all samples was labeled with Cy2. Samples (150 μg) were separated by 2D gel electrophoresis as previously described [7]. Dye swaps were included to exclude preferentially labeled proteins. Relative quantification of matched gel features was performed by using Decyder DIA and BVA software (GE Healthcare, Hoevelaken, the Netherlands). For inter-gel analyses, the internal standard method was used [8]. Protein spots were selected if: 1) fluorescence volume intensity altered more than 1.5 fold pre versus post LVAD samples, 2) the difference between pre-and post LVAD was statistically significant, and 3) spots could be detected in at least 3 patients.

Mass spectrometry

Differentially expressed proteins were excised and identified by tandem mass spectrometry. Selected spots were excised robotically (EttanDalt Spot Cutter, GE Healthcare). Proteins were separated by 12% polyacrylamide gels by SDS-PAGE and stained with Flamingo staining (Bio-Rad). Bands were excised from gel, reduced with dithiothreitol, alkylated with iodoacetamide, and digested with trypsin (Roche, Woerden, the Netherlands) as described [8,9]. Samples were subjected to nanoflow LC (Eksigent Technologies, Dublin, CA, USA) using C18 reverse phase trap columns (Phenomenex; column dimensions 2cm x 100 μm, packed in-house) and subsequently, separated on C18 analytical columns (Reprosil; column dimensions, 20 cm x 50 μm; packed in-house) using a linear gradient from 0 to 40% B (A = 0.1 M acetic acid; B = 95% (v/v) acetonitrile, 0.1 M acetic acid) in 60 min and at a constant flow rate of 150 nl/min. Column eluate was directly coupled to the LTQ-Orbitrap-XL mass spectrometer (Thermo Fisher Scientific Inc, Waltham, MA, USA) operating in positive mode, using Lock spray internal calibration. Data were processed and subjected to database searches using MASCOT software (Matrix Science Inc, Boston, MA, USA) against Swiss Prot and non-redundant NCBI database, with a 10-ppm mass tolerance of precursor and 0.8 Da for the fragment ion.

Quantitative (Q-) PCR for tissue mRNA expression

Total RNA was isolated from 20 frozen tissue sections (10 μm) using miRNeasy Mini Kit (Qiagen, Inc., Austin, USA). Copy DNA was synthesized with the use of superscript III, oligo-dT and random primers (Invitrogen, Oslo, Norway) and not diluted. The Q-PCR mix

consisted of 6,25 μL mastermix, 0.625 μL primer/probe Taqman Gene Expression Assay (Life Technologies, Bleiswijk, the Netherlands) and 3.13 μL H_2O. The expression of the endogenous control Glyceraldehyde 3-phosphate dehydrogenase (GAPDH) was measured for each sample as an endogenous control. Each primer/probe combination was also measured in placental cDNA, which was used as calibrator. Thermal cycling comprised a 10 min denaturation step at 95°C, followed by 40 cycles of 15 sec at 95°Cand 1 min at 60°C. mRNA expression of HPTG was determined by Q-PCR on the LightCycler 480 (Roche Diagnostics BV, Almere, the Netherlands). Data was quantified with the comparative quantification cycle (Cq) method. Relative quantity (RQ) was defined as $2^{-\Delta\Delta Cq}$, in which $\Delta Cq = Cq(target) - Cq$ (endogenous control), $\Delta\Delta Cq = \Delta Cq$ (sample) $- \Delta Cq$ (calibrator). Cq values above 35 were defined as negative.

ELISA for plasma haptoglobin detection

Circulating HPTG was measured in EDTA plasma by ELISA (AssayMax Human HPTG ELISA Kit; Assay Pro, St. Charles, USA), according to the instructions of the manufacturer. In short, the assay diluents were added in a 96 wells plate coated with antibody (polyclonal antibody against HPTG). Standards, controls and samples were added in duplicate. After the first washing step, the streptavidin-peroxidase conjugate was added. The next washing step was followed by the addition of the Substrate Solution. The stop solution was added and wells were read out on a microplate reader.

Immunohistochemistry

From formalin fixed and paraffin embedded tissue, 4 μm thick sections were cut, dried on slides and incubated overnight in a 56°C stove. The sections were deparaffinated and endogenous peroxidase activity was blocked with 5% H_2O_2 for 15 min. Sections were treated with an Antigen Retrieval Solution (ARS) of EDTA. After a wash in PBS, slides were incubated with the primary antibody (anti-HPTG, rabbit polyclonal antibody; 1:200 diluted in PBS/BSA 1%; Abcam, Cambridge, UK) for 1 hr. After a wash in PBS a secondary antibody was used (BrightVision Poly HRP-anti mouse/rabbit/rat IgG; Immunologic, Duiven, the Netherlands). After a washing step with PBS and a washing step with phosphate/citrate solution (pH 5.8), the slides were developed with diaminobenzidine substrate solution for 10 min. The nuclei were counterstained with haematoxylin according to Mayer and dehydrated. In every tissue section, 3 areas were analyzed and the HPTG staining of cardiomyocytes, epithelial and stromal cells was scored from which the modus was calculated. This was performed twice by the same investigator, from which the intra-

5

observer agreement was assessed using unweighted and weighted kappas [10].

Statistical analysis

Categorical data were presented by number (%) and numerical data by median (interquartile range IQR, i.e. 25th - 75th percentile). The pre- and post-LVAD differences of HPTG in myocardial tissue were evaluated with Wilcoxon signed-rank test. Circulating HPTG was log-transformed because of non-normal distribution (histogram, QQ-plot). The log-transformed data were evaluated using the linear mixed model analysis with a random intercept to account for the correlation between repeated measurements within the same person. The differences in plasma levels of HPTG between patients and healthy controls were tested using Mann-Whitney U-test. The intra-observer variability of myocardial HPTG expression was indicated by unweighted and weighted kappas. A p value ≤0.05 is considered significant. All analyses were performed using SPSS, version 20 (SPSS, Inc., Chicago, Illinois).

Results

Baseline characteristics

Patient demographics are presented in *Table 1*. All patients presented initially with class NYHA-IV despite optimal medical therapy, including intravenous inotropic therapy. Twenty-seven patients (73%) were male. The median duration of HF was 1415 days (95-2301) and the median LVAD duration 422 days (195-685). The change in hemoglobin, thrombocytes, LDH and bilirubin during cf-LVAD are presented in *Figure 1*. There was a rapid decrease in hemoglobin (p<0.001) and bilirubin levels (p<0.001) after 1 month of cf-LVAD implantation, whereas the number of thrombocytes increased (p<0.001). Lactate dehydrogenase (LDH) increased significantly during support (pre vs 1 month p=0.001; pre vs 6 months p=0.006).

2D-DIGE reveals a significant decrease in haptoglobin

2D-DIGE on myocardial tissue of 8 DCM patients identified 40 proteins that changed significantly during cf-LVAD support. Nine proteins were significantly up-regulated. Mass spectrometry identified 18 proteins, of which HPTG showed the strongest decline (ratio 6.67; p<0.001) during support (*Figure 2*).

Table 1: Baseline demographics of 37 patients prior to continuous flow LVAD (cf-LVAD) implantation

Age, years	45 (31-54)
Male	27 (73%)
Duration of HF, days	1415 (95-2301)
NYHA[b] classification IV	37 (100%)
bvPM/ICD[c]	22 (56%)
Etiology of non-ischemic DCM	
Idiopathic	12 (31%)
Familial[d]	15 (38%)
Myocarditis	7 (18%)
Peripartum	1 (3%)
Toxic (drugs/medication)	2 (5%)
cf-LVAD support, days	422 (195-685)

[a] Categorical data are presented as number (%) and continuous data as median (25-75% percentile)

[b] NYHA: New York Heart Association Class.

[c] bi-ventriculaire pacemaker/ Implantable Cardioverter Defibrillator.

[d] Familial DCM is defined when de patient has one or more family members who are diagnosed with idiopathic DCM or has a first-degree relative with an unexplained sudden death under the age of 35 years.
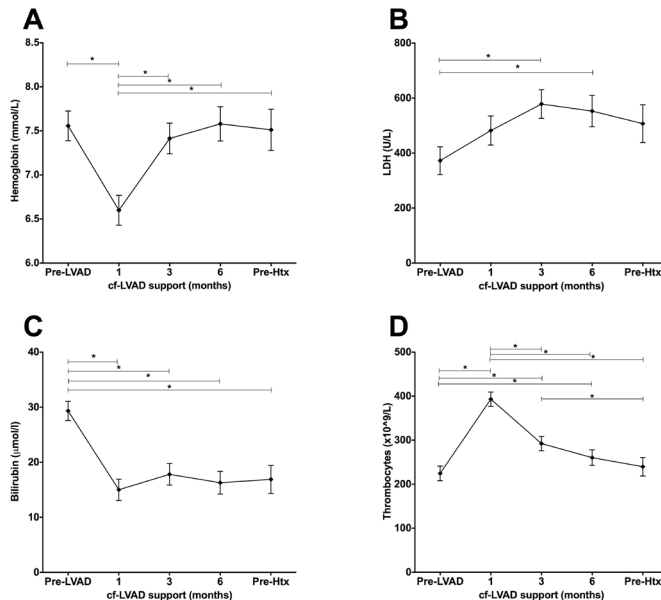
Figure 1: Laboratory parameters before and during continuous flow LVAD (cf-LVAD) support (n=39)
There was a rapid decrease in hemoglobin (*A*; p<0.001) and bilirubin levels (*C*; p<0.001) after 1 month of cf-LVAD implantation, whereas the number of thrombocytes increased (*D*; p<0.001). Lactate dehydrogenase (LDH) increased significantly during support (*B*; pre vs 1 month p=0.001; pre vs 6 months p=0.006). Data are presented as estimated means with standard error. The asterisk (*) represents p<0.05.
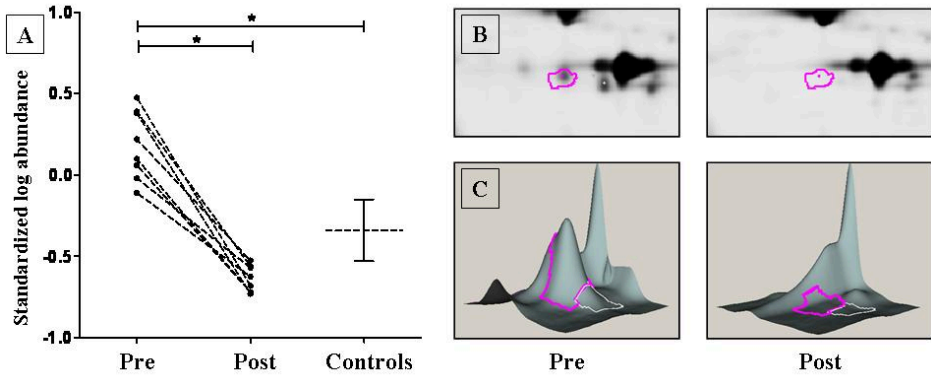
Figure 2: Identification of haptoglobin (HPTG) in myocardial tissue 2D-DIGE
HPTG is significantly elevated pre-LVAD compared to controls (p=0.027) and decreased significantly during support (p=0.008). Each line represents 1 patient. Controls are presented as mean and standard error of the mean (*A*). 2D-DIGE gel of HPTG spot pre- and post cf-LVAD (*B*) with representative images (*C*). The asterisk (*) represents p<0.05.

mRNA expression of HPTG remains stable

The low mRNA expression of HPTG in the myocardium of HF patients did not alter significantly after LVAD support (*Figure 3*).
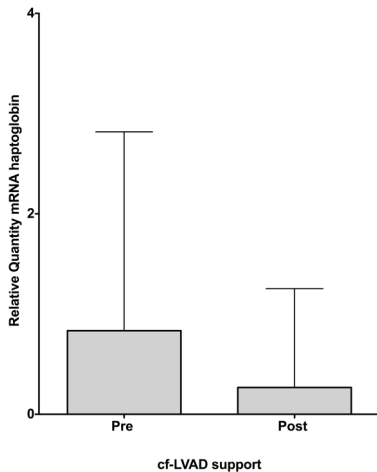
Figure 3: Relative quantity of cardiac mRNA of haptoglobin (HPTG) pre- and post-LVAD
Low mRNA expression of HPTG in the myocardium of heart failure patients did not change significantly after continuous flow LVAD (cf-LVAD) support. Data are presented as median ± interquartile range.

Plasma haptoglobin decreases significantly during support

HPTG levels of end-stage HF patients prior to cf-LVAD implantation were high, but statistically not different from levels in healthy controls (p=0.19; *Figure 4*). After 1 month of cf-LVAD implantation, HPTG levels were significantly lower (p<0.001) than in controls and remained stable thereafter.

Haptoglobin is expressed in the endothelium pre-LVAD and changes during support

In the myocardium, especially the endothelial and stromal cells stained strongly for HPTG pre-LVAD and this intensity decreased dramatically post-LVAD (*Figure 5*). The capillaries in the interstitial fibrotic tissues (epimysium) surrounding the muscles stained more pronounced compared to capillaries in between cardiomyocytes. HPTG expression in cardiomyocytes changed from an alternating pattern pre-LVAD, demonstrating either low or strong expression of HPTG, to a weak diffuse pattern in all cardiomyocytes post-LVAD. The unweighted kappas showed excellent agreement in HPTG staining of cardiomyocytes, endothelial tissue and stromal cells (0.86, 0.88, 0.81, respectively). Moreover, the weighted kappas (linear and quadratic) were even higher (0.88 and 0.91 for cardiomyocytes, 0.93 and 0.97 for endothelial tissue, 0.83 and 0.88 for stromal cells).

5
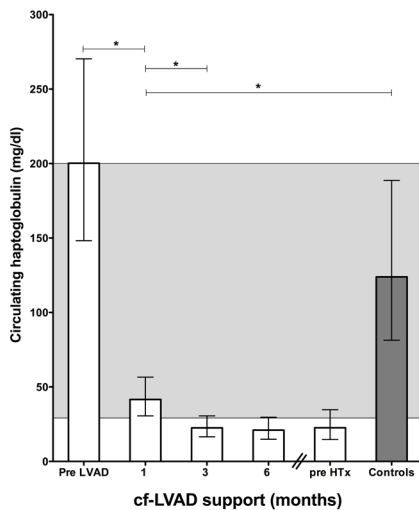
Figure 4: Circulating haptoglobin (HPTG) during continuous flow LVAD (cf-LVAD) support
Prior to cf-LVAD support, HPTG levels were not significantly elevated compared to controls (p=0.18). After cf-LVAD implantation, HPTG levels decreased significantly at 1 month (p<0.001) and at three months (p=0.002; 1 month versus 3 months) and remained stable thereafter. The normal range of circulating HPTG (30-200 mg/dl) is represented as the grey area. Data are presented as the estimated means and 95%-confidence interval. The asterisk (*) represents p<0.05.
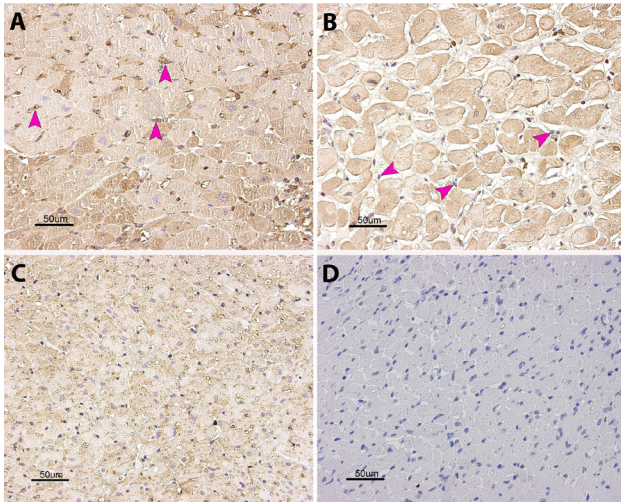
Figure 5: Immunohistochemical (IHC) expression of haptoglobin (HPTG) in the heart
Myocardial tissue of representative heart failure patient pre-LVAD (*A*) and post-LVAD (*B*). Myocardium of healthy control (*C*) and negative IHC control (*D*).
Note the different intra-myocardial staining between pre- (*A*) and post- (*B*) LVAD in stromal elements (pink arrows).

Discussion

There is an urgent need to better understand the cellular events that trigger the cascade of functional and structural changes that results in development of HF, as well as the compensatory changes that take place to preserve cardiac function during LVAD support. Proteomics can be used to obtain a better understanding of these processes and to develop new biomarkers for diagnosis and early detection of cardiovascular disease. By using proteomics in myocardial tissue of pre and post-LVAD HF patients, a strong decline in HPTG levels was observed in patients with end-stage HF after cf-LVAD implantation. It was shown that HPTG was mainly localized in the endothelial and stromal cells in the myocardium before cf-LVAD support, but was almost absent after support. This is of interest, since the expression of mRNA of HPTG in the heart was low, suggesting that the heart is not an important source for HPTG production. Hence, the myocardial HTPG expression must be due to passive uptake from the circulation.

Holme *et al* demonstrated that HPTG-levels predict the risk of acute myocardial infarction, stroke and HF in a large group of healthy volunteers [11]. HPTG can act as a prognostic marker for the development of HF following acute myocardial infarction [12,13]. In addition, HPTG is an acute phase-protein induced by cytokines, such as interleukin-6. Inflammatory activity is important in the pathogenesis and the progression of chronic HF. Increased plasma levels of inflammatory cytokines are described in HF patients [14], which is in concordance with the

high plasma level of HPTG measured in pre-LVAD samples in the present study.

HPTG possesses immune-regulative properties, inhibits prostaglandin synthesis and protects against harmful oxidation processes [15,16]. Yet, the main function of HPTG is the binding and scavenging of free hemoglobin in the extra-vascular compartment. Due to the high rotor speed and interaction with artificial surface in cf-LVADs, red blood cells are damaged leading to free and toxic hemoglobin. This toxicity arises from the heme-iron that, after reaction with endogenous hydrogen peroxide, produces free radicals causing severe oxidative tissue damage [17]. Hemoglobin is a potent scavenger of nitric oxide, leading to impaired regulation of smooth muscle tone, platelet activation and aggregation promoting clot formation [18-21]. HPTG counteracts this hemoglobin toxicity by capturing the released hemoglobin and directing it to CD163-expressing macrophages, which internalize the complex [22].

The HPTG-levels decline rapidly after LVAD implantation and remain low for the rest of the support period. This confirms previous data by Heilmann *et al* [23] that also reported that levels of circulating HPTG remained low after mechanical support, and likewise even below control levels. We hypothesized that the absence of HPTG expression in endothelial and stromal cells in the myocardial tissue post-LVAD can be explained by the binding of HPTG to the increased free hemoglobin by mechanical erythrocyte damage, to prevent heme-iron mediated oxidation. The fact that HPTG mRNA in the myocardium was low and remained low during mechanical support suggested that there is, independently of the condition of the myocardium, no significant HPTG production in the heart. This is supported by our finding that, after cf-LVAD support, hardly any HPTG can be detected in the stromal/endothelial cells of the myocardium. This indicates that the presence of HPTG in the myocardium of HF patients is due to import of HPTG from the circulation, which subsequently binds to the cells.

Conclusion

Haptoglobin (HPTG) decreased both in the extracellular space of the heart and in the plasma of cf-LVAD supported patients. Local production of HPTG in the myocardium seems negligible and the HPTG present in stromal and endothelial cells is most likely imported from the pool of circulating HPTG. During LVAD support, unbound HPTG diminishes, which is probably due to an increase in hemolytic activity and by the decrease in HF with subsequent less inflammatory activity. The clinical consequences of severe hemolysis are unknown and require further investigations.

References

1.   Rose EA, Gelijns AC, Moskowitz AJ, Heitjan DF, Stevenson LW, Dembitsky W, et al. Long-term use of a left ventricular assist device for end-stage heart failure. N. Engl. J. Med. 2001 Nov 15;345(20):1435–43.

2.   Rogers JG, Butler J, Lansman SL, Gass A, Portner PM, Pasque MK, et al. Chronic mechanical circulatory support for inotrope-dependent heart failure patients who are not transplant candidates: results of the INTrEPID Trial. J. Am. Coll. Cardiol. 2007 Aug 21;50(8):741–7.

3.   Soppa GKR, Barton PJR, Terracciano CMN, Yacoub MH. Left ventricular assist device-induced molecular changes in the failing myocardium. CurrOpinCardiol. 2008 May;23(3):206–18.

4.   Birks EJ, George RS. Molecular changes occurring during reverse remodelling following left ventricular assist device support. J CardiovascTransl Res. 2010 Dec;3(6):635–42.

5.   Lok SI, van Mil A, Bovenschen N, van der Weide P, van Kuik J, Van Wichen D, et al. Post-transcriptional Regulation of α-1-Antichymotrypsin by MicroRNA-137 in Chronic Heart Failure and Mechanical Support. Circ Heart Fail. 2013 Jul 1;6(4):853–61.

6.   deWeger RA, Schipper MEI, Siera-de Koning E, van der Weide P, van Oosterhout MFM, Quadir R, et al. Proteomic profiling of the human failing heart after left ventricular assist device support. J Heart Lung Transplant. 2011 May;30(5):497–506.

7.   Bovenschen N, Quadir R, van den Berg AL, Brenkman AB, Vandenberghe I, Devreese B, et al. Granzyme K displays highly restricted substrate specificity that only partially overlaps with granzyme A. J Biol Chem. 2009 Feb 6;284(6):3504–12.

8.   Alban A, David SO, Bjorkesten L, Andersson C, Sloge E, Lewis S, et al. A novel experimental design for comparative two-dimensional gel analysis: two-dimensional difference gel electrophoresis incorporating a pooled internal standard. Proteomics. 2003 Jan 1;3(1):36–44.

9.   Wilm M, Shevchenko A, Houthaeve T, Breit S, Schweigerer L, Fotsis T, et al. Femtomole sequencing of proteins from polyacrylamide gels by nano-electrospray mass spectrometry. Nature. 1996 Feb 1;379(6564):466–9.

10.   Fleiss JL. Statistical methods for rates and proportions.Second edition [Internet]. 1981. Available from: http://books.google.com/books?id=I79_MgAACAAJ&dq=Fleiss+J+L+1981+Statistical+methods+for+rates+and+proportions&cd=14&source=gbs_api.

11.   Holme I, Aastveit AH, Hammar N, Jungner I, Walldius G. Haptoglobin and risk of myocardial infarction, stroke, and congestive heart failure in 342,125 men and women in the ApolipoproteinMOrtalityRISk study (AMORIS). Ann. Med. 2009;41(7):522–32.

12.   Pinet F, Beseme O, Cieniewski-Bernard C, Drobecq H, Jourdain S, Lamblin N, et al. Predicting left ventricular remodeling after a first myocardial infarction by plasma proteome analysis. Proteomics. 2008 May;8(9):1798–808.

13.   Haas B, Serchi T, Wagner DR, Gilson G, Planchon S, Renaut J, et al. Proteomic analysis of plasma samples from patients with acute myocardial infarction identifies haptoglobin as a potential prognostic biomarker. J Proteomics. 2011 Dec 10;75(1):229–36.

14. Anker SD, Haehling von S. Inflammatory mediators in chronic heart failure: an overview. Heart. 2004 Apr;90(4):464–70.

15. Braeckman L, De Bacquer D, Delanghe J, Claeys L, De Backer G. Associations between haptoglobin polymorphism, lipids, lipoproteins and inflammatory variables. Atherosclerosis. 1999 Apr;143(2):383–8.

16. Langlois MR, Delanghe JR. Biological and clinical significance of haptoglobin polymorphism in humans. Clin. Chem. 1996 Oct;42(10):1589–600.

17. Sadrzadeh SM, Graf E, Panter SS, Hallaway PE, Eaton JW. Hemoglobin. A biologic fenton reagent. J Biol Chem. 1984 Dec 10;259(23):14354–6.

18. Rother RP, Bell L, Hillmen P, Gladwin MT. The clinical sequelae of intravascular hemolysis and extracellular plasma hemoglobin: a novel mechanism of human disease. JAMA. 2005 Apr 6;293(13):1653–62.

19. Levy AP, Asleh R, Blum S, Levy NS, Miller-Lotan R, Kalet-Litman S, et al. Haptoglobin: basic and clinical aspects. Antioxid. Redox Signal. 2010 Feb;12(2):293–304.

20. Buehler PW, D'Agnillo F. Toxicological consequences of extracellular hemoglobin: biochemical and physiological perspectives. Antioxid. Redox Signal. 2010 Feb;12(2):275–91.

21. Nielsen MJ, Moestrup SK. Receptor targeting of hemoglobin mediated by the haptoglobins: roles beyond heme scavenging. Blood. 2009 Jul 23;114(4):764–71.

22. Kristiansen M, Graversen JH, Jacobsen C, Sonne O, Hoffman HJ, Law SK, et al. Identification of the haemoglobin scavenger receptor. Nature. 2001 Jan 11;409(6817):198–201.

23. Heilmann C, Geisen U, Benk C, Berchtold-Herz M, Trummer G, Schlensak C, et al. Haemolysis in patients with ventricular assist devices: major differences between systems. Eur J Cardiothorac Surg. 2009 Sep;36(3):580–4.

5
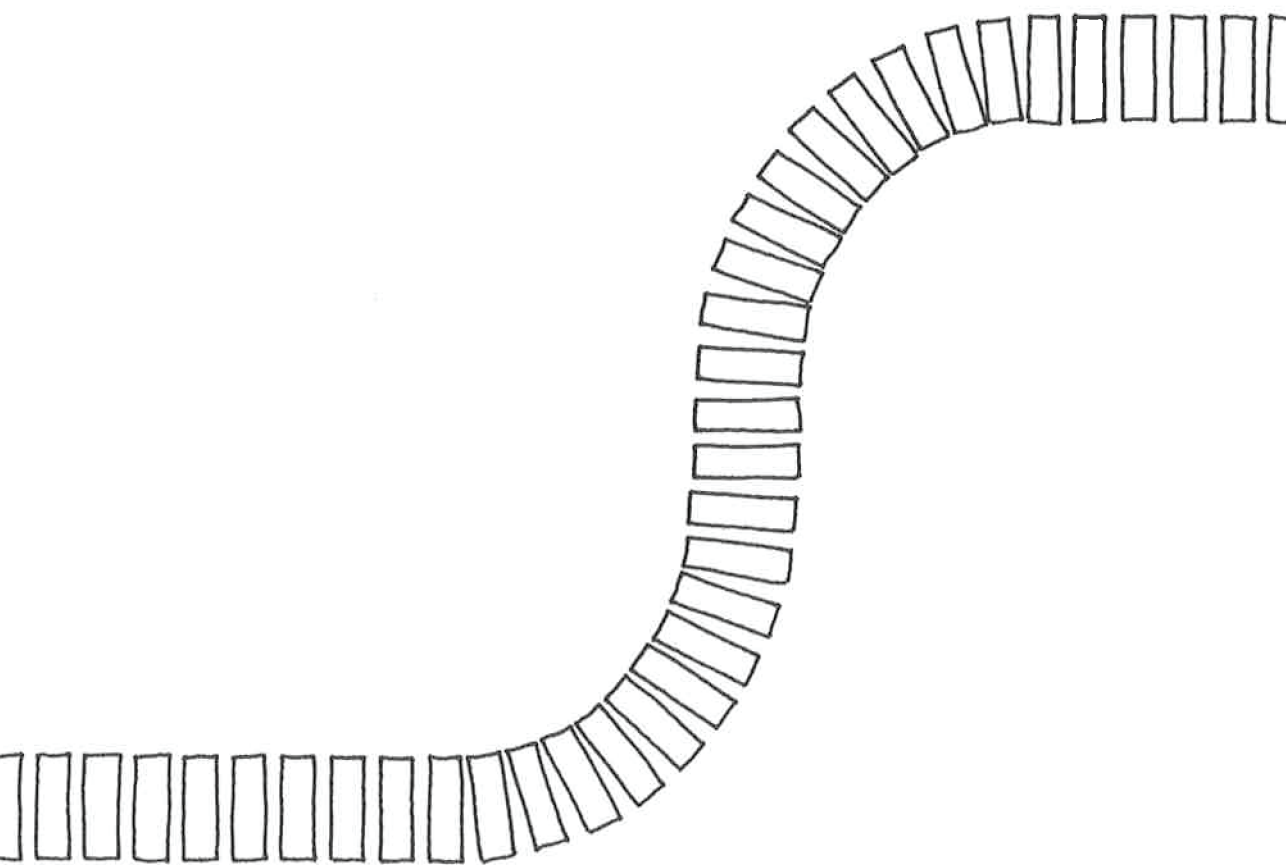
CHAPTER 6

Post-transcriptional regulation of alpha-1-antichymotrypsin by miR-137 in chronic heart failure and mechanical support

Sjoukje I. Lok[1], Alain van Mil[1,5], Niels Bovenschen[2], Petra van der Weide[2], Joyce van Kuik[2], Dick van Wichen[2], Ton Peeters[2], Erica Siera[2], Bjorn Winkens[3], Joost P.G. Sluijter[1,5], Pieter A. Doevendans[1,5], Paula A. da Costa Martins[4], Nicolaas de Jonge[1], Roel A. de Weger[2]

[1] Department of Cardiology, University Medical Centre Utrecht
[2] Department of Pathology, University Medical Center, Utrecht
[3] Department of Methodology and Statistics, University of Maastricht
[4] Department of Cardiology, University of Maastricht
[5] ICIN Netherlands Heart Institute, Utrecht

Abstract

Background: Better understanding of the molecular mechanisms of remodeling has become a major objective of heart failure (HF) research to stop or reverse its progression. Left ventricular assist devices (LVADs) are being used in patients with HF, leading to partial reverse remodeling. In the present study, proteomics identified significant changes in alpha-1-antichymotrypsin (ACT) levels during LVAD support. Moreover, the potential role of ACT in reverse remodeling was studied in detail.

Methods and results: Expression of ACT mRNA (Q-PCR) decreased significantly in post-LVAD myocardial tissue compared to pre-LVAD tissue (n=15; p<0.01). Immunohistochemistry revealed that ACT expression and localization changed during LVAD support. Circulating ACT levels were elevated in HF patients (n=18) as compared to healthy controls (n=6; p=0.001) and normalized upon 6 months of LVAD support. Since increasing evidence implicates that microRNAs (miRs) are involved in myocardial disease processes, we also investigated whether ACT is post-transcriptional regulated by miRs. Bioinformatics analysis pointed miR-137 as a potential regulator of ACT. The miR-137 expression inversely correlated with ACT mRNA in myocardial tissue. Luciferase activity assays confirmed ACT as a direct target for miR-137 and *in situ* hybridization indicated that ACT and miR-137 were mainly localized in cardiomyocytes and stromal cells.

Conclusion: High ACT plasma levels in HF normalized during LVAD support, which coincides with decreased ACT mRNA in heart tissue, whereas miR-137 levels increased. MiR-137 directly targeted ACT, thereby indicating that ACT and miR-137 play a role in the pathophysiology of HF and reverse remodeling during mechanical support.

Introduction

Heart failure (HF) is considered a highly complex clinical syndrome, manifested by many cardiac and extra-cardiac features [1]. The complex sequelae of HF which take place in the heart, are generally referred to as 'cardiac remodeling' and involve molecular and cellular processes that result in changes of size, shape and function of the heart after injury or stress stimulation [1,2]. Left ventricular assist devices (LVADs) provide a unique and valuable opportunity to investigate reverse remodeling in humans, since they provide volume and pressure unloading of the left ventricle, thereby reversing the compensatory responses of the overloaded myocardium [3,4].

There is substantial interest in applying proteomics to obtain better understanding of disease processes and to develop new biomarkers for diagnosis and early detection of cardiovascular diseases [5,6]. The purpose of the present study was to investigate proteomic changes in reverse remodeling during LVAD support. Since the degree of reverse remodeling is more pronounced in patients with non-ischemic dilated cardiomyopathy (DCM) [7], we focused on this subset of patients.

Recently, we have found that levels of alpha-1-antichymotrypsin (ACT) decrease in myocardial tissue during pulsatile flow LVAD (pf-LVAD) support, which was detected by proteomics and confirmed by immunosorbent assays [8]. However, the molecular pathways regulating ACT expression in the heart were not explored.

Clinically, pf-LVAD support is being replaced by continuous flow LVAD (cf-LVAD) support. Therefore, we performed proteomics in plasma and heart tissue of DCM patients, supported with a cf-LVAD. This approach suggested a potential role of ACT during reverse remodeling in cf-LVAD, which was experimentally confirmed in individual patients by ELISA, Q-PCR and protein localization.

MicroRNAs (miRs) are small, non-coding RNAs that bind mRNAs at their 3'-untranslated regions, stimulating mRNA degradation or inhibiting protein translation [9]. Delineating the role of miRs in posttranscriptional gene regulation offers new insight into the mechanisms how the heart adapts to mechanical support. Moreover, miRs can be important hallmarks for recovery or deterioration and can be used as a therapeutic target in HF [10]. Therefore, the post-transcriptional regulation of ACT by miRs was investigated.

This study revealed a potential role of ACT, and its post-transcriptional regulator miR-137 in the pathophysiology of HF and reverse remodeling during mechanical support.

6

Materials and methods

Study population

Eighteen patients were included with a non-ischemic DCM supported with a cf-LVAD (HeartMate II, Thoratec, CA, USA) as bridge to heart transplantation (HTx). Plasma was collected before and 1, 3 and 6 months after LVAD implantation. Control plasma was collected from 6 healthy individuals.

Of the 18 patients included, 15 underwent HTx. Myocardial tissue of each individual patient was collected at time of LVAD implantation (pre-LVAD) and from the explanted left ventricle (post-LVAD), outside the suture area of the inflow cannula. Control myocardial tissue was obtained from 3 donor hearts declined for HTx (due to non-cardiac reasons) and from biopsies of 7 donor hearts during HTx surgery. All LVAD patients gave written informed consent for the use of their tissues for research purposes.

2D-DIGE

With the use of fluorescent 2-dimensional difference gel electrophoresis (2D-DIGE), a comparative analysis was made of protein expression in tissue and plasma of DCM patients prior to and after cf-LVAD implantation. Paired pre- and post-myocardial tissue of 8 patients and 4 controls were analyzed. In addition, EDTA plasma prior to implantation and 6 months after implantation was used of 8 DCM patients and 5 controls (supplementary data). Differentially expressed proteins were excised and identified by tandem mass spectrometry (supplementary data).

Plasma levels of ACT

EDTA-blood was centrifuged at 3,000 rpm for 10 min, plasma was collected and stored at -20° C. Circulating ACT was determined by ELISA (supplementary data).

ACT mRNA and miR-137 levels

Total RNA was isolated from 20 sections of 10-μm snap-frozen myocardial tissue using miRNeasy Mini Kit (Qiagen Inc, Austin, USA). Copy DNA (cDNA) for ACT was synthesized with superscript III, oligo-dT and random primers (Life Technologies, Bleiswijk, the Netherlands). mRNA expression of ACT was determined by Q-PCR on the LightCycler-480 (Roche Diagnostics BV, Almere, the Netherlands) as described previously [11]. A detailed description is provided in the supplementary data. For miR-137, a two-step protocol consisting of reverse transcription with a miR specific primer followed by Q-PCR

with a TaqMan probe was performed on the ViiA 7 (Life Technologies).

Immunohistochemistry (IHC)

The expression of ACT and its major target for proteinase inhibition, cathepsin G (CG), was analyzed by IHC in formalin fixed paraffin embedded sections. Endogenous peroxidase was blocked with H_2O_2 for 15 min. Sections were pre-treated with either citrate (ACT) or EDTA (CG) and incubated with primary antibody diluted in PBS/1% BSA for 1 hr. (ACT, diluted 1:50, rabbit anti-human ACT, Dako, Glostrup, Denmark; CG diluted 1:100, mouse anti-human CG, Abcam, Cambridge, USA). Power Vision poly-Anti-Rabbit IgG (Immunovision Technologies, Hillsborough, USA) and RamPo (diluted 1:500 + 10% Normal Human Serum (NHuS), Polyclonal rabbit anti mouse Immunoglobulin Horseradish Peroxidase (HRP), Dako) were used as secondary antibodies for ACT and CG, respectively. The slides were developed with 3,3'-diaminobenzidine-hydrochloride (DAB) solution for 10 min. The nuclei were counterstained with Mayer's Haematoxylin. In every section, 3 areas were selected at random and the ACT staining of cardiomyocytes, epithelial and stromal cells was scored and the modus was calculated. ACT expression was analyzed using a scoring system; 0=no staining, 1=weak, 2=moderate, 3=strong. This was performed individually by 3 observers, from which the intra-observer agreement was assessed using unweighted and weighted kappas.

Double staining ACT and anti-cardiac actin

After staining with the primary antibody for ACT (diluted 1:50, rabbit anti-human ACT, Dako), slides were incubated with swine anti-rabbit Ig Tetramethylrhodamine isothiocyanate (TRITC)-labeled (Dako, 1:40) in PBS and 10% human AB-serum. After a wash in PBS/Tween-20, the slides were incubated with a solution of PBS and 10% normal rabbit serum (nRBS) for 30 min. After decanting the solution, the slides were horizontally incubated with monoclonal anti-actin (α-Sarcomeric) antibody produced in mouse (Sigma-Aldrich Inc., St. Louis, USA, 1:500) in PBS and 10% nRBS. Incubation was followed by a washing step in PBS/Tween-20. The slides were horizontally incubated with rabbit anti mouse FITC (Dako, 1:50) in PBS and 10 % AB-serum. After a wash with PBS/Tween-20, the slides were incubated with Topro-3 iodide (Life Technologies, 1:500) in PBS Tween-20 and cover slips were mounted onto object glasses using vectashield-mounting medium (VectorLaboratories Inc., Burlingame, USA).

6

In situ hybridization (ISH) for ACT mRNA and miR-137

ISH for ACT mRNA was performed on tissue slides from freshly frozen paired myocardial samples of 4 patients pre- and post-LVAD support and of two controls (donor hearts declined for HTx; supplementary data). Negative (ISH without probe) and positive controls were included. To test the specificity of the ISH signal of ACT, a non-relevant probe (interleukin-2; IL-2) was tested in parallel.

Locked Nucleic Acid (LNA) hybridization probes for miR-137 and negative control miRCURY LNA Sense (scramble) were conjugated with 3'- 5'digoxigenin. Positive control probe U6 was conjugated with 5'digoxigenin. miR *in situ* was performed as described at http://www.exiqon.com/insitu. All LNA reagents were obtained from Exiqon (Vedbaek, Denmark).

miR transfection

The human hepatoma cell line (HepG2) was used as a model to examine expression of ACT mRNA after miR-137 transfection. Cells were re-suspended in normal growth medium to 1x 10^5 cells/500 ml. A total of 0.5 µl of interleukin-6 (IL-6) was added to stimulate ACT production. Pre-miRTM miRNA Precursor Molecules for miR-137 (PM10513) or a Negative Precursor Control (AM17110; non-targeting sequence) were transfected with 1 µl lipofectamine RNAiMax, according to the instruction of the manufacturer (Life Technologies). In addition, some cells were left untreated (non-transfection). As a positive control for HepG2 transfection, miRNA Precursor molecules for miR-1 (PM10617) were transfected and the effect on protein tyrosine kinase-9 (PTK-9), a validated miR-1 target, was determined. After 48 hours, total RNA of the HepG2 cells was isolated as described earlier. The transfection experiments were performed 7 and 10 times for miR-1 and mir-137, respectively.

Luciferase assay

The 3'untranslated region (UTR) of ACT was cloned into the pMIR-REPORT Luciferase vector (Life Technologies). Mutations for the miR-137 target site were generated by QuikChange II Site-Directed Mutagenesis (Agilent Technologies, Amstelveen, the Netherlands). To determine the suppression efficiency of miR-137, 4 luciferase experiments were performed. In each experiment 2 x 10^5 Human Embryonic Kidney-293 (HEK293) cells were co-transfected with 200 ng pMIR-REPORT-ACT-3'UTR Luciferase vector, or the mutated vector and a pMIR-REPORT β-gal control plasmid for normalization of transfection efficiency. In addition, 50 nmol/L precursor miR-137, or a negative control

precursor miR, or a miR without predicted target sites for ACT were introduced by using Lipofectamine 2000 (Life Technologies). Luciferase and β-galactosidase activity was assessed after 48 h with the Luciferase Assay System and β-galactosidase Enzyme Assay System (Promega), respectively, as described before [12].

Statistical analysis

Due to the small sample size and expected non-normality, the ACT isoforms and Q-PCR data (for ACT and miR-137) were presented as median with first and third quartile (Q1-Q3), and evaluated with the Wilcoxon signed-rank test. Plasma data were plotted and evaluated using the mixed model analysis with a random intercept to account for the dependency between repeated measurements within the same patient. Data from patients pre- and post LVAD were compared with healthy controls using Mann-Whitney U test. The inter-observer variability of ACT expression in the heart was indicated by unweighted and weighted kappas. The statistical analysis of 2D-DIGE gel spot volume quantification, transfection experiments and the luciferase reporter assays were presented as mean and standard error of the mean (SEM) and evaluated with the paired samples t-test. A p value ≤0.05 was considered significant. All analyses were performed using SPSS, version 18 (SPSS, Inc., Chicago, Illinois).

Results

Patient characteristics

Patient demographics are shown in *Table 1*. All patients presented initially with HF NYHA IV class despite optimal medical therapy, including intravenous inotropic therapy. Median age was 43 years (Q1-Q3 28-48), 78% (n=14) was male and 44% (n=8) had a familial cause of DCM. A total of 61% (n=11) of the patients had a CRTD or ICD prior to cf-LVAD implantation. The median duration of mechanical support, based on the patients that already underwent HTx (n=15), was 282 days (Q1-Q3 207-521).

2D-DIGE identifies ACT changes in plasma and myocardial tissue during LVAD support

2D-DIGE on myocardial tissue of 8 DCM patients identified 40 proteins that changed significantly during cf-LVAD support, of which 9 were upregulated. 2D-DIGE on plasma of 8 DCM patients identified 97 proteins that were significantly different in the pre- versus the post-pool. Ninety proteins were downregulated and 7 were upregulated. Of all proteins,

6

only ACT changed significantly in *both* tissue and plasma during cf-LVAD support. Five different isoforms of ACT were detected in myocardial tissue of which 2 were significantly down regulated during cf-LVAD support (1.78-2.39 down-fold; *Figure 1 A-F*). Four different isoforms of circulating ACT were detected, all of them being significantly down regulated during cf-LVAD (2.03-2.74 down-fold; *Figure 1 G-J*).

Table 1: Baseline characteristics of patients with end-stage dilated cardiomyopathy (DCM) prior to continuous flow LVAD (cf-LVAD) support.

Patient demographics

Characteristic[a]	Patients (n=18)
Age, years	43.0 (28.0 - 48.0)
Male, %	14 (78%)
Body Mass Index, kg/m^2	24.2 (20.1 - 26.0)
Heart failure duration (days)	1675 (416-1954)
Diabetes mellitus, %	0 (0%)
Hypertension, %	1 (6%)
Hyperlipidemia, %	4 (22%)
CVA/TIA, %	5 (28%)
NYHA classification IV, %	18 (100%)
Etiology of non-ischemic DCM, %	
Idiopathic	5 (28%)
Familial[b]	8 (44%)
Myocarditis	2 (11%)
Peripartum	1 (6%)
Toxic (drugs/medication)	2 (11%)
Pre-operative intervention (CRTD/ICD), %	11 (61%)
Days of LVAD support[c]	282 (207-521)

CVA, cerebrovascular accident; TIA, transient ischemic attack; NYHA, New York Heart Association;
DCM, dilated cardiomyopathy; CRTD, cardiac resynchronization therapy defibrillator;
ICD, implantable cardioverter defibrillator.
[a] Categorical data are presented as number (%) and continuous data as median (25% - 75% percentile)
[b] Familial DCM is defined if the patient has one or more family members diagnosed with idiopathic
DCM or has a first-degree relative with an unexplained sudden death under the age of 35 years
[c] Days of LVAD support are based on the patients who already underwent heart transplantation (n=15).
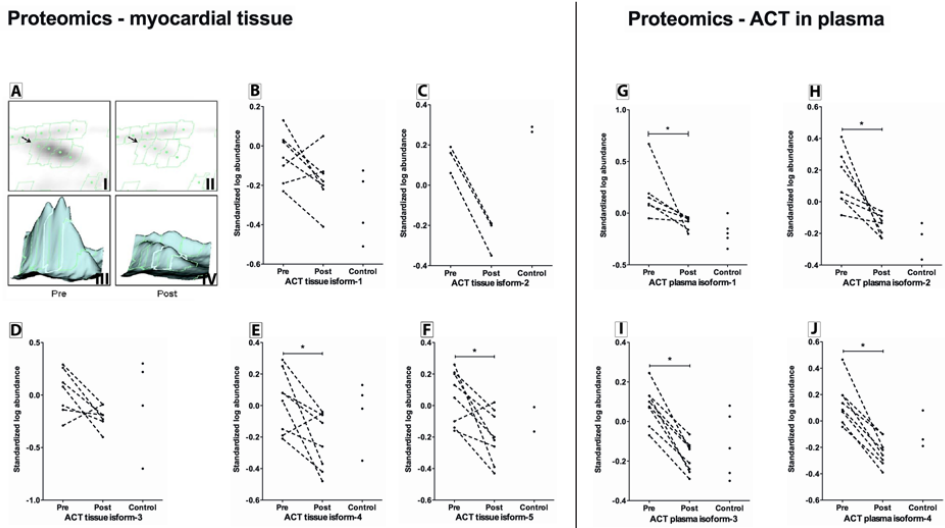
Figure 1: 2D-DIGE of myocardial tissue (n=8 patients, n=4 controls) and plasma (n=8 patients, n=5 controls) prior to and after continuous flow LVAD (cf-LVAD) implantation

Representative 2D-image of alpha-1-antichymotrypsin (ACT) in myocardial tissue pre- and post-LVAD (*A*). Proteomics of myocardial tissue (*B-F*) revealed two out of five ACT isoforms that were significantly down regulated in the post-LVAD sample as compared to pre-LVAD (*E*, * p=0.04; *F*, * p=0.02). Proteomics revealed 4 different isoforms of circulating ACT that changed pre-LVAD as compared to 6 months after LVAD implantation (*G-J*). All isoforms were significantly down regulated (*G*, * p=0.04; *H*, * p=0.02; *I*, * p =0.01; *J*, * p=0.008). Each line represents 1 patient.
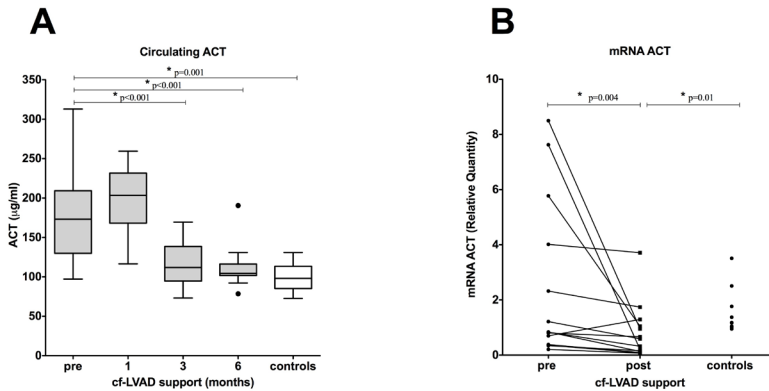
Figure 2: Circulating levels of alpha-1-antichymotrypsin (ACT) and ACT mRNA expression before and after continuous flow LVAD (cf-LVAD) support

Circulating ACT (µg/ml) in end-stage dilated cardiomyopathy patients (n=18 patients, n=6 controls) prior to, and 1, 3 and 6 months after continuous flow LVAD (cf-LVAD) implantation, demonstrated in Tukey boxplots (*A*). After 1 month, there was a non-significant increase followed by normalization after 6 months of support.

mRNA expression of ACT (*B*). After cf-LVAD support, there was a significant decrease in mRNA to levels lower than that of controls (n=15 patients, n=9 controls). Some inter-individual variation was observed.

Elevated circulating ACT levels normalize during mechanical support

ACT plasma levels were significantly elevated in end-stage HF patients prior to LVAD implantation as compared to healthy controls (p=0.001; *Figure 2A*). After 1 month of LVAD support, the concentration of circulating ACT showed a non-significant increase (p=0.08). However, after 3 and 6 months of LVAD support, plasma ACT decreased significantly compared to baseline (both p<0.001) and ultimately reached a similar level as controls (p=0.18).

ACT mRNA and protein expression change during mechanical support

Myocardial mRNA expression of ACT was increased in DCM patients prior to cf-LVAD implantation in comparison to controls, but did not reach significance (p=0.26, *Figure 2B*). After cf-LVAD support, mRNA ACT decreased significantly (median change -0.41, Q1-Q3 -1.71 – -0.17, p=0.004) to levels lower than that of controls (p=0.01).

Localization and distribution of ACT protein in the myocardium during cf-LVAD support was determined by IHC. ACT-expression prior to LVAD support was weak to moderate in the cardiomyocytes, whereas the expression of ACT in the endothelium and stromal cells in the interstitium was strong (arrowheads; *Figure 3A*). If present, inflammatory cells tended to stain as well. After LVAD support (*Figure 3B*), ACT expression in the cardiomyocytes changed from a diffuse pattern towards an alternating pattern demonstrating either low or strong expression of ACT ("on-off effect") in different cardiomyocytes, mainly in the central area of the myocardium. In contrast, expression in the endothelium and in the stromal cells became very low (arrowheads; *Figure 3B*). In controls (*Figure 3C*), cardiomyocytes stained weak with only very occasionally an "on-off effect". Stromal cells and capillaries stained moderately. The unweighted kappas showed excellent agreement in ACT staining of cardiomyocytes, endothelial tissue and stromal cells (0.90, 0.85, 0.91, respectively). Moreover, the weighted kappas (linear and quadratic) were even higher (0.91 and 0.92 for cardiomyocytes, 0.87 and 0.89 for endothelial tissue, and both 0.91 for stromal cells).

To investigate if the "on-off effect" was caused by induced cell death, we performed double immunohistochemical staining (IHC) staining with anti-cardiac actin and ACT. Merging the images clearly showed that the contractile elements were present both in the ACT stained and in the non-stained cells (*Figure 4A-D*), indicating that apoptosis is not related to ACT expression.

Cathepsin G (CG) expression was not localized in cardiomyocytes, endothelium, capillaries or extracellular matrix, but was, but was only present in few scattered mast cells (data not shown).
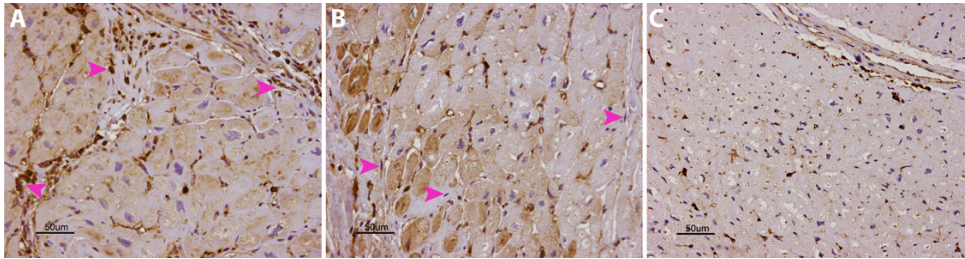
Figure 3: Immunohistochemistry of alpha-1-antichymotrypsin (ACT) before and after continuous flow LVAD (cf-LVAD) support

Myocardial tissue pre-LVAD (*A*), post-LVAD (*B*) support and control (donor hearts declined for heart transplantation; *C*) was stained. Notice the difference in ACT staining in the cardiomyocytes (diffuse vs on-off effect) and in the stromal cells (pink arrowheads; strong vs no/weak staining) between pre- and post LVAD tissue. Control tissue showed diffuse cardiomyocyte staining and weak stromal cell staining.
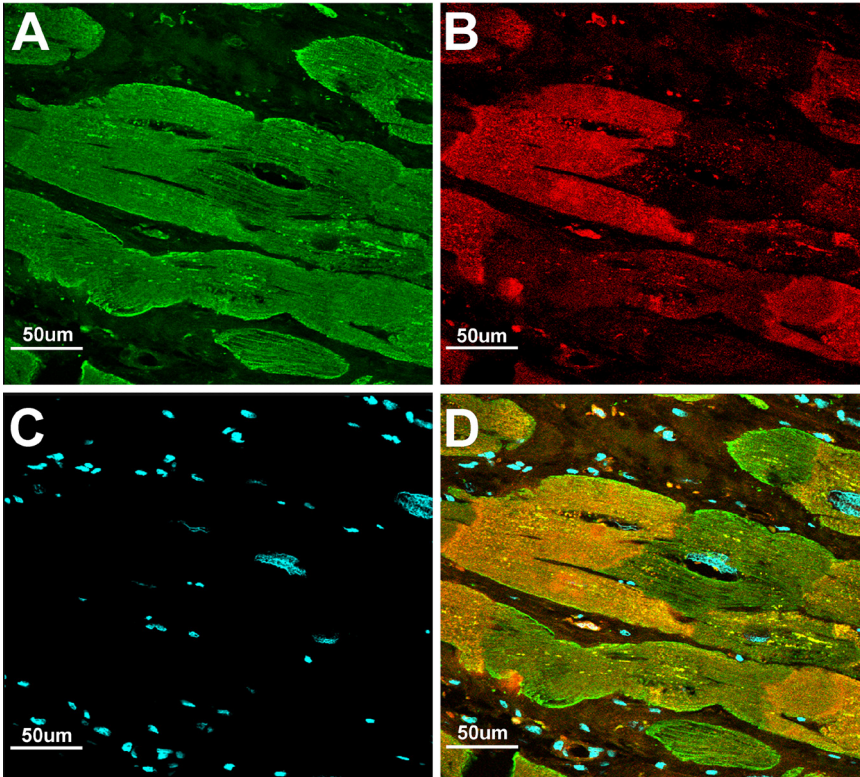
Figure 4: Fluorescence double staining of alpha-1-antichymotrypsin (ACT) and anti-cardiac actin

Fluorescence immunohistochemistry of a dilated heart after continuous flow LVAD support. Anti-cardiac actin (green; *A*), ACT (red; *B*), nuclei of cardiomyocytes (blue; *C*), and merged image (*D*). This indicated that anti-cardiac actin is present both in the cells positive and negative for ACT.

Post-transcriptional regulation of ACT by miR-137

According to two major miR target prediction databases; miRanda 13 and Targetscan 14, ACT is a potential target gene of miR-137. Interestingly, measuring miR-137 levels during cf-LVAD support showed that its expression significantly increased in the myocardial tissue (p=0.01, *Figure 5*).
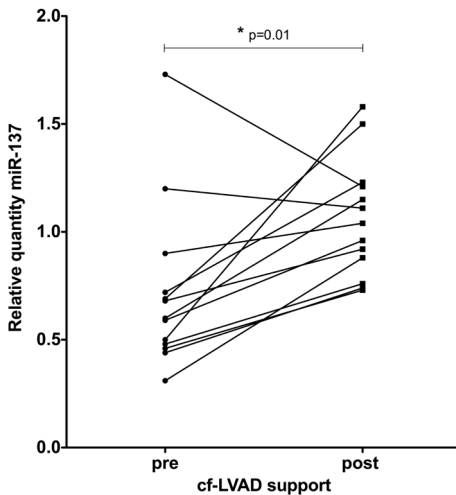
Figure 5: Relative quantification of miR-137 during continuous flow LVAD (cf-LVAD) support The expression of miR-137 was significantly upregulated post-LVAD (n=13).

Whereas in pre-LVAD samples, ACT mRNA was present in cardiomyocytes and stromal cells (*Figure 6A*), in post-LVAD samples it could only be detected in cardiomyocytes (partly in the nuclei; *Figure 6B*) and no "on-off effect" was seen. Furthermore, healthy controls (*Figure 6C*) revealed low expression of ACT mRNA and only in the cardiomyocytes (mainly in the nuclei). ACT mRNA was widely expressed in placental positive control tissue (*Figure 6D*). In the parallel experiment demonstrating the specificity of the ACT-probe, interleukin-2 (IL-2) was only expressed in a few interstitial stromal cells (*Supplemental Figure S1*). Curiously, in pre-LVAD samples (*Figure 7A-B*), miR-137 was moderately expressed in cardiomyocytes whereas post-LVAD, miR-137 was expressed in cardiomyocytes and stromal cells (*Figure 7C-D*). A scrambled miR was used as a negative control, showing only a weak background staining (*Figure 7E*). U6 was used as a positive control, clearly staining the nuclei as expected (*Figure 7F*).

To address the effect of miR-137 expression on ACT mRNA, we transfected HepG2 cells with miR-137 precursor molecules. Transfection of miR-137 resulted in more than 50% reduction of ACT mRNA levels (*Figure 8A*), compared to non-transfected cells (p<0.001;

mean 45.4 ± 7.6 SEM). As a positive control for transfection, delivery of miR-1 gave rise to significantly lesser mRNA of its validated target protein tyrosine kinase-9 in comparison to the nontransfected cells (p=0.001, with outlier p=0.28; *Figure 8B*). Mean mRNA expression of PTK9 in the HepG2 cells after transfection of miR-1 was 34.4 ± 9.7 SEM (without outlier) and 63.6 ± 30.3 SEM (with outlier).
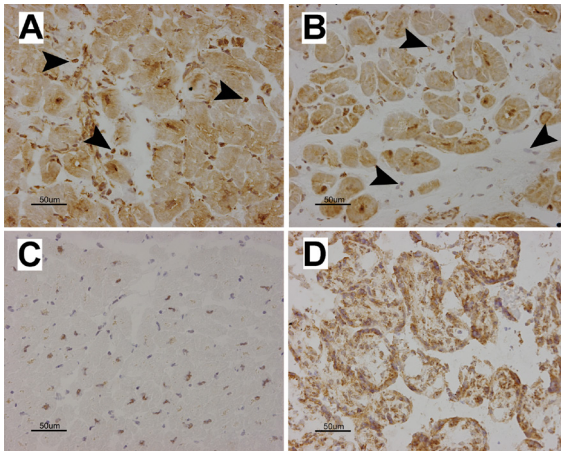
Figure 6: *In situ* hybridization (ISH) of alpha-1-antichymotrypsin (ACT)

mRNA of ACT in pre-LVAD samples was mainly located in the cardiomyocytes and stromal cells (arrowheads; *A*). Post-LVAD mRNA of ACT was only visible in cardiomyocytes, stromal cells stained very weak (arrowheads; *B*). In healthy control, mRNA of ACT was mainly expressed in the nuclei and weakly in the cardiomyocytes (*C*). Placental tissue stained positive for mRNA of ACT (*D*).
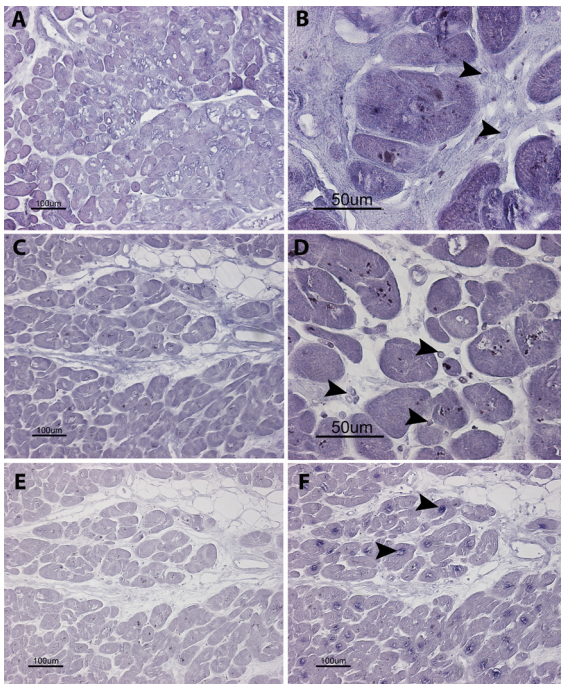
Figure 7: *In situ* hybridization (ISH) of miR-137, scramble and U6

In the pre-LVAD situation (*A-B*), miR-137 expression was weak in cardiomyocytes and almost negative in stromal cells (arrowheads) at 20x (*A*) and at 40x magnification (*B*). Post-LVAD (*C-D*), miR-137 staining was positive in stromal cells (arrowheads) and in the cardiomyocytes at 20x (*C*) and 40x magnification (*D*). No clear on-off effect was observed. In the negative "scramble" ISH (*E*), a weak background staining was observed in the cardiomyocytes (not in the stromal cells). A strong staining of U6 in the nuclei was detected (arrowheads; *F*).

To further confirm the functionality of the miR-137 target site in ACT, we cloned the ACT 3'UTR into a luciferase reporter vector. Firefly luciferase was placed under post-translational control of the native 3'UTR of ACT or an ACT 3'UTR harboring a mutated miR-137 target site. Co-transfection of synthetic miR-137 decreased ACT 3'UTR reporter activity (miR-137 versus non-targeting miR, p=0.006; miR-137 versus no miR, p=0.002), whereas no sensitivity was observed after co-transfection of a control, non-targeting microRNA (*Figure 8C*). In contrast, an ACT 3'UTR reporter with a mutated miR-137 target site showed no sensitivity to miR-137 transfection (*Figure 8D*). Together, these data indicate the presence of a functional miR-137 target site in the 3'UTR of ACT, confirming ACT as a direct target gene of miR-137.
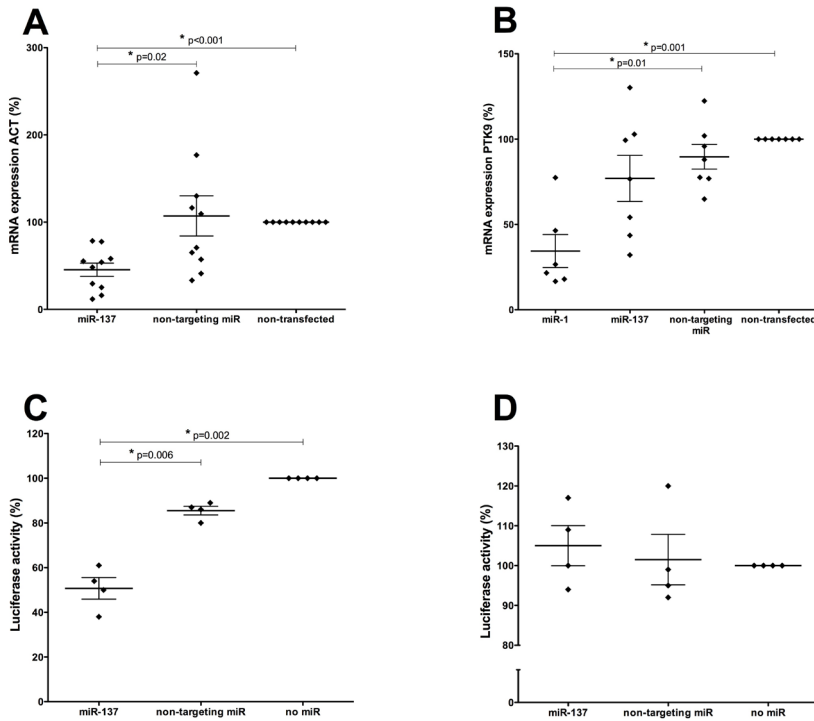
Figure 8: miR-transfection and luciferase reporter assay

Alpha-1-antichymotrypsin (ACT) mRNA (*A*) and protein tyrosine kinase-9 (PTK-9) mRNA (*B*) were significantly downregulated after miR-137 (n=10 experiments) and miR-1 transfection (n=7 experiments), in comparison with the non-transfected cells. The non-transfected human hepato cell line (HepG2 cells) were set on 100 %. There was one outlier in the miR-1 transfection PTK-9 experiment; data are presented without this outlier. In the luciferase reporter assays (n=4 experiments; *C-D*), Luciferase activity was significantly decreased after miR-137 transfection (p<0.05) in comparison to the non-targeting miR or without miR (*C*). The reduction in luciferase activity was completely abrogated after mutating the predicted miR-137 binding site in ACT 3' untranslated region (*D*). Data are presented in scatter-plots as mean and standard error of the mean. The asterisk (*) represents p<0.05.

Discussion

In the present study, it is shown that alpha-1-antichymotrypsin (ACT) levels decrease both in heart tissue and in plasma samples of cf-LVAD supported HF patients, suggesting a possible role for ACT in reverse remodeling. Immunohistochemically, a homogenous expression pattern of ACT within each individual cardiomyocyte was observed post-LVAD, whereas the expression levels of ACT between cardiomyocytes varied. This alternated expression was not due to apoptosis. The ACT staining in stromal cells in between the cardiomyocytes showed a strong decrease after LVAD support, both at protein (IHC) and mRNA (ISH) levels, and could therefore be the main source of the changes observed in plasma ACT during LVAD support. Also the regulatory function of miRs on ACT was studied. According to miR target prediction databases, only miR-137 was predicted to target ACT. We have shown that by transfecting HepG2 cells with miR-137, mRNA of ACT was decreased >50%, and by using luciferase reporter analysis, including target-site mutagenesis that ACT is a direct target of miR-137. MiR-137 was upregulated after cf-LVAD support, which correlates with the reduced mRNA and protein levels of its target ACT. *In situ* hybridization (ISH) showed that miR-137 expression was mainly localized in the cardiomyocytes as well in stromal cells (post-LVAD), as were ACT mRNA and protein. Of note, ISH is quantitatively not reliable and therefore interpretation of levels of miR-137 should be interpreted with caution. Unfortunately, it is not possible to analyze the post-transcriptional role of miR-137 on ACT in a murine HF model, as miR-137 will not bind to the UTR of murine ACT mRNA. ISH ACT showed a more homogeneous staining than miR-137 expression, which may imply that regulation of ACT is not strictly regulated by miR-137 alone, but that regulation of gene transcription is also involved in controlling ACT expression levels.

The role of ACT in HF is unknown. Inflammatory activity is thought to be a key-player in the progression of HF. ACT, serpin peptidase inhibitor, clade A, member 3 (SERPINA3), is an acute-phase protein and induces the pro-inflammatory cytokine tumour necrosis factor (TNF)-α, and NF-κB [15]. Interestingly, TNF-α also controls the synthesis of ACT [16]. TNF-α, which is under the control of nuclear factor NF-κB activation, is produced locally in the context of HF and had been shown to induce cardiomyocyte apoptosis [17] as well as hypertrophic growth [18] and cardiac remodeling. The initial increase in circulating ACT, which we have demonstrated in the present study, might be caused by the surgical procedure of the cf-LVAD implantation.
ACT is the major inhibitor of the extracellular serine protease activity of cathpesin G (CG).

6

Activated neutrophils, macrophages, and mast cells secrete CG into the extracellular space to modulate the immune response [19,20]. The physiological balance between CG and ACT is required for the maintenance of the connective tissue integrity of the heart. Imbalance in favor of CG results in degradation of connective tissue proteins in heart tissue [21] with subsequent cardiomyocyte detachment and apoptosis [22]. A second pathway in which CG can contribute to HF is by converting angiotensin I in angiotensin II, thereby activating the Transforming Growth Factor (TGF)-pathway that results in cardiomyocyte necrosis, hypertrophy and increased fibrosis [23]. Interestingly, ACT expression was present in several micro-array analysis of the failing myocardium [24-27]. These data implicate that ACT limits the proteolytic activity in the human heart by inhibition of CG. LVAD implantation leads to a reversal of HF and accordingly less inflammation and less mast cells and, thereby, less secretion of CG resulting in less need for ACT. This may explain the decrease in ACT during cf-LVAD support in the present study.

ACT has also been associated with the prevention of skeletal muscle degeneration and injury. Circulating ACT increased early after exercise-induced muscle loss [28] and has been related to the preservation of muscle mass in elderly patients [29]. An increased accumulation of ACT has been demonstrated in muscle fibers of patients with inclusion-body myositis, which is an inflammatory muscle disease characterized by progressive muscle weakness and wasting [30]. ACT is also thought to be protective during ischemia-reperfusion by inhibiting neutrophil-accumulation into the ischemic-reperfused myocardium and by inactivating cytotoxic metabolites released from neutrophils [31]. Likewise, ACT was elevated during the first days after an acute coronary syndrome [32,33] and a persistent postoperative increase was noticed after coronary artery bypass grafting [34].

Apart from this important role of ACT as a modulator between inflammation and progression of HF by extracellular mechanisms, it may also have important intracellular effects. ACT has the unique ability amongst serpins to bind to DNA, a property that is independent of its serine protease inhibitory activity [35]. In the present study, mRNA and protein expression of ACT suggest that high amounts of ACT are present within myocardial cells (especially cardiomyocytes and stromal cells) of end-stage HF patients. Moreover, the peculiar staining pattern of ACT in cardiomyocytes that alters during cf-LVAD support, could indicate an intracellular role for ACT. These intracellular aspects of ACT require further investigation to understand its role in HF.

The clinical experience with LVADs has been valuable for the identification of mechanisms of reverse remodeling since myocardial tissue of patients with end-stage HF can be obtained at the time of implantation and at the time of HTx, after a period of unloading. There are, however, some recognized limitations of molecular studies in LVAD patients. Our study size was small and the clinical presentation and duration of support are uncontrolled variables, creating a heterogeneous patients population. Furthermore, the present study comprised relatively young patients with a non-ischemic origin of systolic HF. To generalize our findings, it is important to confirm and extend the results in other HF populations. It remains to be determined whether ACT can also be an aid in clinical decision-making in the management of individual patients. In addition, we tried to confirm our data in murine models. However, the ACT target site for miR-137 in humans is not present in mice.

In summary, plasma ACT is elevated in end-stage HF patients and normalizes during mechanical support. ACT expression is directly regulated by miR-137. ACT and miR-137 are mainly localized in the stromal cells and cardiomyocytes during LVAD support. To the best of our knowledge, miR-137 has not been implicated in cardiovascular disease and this is the first study to show its expression in the human heart, and the shift in expression pattern after unloading the heart by cf-LVAD. Since the expression of ACT is directly regulated by miR-137, and their expression levels are inversely related *in vivo*, it is tempting to speculate that miR-137 and ACT can play an important role in the pathophysiology of HF and either one could possibly serve as a therapeutic target.

Clinical summary

Heart transplantation (HTx) is the choice of treatment in end-stage heart failure (HF). Nevertheless, HTx is available for a minority of patients, because of a lack of donor hearts. Alternatives for HTx are therefore required. Support of the failing heart by a left ventricular assist device (LVAD) has become an important facility in the treatment of HF. During LVAD support, signs and symptoms of HF diminish. The present study showed that plasma levels of alpha-1-antichymotrypsin (ACT) are elevated in end-stage HF patients as compared to healthy controls and is inversely related to miR-137. ACT, an acute phase protein, is a major inhibitor of cathpesin G (CG), the latter being associated with degradation of connective tissue integrity and activation of Transforming Growth Factor (TGF)-pathway. ACT can also bind to DNA, suggesting it may also have an intracellular effect. These data suggest that ACT, and its regulator miR-137, play a role in the pathophysiology of HF and reverse remodeling during mechanical support.

References

1.   Jessup M, Brozena S. Heart failure. N. Engl. J. Med. 2003; 348:2007–2018.

2.   Cohn JN. Structural basis for heart failure. Ventricular remodeling and its pharmacological inhibition. Circulation. 1995; 91:2504–2507.

3.   de Jonge N, van Wichen DF, Schipper MEI, Lahpor JR, Gmelig-Meyling FHJ, Robles de Medina EO, de Weger RA. Left ventricular assist device in end-stage heart failure: persistence of structural myocyte damage after unloading. An immunohistochemical analysis of the contractile myofilaments. J. Am. Coll. Cardiol. 2002; 39:963–969.

4.   Bruggink AH, van Oosterhout MFM, de Jonge N, Ivangh B, van Kuik J, Voorbij RHAM, Cleutjens JPM, Gmelig-Meyling FHJ, de Weger RA. Reverse remodeling of the myocardial extracellular matrix after prolonged left ventricular assist device support follows a biphasic pattern. J Heart Lung Transplant. 2006; 25:1091–1098.

5.   Phizicky E, Bastiaens PIH, Zhu H, Snyder M, Fields S. Protein analysis on a proteomic scale. Nature. 2003; 422:208–215.

6.   Hanash S. Disease proteomics. Nature. 2003; 422:226–232.

7.   Guglin M, Miller L. Myocardial recovery with left ventricular assist devices. Curr Treat Options Cardiovasc Med. 2012; 14:370–383.

8.   de Weger RA, Schipper MEI, Siera-de Koning E, van der Weide P, van Oosterhout MFM, Quadir R, Steenbergen-Nakken H, Lahpor JR, de Jonge N, Bovenschen N. Proteomic profiling of the human failing heart after left ventricular assist device support. J Heart Lung Transplant. 2011; 30:497–506.

9.   Bartel DP. MicroRNAs: genomics, biogenesis, mechanism, and function. Cell. 2004; 116:281–297.

10. da Costa Martins PA, Salic K, Gladka MM, Armand A-S, Leptidis S, Azzouzi el H, Hansen A, Coenen-de Roo CJ, Bierhuizen MF, van der Nagel R, van Kuik J, de Weger R, de Bruin A, Condorelli G, Arbones ML, Eschenhagen T, De Windt LJ. MicroRNA-199b targets the nuclear kinase Dyrk1a in an auto-amplification loop promoting calcineurin/NFAT signalling. Nat. Cell Biol. 2010; 12:1220–1227.

11. Lok SI, Winkens B, Goldschmeding R, van Geffen AJP, Nous FMA, van Kuik J, van der Weide P, Klöpping C, Kirkels JH, Lahpor JR, Doevendans PA, de Jonge N, de Weger RA. Circulating Growth Differentiation Factor-15 correlates with myocardial fibrosis in patients with non-ischemic dilated cardiomyopathy and decreases rapidly after left ventricular assist device support. Eur. J. Heart Fail. 2012; 14:1249-1255.

12. van Mil A, Grundmann S, Goumans M-J, Lei Z, Oerlemans MI, Jaksani S, Doevendans PA, Sluijter JPG. MicroRNA-214 inhibits angiogenesis by targeting Quaking and reducing angiogenic growth factor release. Cardiovasc. Res. 2012; 93:655–665.

13. Betel D, Wilson M, Gabow A, Marks DS, Sander C. The microRNA.org resource: targets and expression. Nucleic Acids Res. 2008; 36:D149–53.

14. Friedman RC, Farh KK-H, Burge CB, Bartel DP. Most mammalian mRNAs are conserved targets of microRNAs. Genome Res. 2009; 19:92–105.

15. Braghin E, Galimberti D, Scarpini E, Bresolin N, Baron P. Alpha1-antichymotrypsin induces TNF-alpha production and NF-kappaB activation in the murine N9 microglial cell line. Neurosci. Lett. 2009; 467:40–42.

16. Palomer X, Alvarez-Guardia D, Rodríguez-Calvo R, Coll T, Laguna JC, Davidson MM, Chan TO, Feldman AM, Vázquez-Carrera M. TNF-alpha reduces PGC-1alpha expression through NF-kappaB and p38 MAPK leading to increased glucose oxidation in a human cardiac cell model. Cardiovasc. Res. 2009; 81:703–712.

17. Krown KA, Page MT, Nguyen C, Zechner D, Gutierrez V, Comstock KL, Glembotski CC, Quintana PJ, Sabbadini RA. Tumor necrosis factor alpha-induced apoptosis in cardiac myocytes. Involvement of the sphingolipid signaling cascade in cardiac cell death. J. Clin. Invest. 1996; 98:2854–2865.

18. Yokoyama T, Nakano M, Bednarczyk JL, McIntyre BW, Entman M, Mann DL. Tumor necrosis factor-alpha provokes a hypertrophic growth response in adult cardiac myocytes. Circulation. 1997; 95:1247–1252.

19. Shapiro SD, Campbell EJ, Senior RM, Welgus HG. Proteinases secreted by human mononuclear phagocytes. J Rheumatol Suppl. 1991; 27:95–98.

20. Pham CTN. Neutrophil serine proteases: specific regulators of inflammation. Nat. Rev. Immunol. 2006; 6:541–550.

21. Heutinck KM, Berge ten IJM, Hack CE, Hamann J, Rowshani AT. Serine proteases of the human immune system in health and disease. Mol. Immunol. 2010; 47:1943–1955.

22. Sabri A, Alcott SG, Elouardighi H, Pak E, Derian C, Andrade-Gordon P, Kinnally K, Steinberg SF. Neutrophil cathepsin G promotes detachment-induced cardiomyocyte apoptosis via a protease-activated receptor-independent mechanism. J Biol Chem. 2003; 278:23944–23954.

23. Jahanyar J, Youker KA, Loebe M, Assad-Kottner C, Koerner MM, Torre-Amione G, Noon GP. Mast cell-derived cathepsin g: a possible role in the adverse remodeling of the failing human heart. J. Surg. Res. 2007; 140:199–203.

24. Yang J, Moravec CS, Sussman MA, DiPaola NR, Fu D, Hawthorn L, Mitchell CA, Young JB, Francis GS, McCarthy PM, Bond M. Decreased SLIM1 expression and increased gelsolin expression in failing human hearts measured by high-density oligonucleotide arrays. Circulation. 2000; 102:3046–3052.

25. Tan F-L, Moravec CS, Li J, Apperson-Hansen C, McCarthy PM, Young JB, Bond M. The gene expression fingerprint of human heart failure. Proc. Natl. Acad. Sci. U.S.A. 2002; 99:11387–11392.

26. Colak D, Kaya N, Al-Zahrani J, Bakheet Al A, Muiya P, Andres E, Quackenbush J, Dzimiri N. Left ventricular global transcriptional profiling in human end-stage dilated cardiomyopathy. Genomics. 2009; 94:20–31.

6

27. Seguchi O, Takashima S, Yamazaki S, Asakura M, Asano Y, Shintani Y, Wakeno M, Minamino T, Kondo H, Furukawa H, Nakamaru K, Naito A, Takahashi T, Ohtsuka T, Kawakami K, Isomura T, Kitamura S, Tomoike H, Mochizuki N, Kitakaze M. A cardiac myosin light chain kinase regulates sarcomere assembly in the vertebrate heart. J. Clin. Invest. 2007; 117:2812–2824.

28. Sietsema KE, Meng F, Yates NA, Hendrickson RC, Liaw A, Song Q, Brass EP, Ulrich RG. Potential biomarkers of muscle injury after eccentric exercise. Biomarkers. 2010; 15:249–258.

29. Schaap LA, Pluijm SMF, Deeg DJH, Visser M. Inflammatory markers and loss of muscle mass (sarcopenia) and strength. Am. J. Med. 2006; 119:526.e9–17.

30. Bilak M, Askanas V, Engel WK. Strong immunoreactivity of alpha 1-antichymotrypsin co-localizes with beta-amyloid protein and ubiquitin in vacuolated muscle fibers of inclusion-body myositis. Acta Neuropathol. 1993; 85:378–382.

31. Murohara T, Guo JP, Lefer AM. Cardioprotection by a novel recombinant serine protease inhibitor in myocardial ischemia and reperfusion injury. J. Pharmacol. Exp. Ther. 1995; 274:1246–1253.

32. Kaźmierczak M, Sobieska M, Wiktorowicz K, Wysocki H. Changes of acute phase proteins glycosylation profile as a possible prognostic marker in myocardial infarction. Int J Cardiol. 1995; 49:201–207.

33. Kopetz VA, Penno MAS, Hoffmann P, Wilson DP, Beltrame JF. Potential mechanisms of the acute coronary syndrome presentation in patients with the coronary slow flow phenomenon - insight from a plasma proteomic approach. Int J Cardiol. 2012; 156:84–91.

34. Banfi C, Parolari A, Brioschi M, Barcella S, Loardi C, Centenaro C, Alamanni F, Mussoni L, Tremoli E. Proteomic analysis of plasma from patients undergoing coronary artery bypass grafting reveals a protease/antiprotease imbalance in favor of the serpin alpha1-antichymotrypsin. J. Proteome Res. 2010; 9:2347–2357.

35. Naidoo N, Cooperman BS, Wang ZM, Liu XZ, Rubin H. Identification of lysines within alpha 1-antichymotrypsin important for DNA binding. An unusual combination of DNA-binding elements. J Biol Chem. 1995; 270:14548–14555.

SUPPLEMENTAL

Supplemental methods

2D-DIGE in tissue and plasma

With the use of fluorescent 2-dimensional difference gel electrophoresis (2D-DIGE), a comparative analysis was made of protein expression in tissue and plasma in DCM patients prior to and after cf-LVAD implantation. High abundant proteins were depleted in plasma using a Human 14 Multiple Affinity Removal System (Agilent Technologies, Wilmington, DE, US) according to manufacturer's instruction. Tissue samples were mixed with 50 mM Tris (pH 7.4), 150 mM NaCl, and 1% NP-40, incubated for 30 min at 4°C. Lysates were cleared by centrifugation at 14,000 rpm for 10 min. Both plasma and tissue pre- and post LVAD samples (75 μg) were precipitated using the Plus One two-dimensional clean-up kit as recommended by the manufacturer (GE Healthcare) and solubilized in 8 M urea, 2 M thiourea, 4% Chaps, 300 mM dithiothreitol, 2% biolyte pH 3–10, and 0.004% bromphenol blue (75 μl). Pre- and post LVAD samples (50 μg) were labeled with 400 pmol of either Cy3 or Cy5 and mixtures (1:1) of all samples were labeled with Cy2, allowing us to adjust for multiple analyses [1,2]. The samples (150 μg) were separated by 2D-DIGE, as previously described [2]. Dye swaps were included to exclude preferentially labeled proteins from the analysis. Relative quantification of matched gel features was performed by using Decyder DIA and BVA software (GE Healthcare). For inter-gel analyses, the internal standard method was used [1]. We selected protein spots if: 1) fluorescence volume intensity was altered more than 1.5 fold (tissue) or 2.0 fold (plasma), 2) with a change in p-value<0.05, 3) spots could be detected in at least 3 patients.

Mass spectrometry

Two dimensional gels were post-stained by mass spectrometry (MS)-compatible Flamingo staining (Bio-Read) and protein spots of interest that showed differential expression between pre-LVAD and post-LVAD samples were excised robotically (Ettan Dalt Spot Cutter, GE Healthcare) and were reduced with dithiothreitol, alkylated with iodoacetamide, and digested with trypsin (Roche) as described [3]. Samples were subjected to nanoflow LC (Eksigent Technologies, Dublin, CA, USA) using C_{18} reverse phase trap columns (Phenomenex; column dimensions 2cm x 100 μm, packed in-house) and subsequently separated on C18 analytical columns (Reprosil; column dimensions, 20 cm x 50 μm; packed in-house) using a linear gradient from 0 to 40% B (A = 0.1 M acetic acid; B = 95% (v/v) acetonitrile, 0.1 M acetic acid) in 60 min and at a constant flow rate of 150 nl/min. Column eluate was directly coupled to a LTQ-Orbitrap-XL mass spectrometer (Thermo Fisher

Scientific) operating in positive mode, using Lock spray internal calibration. Data were processed and subjected to database searches using MASCOT software (Matrixscience) against Swiss Prot and non-redundant NCBI database, with a 10-ppm mass tolerance of precursor and 0.8 Da for the fragment ion.

ACT plasma

Patients: Enzyme-linked-immunosorbent (ELISA) assay plates (96-wells) were coated with monoclonal anti-ACT antibody. Plasma was diluted in an assay buffer, which consisted of PBS containing 0.1% (w/v) Tween-20 and 0.2% (w/v) casein in 100 μl and was incubated for 1 hr at room temperature (RT). Bound ACT was detected with a biotinylated polyclonal antibody against ACT (Dako, Glostrup, Denmark) diluted in 100 μl of assay buffer and incubated for 1 hr at RT. This was followed by incubation with horseradish peroxidase-conjugated streptavidin (Amersham Biosciences, Buckinghamshire, UK) for 1 hr at RT. In between the incubation steps, washing was performed with phosphate-buffered saline containing 0.05% Tween-20. For detection, 100 μl of 3,5,30,50-tetramethylbenzidine (Sigma-Aldrich Co, St. Louis, USA) in 0.11 mmol/liter sodium acetate (pH 5.5) containing 0.003% H_2O_2 was used as substrate. The substrate reaction was stopped by adding 100 μl of 2 mmol/liter H_2O_4. Absorption at 450 nm was determined in a Rainbow Microtiter Plate Reader (SLT, Grading, Austria) corrected for background (540 nm). Purified ACT (Sigma) was employed as reference.

Quantification of ACT mRNA

Total RNA was isolated out of 20 slides of 10-μm frozen tissue, using miRNeasy Mini Kit (Qiagen, Inc., Austin, USA). Copy DNA was synthesized with the use of superscript III, oligo-dT and random primers (Invitrogen, Oslo, Norway). The Q-PCR mix consisted of 6.25 μL mastermix, 0.625 μL primer/probe Taqman Gene Expression Assay (Life Technologies, Bleiswijk, the Netherlands) and 3.13 μL milliQ. The expression of the endogenous control Glyceraldehyde 3-phosphate dehydrogenase (GAPDH) was measured for each sample. Each primer/probe combination was also measured in placental cDNA, which was used as calibrator (positive control). Thermal cycling comprised a 10 minutes denaturation step at 95°C, followed by 40 cycles of 15 sec. at 95°C and 1 min. at 60°C. mRNA expression of ACT was determined on the LightCycler 480 (Roche Diagnostics BV, Almere, the Netherlands). Data was quantified with the comparative quantification cycle (Cq) method. Relative quantity (RQ) was defined as $2^{-\Delta\Delta Cq}$, in which $\Delta Cq= Cq$ (target)-Cq (endogenous control), $\Delta\Delta Cq= \Delta Cq$ (sample)$- \Delta Cq$ (calibrator). Cq values above 35 were defined as negative.

6

ISH ACT mRNA

In this procedure up to the hybridization step, experiments were performed under RNAse free conditions with RNAse free reagents. PCR products were made using specific primers:

ACT forward: ACC-GCC-TTG-GCC-TTC-CTG-TC

ACT reverse: GGC-ACC-ATT-ACC-CAC-TTT-TTC-TTG

PCR products were sequenced and blasted against the human genome to verify their specificity. The PCR products were labeled with digoxigenin by re-PCR in the presence of labeled nucleotides [4]. Frozen slides were fixed in buffered formalin for one hr, rinsed in PBS, endogenous peroxidase was blocked with 1 % H_2O_2 solution for 30 min, rinsed in PBS, incubated with proteinase K (prot.K) solution for 7 min (10 µl prot.K (10 mg/ml) in 100 ml PBS at 37 °C), rinsed in PBS again, fixed in buffered formalin to block prot.K for 5 min, rinsed in PBS, incubated in Triton X-100 in PBS (50 µl Triton X-100 (10%) in 100 ml PBS for 10 min), rinsed in PBS, dehydrated in ethanol 50%, 70%, 96% and 100% and dried at room temperature. The following hybridization mixture was prepared: 30 µl formamide 100 %, 20 µl TE buffer 0.1x 10 µl SSC 20x, 1 µl t-RNA (100 mg\ml), 10 µl Herring Sperm DNA, 10 µl digoxigenin labeled probe, 19 µl RNAse free water, Total volume is 100 µl. This hybridization mixture was boiled in water for 5 min to denature both DNA probes, and cooled on ice for 10 min. Then 25 µl of hybmix was applied to the tissue per slide, and covered with a cover slip. The slides were incubated on a hot plate at 47 °C for 10 min and subsequently, incubated in a humidified chamber overnight in an oven at 37°C. The cover slip was removed and the slides were rinsed in 30% formamide/SSC 2x solution for 10 min at RT. The same solution was preheated in a water bath at 42°C and slides were incubated in this solution at 42°C for 10 min, rinsed in PBS/tween, and incubated in a solution of mouse anti-digoxigenin in a dilution of 1:50 in PBS/BSA 1% for 1 hr. After rinsing in PBS/tween, the slides were incubated with a HRP labeled rabbit anti-mouse antibody diluted 1:100 in PBS supplemented with 10% Normal Human Serum NHS for 30 min, rinsed in PBS/tween, and the slides were incubated with a second HRP labeled swine anti-rabbit antibody diluted 1:100 in PBS supplemented with 10 % NHS for 30 min. After rinsing in PBS the slides were developed with DAB solution for 10 min. The nuclei were counterstained with Mayer's Haematoxylin for 10 sec. The slides were dehydrated with alcohol and xylene series and covered with a cover slip.
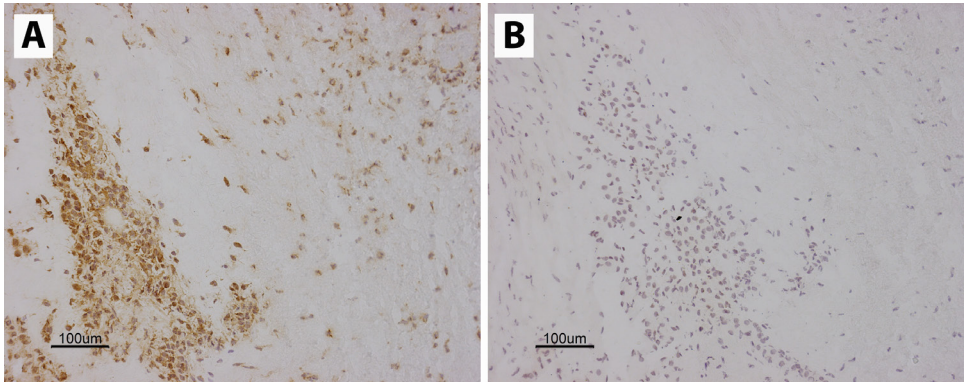
Supplemental Figure S1

In situ hybridization of mRNA interleukin-2 (IL-2) and alpha-1-antichymotrypsin (ACT) in myocardial tissue demonstrating the specificity of the ACT probe. mRNA ACT is strongly expressed in interstitial stromal cells (*A*), whereas IL-2 is only expressed in some (*B*). Placental tissue stained strong for both mRNA ACT and IL-2 (data not shown).

Supplemental references

1. Alban A, David SO, Bjorkesten L, Andersson C, Sloge E, Lewis S, Currie I. A novel experimental design for comparative two-dimensional gel analysis: two-dimensional difference gel electrophoresis incorporating a pooled internal standard. Proteomics. 2003; 3:36–44.

2. Bovenschen N, Quadir R, van den Berg AL, Brenkman AB, Vandenberghe I, Devreese B, Joore J, Kummer JA. Granzyme K displays highly restricted substrate specificity that only partially overlaps with granzyme A. J Biol Chem. 2009; 284:3504–3512.

3. Wilm M, Shevchenko A, Houthaeve T, Breit S, Schweigerer L, Fotsis T, Mann M. Femtomole sequencing of proteins from polyacrylamide gels by nano-electrospray mass spectrometry. Nature. 1996; 379:466–469.

4. Huibers M, de Jonge N, van Kuik J, Koning ES-D, Van Wichen D, Dullens H, Schipper M, de Weger R. Intimal fibrosis in human cardiac allograft vasculopathy. Transpl. Immunol. 2011; 25:124–132.

6
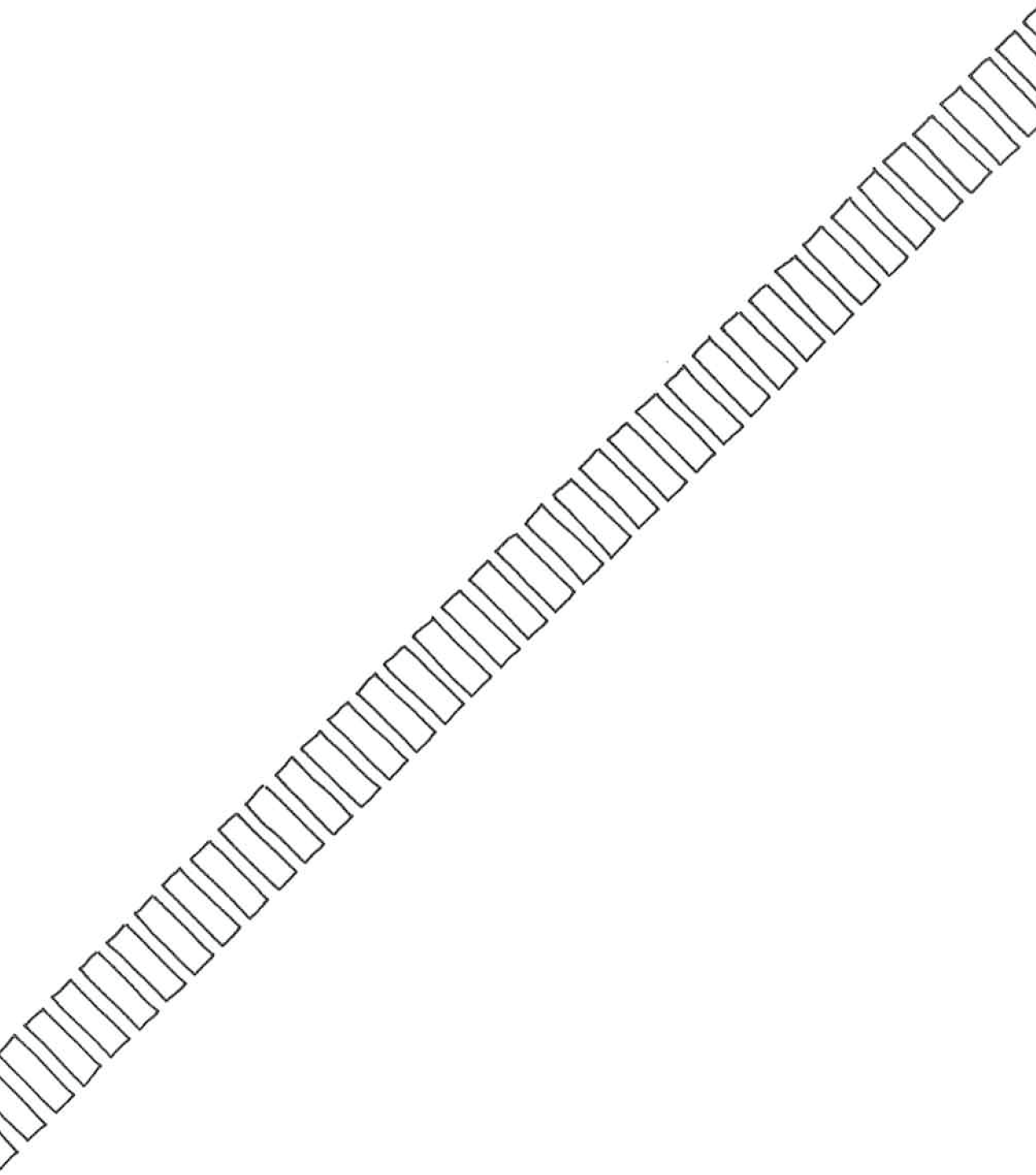
CHAPTER 7

Plasma levels of alpha-1-antichymotrypsin are elevated in patients with chronic heart failure, but are of limited prognostic value

Sjoukje I. Lok[1], Dirk J. Lok[2], Petra van der Weide[3], Bjorn Winkens[4],
Pieta W. Bruggink-André de la Porte[2], Pieter A. Doevendans[1], Roel A. de Weger[3],
Peter van der Meer[5], Nicolaas de Jonge[1]

[1] Department of Cardiology, University Medical Centre Utrecht
[2] Department of Cardiology, Deventer Hospital, Deventer
[3] Department of Pathology, University Medical Center, Utrecht
[4] Department of Methodology and Statistics, University of Maastricht
[5] Department of Cardiology, University Medical Center Groningen, Groningen

Abstract

Background: There is increasing interest in utilizing novel markers of cardiovascular disease risk in chronic heart failure (HF) patients. Recently, it was shown that alpha-1-antichymotrypsin (ACT), an acute phase protein and major inhibitor of cathpesin G, plays a role in the pathophysiology of HF and may serve as a marker for myocardial distress.

Objective: To assess whether ACT is independently associated with long-term mortality in chronic HF patients.

Methods: ACT plasma levels were analysed in EDTA plasma of chronic HF patients and healthy controls. Circulating ACT levels were categorized into quartiles. Survival times were analysed using Kaplan-Meier curves and Cox proportional hazards regression, without and with correction for clinically relevant risk factors, including sex, age, duration of HF, kidney function (MDRD), ischemic HF etiology and NT-proBNP.

Results: A total of 224 patients (mean age 71 years, 72% male, median HF duration 1.6 years) with chronic HF and 20 healthy controls were included. During a median survival time of 5.3 (95% CI 4.5-6.1) years, 159 (71%) patients died. ACT was significantly elevated in HF patients (median 433 μg/ml, IQR 279-680) in comparison to controls (median 214 μg/ml, IQR166-271; p<0.001). Cox regression analysis demonstrated that ACT was not independently related to long-term mortality in chronic HF patients (crude HR = 1.03, 95% CI 0.75-1.41, p=0.871; adjusted HR=1.12, 95% CI 0.78-1.60, p=0.552), which was confirmed by Kaplan Meier curves.

Conclusion: ACT levels are elevated in chronic HF patients, but no independent association with long-term mortality can be established.

Introduction

Despite recent treatment advances, chronic heart failure (HF) continues to impose a substantial health-care burden. Brain Natriuretic Peptide (BNP) and the biologically inactive N-terminal fragment (NT-proBNP) are synthesized by ventricular myocytes in response to hemodynamic stress [1]. Natriuretic peptides (NPs) are useful in the determining the diagnosis and the prognosis of congestive HF and the use of them are subsequently advocated by the American College of Cardiology [2] and the ESC guidelines [3]. However, NPs have limitations that affect the interpretation of results. Elevated NP levels can also be seen in the setting of sepsis [4], acute pulmonary embolism [5] and renal dysfunction [6]. NP levels are higher in women than in men and increase with age [7]. Moreover, NP levels may be reduced in obese patients [8,9]. Consequently, novel biomarkers are currently under intensive investigation and may be of help to improve the prognostication and clinical outcome of HF patients. Recently, we proposed a role of the acute-phase protein alpha-1-antichymotrypsin (ACT; also known as SERPINA3) in reverse remodeling [10]. Our data demonstrated that high ACT plasma and myocardial levels in HF decrease during mechanical support. The goal of this study was to evaluate the prognostic role of ACT levels with respect to long-term mortality in chronic HF patients.

Methods and materials

Study population

Our patient material consisted of plasma and data obtained from the Deventer-Alkmaar Heart Failure study (DEAL-HF) [11,12]. Briefly, 240 patients with typical signs and symptoms of HF were included, combined with echocardiographic or radionuclide ventriculographic findings of a reduced left ventricular systolic function (LVEF ≤ 45%) or diastolic dysfunction. The main exclusion criteria were an expected survival of less than one year and planned hospitalization. In the present study, a complete set of data was available of 224 patients at baseline (due to missing blood samples). Control plasma was collected from 20 anonymous healthy individuals. All patients gave written informed consent.

7

Laboratory assessment

Routine laboratory measurements and blood samples were obtained at baseline. EDTA plasma was separated and stored at minus 70⁰C. Circulating levels of ACT was analyzed according to the description of the manufacturer (Genway Biotech Inc, San Diego, USA). In short, the samples were diluted 1:5,000 in dilution buffer. Standards and samples were added in duplicate in a 96 wells plate coated with antibody and incubated. After the first washing step, the conjugate was added, followed by incubation. The next washing step was followed by the addition of the substrate solution and incubation. The stop solution was added and wells were read out on a microplate reader.

Clinical follow-up

ACT values were assessed for all-cause mortality. Patients were followed up to 10,5 years after randomization at the outdoor patient clinic. In case of no show, information regarding survival was obtained from the hospital system, relatives or general practitioner.

Statistics

Categorical data are presented by number (%) and numerical data by mean ± standard deviation or by median (interquartile range, IQR, i.e. 25th - 75th percentile), where appropriate. Comparisons between patients and healthy controls were performed using independent-samples t-test or Mann-Whitey U-test for numerical variables and Chi-square or Fisher's exact test for categorical variables. Linear regression analysis was performed to assess clinical relevant factors independent related to ACT plasma levels, like sex, age, duration of HF, kidney function (MDRD), ischemic HF etiology and NT-proBNP. Survival times were analysed using Kaplan-Meier curves and Cox proportional hazards (PH) regression, without and with correction for the above mentioned clinically relevant risk factors. Time to event was defined as time between inclusion and death or to end of study/ loss to follow-up (censored). PH assumption was checked using Schoenfeld residuals and linearity assumption by adding and testing mean-centred quadratic terms. A p-value ≤0.05 was considered as statistically significant. All analyses were done with SPSS 20.0 software (SPSS Inc, Chicago, IL).

Methods and materials

Baseline characteristics

Characteristics of the study population are described in *Table 1*.

Table 1: Baseline characteristics

Variable	Total (n=224)	Survivors (n=65)	Non-survivors (n=159)	p-value[1]
Age, years	71 ± 10	67 ± 11	72 ± 9	0.001
Sex, male (%)	72	60	77	0.008
HF etiology, ischemic (%)	65	51	72	0.004
Duration of HF, years	1.6 (0.3-5.8)	0.4 (0.2-3.3)	2.6 (0.4-6.5)	<0.001
NYHA class, III/IV (%)	99	98	99	0.986
Comorbidities				
Diabetes mellitus (%)	30	20	33	0.047
COPD (%)	28	29	27	0.740
CVA (%)	10	8	11	0.417
Hypercholesterolemia (%)	47	48	49	0.853
Anemia (%)	17	8	20	0.023
Laboratory				
Hemoglobin, mmol/L	8.4 ± 1.0	8.6 ± 0.8	8.3 ± 1.0	0.135
Sodium, mmol/L	138 ± 3	139 ± 3	138 ± 3	0.030
Potassium, mmol/L	4.4 ± 0.5	4.4 ± 0.4	4.4 ± 0.5	0.446
Urea, mmol/L	11.0 ± 5.4	9.6 ± 4.1	11.6 ± 5.8	0.005
Creatinine, μmol/L	127 ± 36	115 ± 23	131 ± 40	<0.001
MDRD	52 ± 14	55 ± 13	51 ± 15	0.086
Cockcroft-Gault	54 ± 22	63 ± 25	51 ± 20	0.001
Leukocytes, x10^9/L	7.8 ± 2.2	7.5 ± 1.8	7.9 ± 2.4	0.157
CRP, mg/L	8 (5-16)	6 (3-11)	10 (6-18)	<0.001
NT-proBNP, pg/ml	2089 (973-4364)	1725 (727-3341)	2360 (1074-5776)	0.003
Medication use				
ACE inhibitors (%)	88	91	87	0.419
ARBs (%)	16	17	15	0.711
Beta-blockers (%)	79	89	75	0.022
Calcium blockers (%)	7	8	6	0.769
Digoxin (%)	28	17	33	0.019
Diuretics (%)	99	98	99	0.988
Nitrates (%)	41	42	40	0.750

Values are presented as means ± standard deviations, medians ± interquartile ranges or as frequencies and percentages.
[1] comparison survivors versus non-survivors.
HF, heart failure; NYHA, New York Heart Association; COPD, Chronic Obstructive Pulmonary Disease; CVA, cerebrovascular accident; CRP, C-reactive Protein; NT-proBNP, N-terminal pro brain natriuretic peptide; ACE, Angiotensin converting enzyme; ARB; angiotension receptor blocker.

7

The study cohort consisted of patients with severe chronic HF with a mean age of 71 years, 72% was male with a median HF duration of 1.6 years. Almost all patients (97%) had a left ventricular systolic dysfunction with a reduced ejection fraction with a mean ejection fraction of 31%. At the time of inclusion, an ischemic etiology of HF was present in 146 patients (65%). Non-survivors were older, male subjects with a longer duration of HF, higher CRP and NT-proBNP levels, more often kidney dysfunction and were more often diagnosed with diabetes mellitus, anaemia and ischemic heart disease and were less often treated with beta-blocking agents in comparison to survivors.

Plasma levels of ACT in patients and healthy controls
Figure 1 shows the plasma levels of ACT in patients and healthy controls. A large individual variation of ACT was found. ACT was significantly elevated in patients (median 433 μg/ml, IQR 279-680) in comparison to controls (median 214 μg/ml, IQR 166-271; p<0.001).A linear regression analysis showed that the duration of HF was independently related to ACT plasma levels (patients with a shorter duration of HF had a higher ACT plasma level; p=0.031). Only 5.4% of the variation in ACT plasma levels is explained by the model (R-square = 0.054), which means that the large differences in ACT plasma levels between patients cannot be explained by the variables included in the model.
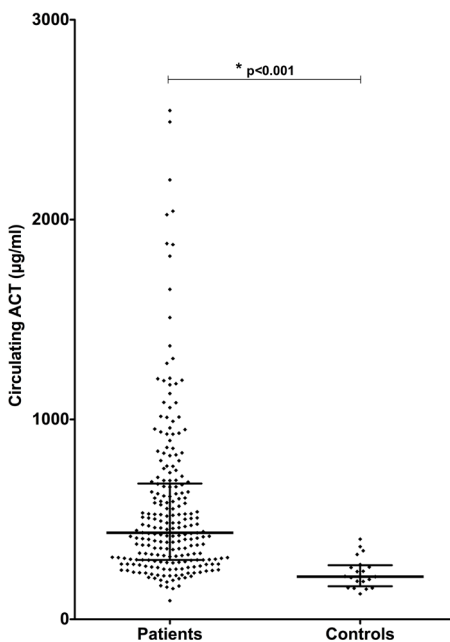
Figure 1: Alpha-1-antichymotrypsin (ACT) plasma levels in chronic heart failure (HF) patients and controls
ACT levels were significantly higher in chronic HF patients in comparison with healthy controls (p<0.001). Each dot represents one patient; the lines indicate median and IQR.

ACT levels and mortality

The mean and median survival time was 5.5 and 5.3 years, respectively. In total, 159 (71%) patients died. Cox-proportional hazard regression models showed that ACT plasma levels (mg/ml) were not significantly related to long-term mortality (crude HR=1.03, 95% CI 0.75-1.41, p=0.871; adjusted HR=1.12, 95% CI 0.78-1.60 ,p=0.552). HR present the effect of ACT per 1000 μg/ml = 1 mg/ml. This non-significant effect of ACT was also confirmed by the Kaplan Meier-curves presented in *Figure 2*, where circulating ACT was divided into quartiles and presented as KM-curves.
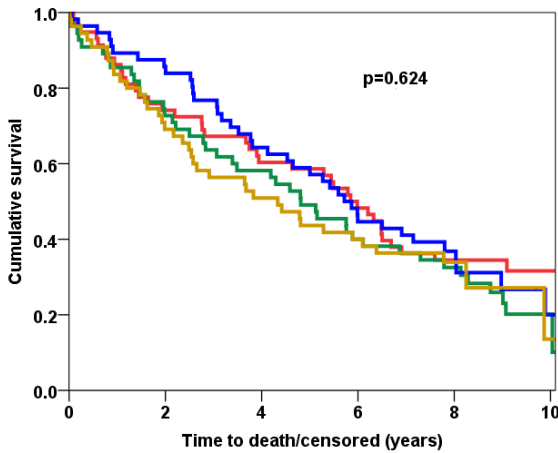
Follow-up (years)	0	2	4	6	8	10
Patients at risk	24	169	131	97	56	7

Figure 2: Kaplan-Meier curves for alpha-1-antichymotrypsin (ACT) levels
ACT levels were categorized in quartiles for presentation purposes. Quartile 1 (red) consists of ACT levels between 93-297 μg/ml, quartile 2 (green) 297-434 μg/ml, quartile 3 (blue) 434-687 μg/ml, quartile 4 (brown) 687-4545 μg/ml. ACT levels were not significant related to mortality.

Discussion

In the present study, ACT levels were significantly elevated in chronic HF patients in comparison to healthy controls and demonstrated that a single measurement of plasma ACT is not an independent risk factor for long-term mortality in these patients.

Multiple microarray analyses have been conducted to screen the gene expression profile of the failing myocardium from patients with dilated cardiomyopathy and suggested elevated ACT expression in the failing heart [13-16]. These findings were corroborated by our previous

work in a small panel of severe end-stage HF patients that demonstrated profound elevated ACT levels in heart tissue as well as plasma at the time of left ventricular assist device (LVAD) implantation. The present study aimed to verify ACT upregulation in a larger cohort of chronic HF patients. We established that ACT plasma levels were significantly elevated in chronic HF patients in comparison to healthy controls. ACT seems to be involved in the pathophysiology of HF. The exact role of ACT in HF is unknown, but several effects on the cardiovascular system have been postulated. ACT is a serine protease inhibitor, mainly of cathepsin G [17]. By eliminating cathepsin G, ACT might prevent the degradation of connective tissue proteins [18] and the activation of the transforming growth factor-pathway [19], with subsequent less cardiomyocyte necrosis, hypertrophy and fibrosis. Also, ACT is an acute-phase protein and induces tumour necrosis factor (TNF)-α and NF-κB [20]. Additionally, ACT is thought to be protective during ischemia-reperfusion by inhibiting neutrophil-accumulation into the ischemic-reperfused myocardium and by inactivating cytotoxic metabolites released from neutrophils [21]. The present study demonstrated that ACT plasma levels were elevated in chronic HF patients, suggesting that ACT might be useful as diagnostic marker in HF. Nevertheless, the present Cox PH regression analyses demonstrated that ACT is not an independent risk factor for long-term mortality in these patients with severe chronic HF. Future studies with plasma samples taken at different time-points and taken from patients with less severe HF are necessary to analyse the potential role of ACT as a prognostic marker in HF.

Limitations

The number of patients after 10 years of follow-up was small. As a sensitivity analysis, data up to 5-years of follow-up were also analysed with Cox-regression, and showed similar results. Only one random plasma sample per patient was available for the present study. As a result, the possible effect of a change in levels of ACT on mortality is unknown. In this study, mainly chronic HF patients with an older age and reduced ejection fraction (HFrEF) were included. Our results cannot be extrapolated to young patients and/or less severe forms of HFrEF, acute HF and HF with a preserved left ventricular systolic function (HFpEF). The main exclusion criteria, expected survival of less than one year and planned hospitalization, may have caused a selection-bias, since these patients are expected to have high ACT levels. The end-point of the present study was all-cause mortality. Therefore, we are not informed about the relation between the novel marker and hospitalizations for HF or other serious events.

References

1. Daniels LB, Maisel AS. Natriuretic peptides. J Am Coll Cardiol 2007;50:2357–2368.

2. Hunt SA, American College of Cardiology, American Heart Association Task Force on Practice Guidelines (Writing Committee to Update the 2001 Guidelines for the Evaluation and Management of Heart Failure). ACC/AHA 2005 guideline update for the diagnosis and management of chronic heart failure in the adult: a report of the American College of Cardiology/American Heart Association Task Force on Practice Guidelines (Writing Committee to Update the 2001 Guidelines for the Evaluation and Management of Heart Failure). J Am Coll Cardiol 2005;46:e1–82.

3. McMurray JJV, Adamopoulos S, Anker SD, Auricchio A, Böhm M, Dickstein K, Falk V, Filippatos G, Fonseca C, Gomez-Sanchez MA, Jaarsma T, Køber L, Lip GYH, Maggioni AP, Parkhomenko A, Pieske BM, Popescu BA, Rønnevik PK, Rutten FH, Schwitter J, Seferovic P, Stepinska J, Trindade PT, Voors AA, Zannad F, Zeiher A, Task Force for the Diagnosis and Treatment of Acute and Chronic Heart Failure 2012 of the European Society of Cardiology, Bax JJ, Baumgartner H, Ceconi C, Dean V, Deaton C, Fagard R, Funck-Brentano C, Hasdai D, Hoes A, Kirchhof P, Knuuti J, Kolh P, McDonagh T, Moulin C, Popescu BA, Reiner Z, Sechtem U, Sirnes PA, Tendera M, Torbicki A, Vahanian A, Windecker S, McDonagh T, et al. ESC guidelines for the diagnosis and treatment of acute and chronic heart failure 2012: The Task Force for the Diagnosis and Treatment of Acute and Chronic Heart Failure 2012 of the European Society of Cardiology. Developed in collaboration with the Heart Failure Association (HFA) of the ESC. Eur J Heart Fail 2012;14:803–869.

4. Rudiger A, Gasser S, Fischler M, Hornemann T, Eckardstein von A, Maggiorini M. Comparable increase of B-type natriuretic peptide and amino-terminal pro-B-type natriuretic peptide levels in patients with severe sepsis, septic shock, and acute heart failure. Crit Care Med 2006;34:2140–2144.

5. Kucher N, Printzen G, Goldhaber SZ. Prognostic role of brain natriuretic peptide in acute pulmonary embolism. Circulation 2003;107:2545–2547.

6. Tsutamoto T, Wada A, Sakai H, Ishikawa C, Tanaka T, Hayashi M, Fujii M, Yamamoto T, Dohke T, Ohnishi M, Takashima H, Kinoshita M, Horie M. Relationship between renal function and plasma brain natriuretic peptide in patients with heart failure. J Am Coll Cardiol 2006;47:582–586.

7. Wang TJ, Larson MG, Levy D, Leip EP, Benjamin EJ, Wilson PWF, Sutherland P, Omland T, Vasan RS. Impact of age and sex on plasma natriuretic peptide levels in healthy adults. Am J Cardiol 2002;90:254–258.

8. Daniels LB, Clopton P, Bhalla V, Krishnaswamy P, Nowak RM, McCord J, Hollander JE, Duc P, Omland T, Storrow AB, Abraham WT, Wu AHB, Steg PG, Westheim A, Knudsen CW, Perez A, Kazanegra R, Herrmann HC, McCullough PA, Maisel AS. How obesity affects the cut-points for B-type natriuretic peptide in the diagnosis of acute heart failure. Results from the Breathing Not Properly Multinational Study. Am Heart J 2006;151:999–1005.

7

9.   Mehra MR, Uber PA, Park MH, Scott RL, Ventura HO, Harris BC, Frohlich ED. Obesity and suppressed B-type natriuretic peptide levels in heart failure. J Am Coll Cardiol 2004;43:1590–1595.

10. Lok SI, van Mil A, Bovenschen N, van der Weide P, van Kuik J, Van Wichen D, Peeters T, Siera E, Winkens B, Sluijter JPG, Doevendans PA, da Costa Martins PA, de Jonge N, de Weger RA. Post-transcriptional Regulation of α-1-Antichymotrypsin by MicroRNA-137 in Chronic Heart Failure and Mechanical Support. Circ Heart Fail 2013;6:853–861.

11. Bruggink-André de la Porte PWF, Lok DJA, Van Wijngaarden J, Cornel JH, Pruijsers-Lamers D, van Veldhuisen DJ, Hoes AW. Heart failure programmes in countries with a primary care-based health care system. Are additional trials necessary? Design of the DEAL-HF study. Eur J Heart Fail 2005;7:910–920.

12. Lok DJA, van der Meer P, la Porte de PWB-A, Lipsic E, Van Wijngaarden J, Hillege HL, van Veldhuisen DJ. Prognostic value of galectin-3, a novel marker of fibrosis, in patients with chronic heart failure: data from the DEAL-HF study. Clin Res Cardiol 2010;99:323–328.

13. Tan F-L, Moravec CS, Li J, Apperson-Hansen C, McCarthy PM, Young JB, Bond M. The gene expression fingerprint of human heart failure. Proc Natl Acad Sci USA 2002;99:11387–11392.

14. Colak D, Kaya N, Al-Zahrani J, Bakheet Al A, Muiya P, Andres E, Quackenbush J, Dzimiri N. Left ventricular global transcriptional profiling in human end-stage dilated cardiomyopathy. Genomics 2009;94:20–31.

15. Yang J, Moravec CS, Sussman MA, DiPaola NR, Fu D, Hawthorn L, Mitchell CA, Young JB, Francis GS, McCarthy PM, Bond M. Decreased SLIM1 expression and increased gelsolin expression in failing human hearts measured by high-density oligonucleotide arrays. Circulation 2000;102:3046–3052.

16. Seguchi O, Takashima S, Yamazaki S, Asakura M, Asano Y, Shintani Y, Wakeno M, Minamino T, Kondo H, Furukawa H, Nakamaru K, Naito A, Takahashi T, Ohtsuka T, Kawakami K, Isomura T, Kitamura S, Tomoike H, Mochizuki N, Kitakaze M. A cardiac myosin light chain kinase regulates sarcomere assembly in the vertebrate heart. J Clin Invest 2007;117:2812–2824.

17. Seguchi O, Takashima S, Yamazaki S, Asakura M, Asano Y, Shintani Y, Wakeno M, Minamino T, Kondo H, Furukawa H, Nakamaru K, Naito A, Takahashi T, Ohtsuka T, Kawakami K, Isomura T, Kitamura S, Tomoike H, Mochizuki N, Kitakaze M. A cardiac myosin light chain kinase regulates sarcomere assembly in the vertebrate heart. J Clin Invest 2007;117:2812–2824.

18. Sabri A, Alcott SG, Elouardighi H, Pak E, Derian C, Andrade-Gordon P, Kinnally K, Steinberg SF. Neutrophil cathepsin G promotes detachment-induced cardiomyocyte apoptosis via a protease-activated receptor-independent mechanism. J Biol Chem 2003;278:23944–23954.

19. Jahanyar J, Youker KA, Loebe M, Assad-Kottner C, Koerner MM, Torre-Amione G, Noon GP. Mast cell-derived cathepsin g: a possible role in the adverse remodeling of the failing human heart. J Surg Res 2007;140:199–203.

20. Braghin E, Galimberti D, Scarpini E, Bresolin N, Baron P. Alpha1-antichymotrypsin induces TNF-alpha production and NF-kappaB activation in the murine N9 microglial cell line. Neurosci Lett 2009;467:40–42.

21. Murohara T, Guo JP, Lefer AM. Cardioprotection by a novel recombinant serine protease inhibitor in myocardial ischemia and reperfusion injury. J Pharmacol Exp Ther 1995;274:1246–1253.

7
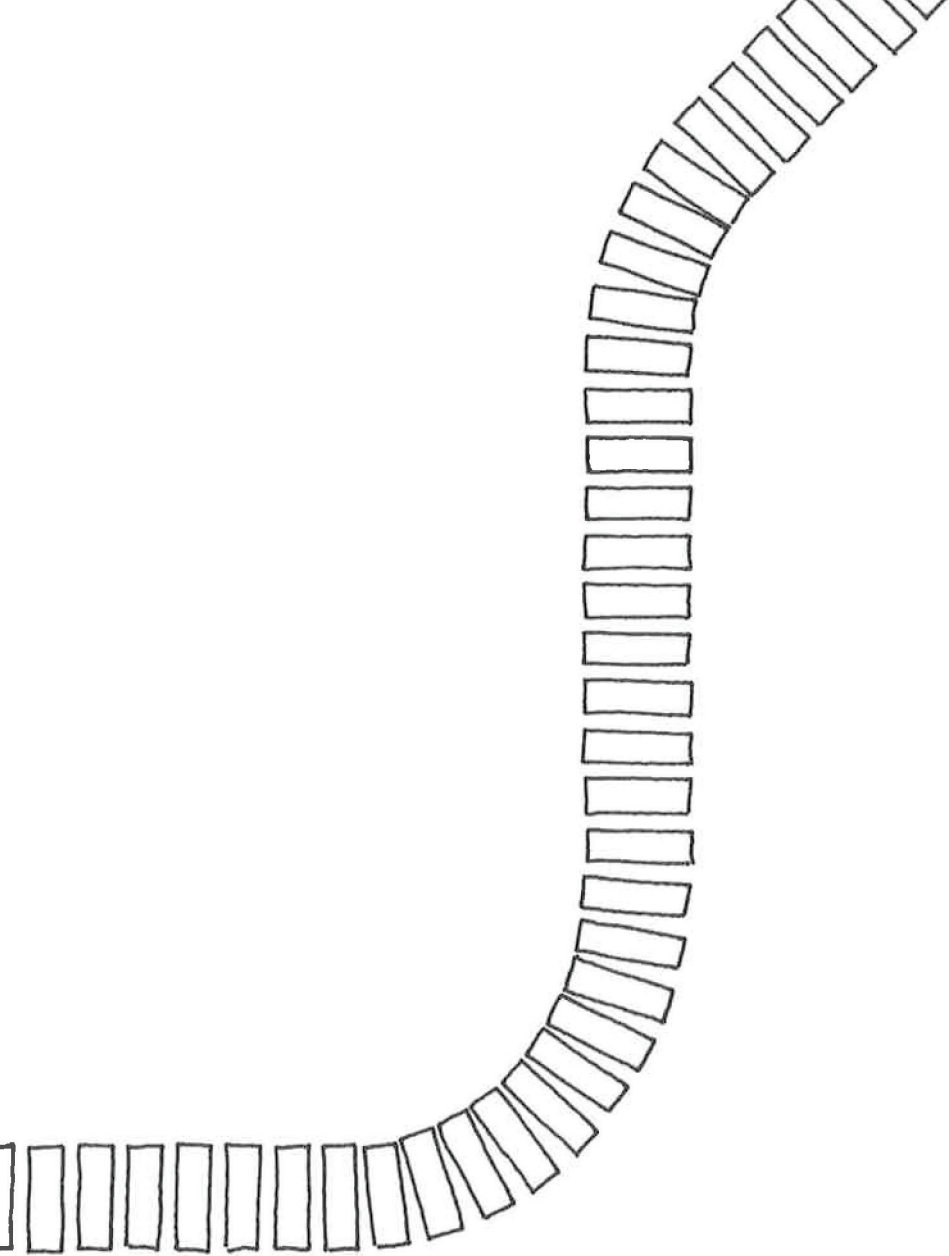
CHAPTER 8

MicroRNA expression in myocardial tissue and plasma of patients with end-stage heart failure during LVAD support: different aspects of continuous versus pulsatile devices

Under revision

Sjoukje I. Lok[1], Nicolaas de Jonge[1], Joyce van Kuik[2], Ankie J. van Geffen[2], Petra van der Weide[2], Erica Siera[2], Bjorn Winkens[3], Pieter A. Doevendans[1], Roel A. de Weger[2], Paula A. da Costa Martins[4]

[1] Department of Cardiology, University Medical Centre Utrecht
[2] Department of Pathology, University Medical Center, Utrecht
[3] Department of Methodology and Statistics, University of Maastricht
[4] Department of Cardiology, CARIM School for Cardiovascular Diseases, Faculty of Health, Medicine and Life Sciences, Maastricht University

Abstract

Aim: In clinical practice, pulsatile flow left ventricular assist devices (pf-LVADs) are being replaced by continuous flow LVADs (cf-LVADs) in patients with end-stage heart failure (HF). MicroRNAs (miRs) play an important role in the onset and progression of HF. In this study, we analyzed cardiac miR expression patterns associated with each type of device.

Methods: Micro-array analysis and quantitative polymerase chain reaction array were performed to identify changes in miR expression in cardiac tissue (n=5) and plasma samples (n=5) during pf- and cf-LVAD support. Selected miRs were analyzed in individual patients supported with a pf-LVAD (n=17), cf-LVAD (n=17) and controls (n=2). In addition, 4 miRs were investigated in plasma of cf-LVAD supported patients (n=18) and healthy controls (n=10).

Results: Array screening revealed that the majority of miRs demonstrated a device-specific change, whereas only few miRs showed uniform expression profiles. Twenty-six miRs were selected and examined in myocardial tissue before and after pf- and cf-LVAD support. Of these, 5 miRs displayed a similar expression pattern among the devices (miR-129*, miR-146a, miR-155, miR-221, miR-222), whereas others only changed significantly during pf-LVAD (miR-let-7i, miR-21, miR-378, miR-378*) or cf-LVAD support (miR-137). Out of the 4 circulating miRs that were analyzed in plasma of cf-LVAD supported patients, miR-21 decreased at 1, 3, and 6 months after LVAD implantation. miR-146a, miR-221 and miR-222 showed a fluctuating time pattern post-LVAD.

Conclusion: Our data show different miR expression profiles amongst pf-LVADs and cf-LVADs, thereby strengthening the concept that the type of unloading can influence different cellular and molecular processes, which might affect clinical outcomes.

Introduction

Heart transplantation (HTx) is the ultimate therapy for patients with end-stage heart failure (HF), despite the discrepancy between the number of donor hearts available and the number of patients awaiting HTx. Left ventricular assist devices (LVADs) were introduced as a bridge to transplantation (BTT) in order to reduce mortality and improve quality of life while waiting for HTx. LVADs provide volume and pressure unloading of the left ventricle, reversing the compensatory responses of the overloaded myocardium, resulting in partial "reverse remodeling" [1-4]. Clinical experience with LVAD support has shown that a subset of patients could be weaned from the device after restoration of basic cardiac function, so called bridge to recovery (BTR) [5,6]. A lot of knowledge has emerged from studies on pulsatile flow LVADs (pf-LVADs), providing insights into the basic mechanisms and limitations of ventricular recovery. However, currently, pf-LVADs have been replaced by continuous flow LVADs (cf-LVAD). Although many studies showed that cf-LVADs are as effective or even better in transplant rate and post-transplant outcomes [7-9], differences in left ventricular unloading between the devices may result in differences between "reverse remodeling" and the experience with pf-LVADs may no longer apply [10-12]. Whereas most of the previous studies remained descriptive by studying the myocardial structure and function as features of reverse remodeling [13,14], not much is known about the specific effects of each system on molecular and signaling pathways. In addition, the lack of validated biomarkers for recovery aggravates uncertainties about ideal timing for LVAD explantation. A hallmark of HF mRNA signatures is that more transcripts are down regulated then up regulated, suggesting the importance of molecular mechanisms that suppress mRNA steady state levels. MicroRNAs (miRs) are small, non-coding RNAs that bind mRNAs at their 3'-untranslated regions, stimulating mRNA degradation or inhibiting protein translation [15]. MiRs are important hallmarks for recovery or deterioration and might be used as a therapeutic target in HF [16-18]. Therefore, delineating their role in posttranscriptional gene regulation offers new insight into the mechanisms how the heart adapts to mechanical support. Because in cf-LVAD, the left ventricle is constantly unloaded throughout the complete cardiac cycle and in pf-LVAD this occurs only at specific time points in the cycle, it is important to compare the physiological effects of such differences. In this context, our goal was to identify changes in miR expression during LVAD support and to investigate whether these expression patterns differ between pf-LVAD and cf-LVAD support, both at tissue and plasma levels. Assessing these differences can help identifying new regulatory players and mechanisms in reverse remodeling during mechanical support.

8

Methods and materials

Study population

Only patients with end-stage non-ischemic dilated cardiomyopathy (DCM) that were supported with a LVAD as BTT were included. To identify which miRs are differentially expressed in tissue during support, microarray analysis of myocardial tissue at time of LVAD implantation from the apical core (pre-LVAD) and from the explanted left ventricle at the time of HTx (post-LVAD) was performed at Exiqon A/S (Vedbeak, Denmark) from paired pf-LVAD (n=5; HeartMate-XVE, HeartMate-VE, Novacor and Thoratec) and cf-LVAD patients (n=5; HeartMate II, Thoratec) and controls (n=2). Furthermore, 26 miRs were selected and analyzed in myocardial tissue pre- and post-LVAD from individual pf-LVAD (n=17) and cf-LVAD patients (n=17) using a custom made Q-PCR array from Qiagen. Myocardial tissue was obtained outside the suture area of the inflow cannula. Control myocardial tissue was collected from 2 donor hearts declined for HTx (due to non-cardiac reasons).

In order to investigate which miRs are present in the circulation and change during cf-LVAD support, a quantitative polymerase chain reaction (QPCR)-based array was performed on pooled plasma samples from 5 patients prior to and 6 months after LVAD implantation (n=2). Four miRs were selected and studied in the plasma of 18 individual cf-LVAD supported patients prior to and 1, 3, and 6 months after implantation and prior to HTx (using Taqman Gene Expression Assays from Life Technologies). Control plasma was collected from 10 healthy individuals.

All subjects included in this study gave written informed consent for the use of their tissues for research purposes. The experimental design of the study is depicted in *Supplemental Figure 1* (*Figure S1*).

Tissue and plasma arrays (Pre-screening)

All array experiments were conducted at Exiqon Services (Copenhagen, Denmark) according to the manufacturer's protocol.

For tissue: Myocardial tissue was collected pre- and post pf/cf-LVAD implantation and from healthy controls. Total RNA was isolated from 20 sections of 10-μm snap-frozen tissue using miRNeasy Mini Kit according to the manufacturer's instructions (Qiagen Inc, Austin, USA). The RNA quality was verified by an Agilent 2100 Bioanalyzer profile. 500 ng total RNA from both samples and reference were labeled with a Hy3™ and HY5™ fluorescent label, respectively, using the miRCURY LNA™ microRNA array Hi-Power Labeling

Kit, Hy3™ /HY™. The Hy3™-labeled samples and the HY5™-labeled reference RNA sample were mixed pair-wise and hybridized to the miRCURY LNA™ microRNA Array (6th Gen, consisting of 3100 probe sets). The quantified signals were background corrected (Normexp with offset value 10) and normalized using the global Lowess (LOcally WEighted Scatterplot Smoothing) regression algorithm. Data quality assessment showed that the labeling was successful for all capture probes since the control spike-in oligo nucleotides produced signals in the expected range. Samples that showed lowered correlation of the spike-on-controls compared to the remaining samples were, therefore, excluded from further analysis.

For plasma: Plasma from patients was collected prior to cf-LVAD implantation and 6 months thereafter. Total RNA was isolated from 200μl plasma per sample using miRNeasy Mini Kit (Qiagen Inc). Each RNA sample was reverse transcribed into cDNA and run on the miRCURY LNA™ Universal RT miR PCR Human panel I and II, which contain together, 742 miR assays. Each PCR panel contained a PCR control (three replicates of an inter-plate calibrator) and 3 primer sets for reference genes. In addition, one enzyme control (reverse transcriptase replaced by water) was included as negative control. The negative controls were used to set the threshold for sample detection, to which a value of 42 was assigned. The criterion for including an assay in the further analysis is that the quantification cycle (Cq) must be 5 cycles lower than the negative control.

An additional step in the real time PCR analysis, by generating a melting curve for each reaction, was performed to evaluate the specificity of the assays. Any assays that showed multiple peaks have been excluded from the data set. The amplification curves were analyzed using the Roche LC software, both for determination of Cq and for melting curve analyses. PCR efficiency was also assessed by analysis of the PCR amplification curve using algorithms similar to the LinReg software. The average efficiencies ranged between 1.8 and 2.1. Individual reactions that gave an efficiency<1.6 were excluded from the dataset. The melting temperature was furthermore checked to be within the specifications of the individual assays. For normalization of the data, the average of the assays detected in all samples has been applied. These were 152 assays. By using the formula *normalized Cq = Average Cq (n=152) – assay Cq* to calculate the normalized Cq values, lower values will indicate that a specific miR is more abundant in that specific sample.

miR selection criteria
The selection of the investigated miRs was made based on the results from the prescreening (Exiqon arrays) combined with previously obtained (unpublished) miR array data from our

8

group and literature studies.

For tissue, the Exiqon array data did not show profound changes between pre- and post-LVAD samples. This can be due to the strict statistical analysis; the low amount of samples used or the lower sensitivity of the technique compared with, for instance, Q-PCR. A less strict array analysis (excluding correction for multiple testing) resulted in a few miRs that were differentially expressed between pre- and post pf-LVAD, or pre- and post cf-LVAD, respectively. From these we selected 12 miRs for validation and added up to 26 miRs using our own unpublished miR data and literature studies. Testing these miRs in a larger patient panel using a more sensitive technique (Q-PCR) may result in more significant differences. For plasma we used the results of our custom made PCR-array for tissue as a starting point, to secure that the plasma miRs we selected could be derived from heart tissue. The plasma data from the Exiqon PCR array was used to check if the selected miRs were detectable in plasma.

Q-PCR analysis of miR expression in tissue

Twenty-six miRs were selected for investigation of their expression levels in a larger pf-LVAD (n=17) and cf-LVAD (n=17) patient cohort. RNA was isolated from 20 snap frozen 10μm sections of myocardial tissue (pre- and post-LVAD) using the miRNeasy Mini Kit (Qiagen Inc, Austin, USA) according to the manufacturer. For cDNA synthesis and Q-PCR analysis, the miScript II RT kit and a custom made miScript PCR Array (based on the 26 selected miRs and 6 controls and in a 96-wells format) were used (Qiagen Inc). In short, 250 ng of total RNA was converted into cDNA using the 5x miScript HiSpec buffer. Thermal cycling was done using the ViiA™ 7 Real-Time PCR system (Life Technologies, USA) and consisted of a 15 minute hot start at 95°C followed by 40 cycles of 94°C for 15 sec, 55°C for 30 sec and 70°C for 30 sec.

Of the custom made array, candidate stable references (miR-340, miR-664) were selected, based upon their stable expression in the previously performed Exiqon array. Also, SNORD68 and RNU6-2 were chosen because these small RNAs have been verified to have relatively stable expression levels across tissues (miScript Manual). The standard deviation (SD) of the Cq values of all samples was determined for the candidate reference genes (SD for miR-340 =0.46, SD for miR-664 = 0.40, SD for RNU6-2 = 0.47, SD for SNORD68 = 0.48). Expression levels of miR-664 were used for data normalization, because the expression pattern of this miR was very stable among all samples tested. The other 2 controls were a reverse transcription control (miRTC) and a positive PCR control (PPC). The relative quantity (RQ) was calculated using the ΔΔCq method.

Q-PCR analysis of miR expression in plasma

From the custom array on tissue, specific miRs were selected to further investigate their expression levels in plasma. RNA was isolated from 500 µl plasma at different time points (pre cf-LVAD support, 1, 3 and 6 months after cf-LVAD implantation, and pre-HTx) using the miRVana™ PARIS™ kit (part# AM1556, Life Technologies, USA) according to the manufacturer's instructions.

cDNA synthesis for miRs was performed using the TaqMan®MicroRNA Reverse Transcription Kit Life Technologies, USA). Q-PCR was performed using TaqMan® MicroRNA assays (Life Technologies, USA). PCR reactions were performed on the ViiA™ 7Real-Time PCR system (Life Technologies, USA). Thermal cycling conditions consisted of a denaturation step at 95 °C for 10 min, followed by 40 cycles of 95 °C for 15 sec and 60°C for 1 min. Cq values above 35 were defined negative. A stable miR from the previously performed Exiqon array on plasma (miR-148b) was used as reference and the relative quantity (RQ) was calculated using the ΔΔCq method.

Statistical analysis

Categorical and continuous data are presented by number (%) and by mean (SD) or median (interquartile range IQR, i.e. 25th - 75th percentile), where appropriate. Independent-samples t-tests were used for comparing miR expression arrays (Exiqon). Due to the high number of miRs being tested in parallel, micro-arrays are prone to give false positive results. The false positive rate is controlled by multiple testing corrections that adjust p-values derived from multiple statistical tests. Therefore, p-values were calculated with and without the Benjamin and Hochberg multiple testing adjustment method [19]. For miR Q-PCR array (Qiagen) data, the groups were compared using paired-samples t-test and Wilcoxon signed rank test, where appropriate. For miR expression profiling in plasma, the longitudinal detection pattern of circulating miRs (from pre-LVAD until pre Htx) was evaluated using the mixed model analysis with a random intercept to account for the correlation between repeated measurements within the same person. The data from this model are presented by estimated mean ± standard error. The miR expression pre LVAD was compared with healthy controls using Mann-Whitney U test. P-values ≤ 0.05 were considered statistically significant. Mixed model analysis was applied using SPSS, version 20 (SPSS, Inc., Chicago, Illinois, USA). All other analyses were performed using GraphPad Prism version 5.0 (GraphPad Software Inc., La Jolla, CA, USA).

8

Results

Patient demographics

Baseline characteristics of all patients involved in the study are presented in *Table 1* and *Table 2*. Patients supported with a pf-LVAD (n=17) had a mean age of 45 years, 82% (n=14) were male, with a median HF duration of 1754 days (IQR 750-2489) and LVAD duration of 282 (IQR 197-512) days (*Table 2*). The majority of the patients (70%) was supported with a HeartMate-(X)VE. The cf-LVAD supported group (n=17) consisted of patients with a mean age of 39 years and 94% (n=16) were male. The median duration of HF was 398 days (IQR 49-1344) and the LVAD duration was 206 (IQR 190-317) days. In the cf-LVAD group, all patients were supported with a HeartMate II device (*Table 2*).

Table 1: Baseline demographics of the patients (n=15) selected for microarray analysis (pre-screening)

	Tissue		Plasma
	pf-LVAD (n=5)	**cf-LVAD** (n=5)	**cf-LVAD** (n=5)
Age, years	38 ± 7	49 ± 6	42 ± 6
Male, %	5 (100%)	4 (80%)	2 (40%)
HF duration (days)	261 (26-1023)	1747 (1531-3316)	1754 (723-1884)
Body Mass Index, kg/m2	22.7 ± 1.5	26.2 ± 1.86	24.1 ± 1.47
Diabetes mellitus, %	0 (0%)	0 (0%)	0 (0%)
Hypertension, %	0 (0%)	0 (0%)	0 (0%)
CVA/TIA, %	1 (20%)	2 (40%)	2 (40%)
NYHA classification IV, %	5 (100%)	5 (100%)	5 (100%)
Etiology of non-ischemic DCM, %			
Idiopathic	2 (40%)	3 (60%)	2 (40%)
Familial[a]	1 (20%)	2 (40%)	3 (60%)
Toxic (drugs)	1 (20%)	0 (0%)	0 (0%)
Myocarditis	1 (20%)	0 (0%)	0 (0%)
CRTD/ICD before LVAD implant, %	2 (40%)	4 (80%)	3 (60%)
Type of LVAD			
HeartMate II	0	5 (100%)	5 (100%)
HeartMate (X)VE	3 (60%)	0 (0%)	0 (0%)
Thoratec	1 (20%)	0 (0%)	0 (0%)
Novacor	1 (20%)	0 (0%)	0 (0%)
Days of LVAD support[b]	204 (180-301)	489 (238-897)	500 (260-1082)

HF, heart failure; CVA, cerebrovascular accident; TIA, transient ischemic attack;
NYHA, New York Heart Association; DCM, dilated cardiomyopathy;
CRTD, cardiac resynchronization therapy defibrillator; ICD, implantable cardioverter defibrillator.
Categorical data are presented as number (%), continuous data as mean±SEM or median (IQR), respectively.
[a] Familial DCM is defined if the patient has one or more family members diagnosed with idiopathic DCM or has a first-degree relative with an unexplained sudden death under the age of 35 years.
[b] Days of LVAD support are based on patients who already underwent HTx.

Table 2: Baseline demographics of the patients supported with a pulsatile flow LVAD (pf-LVAD) and continuous flow LVAD (cf-LVAD) (validation).

	Tissue		Plasma
	pf-LVAD (n=17)	**cf-LVAD** (n=17)	**cf-LVAD** (n=18)
Age, years	45 ± 3	39 ± 3	45 ± 3
Male, %	14 (82%)	16 (94%)	14 (78%)
Body Mass Index, kg/m2	25.7 ± 1.8	22.8 ± 0.87	24.3 ± 1.3
HF duration (days)	1754 (750-2489)	398 (49-1344)	1872 (424-2343)
Smoking			
No	9 (53%)	13 (76%)	11 (61%)
Yes	3 (18%)	2 (12%)	2 (11%)
Former	5 (29%)	2 (12%)	5 (28%)
Diabetes mellitus, %	1 (6%)	0 (0%)	2 (11%)
Hypertension, %	1 (6%)	0 (0%)	0 (0%)
Hyperlipidemia, %	2 (12%)	1 (6%)	2 (11%)
CVA/TIA before LVAD, %	6 (35%)	1 (6%)	5 (28%)
NYHA classification IV, %	18 (100%)	17 (100%)	18 (100%)
Etiology of non-ischemic DCM, %			
Idiopathic	8 (47%)	10 (59%)	6 (33%)
Familial[a]	6 (35%)	4 (24%)	7 (39%)
Myocarditis	2 (12%)	1 (6%)	3 (17%)
Toxic	0 (0%)	1 (6%)	1 (6%)
Peripartum cardiomyopathy	0 (0%)	1 (6%)	0 (0%)
Systemic disease	1 (6%)	0 (0%)	1 (6%)
CRTD/ICD before implantation, %	13 (61%)	8 (47%)	11 (61%)
Type of LVAD			
HeartMate-II	0 (0%)	17 (100%)	18 (100%)
HeartMate-(X)VE	12 (70%)	0 (0%)	0 (0%)
Thoractec	3 (18%)	0 (0%)	0 (0%)
Novacor	1 (6%)	0 (0%)	0 (0%)
HeartMate-IP	1 (6%)	0 (0%)	0 (0%)
Days of LVAD support[b]	282 (197-512)	206 (190-317)	386 (227-510)

HF, heart failure; CVA, cerebrovascular accident; TIA, transient ischemic attack;
NYHA, New York Heart Association; DCM, dilated cardiomyopathy;
CRTD, cardiac resynchronization therapy defibrillator; ICD, implantable cardioverter defibrillator.
Categorical data are presented as number (%), continuous data as mean±SEM or median (IQR), respectively.
[a] Familial DCM is defined if the patient has one or more family members diagnosed with idiopathic DCM or has a first-degree relative with an unexplained sudden death under the age of 35 years.
[b] Days of LVAD support are based on patients who already underwent HTx.

8

Differential human miR expression pattern in pre- and post-LVAD myocardial tissue

From the 30 miRs that were most differentially expressed in pf-LVAD (logFC>1), seven (23%) were also differentially expressed in (the 20 most differentially expressed miR) cf-LVAD, when comparing control tissue with pre-LVAD tissue (*Figure 1A, Tables S2-S3*). This number increased to 11 (37%), comparing controls vs post-LVAD tissue (*Figure 1B*, *Tables S4-S5*).

Micro-array analysis of miR expression in myocardial samples revealed distinct miR expression profiles between pre- and post-LVAD, for both types of devices. Unfortunately, the array analysis did not identify any differentially expressed miRs (logFC>1) when comparing the pre- and post-sample groups, after correcting for multiple testing using the Bonferroni method. An array analysis excluding the Bonferroni correction, resulted in the detection of either 19 or 13 miRs that were differentially expressed between pre- and post pf-LVAD, or pre- and post cf-LVAD, respectively (*Tables S6-S7*). From these, we selected 12 miRs for validation and added up to 26 miRs using our own unpublished miR data and literature studies (*Table S1*). To evaluate whether the expression changed significantly during LVAD support, selected miRs were tested in a larger patient panel (before and after pf-LVAD/cf-LVAD support) using a more sensitive technique (Q-PCR).

Out of the 26 selected miRs, 5 miRs showed a similar pattern during pf-LVAD and cf-LVAD support. miR-129* and miR-146a were downregulated in pre-LVAD supported patients and increased during mechanical support (*Figure 2A-B*). In contrast, miR-155, miR-221 and miR-122 were upregulated in pre-LVAD and decreased upon implantation (*Figure 2C-E*).

Several miRs showed a significant change in either pf-LVAD or cf-LVAD support. Five miRs changed in expression after pf-LVAD (miR-let-7i, miR-21, miR-378 and miR-378*, *Figure 3A-D*), whereas the expression of miR-137 only changed significantly during cf-LVAD support (*Figure 3E*). Of note, miR-21 changed non-significantly in cf-LVAD tissue, but showed the same trend as in pf-LVAD.

Curiously, several miRs that have previously been reported to be differentially expressed between pre- and post pf-LVAD [20], did not significantly change in cf-LVAD. This was the case for miR-133a, miR-133b, miR-1, miR-151, miR-7a and miR-378 (*Figure S2A-F*).
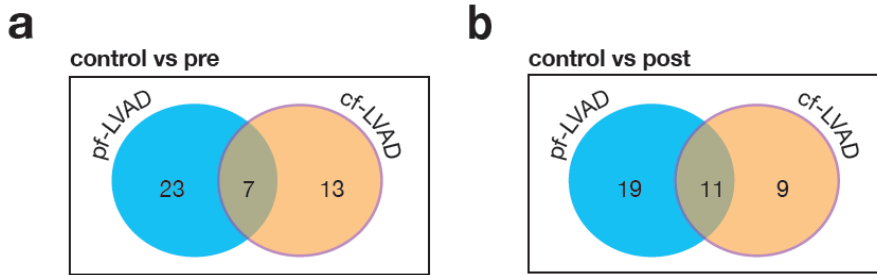
Figure 1: Distribution of miR-expression in cardiac tissue of LVAD patients and controls
MiR expression in patients prior to pulsatile flow (pf-LVAD) and continuous flow LVAD (cf-LVAD) implantation versus controls (*A*) and post pf/cf-LVAD versus controls (*B*), respectively. Micro-array analysis revealed distinct miR-expression profiles between pre- and post-LVAD, for both type of devices.
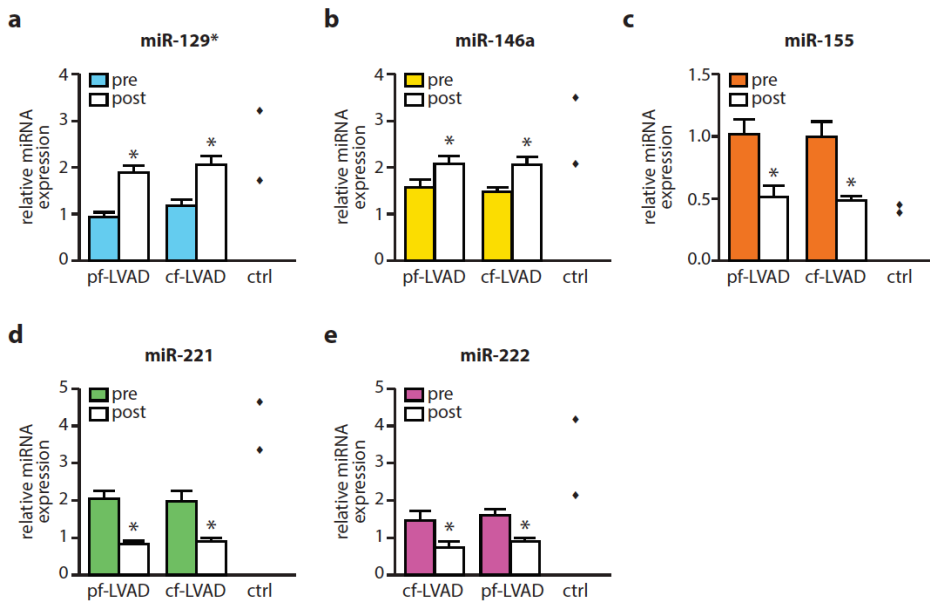
Figure 2: Similar changes in miR expression in pulsatile flow (pf-LVAD) and continuous flow LVAD (cf-LVAD)
Alteration in miR-expression in myocardial tissue of both pf-LVAD (n=17) and cf-LVAD (n=17) patients and controls (ctrl). miR-129* and miR-146a are upregulated in post-LVAD in comparison to pre-LVAD, whereas miR-155, miR-121 and miR-122 are downregulated in both devices. The asterisk (*) represents p<0.05.

8
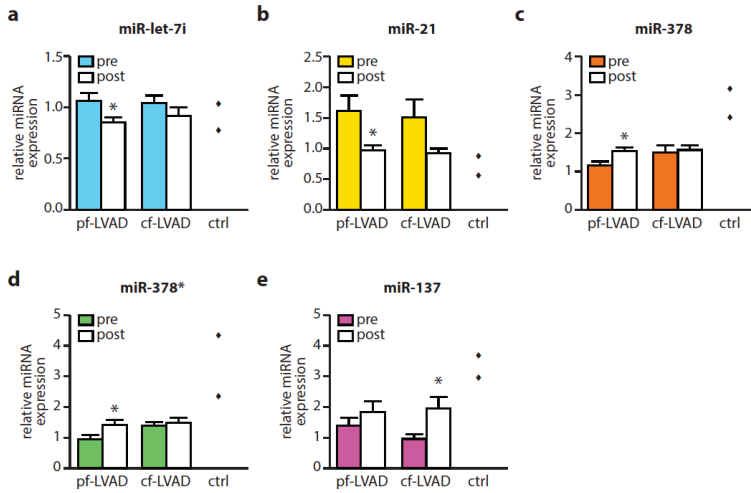
Figure 3: Device specific changes in miR expression

Selection of myocardial miRs that changed only in pulsatile flow (pf-LVAD; *A-D*) or continuous flow LVAD (cf-LVAD; *E*), respectively. Controls are presented as ctrl. During pf-LVAD support, miR-let-7i, miR-21, miR-378 and miR-378* changed significantly post LVAD, whereas in cf-LVAD these miRs did not differ significantly. In cf-LVAD, only miR-137 changed significantly post-LVAD. The asterisk (*) represents $p<0.05$.
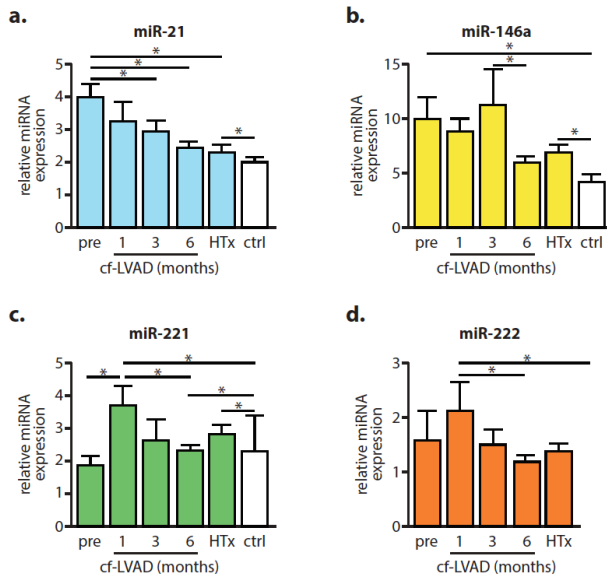
Figure 4: Changes in plasma miR expression after continuous flow LVAD (cf LVAD) implantation

Expression of 4 circulating miRs during cf-LVAD support prior to and 1,3, and 6 months after implantation and before HTx (n=18 patients and n=10 controls). In miR-222, no reliable duplicates on controls could be measured. The asterisk (*) represents $p<0.05$.

Differential human miR expression pattern in pre- and post-LVAD-derived plasma

Plasma samples from patients were collected prior to cf-LVAD implantation and 6 months thereafter. From a total of 742 miRs investigated, we were able to detect the expression of 352 miRs. The most differentially regulated miRs are depicted in *Table S8*. Based on miR expression in tissue obtained by the custom Qiagen arrays and the expression profile in plasma (the miRs had to be detectable in plasma), 4 miRs that changed significantly (or near significant) in cf-LVAD supported patients were selected for further validation in plasma by Q-PCR: miR-21, miR-146a, miR-221 and miR-222. Prior to cf-LVAD implantation, levels of miR-21 were doubled compared to controls, decreased significantly during support, but did not normalize (*Figure 4A*). Levels of miR-146a were also increased pre-LVAD compared to controls, but revealed a fluctuating expression pattern during support with a tendency to decrease (*Figure 4B*). The expression patterns for miR-221 and miR-222 were alike, with both miRs upregulated after 1 month followed by downregulation (*Figure 4C-D*).

Discussion

In the present study, we demonstrate distinct differences in miR expression not only in non-failing versus LVAD-supported hearts, but also more specific differences in miR expression patterns in pulsatile flow (pf-LVAD) versus continuous flow LVAD (cf-LVAD) supported myocardium.

The use of cf-LVADs has been increasing over the last years and this is mostly related to its many advantages over pf-LVADs: smaller size, reducing surgical trauma, higher mechanical reliability, limited-blood containing surfaces, better energy efficiency and decreased risk of device-related infections [9,21]. Nevertheless, because cf-LVADs generate less pulsatile hemodynamics, there are still some reservations regarding the effect of long-term continuous blood flow mainly regarding cardiovascular remodeling, perfusion of end-organs and long-term patient outcome. Accordingly, it has been suggested that BTR is more likely in pf-LVAD support than in cf-LVAD support [22]. Whereas, most studies, so far, have compared the myocardial contractile profiles and cellular/hemodynamic responses of the failing myocardium in pf-LVAD versus cf-LVADs, the exact biochemical and molecular changes related to each type of device are still unclear. In this context and to our best knowledge, this study is the first to apply a miR expression profiling strategy to evaluate the molecular regulatory role of miRs during long-term LVAD support and to provide more insight in the molecular mechanisms that are affected by each type of device.

8

miRs are established main players in the pathological cardiac remodeling process leading to HF [16,23-25]. LVAD support is able to partially reverse structural and mechanistic changes and this may be related to changes in miR expression patterns. To date, only three studies have addressed changes in miRs during LVAD support [20,26,27]. Ramani *et al* examined the expression levels of 376 miRs in myocardial tissue of 28 patients to determine whether there was an association between the expression levels at the time of LVAD implantation and the ability of the heart to recover during support [27]. In addition, 7 non-failing hearts were investigated. Fourteen of the patients underwent removal of their LVAD. The level of miR-15b, miR-23a, miR-26a and miR-195 were significantly decreased in the left ventricle of the recovery hearts when compared to LVAD dependent hearts. Remarkably, LVAD support did not alter the expression of any of these miRs. Moreover, the expression levels of miR-23a and miR-195 in the recovery group were similar to those of non-failing hearts. An editorial comment of Mann and Burkhoff suggest therefore, that degree of recovery may relate more to the severity and nature of the underlying HF at the time of LVAD implantation, rather than to the effect of mechanical unloading [28]. Matkovich *et al* performed a parallel miR and mRNA micro-array profiling on myocardial tissue from non-failing hearts, failing hearts, and failing hearts supported with a LVAD [26]. They showed that 28 miRs were 2-fold increased in failing hearts, and there was near complete normalization of the miR signature in the LVAD supported hearts. By contrast, 444 mRNAs were altered by 1.3 fold in failing hearts, and only 29 of these normalized by 25% in the LVAD supported hearts. This suggests that miRs may be more sensitive than mRNAs to functional changes related to end-stage HF. In fact, previous work from our group [20] focusing on the differential expression of four specific miRs known to be expressed in the heart and to have functional roles in progression of HF (miR-1, miR-133a, miR-133b and miR-208), showed that expression of these miRs is restored during pf-LVAD support. However, this was only observed in ischemic heart disease patients and not in DCM patients. Similarly, in the present study, we showed that expression of these miRs did not change significantly in cf-LVAD supported myocardial tissue of DCM patients (*Figure S2*).

There is a specific set of miRs that showed the same expression pattern after cf- and pf-LVAD support, with some of them being restored to expression levels of controls after LVAD support. Curiously, when examining the temporal expression pattern of miR-21 after implantation and just before HTx, it revealed a consistent decreasing pattern until control levels were reached. miR-21 is very abundant in the cardiovascular system and several studies have revealed that its expression is deregulated in heart and vasculature under cardiovascular disease conditions, such as proliferative vascular disease, cardiac

hypertrophy, HF, and ischemic heart disease [29-31]. There are, however, some miRs that were further depleted or induced after support and therefore, have an expression behavior very different from healthy hearts. miR-221 and miR-222, are examples of miRs that are repressed in HF and this repression is even more accentuated after support. This kind of response may reflect the role of these miRs in regulating vascular inflammation and therefore, their function as mediators of endothelial cell pathophysiology [32,33] may provide clues as to why cardiac function is not completely normalized in most LVAD patients.

More importantly, our data confirms the hypothesis that different type of support devices result in different miR expression profiles. From all the differentially expressed miRs in LVAD-supported myocardium, only 30% are common to both types of devices, suggesting that all others are specific for cf- or pf-LVAD. In agreement, as miR-137 seems to be a cf-LVAD-specific miR, miRs such as miR- let7i, -21, -378 and -378* show a more pronounced change in pf-LVAD as compared to cf-LVAD. Interestingly, all these miRs are not only implicated in vascular inflammation but also in cell growth and vascularization in several types of cancer [34,35]. miR-378 and miR-378* are also implicated in cardiac pathological remodeling as being negative regulators of cardiac hypertrophic growth [36,37]. In agreement, our results show a significant increase in miR-378 and miR-378* in post pf-LVAD, indicating that increased expression levels of these miRs contribute to better cardiac function and therefore positive cardiac remodeling. Furthermore, we have very recently shown that miR-137 is implicated in reverse remodeling during cf-LVAD support by directly regulating alpha-1-antichymotrypsin (ACT), a potential new biomarker of HF [18].

The differences observed between miR expression profiles related to cf- and pf-LVAD might explain the different patient outcome observed after myocardial support by each type of device. In fact, previous profiling studies have detected that mRNA signatures do not always reflect the improvements delivered by biomechanical support such as that provided by LVADs [38,39]. From a total of 3088 mRNA transcripts exhibiting abnormal abundance in HF, only 11% of these genes exhibit partial recovery and only 5% showed true normalization (38). These numbers may reflect the fact that not all secondary effects of LVAD support are beneficial. In a similar way, also the specific miR expression profiles induced by either pulsatile or continuous flow will affect the clinical outcome of those patients either by restoring protein levels (in some cases just to a certain extent) or even accentuate the unbalance between pre and post-LVAD.

Altogether, our data strongly suggests that specific and different signaling molecules are implied in the reverse remodeling associated to pf-LVAD and cf-LVAD support respectively.

8

More precisely, specific miRs are differentially regulated in a device specific manner, strengthening the concept that selection of device type can influence different cellular and molecular processes, directly affecting clinical outcomes. As pf-LVADs are no longer used, studies like ours should be taken into consideration for further improvements and optimization of the currently used cf-LVADs.

References

1. Wohlschlaeger J, Schmitz KJ, Schmid C, Schmid KW, Keul P, Takeda A, Weis S, Levkau B, Baba HA. Reverse remodeling following insertion of left ventricular assist devices (LVAD): a review of the morphological and molecular changes. Cardiovasc. Res. 2005 Dec 1;68(3):376–386.

2. Ambardekar AV, Buttrick PM. Reverse remodeling with left ventricular assist devices: a review of clinical, cellular, and molecular effects. Circ Heart Fail. 2011 Mar;4(2):224–233.

3. Hall JL, Fermin DR, Birks EJ, Barton PJR, Slaughter M, Eckman P, Baba HA, Wohlschlaeger J, Miller LW. Clinical, molecular, and genomic changes in response to a left ventricular assist device. J. Am. Coll. Cardiol. 2011 Feb 8;57(6):641–652.

4. Bruggink AH, van Oosterhout MFM, de Jonge N, Ivangh B, van Kuik J, Voorbij RHAM, Cleutjens JPM, Gmelig-Meyling FHJ, de Weger RA. Reverse remodeling of the myocardial extracellular matrix after prolonged left ventricular assist device support follows a biphasic pattern. J Heart Lung Transplant. 2006 Sep;25(9):1091–1098.

5. Birks EJ, Tansley PD, Hardy J, George RS, Bowles CT, Burke M, Banner NR, Khaghani A, Yacoub MH. Left ventricular assist device and drug therapy for the reversal of heart failure. N. Engl. J. Med. 2006 Nov 2;355(18):1873–1884.

6. Müller J, Wallukat G, Weng YG, Dandel M, Spiegelsberger S, Semrau S, Brandes K, Theodoridis V, Loebe M, Meyer R, Hetzer R. Weaning from mechanical cardiac support in patients with idiopathic dilated cardiomyopathy. Circulation. 1997 Jul 15;96(2):542–549.

7. Pruijsten RV, Lok SI, Kirkels HH, Klöpping C, Lahpor JR, de Jonge N. Functional and hemodynamic recovery after implantation of continuous-flow left ventricular assist devices in comparison with pulsatile left ventricular assist devices in patients with end-stage heart failure. Eur. J. Heart Fail. 2012 Mar;14(3):319–325.

8. Garatti A, Bruschi G, Colombo T, Russo C, Lanfranconi M, Milazzo F, Frigerio M, Vitali E. Clinical outcome and bridge to transplant rate of left ventricular assist device recipient patients: comparison between continuous-flow and pulsatile-flow devices. Eur J Cardiothorac Surg. 2008 Aug;34(2):275–80; discussion 280.

9. Slaughter MS, Rogers JG, Milano CA, Russell SD, Conte JV, Feldman D, Sun B, Tatooles AJ, Delgado RM, Long JW, Wozniak TC, Ghumman W, Farrar DJ, Frazier OH, HeartMate II Investigators. Advanced heart failure treated with continuous-flow left ventricular assist device. N. Engl. J. Med. 2009 Dec 3;361(23):2241–2251.

10. Klotz S, Deng MC, Stypmann J, Roetker J, Wilhelm MJ, Hammel D, Scheld HH, Schmid C. Left ventricular pressure and volume unloading during pulsatile versus nonpulsatile left ventricular assist device support. Ann. Thorac. Surg. 2004 Jan;77(1):143–9; discussion 149–50.

11. Bartoli CR, Giridharan GA, Litwak KN, Sobieski M, Prabhu SD, Slaughter MS, Koenig SC. Hemodynamic responses to continuous versus pulsatile mechanical unloading of the failing left ventricle. ASAIO J. 2010 Aug 31;56(5):410–416.

8

12.   Haft J, Armstrong W, Dyke DB, Aaronson KD, Koelling TM, Farrar DJ, Pagani FD. Hemodynamic and exercise performance with pulsatile and continuous-flow left ventricular assist devices. Circulation. 2007 Sep 11;116(11 Suppl):I8–15.

13.   Kato TS, Chokshi A, Singh P, Khawaja T, Cheema F, Akashi H, Shahzad K, Iwata S, Homma S, Takayama H, Naka Y, Jorde U, Farr M, Mancini DM, Schulze PC. Effects of continuous-flow versus pulsatile-flow left ventricular assist devices on myocardial unloading and remodeling. Circ Heart Fail. 2011 Sep 1;4(5):546–553.

14.   Garcia S, Kandar F, Boyle A, Colvin-Adams M, Lliao K, Joyce L, John R. Effects of pulsatile- and continuous-flow left ventricular assist devices on left ventricular unloading. J Heart Lung Transplant. 2008 Mar;27(3):261–267.

15.   Bartel DP. MicroRNAs: genomics, biogenesis, mechanism, and function. Cell. 2004 Jan 23;116(2):281–297.

16.   da Costa Martins PA, Salic K, Gladka MM, Armand A-S, Leptidis S, Azzouzi el H, Hansen A, Coenen-de Roo CJ, Bierhuizen MF, van der Nagel R, van Kuik J, de Weger R, de Bruin A, Condorelli G, Arbones ML, Eschenhagen T, De Windt LJ. MicroRNA-199b targets the nuclear kinase Dyrk1a in an auto-amplification loop promoting calcineurin/NFAT signalling. Nat. Cell Biol. 2010 Dec;12(12):1220–1227.

17.   Leptidis S, Azzouzi el H, Lok SI, de Weger R, Olieslagers S, Kisters N, Silva GJ, Heymans S, Cuppen E, Berezikov E, De Windt LJ, da Costa Martins P. A deep sequencing approach to uncover the miRNOME in the human heart. PLoS ONE. 2013;8(2):e57800.

18.   Lok SI, van Mil A, Bovenschen N, van der Weide P, van Kuik J, Van Wichen D, Peeters T, Siera E, Winkens B, Sluijter JPG, Doevendans PA, da Costa Martins PA, de Jonge N, de Weger RA. Post-transcriptional Regulation of α-1-Antichymotrypsin by MicroRNA-137 in Chronic Heart Failure and Mechanical Support. Circ Heart Fail. 2013 Jul 1;6(4):853–861.

19.   Benjamini Y, Hochberg Y. JSTOR: Journal of the Royal Statistical Society. Series B (Methodological), Vol. 57, No. 1 (1995), pp. 289-300. Journal of the Royal Statistical Society Series B (Methodolocial). 1995;57:289–300.

20.   Schipper MEI, van Kuik J, de Jonge N, Dullens HFJ, de Weger RA. Changes in regulatory microRNA expression in myocardium of heart failure patients on left ventricular assist device support. J Heart Lung Transplant. 2008 Dec;27(12):1282–1285.

21.   Schaffer JM, Allen JG, Weiss ES, Arnaoutakis GJ, Patel ND, Russell SD, Shah AS, Conte JV. Infectious complications after pulsatile-flow and continuous-flow left ventricular assist device implantation. J Heart Lung Transplant. 2011 Feb;30(2):164–174.

22.   Krabatsch T, Schweiger M, Dandel M, Stepanenko A, Drews T, Potapov E, Pasic M, Weng Y-G, Huebler M, Hetzer R. Is bridge to recovery more likely with pulsatile left ventricular assist devices than with nonpulsatile-flow systems? Ann. Thorac. Surg. 2011 May;91(5):1335–1340.

23.   van Rooij E, Sutherland LB, Liu N, Williams AH, McAnally J, Gerard RD, Richardson JA, Olson EN. A signature pattern of stress-responsive microRNAs that can evoke cardiac hypertrophy and heart failure. Proc. Natl. Acad. Sci. U.S.A. 2006 Nov 28;103(48):18255–18260.

24. Ikeda S, Kong SW, Lu J, Bisping E, Zhang H, Allen PD, Golub TR, Pieske B, Pu WT. Altered microRNA expression in human heart disease. Physiol. Genomics. 2007 Nov 14;31(3):367–373.

25. Thum T, Galuppo P, Wolf C, Fiedler J, Kneitz S, van Laake LW, Doevendans PA, Mummery CL, Borlak J, Haverich A, Gross C, Engelhardt S, Ertl G, Bauersachs J. MicroRNAs in the human heart: a clue to fetal gene reprogramming in heart failure. Circulation. 2007 Jul 17;116(3):258–267.

26. Matkovich SJ, Van Booven DJ, Youker KA, Torre-Amione G, Diwan A, Eschenbacher WH, Dorn LE, Watson MA, Margulies KB, Dorn GW. Reciprocal regulation of myocardial microRNAs and messenger RNA in human cardiomyopathy and reversal of the microRNA signature by biomechanical support. Circulation. 2009 Mar 10;119(9):1263–1271.

27. Ramani R, Vela D, Segura A, McNamara D, Lemster B, Samarendra V, Kormos R, Toyoda Y, Bermudez C, Frazier OH, Moravec CS, Gorcsan J, Taegtmeyer H, McTiernan CF. A micro-ribonucleic acid signature associated with recovery from assist device support in 2 groups of patients with severe heart failure. J. Am. Coll. Cardiol. 2011 Nov 22;58(22):2270–2278.

28. Mann DL, Burkhoff D. Myocardial expression levels of micro-ribonucleic acids in patients with left ventricular assist devices signature of myocardial recovery, signature of reverse remodeling, or signature with no name? J. Am. Coll. Cardiol. 2011 Nov 22;58(22):2279–2281.

29. Cheng Y, Ji R, Yue J, Yang J, Liu X, Chen H, Dean DB, Zhang C. MicroRNAs are aberrantly expressed in hypertrophic heart: do they play a role in cardiac hypertrophy? Am. J. Pathol. 2007 Jun;170(6):1831–1840.

30. Thum T, Gross C, Fiedler J, Fischer T, Kissler S, Bussen M, Galuppo P, Just S, Rottbauer W, Frantz S, Castoldi M, Soutschek J, Koteliansky V, Rosenwald A, Basson MA, Licht JD, Pena JTR, Rouhanifard SH, Muckenthaler MU, Tuschl T, Martin GR, Bauersachs J, Engelhardt S. MicroRNA-21 contributes to myocardial disease by stimulating MAP kinase signalling in fibroblasts. Nature. 2008 Dec 18;456(7224):980–984.

31. Sayed D, Hong C, Chen I-Y, Lypowy J, Abdellatif M. MicroRNAs play an essential role in the development of cardiac hypertrophy. Circ. Res. 2007 Feb 16;100(3):416–424.

32. Duan M, Yao H, Hu G, Chen X, Lund AK, Buch S. HIV Tat Induces Expression of ICAM-1 in HUVECs: Implications for miR-221/-222 in HIV-Associated Cardiomyopathy. PLoS ONE. 2013;8(3):e60170.

33. Zhang Q, Kandic I, Kutryk MJ. Dysregulation of angiogenesis-related microRNAs in endothelial progenitor cells from patients with coronary artery disease. Biochem. Biophys. Res. Commun. 2011 Feb 4;405(1):42–46.

34. Feng M, Li Z, Aau M, Wong CH, Yang X, Yu Q. Myc/miR-378/TOB2/cyclin D1 functional module regulates oncogenic transformation. Oncogene. 2011 May 12;30(19):2242–2251.

35. Lee DY, Deng Z, Wang C-H, Yang BB. MicroRNA-378 promotes cell survival, tumor growth, and angiogenesis by targeting SuFu and Fus-1 expression. Proc. Natl. Acad. Sci. U.S.A. 2007 Dec 18;104(51):20350–20355.

8

36.   Nagalingam RS, Sundaresan NR, Gupta MP, Geenen DL, Solaro RJ, Gupta M. A Cardiac-enriched MicroRNA, miR-378, Blocks Cardiac Hypertrophy by Targeting Ras Signaling. J Biol Chem. 2013 Apr 19;288(16):11216–11232.

37.   Ganesan J, Ramanujam D, Sassi Y, Ahles A, Jentzsch C, Werfel S, Leierseder S, Loyer X, Giacca M, Zentilin L, Thum T, Laggerbauer B, Engelhardt S. MiR-378 Controls Cardiac Hypertrophy by Combined Repression of MAP Kinase Pathway Factors. Circulation. 2013 May 28;127(21):2097-106.

38.   Margulies KB, Matiwala S, Cornejo C, Olsen H, Craven WA, Bednarik D. Mixed messages: transcription patterns in failing and recovering human myocardium. Circ. Res. 2005 Mar 18;96(5):592–599.

39.   Dorn GW, Matkovich SJ. Put your chips on transcriptomics. Circulation. 2008 Jul 15;118(3):216–218.

SUPPLEMENTAL

Supplemental Figure S1: Experimental design of the study

pre-screening				
Device	pfLVAD	control	cfLVAD	cfLVAD
Sample	myocardium	myocardium	myocardium	plasma
Timing Sample	pre/post		pre/post	pre/6months post
Number	n=5	n=2	n=5	n=5
Test System	microarray	microarray	microarray	QPCR-based array
Firm	Exiqon	Exiqon	Exiqon	Exiqon
Selected miRs	26		26	4

validation				
Device	pfLVAD	control	cfLVAD	cfLVAD	control
Sample	myocardium	myocardium	myocardium	plasma	plasma
Timing Sample	pre/post		pre/post	pre/1,3,6months post	
Number	n=17	n=2	n=17	n=18	n=10
Test System	QPCR array	QPCR array	QPCR array	QPCR array	QPCR array
Firm	Qiagen	Qiagen	Qiagen	Life Technologies	Life Technologies

Supplemental Figure S2
These selected miRs have previously been investigated in pulsatile flow LVAD (pf-LVAD) supported patients and changed significantly. Whereas these figures represents no significant change in miR expression during continuous flow LVAD (cf-LVAD) support.

Supplemental Table S1: Selected miRs

Annotation	Selection
hsa-miR-208a	literature [1-4]
hsa-let-7i	literature [5,6]
hsa-miR-137	literature [7]
hsa-miR-23a*	literature [8-10]
hsa-miR-199b-5p	literature [11,12]
hsa-miR-320d	literature [13,14]
hsa-miR-133b	literature [1,15-18]
hsa-miR-21	literature [19-23]
hsa-miR-199a-5p	micro-array
hsa-miR-29b-1*	micro-array
hsa-miR-17*	micro-array
hsa-miR-92a	micro-array
hsa-miR-25	micro-array
hsa-miR-146a	micro-array
hsa-miR-221	micro-array
hsa-miR-23a	micro-array
hsa-miR-378	micro-array
hsa-miR-1	micro-array
hsa-miR-155	micro-array
hsa-miR-22	micro-array
hsa-miR-378*	micro-array
hsa-miR-129*	micro-array
hsa-miR-142-5p	micro-array
hsa-miR-136	micro-array
hsa-miR-222	micro-array

List of miRs that were evaluated by real time PCR in individual patients before and after pf/cf-LVAD support

8

Supplemental Table S2: Microarray analysis of miR expression in cardiac tissue of pulsatile flow LVAD (pf-LVAD) patients (control versus pre-LVAD)

Probe ID	Annotation	Control	pre-LVAD	LogFC	Average HY3
29802	hsa-miR-144	-5.092	-1.226	3.866	9.381
42866	hsa-miR-451	-5.736	-2.105	3.631	10.647
46620	hsa-miR-1275	-2.141	0,961	3.102	12.036
46921	hsa-miR-1290	-2.605	-0,003	2.602	10.834
10916	hsa-miR-1	1.085	-1,1	-2,185	12.385
147820	hsa-miR-3133	0,814	-1.257	-2.072	7.432
148642	hsa-miR-1246	-2.079	-0,079	2.000	11.371
1477767	hsa-miR-4279	-0,361	1.973	-1.612	10.883
147636	hsa-miR-4284	0,921	-0,658	-1.579	14.123
148032	hsa-miR-3685	0,806	-0,670	-1.476	9.068
11053	hsa-miR-32	0,568	-0,886	-1.454	7.381
42571	hsa-miR-129*	1.046	-0,296	-1.342	8.232
10964	hsa-miR-155	-0,137	1.203	1.340	7.753
148599	hsa-miR-3680	0,996	-0,274	-1.270	7.008
46944	hsa-miR-1297	0,418	-0,808	-1.225	7.763
145852	hsa-miR-210	-0,176	1.026	1.202	8.488
42654	hsa-miR-483-5p	-1.221	-0,020	1.201	7.359
148396	hsa-miR-642b	-1.762	-0,602	1.160	8.163
148682	hsa-miR-483-3p	-0,573	-1.718	-1.145	10.587
146165	hsa-miR-1973	-0,056	1.085	1.140	10.477
146008	hsa-miR-26b	0,166	-0,954	-1.120	10.233
147691	hsa-miR-320e	-0,364	0,755	1.120	9.345
46324	hsa-miR-320b	-0,208	0,894	1.102	9.737
147942	hsa-miR-4268	-0,680	-1.778	-1.098	9.812
145798	hsa-miR-142-5p	-1.668	-0,574	1.093	7.297
46228	hsa-miR-320c	-0,196	0,889	1.085	9.420
42761	hsa-miR-675	-1.501	-0,438	1.064	7.340
42872	hsa-miR-138-1*	0,707	-0,349	-1.056	9.275
27533	hsa-miR-320a	-0,175	0,862	1.037	9.749
148228	hsa-miR-3656	-1.118	-0,087	1.031	8.434

Supplemental Table S3: Microarray analysis of miR expression in cardiac tissue of continuous flow LVAD (cf-LVAD) patients (control versus pre-LVAD)

Probe ID	Annotation	Control	pre-LVAD	LogFC	Average HY3
42866	hsa-miR-451	-6,10	-1,68	4,42	12.577
29802	hsa-miR-144	-5,72	-1,58	4,14	10.658
46921	hsa-miR-1290	-2,99	-0,63	2,36	11.006
148642	hsa-miR-1246	-2,82	-0,62	2,20	11.568
46620	hsa-miR-1275	-2,29	-0,26	2,04	11.274
147604	hsa-miR-4285	-1,67	-0,26	1,41	10.021
148687	hsa-miR-1908	-1,48	-0,16	1,32	9.708
147817	hsa-miR-3196	-1,51	-0,27	1,24	8.398
147667	hsa-miR-3182	-1,19	0,01	1,20	10.992
147920	hsa-miR-4290	-1,21	-0,05	1,16	10.546
148396	hsa-miR-642b	-1,87	-0,77	1,10	8.223
145768	hsa-miR-665	-1,56	-0,47	1,09	7.610
11065	hsa-miR-335	-1,51	-0,43	1,08	8.272
145798	hsa-miR-142-5p	-1,79	-0,71	1,08	7.612
17810	hsa-miR-29b-1*	1,07	0,02	-1,06	6.507
29562	hsa-miR-199a-5p	-0,88	0,18	1,06	11.069
17885	hsa-miRPlus-A1086	-1,07	-0,05	1,02	8.691
147636	hsa-miR-4284	0,94	-0,08	-1,02	13.564
17377	hsa-miR-600	0,98	-0,03	-1,01	8.622

8

Supplemental Table S4: Microarray analysis of miR expression in cardiac tissue of pulsatile flow LVAD (pf-LVAD) patients (control versus post-LVAD)(>logFC>1)

Probe ID	Annotation	Control	post-LVAD	LogFC	Average HY3
10916	hsa-miR-1	1.085	-1.021	-2.106	12.036
147820	hsa-miR-3133	0,814	-1.108	-1.922	7.340
11022	hsa-miR-221	1.245	-0,402	-1.647	9.339
147636	hsa-miR-4284	0,921	-0,677	-1.598	13.871
11053	hsa-miR-32	0,568	-1.011	-1.579	7.266
147767	hsa-miR-4279	-0,361	-1.887	-1.526	10.917
148032	hsa-miR-3685	0,806	-0,656	-1.462	9.111
147588	hsa-miR-4288	1.178	-0,256	-1.433	9.970
33596	hsa-miR-126*	0,594	-0,742	-1.336	9.679
42571	hsa-miR-129*	1.046	-0,288	-1.335	8.106
46944	hsa-miR-1297	0,418	-0,867	-1.284	7.653
148599	hsa-miR-3680	0,996	-0,208	-1.204	6.979
148682	hsa-miR-483-3p	-0,573	-1.734	-1.161	10.676
146112	hsa-miR-30b	0,634	-0,523	-1.157	11.486
4610	hsa-miR-126	0,596	-0,551	-1.147	11.911
145844	hsa-miR-374a	0,315	-0,800	-1.115	7.757
146008	hsa-miR-26b	0,166	-0,936	-1.101	10.009
46483	hsa-miR-27a	0,382	-0,695	-1.077	9.866
147942	hsa-miR-4268	-0,680	-1.738	-1.058	9.864
27536	hsa-miR-190	0,613	-0,404	-1.017	7.338
147817	hsa-miR-3196	-1.443	-0,436	1.007	8.510
42581	hsa-miR-513a-5p	-0,499	0,533	1.032	9.179
145798	hsa-miR-142-5p	-1.668	-0,604	1.063	7.393
10964	hsa-miR-155	-0,137	1.147	1.284	7.884
146165	hsa-miR-1973	-0,056	1.309	1.365	10.535
148642	hsa-miR-1246	-2.079	-0,600	1.478	11.505
46921	hsa-miR-1290	-2.605	-0,623	1.982	10.970
42866	hsa-miR-451	-5.736	-3.424	2.311	10.696
29802	hsa-miR-144	-5.092	-2.474	2.618	9.586
46620	hsa-miR-1275	-2.141	0,649	2.790	12.303

Supplemental Table S5: Microarray analysis of miR expression in cardiac tissue of continuous flow LVAD (cf-LVAD) patients (control versus post-LVAD)

Probe ID	Annotation	Control	post-LVAD	LogFC	Average HY3
42866	hsa-miR-451	-6,10	-1,84	4,27	12.577
29802	hsa-miR-144	-5,72	-1,66	4,07	10.658
46921	hsa-miR-1290	-2,99	-0,52	2,47	11.006
148642	hsa-miR-1246	-2,82	-0,48	2,34	11.568
147588	hsa-miR-4288	1,13	-0,80	-1,93	9.525
11022	hsa-miR-221	1,16	-0,64	-1,81	9.041
46620	hsa-miR-1275	-2,29	-0,59	1,70	11.274
145798	hsa-miR-142-5p	-1,79	-0,42	1,37	7.612
147604	hsa-miR-4285	-1,67	-0,34	1,32	10.021
11065	hsa-miR-335	-1,51	-0,18	1,32	8.272
147817	hsa-miR-3196	-1,51	-0,19	1,32	8.398
147636	hsa-miR-4284	0,94	-0,33	-1,27	13.564
145768	hsa-miR-665	-1,56	-0,30	1,26	7.610
148687	hsa-miR-1908	-1,48	-0,24	1,23	9.708
148396	hsa-miR-642b	-1,87	-0,67	1,20	8.223
29562	hsa-miR-199a-5p	-0,88	0,31	1,19	11.069
147920	hsa-miR-4290	-1,21	-0,03	1,19	10.546
17377	hsa-miR-600	0,98	-0,18	-1,16	8.622
11023	hsa-miR-222	0,80	-0,33	-1,13	9.578
148599	hsa-miR-3680	0,81	-0,29	-1,10	7.427

8

Supplemental Table S6: Microarray analysis of miR expression in cardiac tissue of pulsatile flow LVAD (pf-LVAD) (pre-LVAD versus post-LVAD)

Probe ID	Annotation	LogFC	Average HY3	p-value
17822	hsa-miR-490-5p	0,14	6.528	0,007
29802	hsa-miR-144	-1,21	9.366	0,010
17885	hsa-miRPlus-A1086	-0,51	7.069	0,010
11020	**hsa-miR-22**	**-0,30**	**13.827**	**0,011**
147616	hsa-miR-4291	-0,23	10.378	0,011
11092	**hsa-miR-378***	**0,43**	**7.241**	**0,019**
10943	**hsa-miR-136**	**0,15**	**8.260**	**0,023**
17608	hsa-miR-425	-0,26	7.292	0,025
46558	hsa-miR-1268/hsa-miR-1268b	0,40	5.865	0,026
46258	hsa-miR-1184	0,14	7.150	0,026
148085	hsa-miR-3687	-0,40	6.495	0,028
147744	hsa-miR-4286	0,10	14.105	0,029
42845	hsa-miR-125b-2*	0,11	6.056	0,034
11023	**hsa-miR-222**	**-0,75**	**9.601**	**0,040**
42744	**hsa-miR-23a**	**-0,14**	**12.563**	**0,041**
148668	**hsa-miR-378**	**0,40**	**12.140**	**0,043**
11105	hsa-miR-378/hsa-miR-378c/hsa-miR-378d	0,35	11.663	0,044
17848	hsa-miRPlus-A1087	-0,62	7.892	0,046
148420	hsa-miR-3607-3p	0,27	9.547	0,047
10916	hsa-miR-1	0,310	12.478	0,673
19588	hsa-miR-17*	0,056	8.368	0,701
147512	hsa-miR-21	-0,629	9.104	0,191
42638	hsa-miR-23a*	-0,097	6.580	0,166
42682	hsa-miR-25	-0,088	7.693	0,288
17810	hsa-miR-29b-1*	-0,015	6.804	0,896
145693	hsa-miR-92a	-0,012	8.753	0,934
42571	hsa-miR-129*	0,201	8.318	0,626
146160	hsa-miR-133b	0,081	13.895	0,664
x	hsa-miR-137	x	x	x
145798	hsa-miR-142-5p	-0,215	7.191	0,105
10952	hsa-miR-146a	0,239	6.839	0,177
10964	hsa-miR-155	-0,237	7.667	0,555
29562	hsa-miR-199a-5p	0,093	9.939	0,549
19591	hsa-miR-199b-5p	0,086	8.300	0,845
5730	hsa-miR-208a	0,000	10.140	0,997
11022	hsa-miR-221	-0,833	9.510	0,094
46870	hsa-miR-320d	-0,205	9.170	0,245
9938	hsa-let-7i	-0,066	6.161	0,646

Grey: miRs that were differentially expressed between pre- and post-LVAD
MiRs selected for real time PCR analyses are depicted in bold.

Supplemental Table S7: Microarray analysis of miR expression in cardiac tissue of continuous flow LVAD (cf-LVAD) patients (pre-LVAD versus post-LVAD)

Probe ID	Annotation	LogFC	Average HY3	p-value
19588	**hsa-miR-17***	**0,19**	**6.561**	**0,002**
10943	**hsa-miR-136**	**0,38**	**8.359**	**0,002**
42682	**hsa-miR-25**	**0,20**	**7.758**	**0,010**
145693	**hsa-miR-92a**	**0,23**	**8.658**	**0,020**
11022	**hsa-miR-221**	**-0,96**	**9.041**	**0,021**
147588	hsa-miR-4288	-1,06	9.525	0,025
11023	**hsa-miR-222**	**-0,62**	**9.578**	**0,027**
145897	hsa-miR-92b	0,14	6.270	0,028
10952	**hsa-miR-146a**	**0,41**	**7.137**	**0,038**
17810	**hsa-miR-29b-1***	**0,18**	**6.507**	**0,038**
42739	hsa-miR-339-5p	-0,11	6.622	0,040
42538	hsa-miR-196a*	-0,08	6.931	0,040
42743	hsa-let-7e*	0,17	5.848	0,046
10916	hsa-miR-1	-0,10	12.669	0,880
147512	hsa-miR-21	-0,28	9.503	0,413
11020	hsa-miR-22	-0,04	13.845	0,820
42744	hsa-miR-23a	0,00	12.845	0,988
42638	hsa-miR-23a*	0,31	6.232	0,124
42571	hsa-miR-129*	-0,03	7.593	0,945
146160	hsa-miR-133b	-0,07	13.869	0,704
x	hsa-miR-137	x	x	x
145798	hsa-miR-142-5p	0,30	7.612	0,303
10964	hsa-miR-155	-0,14	7.197	0,676
29562	hsa-miR-199a-5p	0,13	11.069	0,351
19591	hsa-miR-199b-5p	-0,19	9.325	0,663
5730	hsa-miR-208a	-0,28	9.944	0,395
46870	hsa-miR-320d	0,03	9.350	0,865
148668	hsa-miR-378	0,15	12.247	0,351
11092	hsa-miR-378*	0,15	6.957	0,479
9938	hsa-let-7i	0,06	11.024	0,524

Grey: miRs that were differentially expressed betwwen pre- and post-LVAD.
MiRs selected for real time PCR analysis are in depicted in bold and also in the below section (white).

8

Supplemental Table S8: Microarray analysis of miRs expression in plasma of continuous flow LVAD (cf-LVAD) patients

| Annotation	post cf-LVAD	pre cf-LVAD	SD
hsa-miR-22*	-3,37	0,19	2,51
hsa-miR-1974	5,58	2,03	2,51
hsa-miR-1908	-3,87	-1,50	1,68
hsa-miR-30e*	-3,73	-1,59	1,51
hsa-miR-127-3p	0,49	-1,60	1,47
hsa-miR-155	-2,67	-4,76	1,47
hsa-miR-877	-2,37	-4,33	1,38
hsa-let-7f	0,46	-1,48	1,38
hsa-miR-338-3p	-1,68	0,06	1,23
hsa-miR-29c	-2,59	-0,90	1,20
hsa-miR-19a	-3,84	-2,17	1,18
hsa-miR-133b	-2,95	-4,49	1,09
hsa-miR-301b	-3,12	-4,63	1,07
hsa-miR-191	-1,97	-0,47	1,06
hsa-miR-29a	-3,09	-1,60	1,06
hsa-miR-339-3p	0,49	-0,99	1,05
hsa-miR-21	3,93	4,26	0,23
hsa-miR-146a	1,42	1,63	0,15
hsa-miR-222	1,92	2,01	0,07
hsa-miR-221	4,80	4,77	0,02

Grey: miRs that were differentially expressed between pre- and post-LVAD

Supplemental references

1. Widera C, Gupta SK, Lorenzen JM, Bang C, Bauersachs J, Bethmann K, Kempf T, Wollert KC, Thum T. Diagnostic and prognostic impact of six circulating microRNAs in acute coronary syndrome. J Mol Cell Cardiol. 2011; 51:872–875.

2. Montgomery RL, Hullinger TG, Semus HM, Dickinson BA, Seto AG, Lynch JM, Stack C, Latimer PA, Olson EN, van Rooij E. Therapeutic inhibition of miR-208a improves cardiac function and survival during heart failure. Circulation. 2011; 124:1537–1547.

3. Oliveira-Carvalho V, Carvalho VO, Bocchi EA. The emerging role of miR-208a in the heart. DNA Cell Biol. 2013; 32:8–12.

4. Callis TE, Pandya K, Seok HY, Tang R-H, Tatsuguchi M, Huang Z-P, Chen J-F, Deng Z, Gunn B, Shumate J, Willis MS, Selzman CH, Wang D-Z. MicroRNA-208a is a regulator of cardiac hypertrophy and conduction in mice. J. Clin. Invest. 2009; 119:2772–2786.

5. Satoh M, Minami Y, Takahashi Y, Tabuchi T, Nakamura M. A cellular microRNA, let-7i, is a novel biomarker for clinical outcome in patients with dilated cardiomyopathy. J Card Fail. 2011; 17:923–929.

6. Satoh M, Tabuchi T, Minami Y, Takahashi Y, Itoh T, Nakamura M. Expression of let-7i is associated with Toll-like receptor 4 signal in coronary artery disease: effect of statins on let-7i and Toll-like receptor 4 signal. Immunobiology. 2012; 217:533–539.

7. Lok SI, van Mil A, Bovenschen N, van der Weide P, van Kuik J, Van Wichen D, Peeters T, Siera E, Winkens B, Sluijter JPG, Doevendans PA, da Costa Martins PA, de Jonge N, de Weger RA. Post-transcriptional Regulation of α-1-Antichymotrypsin by MicroRNA-137 in Chronic Heart Failure and Mechanical Support. Circ Heart Fail. 2013; 6:853–861.

8. Wang J, Xu R, Lin F, Zhang S, Zhang G, Hu S, Zheng Z. MicroRNA: novel regulators involved in the remodeling and reverse remodeling of the heart. Cardiology. 2009; 113:81–88.

9. Lin Z, Murtaza I, Wang K, Jiao J, Gao J, Li P-F. miR-23a functions downstream of NFATc3 to regulate cardiac hypertrophy. Proc. Natl. Acad. Sci. U.S.A. 2009; 106:12103–12108.

10. Wang K, Lin Z-Q, Long B, Li J-H, Zhou J, Li P-F. Cardiac hypertrophy is positively regulated by MicroRNA miR-23a. J Biol Chem. 2012; 287:589–599.

11. Greco S, Fasanaro P, Castelvecchio S, D'Alessandra Y, Arcelli D, Di Donato M, Malavazos A, Capogrossi MC, Menicanti L, Martelli F. MicroRNA dysregulation in diabetic ischemic heart failure patients. Diabetes. 2012; 61:1633–1641.

12. da Costa Martins PA, Salic K, Gladka MM, Armand A-S, Leptidis S, Azzouzi el H, Hansen A, Coenen-de Roo CJ, Bierhuizen MF, van der Nagel R, van Kuik J, de Weger R, de Bruin A, Condorelli G, Arbones ML, Eschenhagen T, De Windt LJ. MicroRNA-199b targets the nuclear kinase Dyrk1a in an auto-amplification loop promoting calcineurin/NFAT signalling. Nat. Cell Biol. 2010; 12:1220–1227.

13. Ren X-P, Wu J, Wang X, Sartor MA, Qian J, Jones K, Nicolaou P, Pritchard TJ, Fan G-C. MicroRNA-320 is involved in the regulation of cardiac ischemia/reperfusion injury by targeting heat-shock protein 20. Circulation. 2009; 119:2357–2366.

8

14. Wang XH, Qian RZ, Zhang W, Chen SF, Jin HM, Hu RM. MicroRNA-320 expression in myocardial microvascular endothelial cells and its relationship with insulin-like growth factor-1 in type 2 diabetic rats. Clin. Exp. Pharmacol. Physiol. 2009; 36:181–188.

15. Bostjancic E, Zidar N, Stajer D, Glavac D. MicroRNAs miR-1, miR-133a, miR-133b and miR-208 are dysregulated in human myocardial infarction. Cardiology. 2010; 115:163–169.

16. Schipper MEI, van Kuik J, de Jonge N, Dullens HFJ, de Weger RA. Changes in regulatory microRNA expression in myocardium of heart failure patients on left ventricular assist device support. J Heart Lung Transplant. 2008; 27:1282–1285.

17. Xiao L, Xiao J, Luo X, Lin H, Wang Z, Nattel S. Feedback remodeling of cardiac potassium current expression: a novel potential mechanism for control of repolarization reserve. Circulation. 2008; 118:983–992.

18. Sucharov C, Bristow MR, Port JD. miRNA expression in the failing human heart: functional correlates. J Mol Cell Cardiol. 2008; 45:185–192.

19. Yang K-C, Ku Y-C, Lovett M, Nerbonne JM. Combined deep microRNA and mRNA sequencing identifies protective transcriptomal signature of enhanced PI3Kα signaling in cardiac hypertrophy. J Mol Cell Cardiol. 2012; 53:101–112.

20. Hu S, Huang M, Nguyen PK, Gong Y, Li Z, Jia F, Lan F, Liu J, Nag D, Robbins RC, Wu JC. Novel microRNA prosurvival cocktail for improving engraftment and function of cardiac progenitor cell transplantation. Circulation. 2011; 124:S27–34.

21. Patrick DM, Montgomery RL, Qi X, Obad S, Kauppinen S, Hill JA, van Rooij E, Olson EN. Stress-dependent cardiac remodeling occurs in the absence of microRNA-21 in mice. J. Clin. Invest. 2010; 120:3912–3916.

22. da Costa Martins PA, De Windt LJ. miR-21: a miRaculous Socratic paradox. Cardiovasc. Res. 2010; 87:397–400.

23. Thum T, Gross C, Fiedler J, Fischer T, Kissler S, Bussen M, Galuppo P, Just S, Rottbauer W, Frantz S, Castoldi M, Soutschek J, Koteliansky V, Rosenwald A, Basson MA, Licht JD, Pena JTR, Rouhanifard SH, Muckenthaler MU, Tuschl T, Martin GR, Bauersachs J, Engelhardt S. MicroRNA-21 contributes to myocardial disease by stimulating MAP kinase signalling in fibroblasts. Nature. 2008; 456:980–984.
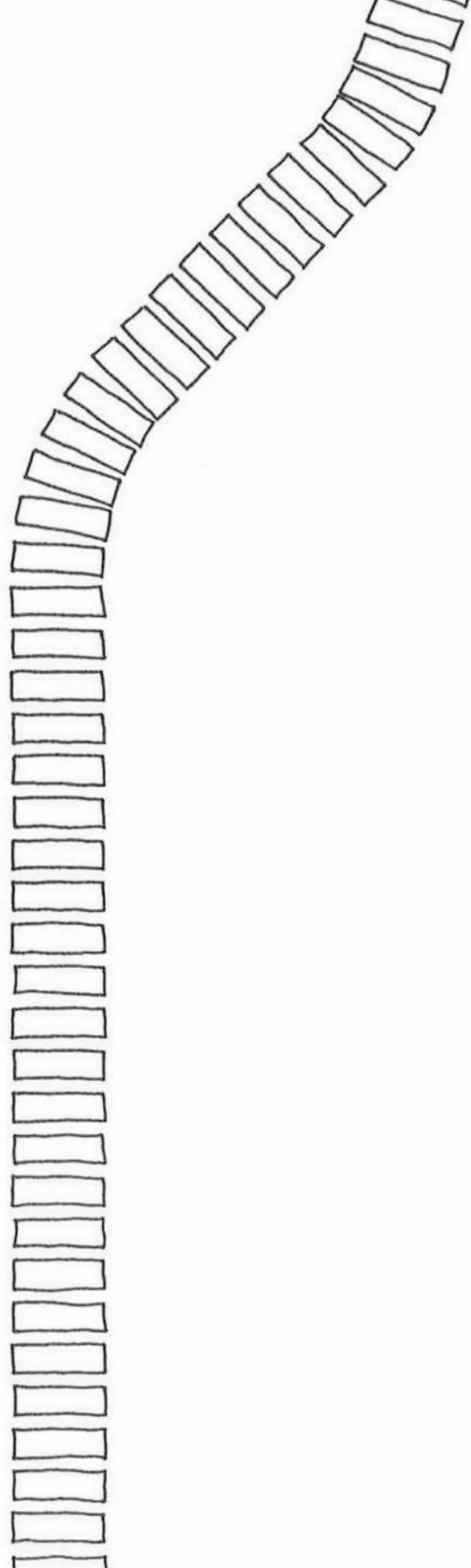
CHAPTER 9

General discussion

General discussion

In this thesis, we evaluated the clinical experience, histological and immunological changes and the expression of biomarkers during continuous flow left ventricular assist device (cf-LVAD) support as bridge to transplantation (BTT) and bridge to recovery (BTR) in end-stage heart failure (HF) patients in the University Medical Center in Utrecht.

Clinical experience

In chapter 2, the outcome of 85 patients supported with a HeartMate II cf-LVAD was described. The 1- and 2-year actuarial survival rates during support were 83% and 76%, consistent with other recent single-centre experiences [1,2]. Studies have demonstrated that cf-LVAD support provides adequate perfusion, leading to improved end-organ function for durations up to 15 months [3-5]. Similarly, our experience showed improved liver- and renal function for up to 1 year post-implant. In addition, left ventricular end-diastolic dimension (LVEDD) and left ventricular end-systolic dimension (LVESD) decreased significantly after 3 months of mechanical support and the LVESD further decreased significantly after 12 months compared with 3 months. Based on these and other results, cf-LVAD therapy can be considered as a successful life-saving therapy. Yet, there is a price to pay in terms of risk of adverse events during support. The most common adverse events in our patient population were: infections, cardiac arrhythmias and peri-operative bleeding. Cerebrovascular events may be considered as the most serious adverse events. In our patient cohort, 21 neurological events occured in 17 patients, of which 13 CVAs. Of these CVAs, 4 were fatal, 6 resulted in minor limitations and 3 in major limitations of daily life activities. The cumulative risk of the adverse events will shape the debate about the eventual cost-effectiveness of cf-LVADs for end-stage HF patients. Emphasis should be laid on optimal anti-coagulation regimen, the management of ventricular arrhythmias, device-related infections and haemolysis.

Histological and immunological changes

In chapter 3, histological changes during mechanical support were evaluated. cf-LVAD support is characterized by an overall increase in myocardial fibrosis and lengthening of cardiomyocytes. This is in contrast to previous studies with pulsatile flow LVAD (pf-LVAD) support, where a substantial decrease in cardiomyocyte diameter and length has been demonstrated [6-8]. This difference in response of cardiomyocyte size between devices is thought to be consistent with less ventricular unloading during cf-LVAD support [9,10]. However, as our study group previously demonstrated, elevated brain natriuretic peptide

9

(BNP) levels decrease equally between cf-LVAD and pf-LVAD treatment [11], suggesting no difference in volume unloading between the devices. The cardiomyocyte size in patients supported with cf-LVAD could also be influenced by the physiological effect of long-term continuous flow on the peripheral vasculature [12]. The response of collagen concentration during mechanical unloading remains controversial. Some studies have found a reduction in collagen during support [9,13,14], whereas most studies showed an increase [8,15-22]. Differences in techniques, concomitant medication, HF etiology, and duration of support could account for some of these discrepancies in total collagen measurement. In our patient population, the use of angiotensin-converting-enzyme (ACE) inhibitors and aldosterone antagonists did not differ before and after LVAD therapy. To date, no studies have been performed to evaluate the effect on maximal therapy in addition to LVAD support on myocardial recovery. Although these data are warranted, patient groups are small and, as a consequence, patient recruitment will be difficult.

Biomarkers

Achieving sustained myocardial recovery, allowing LVAD removal is one of the most desirable goals. For these patients LVAD support could postpone and/or reduce the need for heart transplantation (HTx). Clearly, the ability to identify BTR patients, for instance with the use of biomarkers, could reduce the need for donor hearts. The current era of genomics, proteomics, and metabolomics has led to the discovery of an immense number of novel candidate biomarkers. The American Heart Association emphasized the critical appraisal of novel markers to determine their clinical utility [23]. Several novel fibrotic markers, such as Galectin-3 (Gal-3), Osteopontin (OPN), Connective Tissue Growth Factor (CTGF) and Transforming Growth Factor β-1 (TGFβ-1) are being tested and introduced for clinical use in chronic HF. The additive value of these markers during LVAD support is still unclear. In chapter 3, we describe the expression of plasma levels and cardiac mRNA of these markers in comparison to BNP in patients with end-stage HF during cf-LVAD support as BTT and BTR. BNP, Gal-3, CTGF and OPN were significantly elevated pre-LVAD in comparison to controls. BNP decreased significantly after 1 month of cf-LVAD support to near-normal levels, whereas the other pro-fibrotic markers remained elevated in comparison to controls. No difference in expression of fibrotic markers could be detected between recovered and non-recovered patients, although only few patients could be weaned from the device.

Recently, Growth Differentiation Factor (GDF)-15 has come under increasing scrutiny as a biomarker in patients with acute and chronic cardiovascular disease [24-26]. Still, the role of GDF-15 in chronic HF patients remains unclear. In chapter 4, we described the change

of mRNA and circulating levels of GDF-15 in 30 patients with NYHA class IV with non-ischemic HF during cf-LVAD support. We demonstrated that 96% of the patients had elevated circulating GDF-15 levels prior to cf-LVAD implantation and that this percentage decreased to 25% after 6 months of mechanical unloading. As written in an editorial by Wollert and Kempf, our data indicate, for the first time, that high levels of GDF-15 are to some extent reversible, and that circulating GDF-15 can decline in response to LVAD implantation [27]. Kempf *et al* previously demonstrated an increase in GDF-15 expression in cardiomyocytes exposed to ischemia [28] and increased wall stress [29]. Consistently, previous data indicated that expression of GDF-15 was increased in dilated hearts of mice [30]. Remarkably, in our study with patients with end-stage non-ischemic dilated cardiomyopathy, we did not detect appreciable cardiac mRNA and protein expression of GDF-15, suggesting that the heart is not an important source of GDF-15 production in these patients. If GDF-15 is produced predominantly outside the heart in advanced HF, the substantial decreases in GDF-15 after LVAD implantation must reflect the peripheral effects. If not the heart, where does GDF-15 synthesis take place in end-stage HF patients? We demonstrated that circulating levels of GDF-15 prior to LVAD implantation correlate closely with creatinine and aspartate transaminase (AST). Along this line, changes in GDF-15 after LVAD implantation were related to the changes in creatinine and AST. Experimental data indicate that the kidneys produce GDF-15 in response to ischemic stress or injury [31]. Elevated GDF-15 levels in HF may therefore reflect to some extent the deleterious reciprocal relationship between cardiac and renal dysfunction. More studies are needed to investigate whether the kidneys are the main source of GDF-15 production in HF patients.

There is substantial interest in both applying proteomics to better understand disease processes and to develop new biomarkers for diagnosis and early detection of cardiovascular diseases [32,33]. We performed proteomics and immunosorbent assays of <u>myocardial tissue</u> that was collected before and after cf-LVAD implantation (n=8). In this thesis we discovered 40 proteins that changed significantly in heart tissue during support. Of these, haptoglobin (HPTG), an acute phase protein, showed the most profound reduction and was further evaluated and described in chapter 5. We showed that circulating HPTG decreased significantly during cf-LVAD support to levels below that of healthy controls. HPTG was mainly localized in the endothelial and stromal cells in the myocardium before cf-LVAD support, but was almost absent post-LVAD. This is of interest, since the expression of mRNA in the heart was low, suggesting that the heart is not an important source for HPTG production. During mechanical support, signs of HF decline, accompanied by decreased levels of cytokines and inflammatory markers and low HTPG levels. The decline in HTPG

9

could also be explained by persistent hemolysis during support.

In addition, we performed proteomics and immunosorbent assays of <u>plasma</u> of cf-LVAD supported patients. A total of 97 circulating proteins were identified that were significantly different in the pre- versus the post-pool. Of all proteins identified by proteomics, only alpha-1-antichymotrypsin (ACT) changed significantly in both tissue *and* plasma during cf-LVAD support and is further described in chapter 6 and 7. In chapter 6, we validated that ACT levels decrease both in heart tissue and in plasma samples of individual cf-LVAD supported HF patients. Immunohistochemistry revealed that ACT expression and localization changed during LVAD support. Since increasing evidence indicates that microRNAs (miRs) are involved in myocardial disease processes, we also investigated whether ACT is post-transcriptional regulated by miRs. Bioinformatics analysis pointed miR-137 as a potential regulator of ACT. The miR-137 expression inversely correlated with ACT mRNA in myocardial tissue. Luciferase activity assays confirmed ACT as a direct target for miR-137 and *in situ* hybridization indicated that ACT and miR-137 were mainly localized in cardiomyocytes and stromal cells. As the expression of ACT is directly regulated by miR-137, and their expression levels are inversely related *in vivo*, it is tempting to speculate that miR-137 and ACT play an important role in the pathophysiology of HF and either one could possibly serve as a therapeutic target. However, our patient population consisted of relatively young patients with a non-ischemic origin of systolic HF. To generalize our findings, we evaluated the role of ACT levels with respect to long-term mortality in chronic HF patients, as described in chapter 7. A total of 224 patients with severe chronic HF were included (mean age 71 years). During a median survival time of 5.3 years, 159 (71%) patients died. ACT was significantly elevated in these patients (median 433 μg/ml) in comparison to controls (median 214 μg/ml). No independent association to long-term mortality could be established. Future studies in patients with less severe HF and evaluation of plasma samples taken at different time-points are necessary to analyse the potential role of ACT as a marker in HF.

A hallmark of HF mRNA signatures is that more transcripts are down-regulated than up-regulated, suggesting the importance of molecular mechanisms that suppress mRNA steady state levels [34]. miRs are small non-coding RNAs that bind to mRNAs stimulating mRNA degradation of inhibiting protein translation [35]. Delineating the role of miRs in posttranscriptional gene regulation offers new insight into the mechanisms how the heart adapts to mechanical support. Moreover, miRs can be important hallmarks for recovery or deterioration and could be used as a therapeutic target in HF [36]. Hence, we investigated changes in miRs in plasma and myocardial tissue during LVAD support and analyzed

whether these miR-expression patterns differ between pf-LVAD and cf-LVAD support. Chapter 8 demonstrated that levels of different miRs change amongst pf-LVAD and cf-LVADs. Twenty-six miRs were selected and examined in myocardial tissue. Of these, 5 miRs (miR-129*, miR-146a, miR-155, miR-221, miR-222) displayed a similar pattern among the devices, whereas some changed only significantly during pf-LVAD or cf-LVAD support. The differences observed between miR expression profiles related to cf- and pf-LVAD might explain the different patient outcome observed after myocardial support by each type of device. Also, the specific miR expression profiles induced by either continuous or pulsatile flow could affect the clinical outcome of those patients either by restoring protein levels or even accentuate the unbalance between pre- and post-LVAD. Out of the 4 circulating miRs that were analysed in plasma of cf-LVAD supported patients, miR-21 decreased at 1,3 and 6 months after LVAD implantation. MiR-21 is very abundant in the cardiovascular system and several studies have revealed that it's expression is increased in failing human hearts.

Reverse remodeling and myocardial recovery

Cellular and molecular reverse remodeling is more pronounced than clinical cardiac recovery. As reviewed by Drakos *et al*, there are several explanations for the difference between clinical and biological outcomes [37]. One potential explanation is that reverse remodeling results in improvement of the pathological condition, but not in complete normalization [38]. Several lines of evidence support this view. First, gene expression profiling studies have shown that only about 5% of the dysregulated HF genes revert back to normal, despite typical morphological and functional responses to LVAD support [39]. It is unlikely that myocardial recovery is driven by a few unique genes. Second, the majority of the studies have demonstrated that the extracellular matrix (ECM) does not revert to normal during mechanical support, and can actually be characterized by increased myocardial fibrosis [8,15-22]. Moreover, studies suggested that LVAD support does not result in normalization of left ventricular wall stress [37,40]. Finally, although maximal calcium saturated force generation is improved in cardiomyocytes after LVAD support, force generation is still less than in cardiomyocytes from non-failing controls, despite reversal of cardiomyocyte hypertrophy [41]. These observations suggest that reverse remodeling occurs in the vast majority of patients during long-term LVAD support, but only rarely results in myocardial recovery. This is in accordance with our patient cohort, where only 4% of the patients experienced myocardial recovery with subsequent LVAD explantation. If reverse remodeling represents a partial normalization of the HF phenotype, does myocardial recovery represent a more complete normalization or does it represent a unique biological process that is different

9

from reverse remodeling [38]? Unfortunately, current literature is insufficient to address this question and more studies addressing these issues are needed. Mann *et al* proposed that reverse remodeling is accompanied by 2 different outcomes; myocardial remission and myocardial recovery (*Figure 1*). Myocardial remission represents reversal of the HF phenotype superimposed on hearts that have sustained irreversible damage (so called "plastic deformation"), characterized by recurrence of HF events. On the other hand, myocardial recovery represents reversal of the HF phenotype superimposed on hearts that do not suffer sustained irreversible damage ("elastic deformation"), with freedom from future cardiac events [41]. It would be of interest to distinguish and recognize patients with plastic versus elastic deformation before LVAD implantation. Patients likely to develop elastic deformation (eg myocarditis, peripartum cardiomyopathy) are probably better of with pf-LVADs, since they provide profound volume unloading and are associated with a higher BTR rate compared with cf-LVADs.
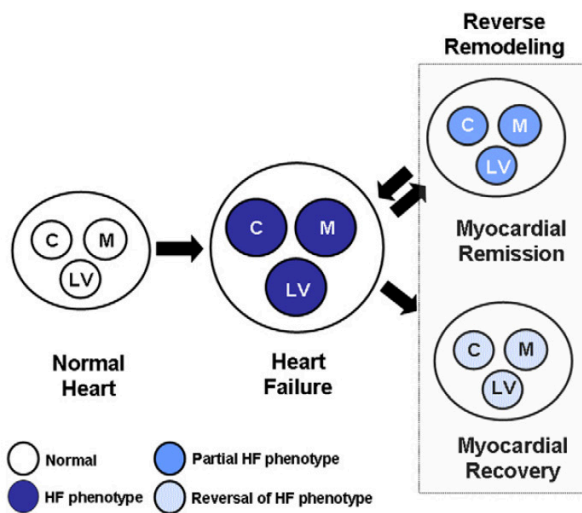
Figure 1: Different outcome of reverse remodeling
Cardiac remodeling results from abnormalities that arise in the biology of the cardiomyocytes (C), the myocardium (M) as well as LV geometry (LV). Reverse remodeling can lead to myocardial recovery, characterized by freedom from future heart failure (HF) events or myocardial remission, characterized by recurrence of HF events. Source: Mann DL, Barger PM, Burkhoff D. Myocardial recovery and the failing heart: myth, magic or molecular target? J Am Coll Cardiol, 2012.
Reproduced with permission.

Future aspects

Although the present thesis provides some answers with regard to clinical and histological changes during cf-LVADs, others have been raised and need to be addressed in future studies [49].

First, we need to understand why myocardial recovery is a rare phenomenon. In line with this thesis, evidence has been gathered to re-induce pulsatile flow in order to optimize myocardial recovery. More studies have to be performed since many questions remain. What is the impact of partial or complete unloading on myocardial blood flow and metabolism? Is there a degree of pulsatility of unloading, which may optimize myocardial recovery? And does a pulsatile rotary pump indeed leads to more profound reverse remodeling with a subsequent higher rate of BTR?

Also, more studies are needed to investigate optimal medical treatment during LVAD support. Approaches in which LVAD support is combined with one or more other treatment modalities, such as drugs, stem cells or gene therapy to promote myocardial recovery and to prevent post-LVAD explant remodeling may be of interest. It is intriguing whether the promising results with regard to Clenbuterol and Ivabradine can enhance myocardial recovery [50,51]. Before using this medical regime in end-stage HF patients during LVAD support, more studies are needed to evaluate side effects, cost-effectiveness and, most importantly, clinical outcomes of these pharmacological agents.

Although device durability has been enhanced with cf-LVAD support, the inherent risk of bleeding, stroke and infection are of concern. The optimal regime of antiplatelet and anticoagulation to minimize both thromboembolic and hemorrhagic stroke is unknown. In our center, the international normalized ratio (INR) goal was 1.5-2, as advocated in the literature [52]. Extended or lifetime mechanical support is increasingly common. LVAD use expands to older patient population, and it is clear that advanced age remains an important risk factor for stroke. Therefore, stroke risk should be part of counseling before elective LVAD implantation. Besides stroke and bleeding, infection of the percutaneous driveline, pump pocket or both is a major concern for long-term LVAD support. Immobilization of the driveline may help avoid torsion and breakdown of the cutaneous junction, the most common entry point for infection. Further minimally invasive surgical implantation techniques in combination with newer miniaturized pumps may reduce the post-operative risk. Currently, a transcutaneous energy transfer system (TETS) is under the development to wirelessly power implantable devices [53]. Unfortunately, this system has poor efficiency and suffers from technical concerns [54]. Another alternative is the invasive skull pedestal power delivery technique, but this is associated with a low quality of life [55]. Recent studies

9

of wireless power transfer based on the free-range resonant electrical delivery (FREE-D) appear promising, but more research is needed.

Pump thrombosis has been reported in cf-LVAD supported patients [56,57]. LVAD supported patients have a significant risk of device thrombosis and thromboembolism, despite anticoagulation. The LVAD system is a thrombin generator and clot matrix substrate [58,59]. Because the endothelium is missing on artificial surfaces, it cannot exert its antithrombotic actions, increasing the risk for occlusive thrombosis or thromboembolic events. Despite the fact that surfaces of the HM II are textured and thrombo-resistant, long-term anticoagulation is indicated with a subsequent risk of bleeding. Biogenic LVADs that are lined with the patient's endothelial progenitor cells, might become available in the nearest future [60]. Such a lining may prevent platelet adhesion and thrombi formation in areas of low flow and stasis. More investigations are needed to understand the complex molecular structures and interactions between endothelial cells and device surfaces.

It has been suggested that patients supported by cf-LVAD may have a higher risk of bleeding compared to pf-LVAD, mostly of gastrointestinal and nasal mucosal origin [61-63]. This increased prevalence might be caused by the use of anticoagulation therapy and the acquired von Willebrand disease. The von Willebrand factor (vWF) molecule is a protein expressed by vascular endothelial cells that bind to exposed collagen of damaged blood vessels. It has been hypothesized that the high shear stress forces changes in the shape of the vWF molecule, leading to proteolysis of the high molecular weight multimers of vWF [64]. Slaughter advocates hematologic screening in all patients prior to LVAD implantation. If von Willebrand disease is diagnosed, antifibrinolytics and vWF replacement should be prescribed as preventive treatment [65].

Finally, as pump design has evolved, so has the population of patients with end-stage HF supported with a LVAD. With the recent expansion in use of the cf-LVAD as DT, there is now a meaningful cohort of patients who are receiving permanent LVAD support. The success of LVAD therapy has generated debate about the severity of HF that should prompt implantation of a device. The REVIVE-IT trial includes patients who have advanced HF with significant functional impairment and who are ineligible for transplant, but who have not yet manifested serious consequences of end-stage HF. The results from this trial are of interest, and may lead to implantation of LVADs in "less sick patients" with advanced HF. Similarly, it remains to be investigated whether LVADs as DT should be considered as standard care for patients with refractory HF who are ineligible for HTx [66]. The major improvements in survival and device durability will certainly have a great impact on expected cost-effectiveness of LVADs. Currently, the costs of providing cf-LVAD treatment

to an ever-increasing patient population have raised additional concerns regarding its financial sustainability [67]. Less expensive cf-LVADs, that can incorporate pulsatility, are needed in end-stage HF patients.

Conclusion

Taken together, this thesis should provide the reader an overview of the clinical and myocardial changes of end-stage heart failure patients during continuous flow left ventricular assist device (cf-LVAD) support.

Our study results indicate that cf-LVADs can be considered as a life-saving therapy in end-stage heart failure patients. Hitherto, there is a price to pay in terms of risk of serious adverse events during support. Perhaps, the greatest risks that remain of concern are the neurological adverse events. Future emphasis should be focused on minimizing adverse events, while improving survival and quality of life while on LVAD support.

We have provided evidence that long-term cf-LVAD support is associated with lengthening of cardiomyocytes, without alterations in diameter size. Remarkably, myocardial fibrosis increased during support, as well as circulating pro-fibrotic markers, suggesting insufficient remodeling of the extracellular matrix composition. In search of novel biomarkers for reverse remodeling, we used proteomics and selected two proteins (haptoglobin; HPTG and alpha-1-antichymotrypsin; ACT) that changed significantly in myocardial tissue and plasma during cf-LVAD support. Further investigation of the selected proteins in individual patients demonstrated that both circulating HPTG and ACT decreased significantly during cf-LVAD support to levels similar or even lower than those of healthy controls. Besides these proteins, we evaluated established heart failure markers, such as Brain Natriuretic Peptide (BNP) and Growth Differentiation Factor (GDF)-15 in plasma and myocardial tissue after cf-LVAD implantation. After one month of implantation, circulating BNP and GDF-15 decreased profoundly and remained stable thereafter. Remarkably, GDF-15 mRNA and protein expression were hardly detectable in non-ischemic dilated hearts, indicating that the myocardium is not an important source of GDF-15 in these patients. Moreover, microRNA (miR) expression profiles were evaluated in patients during pulsatile flow LVAD (pf-LVAD) versus cf-LVAD support. This thesis demonstrated that the type of device was associated with a different miR expression profile, which might affect the clinical outcome by restoring protein levels. While significant steps have been made to evaluate cellular and molecular reverse remodeling, we still have to figure out why myocardial recovery is a rare phenomenon with often only a temporary duration. Also, the lack of validated biomarkers for myocardial recovery aggravates uncertainties about ideal timing for LVAD explantation.

9

References

1. Starling RC, Naka Y, Boyle AJ, Gonzalez-Stawinski G, John R, Jorde U, Russell SD, Conte JV, Aaronson KD, McGee EC, Cotts WG, DeNofrio D, Pham DT, Farrar DJ, Pagani FD. Results of the post-U.S. Food and Drug Administration-approval study with a continuous flow left ventricular assist device as a bridge to heart transplantation: a prospective study using the INTERMACS (Interagency Registry for Mechanically Assisted Circulatory Support). J. Am. Coll. Cardiol. 2011; 57:1890–1898.

2. John R, Naka Y, Smedira NG, Starling R, Jorde U, Eckman P, Farrar DJ, Pagani FD. Continuous flow left ventricular assist device outcomes in commercial use compared with the prior clinical trial. Ann. Thorac. Surg. 2011; 92:1406–13– discussion 1413.

3. Hasin T, Topilsky Y, Schirger JA, Li Z, Zhao Y, Boilson BA, Clavell AL, Rodeheffer RJ, Frantz RP, Edwards BS, Pereira NL, Joyce L, Daly R, Park SJ, Kushwaha SS. Changes in renal function after implantation of continuous-flow left ventricular assist devices. J. Am. Coll. Cardiol. 2012; 59:26–36.

4. Kamdar F, Boyle A, Liao K, Colvin-Adams M, Joyce L, John R. Effects of centrifugal, axial, and pulsatile left ventricular assist device support on end-organ function in heart failure patients. J Heart Lung Transplant. 2009; 28:352–359.

5. Radovancevic B, Vrtovec B, de Kort E, Radovancevic R, Gregoric ID, Frazier OH. End-organ function in patients on long-term circulatory support with continuous- or pulsatile-flow assist devices. J Heart Lung Transplant. 2007; 26:815–818.

6. de Jonge N, van Wichen DF, Schipper MEI, Lahpor JR, Gmelig-Meyling FHJ, Robles de Medina EO, de Weger RA. Left ventricular assist device in end-stage heart failure: persistence of structural myocyte damage after unloading. An immunohistochemical analysis of the contractile myofilaments. J. Am. Coll. Cardiol. 2002; 39:963–969.

7. Maybaum S, Mancini D, Xydas S, Starling RC, Aaronson K, Pagani FD, Miller LW, Margulies K, McRee S, Frazier OH, Torre-Amione G, LVAD Working Group. Cardiac improvement during mechanical circulatory support: a prospective multicenter study of the LVAD Working Group. Circulation. 2007; 115:2497-2505.

8. Drakos SG, Kfoury AG, Hammond EH, Reid BB, Revelo MP, Rasmusson BY, Whitehead KJ, Salama ME, Selzman CH, Stehlik J, Clayson SE, Bristow MR, Renlund DG, Li DY. Impact of mechanical unloading on microvasculature and associated central remodeling features of the failing human heart. J. Am. Coll. Cardiol. 2010; 56:382–391.

9. Kato TS, Chokshi A, Singh P, Khawaja T, Cheema F, Akashi H, Shahzad K, Iwata S, Homma S, Takayama H, Naka Y, Jorde U, Farr M, Mancini DM, Schulze PC. Effects of continuous-flow versus pulsatile-flow left ventricular assist devices on myocardial unloading and remodeling. Circ Heart Fail. 2011; 4:546–553.

10. Klotz S, Deng MC, Stypmann J, Roetker J, Wilhelm MJ, Hammel D, Scheld HH, Schmid C. Left ventricular pressure and volume unloading during pulsatile versus nonpulsatile left ventricular assist device support. Ann. Thorac. Surg. 2004; 77:143–9; discussion 149–50.

11.   Pruijsten RV, Lok SI, Kirkels HH, Klöpping C, Lahpor JR, de Jonge N. Functional and hemodynamic recovery after implantation of continuous-flow left ventricular assist devices in comparison with pulsatile left ventricular assist devices in patients with end-stage heart failure. Eur. J. Heart Fail. 2012; 14:319–325.

12.   Margulies KB, Rame JE. Adaptations to pulsatile versus nonpulsatile ventricular assist device support. Circ Heart Fail. 2011; 4:535–537.

13.   Thohan V, Stetson SJ, Nagueh SF, Rivas-Gotz C, Koerner MM, Lafuente JA, Loebe M, Noon GP, Torre-Amione G. Cellular and hemodynamics responses of failing myocardium to continuous flow mechanical circulatory support using the DeBakey-Noon left ventricular assist device: a comparative analysis with pulsatile-type devices. J Heart Lung Transplant. 2005; 24:566–575.

14.   Bruckner BA, Stetson SJ, Perez-Verdia A, Youker KA, Radovancevic B, Connelly JH, Koerner MM, Entman ME, Frazier OH, Noon GP, Torre-Amione G. Regression of fibrosis and hypertrophy in failing myocardium following mechanical circulatory support. J Heart Lung Transplant. 2001; 20:457–464.

15.   Klotz S, Foronjy RF, Dickstein ML, Gu A, Garrelds IM, Danser AHJ, Oz MC, D'Armiento J, Burkhoff D. Mechanical unloading during left ventricular assist device support increases left ventricular collagen cross-linking and myocardial stiffness. Circulation. 2005; 112:364–374.

16.   Barbone A, Holmes JW, Heerdt PM, The AH, Naka Y, Joshi N, Daines M, Marks AR, Oz MC, Burkhoff D. Comparison of right and left ventricular responses to left ventricular assist device support in patients with severe heart failure: a primary role of mechanical unloading underlying reverse remodeling. Circulation. 2001; 104:670–675.

17.   Madigan JD, Barbone A, Choudhri AF, Morales DL, Cai B, Oz MC, Burkhoff D. Time course of reverse remodeling of the left ventricle during support with a left ventricular assist device. J. Thorac. Cardiovasc. Surg. 2001; 121:902–908.

18.   Matsumiya G, Monta O, Fukushima N, Sawa Y, Funatsu T, Toda K, Matsuda H. Who would be a candidate for bridge to recovery during prolonged mechanical left ventricular support in idiopathic dilated cardiomyopathy? J. Thorac. Cardiovasc. Surg. 2005; 130:699–704.

19.   McCarthy PM, Nakatani S, Vargo R, Kottke-Marchant K, Harasaki H, James KB, Savage RM, Thomas JD. Structural and left ventricular histologic changes after implantable LVAD insertion. Ann. Thorac. Surg. 1995; 59:609–613.

20.   Nakatani S, McCarthy PM, Kottke-Marchant K, Harasaki H, James KB, Savage RM, Thomas JD. Left ventricular echocardiographic and histologic changes: impact of chronic unloading by an implantable ventricular assist device. J. Am. Coll. Cardiol. 1996; 27:894–901.

21.   McGowan BS, Scott CB, Mu A, McCormick RJ, Thomas DP, Margulies KB. Unloading-induced remodeling in the normal and hypertrophic left ventricle. Am. J. Physiol. Heart Circ. Physiol. 2003; 284:H2061–8.

22.   Klotz S, Danser AHJ, Foronjy RF, Oz MC, Wang J, Mancini D, D'Armiento J, Burkhoff D. The impact of angiotensin-converting enzyme inhibitor therapy on the extracellular collagen matrix during left ventricular assist device support in patients with end-stage heart failure. J. Am. Coll. Cardiol. 2007; 49:1166–1174.

9

23.   Hlatky MA, Greenland P, Arnett DK, Ballantyne CM, Criqui MH, Elkind MSV, Go AS, Harrell FE, Hong Y, Howard BV, Howard VJ, Hsue PY, Kramer CM, McConnell JP, Normand S-LT, O'Donnell CJ, Smith SC, Wilson PWF, American Heart Association Expert Panel on Subclinical Atherosclerotic Diseases and Emerging Risk Factors and the Stroke Council. Criteria for evaluation of novel markers of cardiovascular risk: a scientific statement from the American Heart Association. Circulation. 2009; 119:2408–2416.

24.   Kempf T, Björklund E, Olofsson S, Lindahl B, Allhoff T, Peter T, Tongers J, Wollert KC, Wallentin L. Growth-differentiation factor-15 improves risk stratification in ST-segment elevation myocardial infarction. Eur. Heart J. 2007; 28:2858–2865.

25.   Wollert KC, Kempf T, Peter T, Olofsson S, James S, Johnston N, Lindahl B, Horn-Wichmann R, Brabant G, Simoons ML, Armstrong PW, Califf RM, Drexler H, Wallentin L. Prognostic value of growth-differentiation factor-15 in patients with non-ST-elevation acute coronary syndrome. Circulation. 2007; 115:962–971.

26.   Eggers KM, Kempf T, Lagerqvist B, Lindahl B, Olofsson S, Jantzen F, Peter T, Allhoff T, Siegbahn A, Venge P, Wollert KC, Wallentin L. Growth-differentiation factor-15 for long-term risk prediction in patients stabilized after an episode of non-ST-segment-elevation acute coronary syndrome. Circ Cardiovasc Genet. 2010; 3:88–96.

27.   Wollert KC, Kempf T. GDF-15 in heart failure: providing insight into end-organ dysfunction and its recovery? Eur. J. Heart Fail. 2012; 14:1191–1193.

28.   Kempf T, Haehling von S, Peter T, Allhoff T, Cicoira M, Doehner W, Ponikowski P, Filippatos GS, Rozentryt P, Drexler H, Anker SD, Wollert KC. Prognostic utility of Growth Differentiation Factor-15 in patients with chronic heart failure. J. Am. Coll. Cardiol. 2007; 50:1054–1060.

29.   Kempf T, Zarbock A, Widera C, Butz S, Stadtmann A, Rossaint J, Bolomini-Vittori M, Korf-Klingebiel M, Napp LC, Hansen B, Kanwischer A, Bavendiek U, Beutel G, Hapke M, Sauer MG, Laudanna C, Hogg N, Vestweber D, Wollert KC. GDF-15 is an inhibitor of leukocyte integrin activation required for survival after myocardial infarction in mice. Nat. Med. 2011; 17:581–588.

30.   Harding P, Yang X-P, Yang J, Shesely E, He Q, LaPointe MC. Gene expression profiling of dilated cardiomyopathy in older male EP4 knockout mice. Am. J. Physiol. Heart Circ. Physiol. 2010; 298:H623–32.

31.   Lajer M, Jorsal A, Tarnow L, Parving H-H, Rossing P. Plasma Growth Differentiation Factor-15 independently predicts all-cause and cardiovascular mortality as well as deterioration of kidney function in type 1 diabetic patients with nephropathy. Diabetes Care. 2010; 33:1567–1572.

32.   Phizicky E, Bastiaens PIH, Zhu H, Snyder M, Fields S. Protein analysis on a proteomic scale. Nature. 2003; 422:208–215.

33.   Hanash S. Disease proteomics. Nature. 2003; 422:226–232.

34.   Matkovich SJ, Van Booven DJ, Youker KA, Torre-Amione G, Diwan A, Eschenbacher WH, Dorn LE, Watson MA, Margulies KB, Dorn GW. Reciprocal regulation of myocardial microRNAs and messenger RNA in human cardiomyopathy and reversal of the microRNA signature by biomechanical support. Circulation. 2009; 119:1263–1271.

35.   Bartel DP. MicroRNAs: genomics, biogenesis, mechanism, and function. Cell. 2004; 116:281–297.

36.   da Costa Martins PA, Salic K, Gladka MM, Armand A-S, Leptidis S, Azzouzi el H, Hansen A, Coenen-de Roo CJ, Bierhuizen MF, van der Nagel R, van Kuik J, de Weger R, de Bruin A, Condorelli G, Arbones ML, Eschenhagen T, De Windt LJ. MicroRNA-199b targets the nuclear kinase Dyrk1a in an auto-amplification loop promoting calcineurin/NFAT signalling. Nat. Cell Biol. 2010; 12:1220–1227.

37.   Drakos SG, Kfoury AG, Stehlik J, Selzman CH, Reid BB, Terrovits JV, Nanas JN, Li DY. Bridge to recovery: understanding the disconnect between clinical and biological outcomes. Circulation. 2012; 126:230–241.

38.   Mann DL, Burkhoff D. Is myocardial recovery possible and how do you measure it? Curr Cardiol Rep. 2012; 14:293–298.

39.   Margulies KB, Matiwala S, Cornejo C, Olsen H, Craven WA, Bednarik D. Mixed messages: transcription patterns in failing and recovering human myocardium. Circ. Res. 2005; 96:592–599.

40.   Burkhoff D, Klotz S, Mancini DM. LVAD-induced reverse remodeling: basic and clinical implications for myocardial recovery. J Card Fail. 2006; 12:227–239.

41.   Mann DL, Barger PM, Burkhoff D. Myocardial recovery and the failing heart: myth, magic, or molecular target? J. Am. Coll. Cardiol. 2012; 60:2465–2472.

42.   Martina JR, Schipper MEI, de Jonge N, Ramjankhan F, de Weger RA, Lahpor JR, Vink A. Analysis of aortic valve commissural fusion after support with continuous-flow left ventricular assist device. Interact Cardiovasc Thorac Surg. 2013; 17:616-24.

43.   Martina J, de Jonge N, Sukkel E, Lahpor J. Left ventricular assist device-related systolic aortic regurgitation. Circulation. 2011; 124:487–488.

44.   Caccamo M, Eckman P, John R. Current state of ventricular assist devices. Curr Heart Fail Rep. 2011; 8:91–98.

45.   John R, Kamdar F, Eckman P, Colvin-Adams M, Boyle A, Shumway S, Joyce L, Liao K. Lessons Learned From Experience With Over 100 Consecutive HeartMate II Left Ventricular Assist Devices. Ann. Thorac. Surg. 2011; 92:1593–1600.

46.   Thompson LO, Loebe M, Noon GP. What price support? Ventricular assist device induced systemic response. ASAIO J. 2003; 49:518–526.

47.   Frazier OH. Unforeseen consequences of therapy with continuous-flow pumps. Circ Heart Fail. 2010; 3:647–649.

48.   Krabatsch T, Schweiger M, Dandel M, Stepanenko A, Drews T, Potapov E, Pasic M, Weng Y-G, Huebler M, Hetzer R. Is bridge to recovery more likely with pulsatile left ventricular assist devices than with nonpulsatile-flow systems? Ann. Thorac. Surg. 2011; 91:1335–1340.

49.   Pirbodaghi T, Asgari S, Cotter C, Bourque K. Physiologic and hematologic concerns of rotary blood pumps: what needs to be improved? Heart Fail Rev. 2013, epub ahead of print.

9

50. Birks EJ, Tansley PD, Hardy J, George RS, Bowles CT, Burke M, Banner NR, Khaghani A, Yacoub MH. Left ventricular assist device and drug therapy for the reversal of heart failure. N. Engl. J. Med. 2006; 355:1873–1884.

51. Navaratnarajah M, Ibrahim M, Siedlecka U, van Doorn C, Shah A, Gandhi A, Dias P, Sarathchandra P, Yacoub MH, Terracciano CM. Influence of ivabradine on reverse remodelling during mechanical unloading. Cardiovasc. Res. 2013; 97:230–239.

52. Boyle AJ, Russell SD, Teuteberg JJ, Slaughter MS, Moazami N, Pagani FD, Frazier OH, Heatley G, Farrar DJ, John R. Low thromboembolism and pump thrombosis with the HeartMate II left ventricular assist device: analysis of outpatient anti-coagulation. J Heart Lung Transplant. 2009; 28:881–887.

53. Sherman C, Clay W, Dasse K, Daly B. Energy transmission across intact skin for powering artificial internal organs. Trans Am Soc Artif Intern Organs. 1981; 27:137–141.

54. Slaughter MS, Myers TJ. Transcutaneous energy transmission for mechanical circulatory support systems: history, current status, and future prospects. J Card Surg. 2010; 25:484–489.

55. Westaby S, Siegenthaler M, Beyersdorf F, Massetti M, Pepper J, Khayat A, Hetzer R, Frazier OH. Destination therapy with a rotary blood pump and novel power delivery. Eur J Cardiothorac Surg. 2010; 37:350–356.

56. Bashir J, Cheung A, Kaan A, Kearns M, Ibey A, Ignaszewski A. Thrombosis and failure of a HeartMate II device in the absence of alarms. J Heart Lung Transplant. 2011; 30:1197–1199.

57. Meyer AL, Kuehn C, Weidemann J, Malehsa D, Bara C, Fischer S, Haverich A, Strüber M. Thrombus formation in a HeartMate II left ventricular assist device. J. Thorac. Cardiovasc. Surg. 2008; 135:203–204.

58. Spanier TB, Chen JM, Oz MC, Stern DM, Rose EA, Schmidt AM. Time-dependent cellular population of textured-surface left ventricular assist devices contributes to the development of a biphasic systemic procoagulant response. J. Thorac. Cardiovasc. Surg. 1999; 118:404–413.

59. Nielsen VG, Kirklin JK, Holman WL, Steenwyk BL, George JF, Zhou F, Parks DA, Ellis TC. Mechanical circulatory device thrombosis: a new paradigm linking hypercoagulation and hypofibrinolysis. ASAIO J. 2008; 54:351–358.

60. Yoder MC, Mead LE, Prater D, Krier TR, Mroueh KN, Li F, Krasich R, Temm CJ, Prchal JT, Ingram DA. Redefining endothelial progenitor cells via clonal analysis and hematopoietic stem/progenitor cell principals. Blood. 2007; 109:1801–1809.

61. Crow S, John R, Boyle A, Shumway S, Liao K, Colvin-Adams M, Toninato C, Missov E, Pritzker M, Martin C, Garry D, Thomas W, Joyce L. Gastrointestinal bleeding rates in recipients of nonpulsatile and pulsatile left ventricular assist devices. J. Thorac. Cardiovasc. Surg. 2009; 137:208–215.

62. Stern DR, Kazam J, Edwards P, Maybaum S, Bello RA, D'Alessandro DA, Goldstein DJ. Increased incidence of gastrointestinal bleeding following implantation of the HeartMate II LVAD. J Card Surg. 2010; 25:352–356.

63. Morgan JA, Paone G, Nemeh HW, Henry SE, Patel R, Vavra J, Williams CT, Lanfear DE, Tita C, Brewer RJ. Gastrointestinal bleeding with the HeartMate II left ventricular assist device. J Heart Lung Transplant. 2012; 31:715–718.

64. Uriel N, Pak S-W, Jorde UP, Jude B, Susen S, Vincentelli A, Ennezat P-V, Cappleman S, Naka Y, Mancini D. Acquired von Willebrand syndrome after continuous-flow mechanical device support contributes to a high prevalence of bleeding during long-term support and at the time of transplantation. J. Am. Coll. Cardiol. 2010; 56:1207–1213.

65. Slaughter MS. Hematologic effects of continuous flow left ventricular assist devices. J Cardiovasc Transl Res. 2010; 3:618–624.

66. Mehra MR, Domanski MJ. Should left ventricular assist device should be standard of care for patients with refractory heart failure who are not transplantation candidates?: left ventricular assist devices should be considered standard of care for patients with refractory heart failure who are not transplantation candidates. Circulation. 2012; 126:3081–3087.

67. Neyt M, Van den Bruel A, Smit Y, de Jonge N, Erasmus M, Van Dijk D, Vlayen J. Cost-effectiveness of continuous-flow left ventricular assist devices. Int J Technol Assess Health Care. 2013; 29:254–260.

9
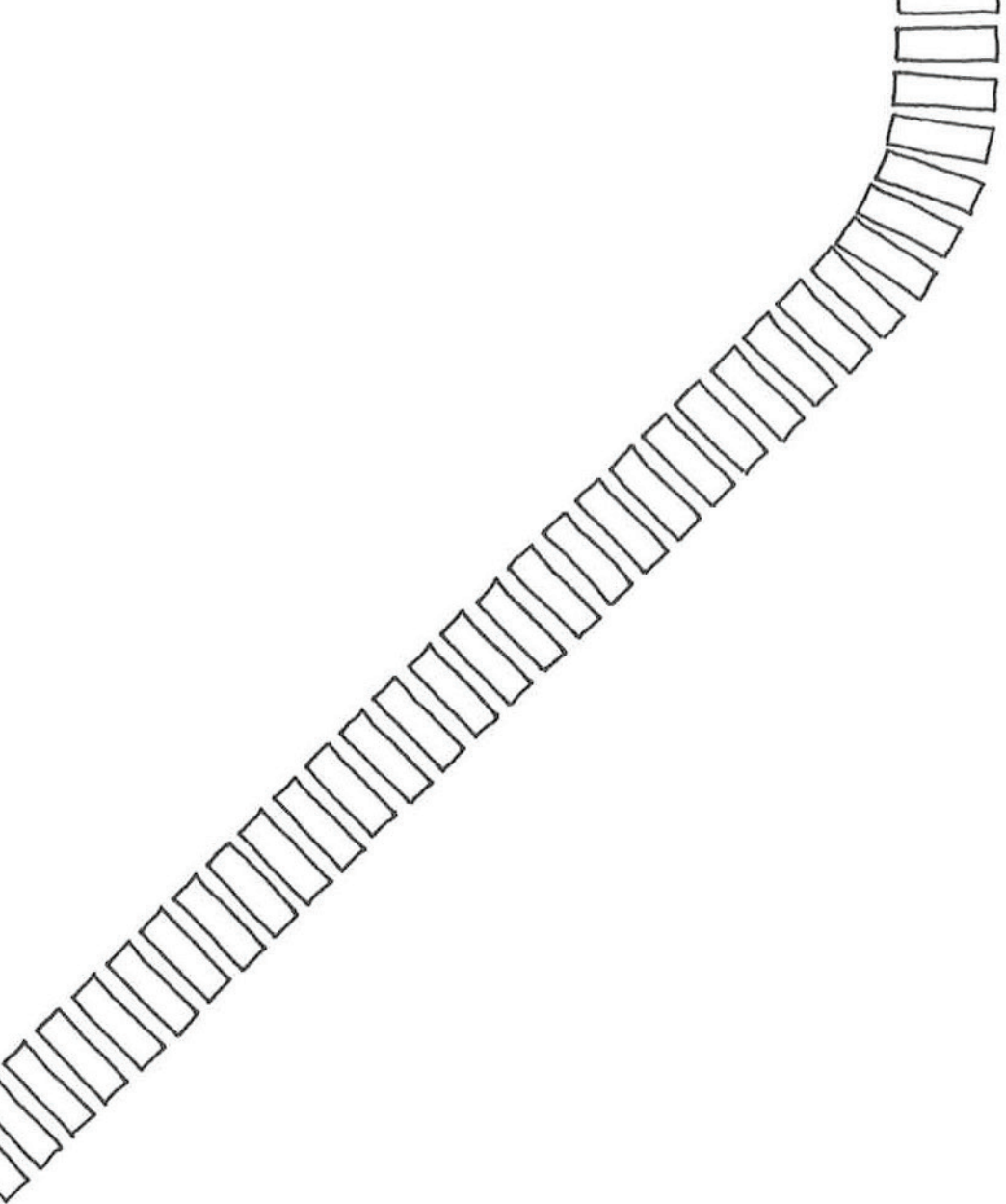
NEDERLANDSE SAMENVATTING

Nederlandse samenvatting

Hartfalen is wereldwijd een groeiend probleem. Van alle Nederlanders, van 55 jaar of ouder, zal ongeveer een op de drie hartfalen ontwikkelen. Harttransplantatie is de ultieme behandeling voor patiënten met eindstadium hartfalen. Door het gering aantal donorharten komt echter slechts een klein deel van de patiënten met eindstadium hartfalen in aanmerking voor transplantatie. Ter overbrugging naar een harttransplantatie kan een steunhart worden overwogen.

Een steunhart is een mechanische pomp die de hartfunctie ondersteunt. De meeste steunharten worden aangewend voor de linker hartkamer en worden "Left Ventricular Assist Devices" (LVADs) genoemd. Een LVAD wordt in de buik geplaatst en verbonden aan hart en aorta door middel van canules.

Momenteel wordt een LVAD met name gebruikt als overbrugging naar een harttransplantatie (*Bridge To Transplantation, BTT*) bij patiënten die zo snel verslechteren dat zij dreigen te overlijden voordat een donorhart beschikbaar komt. Het grote voordeel van een LVAD is, dat patiënten na implantatie volledig mobiel worden. Patiënten zijn tijdens LVAD therapie zelfs in staat bijna net zoveel inspanning te leveren als na een harttransplantatie. Naast de klinische verbetering, is ook een verbetering van de gestoorde functie van het hart waarneembaar. Onderzoek naar hartweefsel, voor en na LVAD implantatie, laat zien dat het hart deels herstelt tijdens LVAD ondersteuning. De hartspiercellen (cardiomyocyten) van de patiënten met ernstig hartfalen zijn veelal te lang en verbreed. Tijdens LVAD ondersteuning worden de cardiomyocyten smaller en korter en neemt de hoeveelheid littekenweefsel (fibrose) af.

Bij een klein deel van de patiënten (± 5%) is de mate van herstel van de hartfunctie zodanig dat de LVAD kan worden verwijderd zonder dat harttransplantatie nog nodig is. In dit geval dient een LVAD als brug naar herstel (*Bridge To Recovery, BTR*). In enkele gevallen ontwikkelen patiënten na verwijdering van de LVAD na een BTR opnieuw hartfalen. Er zijn momenteel geen goede parameters om te voorspellen bij welke patiënten de LVAD wel of niet kan functioneren als succesvolle BTR.

De overleving met LVAD-therapie bij patiënten met een eindstadium hartfalen is na de implantatie van de LVAD zeer bemoedigend. Ruim 85% van de patiënten overleeft de perioperatieve periode en meer dan 75% ondergaat een harttransplantatie. Vanwege de relatief gunstige overleving en het groeiend tekort aan donorharten, kan een LVAD ook als min of meer permanente behandeling worden gebruikt als alternatief voor een

harttransplantatie (*Destination Therapy, DT*), bijvoorbeeld bij patiënten met een contra-indicatie voor transplantatie.

De eerste generatie "pulsatiele- LVADs" (pf-LVADs) is ondertussen vervangen door "LVADs- met-continue-flow" (cf-LVADs), die aanzienlijk langer kunnen functioneren dan de oudere pompen. pf-LVADs hebben een flexibel diafragma dat een pompkamer comprimeert, waarbij kleppen zorgen voor een bloedstroom in de goede richting. cf-LVADs daarentegen, hebben een elektrisch aangedreven rotor die met een hoog toerental zorgt voor een continue stroom van het bloed vanuit de linker ventrikel naar de aorta.
Veel onderzoek is gedaan naar de effecten van klinische en histologische veranderingen tijdens ondersteuning met pf-LVADs. Dit proefschrift richt zich met name op veranderingen tijdens ondersteuning met de meer moderne cf-LVADs.

Klinische ervaring
Hoofdstuk 2 beschrijft de kliniek van 85 patiënten die een cf-LVAD implantatie hebben ondergaan in het Universiteit Medisch Centrum in Utrecht. De 6 maanden, 1-, 2-, 3- en 4-jaar overleving na cf-LVAD implantatie is respectievelijk 85, 81, 76, 76 en 68%. Deze resultaten zijn vergelijkbaar met andere centra.
Van de 85 patiënten zijn 17 patiënten overleden tijdens LVAD ondersteuning (10 van hen ≤ 30 dagen na implantatie, 7 patiënten >30 dagen). De meest voorkomende complicaties in ons patiënten-cohort zijn infecties, hartritmestoornissen en perioperatieve bloedingen. Trombo-embolische complicaties zijn zeer berucht in verband met hun invaliderende uitwerking en het risico op overlijden. Zeventien patiënten hebben 21 neurologische aandoeningen ontwikkeld waarvan 13 cerebrovasculaire aandoeningen (CVA's). Bij vier patiënten hebben de CVA's geresulteerd in het overlijden van de patiënt, bij 6 zijn minimale restverschijnselen opgetreden en bij 3 patiënten ernstige beperkingen in het dagelijks leven. In ons centrum hebben wij relatief weinig gastro-intestinale bloedingen gezien. Mogelijk komt dit door de relatief jongere patiëntenpopulatie en het standaard gebruik van protonpomp inhibitie.
Van alle 85 patiënten is de New York Heart Association (NYHA) classificatie voor hartfalen verbeterd en is de inspanningstolerantie sterk toegenomen. Toch hebben slechts 3 patiënten (4%) een LVAD explantatie ondergaan. Waarom maar 4% van de patiënten zodanig herstelt dat LVAD explantatie mogelijk is, is reden geweest voor nader onderzoek en wordt nader beschreven in dit proefschrift.

Histologie

Tijdens een LVAD implantatie moet een stukje van de linkerkamer (pre-LVAD) worden verwijderd voor de implantatie van de LVAD canule. Na de harttransplantatie kan het verwijderde hart van de patiënten ook gebruikt worden voor onderzoek (post-LVAD). Door het stukje hart (pre-LVAD) te vergelijken met gezonde individuen kan de architectuur (histologie) van het falende hart bestudeerd worden.

In hoofdstuk 3 wordt beschreven dat patiënten met hartfalen meer fibrose in het hart hebben en dat de diameter van de cardiomyocyten groter is dan die bij gezonde individuen. Door pre-LVAD met post-LVAD te vergelijken, kan het effect van een LVAD op het hart worden onderzocht. Eerder onderzoek heeft aangetoond dat het hart van patiënten tijdens pf-LVAD ondersteuning lijkt te verbeteren, namelijk de cardiomyocyten worden kleiner en korter. Het effect van de pf-LVAD ondersteuning op de hoeveelheid fibrose is niet duidelijk. De ene groep onderzoekers beschrijft een toename van fibrose, terwijl andere groepen juist een afname aantonen. In dit proefschrift tonen wij aan dat tijdens cf-LVAD therapie (in tegenstelling tot pf-LVAD ondersteuning), de cardiomyocyten juist langer worden en de hoeveelheid fibrose toeneemt. De duur van cf-LVAD ondersteuning heeft geen invloed op de hoeveelheid fibrose. Waarom het verschil in ontlasting van de linkerkamer (pulsatiel versus continu) van invloed is op de histologie, is vooralsnog onduidelijk.

Biomarkers

In de cardiologie wordt veel gebruik gemaakt van circulerende signaalmoleculen (biomarkers) voor het stellen van de diagnose en bepalen van de prognose van hartfalen. Omdat fibrose lijkt toe te nemen tijdens cf-LVAD ondersteuning en zodoende het herstel van het hart negatief beïnvloedt, wordt in hoofdstuk 3 de verandering van fibrose-gerelateerde biomarkers beschreven in het plasma en hartweefsel van patiënten tijdens cf-LVAD ondersteuning. De hoeveelheid Brain-Natriuretic Peptide (BNP), Galectin-3 (Gal-3), Connective Tissue Growth Factor (CTGF) en Osteopontin (OPN) in het bloed is significant verhoogd bij patiënten met eindstadium hartfalen voor cf-LVAD implantatie in vergelijking met gezonde individuen. Tijdens support met een cf-LVAD blijven deze echter verhoogd aanwezig, waardoor mogelijk de toename van de fibrose in het hart verklaard kan worden. Naast deze bekende pro-fibrotische biomarkers worden in dit proefschrift veranderingen van Growth Differentiation Factor 15 (GDF-15) tijdens cf-LVAD ondersteuning beschreven. Eerder onderzoek heeft laten zien dat circulerend GDF-15 is verhoogd na een acuut myocard infarct. Hoofdstuk 4 laat zien dat GDF-15 ook is verhoogd bij patiënten met eindstadium hartfalen. Na cf-LVAD implantatie normaliseert de hoeveelheid circulerend

GDF-15. Opmerkelijk is dat messenger RNAs (mRNA) en de eiwit expressie van GDF-15 niet in het hart gedetecteerd kunnen worden. Dit suggereert dat GDF-15 niet in het hart, maar elders geproduceerd wordt. Vermoedelijk is de daling van GDF-15 een weerspiegeling van de verbeterde orgaanperfusie tijdens cf-LVAD ondersteuning.

Eiwitten spelen een belangrijke rol bij veel processen in het lichaam. Met behulp van eiwitstudies (proteomics) kunnen veranderingen van eiwitten worden bestudeerd. In dit promotieonderzoek is gekeken naar de verandering van eiwitten in het plasma en hartspierweefsel van patiënten tijdens cf-LVAD therapie. De verandering van twee individuele eiwitten, te weten haptoglobine (HPTG) en alpha-1-antichymotrypsine (ACT), wordt nader beschreven in hoofdstukken 4 en 5. Hoofdstuk 4 toont aan dat circulerend HPTG daalt na LVAD implantatie. HPTG is een acuut fase eiwit en speelt een rol bij de afbraak van rode bloedcellen (hemolyse). Vermoedelijk dat de daling in HPTG tijdens LVAD tweeledig is- enerzijds door de verminderde inflammatoire activiteit, anderzijds door de beschadiging van rode bloedcellen door de cf-LVAD.

Hoofdstuk 5 beschrijft de verandering van alpha-1-antichymotrypsine (ACT) voor en na cf-LVAD implantatie. De hoeveelheid ACT is verhoogd bij patiënten met eindstadium hartfalen voor implantatie. Na cf-LVAD implantatie daalt de hoeveelheid ACT in zowel het plasma als in het hartspierweefsel. ACT wordt gereguleerd door microRNA (miR)-137. Mogelijk dat ACT een belangrijke rol speelt bij de pathofysiologie van hartfalen. De exacte rol van ACT in hartfalen is onduidelijk, maar in de literatuur worden enkele effecten op het cardiovasculaire systeem beschreven. ACT is een serine protease remmer, voornamelijk van cathepsine G. Door het remmen van cathepsine G voorkomt ACT de degradatie van bindweefsel en de activatie van Transforming Growth Factor (TGF). ACT, een acuut fase eiwit, induceert tevens Tumour Necrosis Factor-α (TNF-α) en Nucleaire Factor Kappa B (NF-kB), eiwitten die een sleutelrol spelen bij het opwekken van een ontstekingsreactie. Tenslotte lijkt ACT beschermend te werken gedurende ischemie-reperfusie, doordat het de accumulatie van neutrofielen in het ischemische gebied remt.

De expressie van ACT is destijds nader onderzocht in patiënten met chronisch systolisch hartfalen uit de Deventer-Alkmaar Hartfalen (DEAL-HF) studie. Hoofdstuk 7 bevestigt dat de hoeveelheid ACT significant verhoogd is in plasma van patiënten met hartfalen vergeleken met dat van gezonde individuen. Desalniettemin blijkt ACT geen goede voorspeller te zijn voor de kans op overlijden. Meerdere plasma-metingen zijn vermoedelijk nodig om meer te kunnen zeggen over de voorspellende rol van ACT in patiënten met hartfalen.

In dit proefschrift is ook gekeken naar het gedrag van microRNAs (miRs) tijdens LVAD

ondersteuning. miRs zijn kleine stukjes RNA, die de expressie van genen beïnvloeden- zij beïnvloeden vele cellulaire processen door binding aan specifieke target mRNAs, hetgeen kan leiden tot remming van target eiwit productie. Daarnaast zijn miRs belangrijk voor normale lichaamsprocessen maar spelen ook een rol bij de pathofysiologie van hartfalen. Het zijn mogelijk aangrijpingspunten voor therapie. Hoofdstuk 8 geeft de expressie weer van miRs tijdens pf-LVAD en cf-LVAD ondersteuning. Na pf-LVAD implantatie is de verandering in miR expressie in het hartspierweefsel meer geprononceerd in vergelijking met patiënten die worden ondersteund met een cf-LVAD. Dit verschil wordt vermoedelijk verklaard door de toegenomen volume- en drukbelasting van de pf-LVAD ten opzichte van een cf-LVAD. Vier miRs zijn nader onderzocht in het plasma van patiënten, ondersteund met een cf-LVAD, waarbij miR-21 daalt (1, 3, en 6 maanden na LVAD implantatie) terwijl de miR-146a, miR-221 en miR-222 een fluctuerend patroon laten zien na implantatie.

Samenvattend toont dit proefschrift aan, dat cf-LVAD ondersteuning een levensreddende therapie is voor patiënten met eindstadium hartfalen. LVAD ondersteuning resulteert in een relatief goede overleving. Desalniettemin zijn er belangrijke cf-LVAD gerelateerde complicaties, waaronder infecties, hartritmestoornissen, perioperatieve bloedingen en trombo-embolische aandoeningen. Klinisch laten alle patiënten een zekere mate van herstel zien tijdens LVAD ondersteuning. Tijdens cf-LVAD therapie verbeteren de eindorgaan perfusie en de NYHA classificatie. Echter, volledig herstel van de hartfunctie met secundair succesvolle cf-LVAD explantatie treedt slechts weinig op. Mogelijk dat de persisterende inflammatoire status, de toename in fibrose en de lange cardiomyocyten mede bepalend zijn voor het relatief geringe aantal patiënten bij wie de cf-LVAD kan worden geëxplanteerd. Vermoedelijk is de oorzaak van het hartfalen van bijzonder grote invloed op de mate van herstel van het hart tijdens LVAD therapie. Momenteel wordt veel onderzoek verricht naar biomarkers om dit herstel te kunnen voorspellen. Met name de miRs lijken succesvol als diagnostische en prognostische biomarkers.
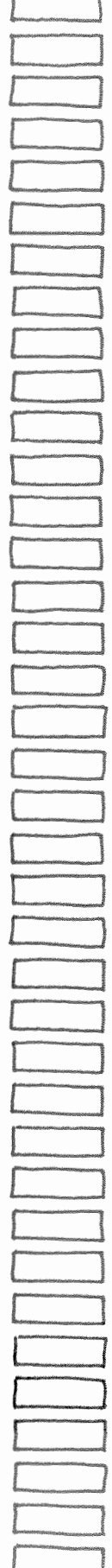
DANKWOORD

Dankwoord

Dit promotieboek gaat over een steunhart als behandeling voor patiënten met eind-stadium hartfalen.

Overdrachtelijk gezien ging ik met een familiare predispositie mijn promotietraject tegemoet. Expressie trad vrij snel op na aankomt in het laboratorium. Symptomen bestonden uit benauwdheid, hartkloppingen, motorische en sensibele onrust en slapeloosheid. Alle biomarkers waren sterk verhoogd. Vrije radicalen kwamen mijn neus uit. Messenger RNAs met antiproliferatieve eigenschappen kwamen onvoldoende tot expressie. Een opname in een wetenschappelijk team in het UMC-Utrecht was geïndiceerd …….

Het is een voorrecht geweest om vier jaar lang te werken met slimme gepassioneerde collega's in de zorg. Aan het tot stand komen van mijn proefschrift hebben veel mensen bijgedragen.

Allereerst de patiënten met eind-stadium hartfalen. Veel dank zijn wij u verschuldigd. Door jullie bijdrage hebben wij meer inzicht gekregen in de reactie van het hart op LVAD support.

Geachte professor Doevendans, ik ben blij dat ik onder uw begeleiding aan mijn promotie heb mogen werken. Mijn promotie-onderzoek is te vergelijken met de fietstocht van Amsterdam naar Stockholm, waaraan wij beiden deelnamen. Geef mij "1-minuut" om u in wielertermen toe te spreken. De promotietocht kenmerkte zich door veel vals plat en kasseien. Het was stoempen, buffelen, vierkant rijden, voortdurend een tandje erbij, terughalen en gelost worden, maar ook recupereren en doorkachelen. Als patron bepaalde u de course, kon ik knallen en als een ware Flandrien met turbodijen over de meet gaan.

Beste Nicolaas, dank voor jouw geduld en wijsheid. Jij fungeert als onmisbare schakel tussen de pathologie en de kliniek. Van al jouw levenslessen vertegenwoordig jij de stelling "schrijf niet wat je weet, maar weet wat je schrijft".

Roel, "pater familias" van de pathologie en in het bijzonder van mijn promotietraject. Jij weet het beste in elk mens naar boven te halen, deuren letterlijk en figuurlijk te openen en een luisterend oor te bieden.

Beste paranimfen. Bjorn, jij bent de man van het eerste uur. Ten tijde van mijn wetenschappelijke stage als geneeskunde student in Maastricht klopte ik aan en ben nooit meer weg gegaan. De voorspelde kans dat een statisticus een goede vriend van mij zou worden lag eerder bij de 0, dan bij de 1. Jij bent *het* bewijs dat kansberekingen slechts voorspellend en nooit bewijzend zijn.

Samora, Sam. Wat begon als collega's op de verpleegafdeling cardiologie, ontwikkelde zich tot een goede vriendschap, pipet-maatjes ("Like a G6") en nu zelfs familie. Jou raak ik gelukkig nooit meer kwijt!

Heren, ik voel mij gesterkt dat jullie, ook tijdens mijn verdediging, naast mij zullen staan!"

Ik wil de hele afdeling Pathologie in het UMC-Utrecht bedanken.

Allereerst de harttransplantatiegroep. Joyce, wij vertegenwoordigen het yin-en-yang-principe en vormen een dynamisch evenwicht. Jij maakte mij vertrouwd met de LightCycler, bracht rust, zorgde voor controle en vertrok toen als "Q-PCR-queen" naar San Diego. Petra, empathisch en groeibriljant van het laboratorium. Bovendien expert in ELISA's en miR-137 transfecties. Erica, fervent proteomics-master en groot supplier van stroopwafels voor bij de koffie. Dick, ruwe bolster, blanke pit. Van molens en muizen tot aan dubbelkleuringen en cardiale allograft vasculopathie; jij bent en blijft onmisbaar in het team. Ton, optimist en legendarische grappenmaker. Jij liet beginnende assistenten dekglaasjes schoonmaken in verband met de bezuiniging en adviseerde hen een testikelketting als sieraad. Naast al jouw grappen blonk jij uit in *in situ* hybridisaties. Kim, kamergenoot in de camera obscura, creatief en ambitieus. Onmisbare Manon, ambitieuze inspirator, Yale student en chirurg van Pien 1, 2, 3…87. Jullie zijn allen onmisbaar gebleken voor de werksfeer en het tot stand komen van dit proefschrift.

Daarnaast wil ik alle pathologen bedanken, in het bijzonder Marguerite, Roel G. en Aryen. Jullie hebben een essentiële bijdrage geleverd aan mijn promotieonderzoek. Niet alleen door het delen van kennis over myofibroblasten, CTGF en Masson Trichrome. Maar ook als medeauteurs van menig artikel en poster.

Daarnaast dank ik allen die werkzaam zijn op de histologie, moleculaire pathologie en immuunhistochemie, inclusief het secretariaat en "last-but-not-least" de mortuarium medewerkers; Aad en Willem! Als arts assistent cardiologie ben ik, zonder ervaring in het laboratorium, met open armen ontvangen. Langzamerhand ben ik vertrouwd geraakt met pipetpunten, rubber policeman en -dankzij Roel B- photoshop. En bovenal, wat hebben wij een plezier gehad. Van de jaarlijkse TourPool met gele trui en kerstborrels tot zelfs een bruiloft van Remco en Joyce!

Zonder de medewerking van studenten had mijn promotieonderzoek zoveel langer geduurd. De groep bleef hecht, mede door onze gezamenlijke waddentocht. Heleen, nuchtere Zeeuwse met een hoog emotioneel en intelligent quotiënt, liep voorop tijdens onze tocht. Fay, met oorbellen en hakken, liefhebster van kasteelbier (met name in de fontein), summa - en nu vooraanstaand Harvard studente, bevlogen en enthousiast. Ankie, jij bent bereid veel dingen te ontdekken, zelfs nieuwe haring, en bleek expert in immunohistochemische kleuringen. Maartje, alias prinses Rapunzel, organisator van de restaurantweek en Engelandvaarder, jij hielp mee met de microRNAs. Evenals Dianne, tevens ex-lerares en expert in Ikea-kasten. Bastiaan, de bedachtzame econoom van het gezelschap, jij ontwikkelde je tot specialist van *in situ* hybridisaties. Danielle en Fabian legden menig onderzoek schriftelijk vast. Allen dank voor jullie gezelligheid en loyaliteit.

Verschillende disciplines hebben meegewerkt aan mijn promotie onderzoek. Allereerst de werknemers op de Experimentele cardiologie, Alain en Joost, onze samenwerking resulteerde in een prachtig artikel waar ik trots op ben. Noortje en Loes, jullie waren onmisbaar bij het verzamelen van patiënten materiaal ten tijde van de TRIUMPH. Hans Kemperman vanuit het laboratorium klinische chemie en haematologie, dank voor de BNP analyse.

Veel dank gaat uit naar de afdeling cardiologie, met in het bijzonder het harttransplantatie team. Beste Hans, jouw wijze les "less is more" is "more than less"! Corinne, ik heb veel bewondering voor de wijze waarop jij opkomt voor de patiënten.
Het stafsecretariaat vertegenwoordigd door Hanneke, Nan en Albert is erg waardevol gebleken.
Ook de staf van de cardiothoracale chirurgie en met name prof Lahpor en dr. Ramjankhan wil ik bedanken. Jullie leverden patiënten materiaal, essentieel voor dit promotieonderzoek. Het LVAD team, bestaande uit Ben en Nelienke, dank voor jullie bijdrage. Jerry, fenominaal is jouw kennis over hartvolumes, bloeddruk en aortakleppen. Een goede samenwerking bracht ons van Utrecht tot aan Montreal ("of was het nou Vancouver..?"). Wij hebben ons door vele LVAD complicaties geworsteld met een vooruitstrevend artikel als eindresultaat. De echolaboranten van de hart- en longfunctie afdeling horen uiteraard ook in dit rijtje thuis. Alsmede de ICT medewerkers, waaronder Tjander en Nikolas, van zowel de afdeling cardiologie als de pathologie.
Alle mede-onderzoekers bedankt! Marieke, Irene, Moniek, Mari-Sevi, Judith, Mieke, Tycho, Frebus, Stefan, Jetske, Anouar, Manon, Willemien, Sofie, Rosemarijn, Tim Hesselink en vele

anderen… Enkele van jullie zijn tevens huidige collega's geworden, te weten Geert, Margot, Anneke en Freerk. Ik ben blij dat wij nu ook in Amersfoort samen kunnen werken. Ook de rest van mijn huidige collega's en verpleegkundigen in zowel het UMC Utrecht als in het Meander Medisch Centrum wil ik bedanken voor hun belangstelling voor mijn onderzoek.

Beste Paula da Costa Martins, vanuit mijn oude studentenstad begeleidde jij mij bij de microRNAs. Veel dank voor de samenwerking en de waardevolle gesprekken naast ons onderzoek.

Met alleen schrijven kom je er niet. Een promotie is top-sport. Vandaar dat ik ploegleider Koos en de fietsclub "Hart voor Vrouwen" wil bedanken. Tiny Terror T, naast een vriendin, ben jij een ware pedaalridder.

Het wel of niet willen lezen van een boek begint bij de omslag. De format en lay-out van dit proefschrift werd mogelijk gemaakt door Anouk Haegens. Alleen al aan de format te zien, zou dit boekje wel eens een bestseller kunnen worden…

De leescommissie, bestaande uit Leon de Windt, Roel Goldschmeding, Jaap Lahpor, Gerard Pasterkamp en Dirk Jan van Veldhuisen wil ik bedanken voor het lezen en beoordelen van dit proefschrift.

Een promotie-onderzoek is een ultieme stress-test voor vriendschap. Lieve vrienden, jullie hebben veel geduld moeten hebben met mijn sociale afzondering, welke nodig was om dit proefschrift tot een goed einde te brengen. Ik heb altijd jullie steun gevoeld. Ik wil enkelen persoonlijk benoemen. Laura, ik heb zoveel zin om samen met jou veel te kleine dorpjes in veel te grote landen te ontdekken. Jij bent een vriendin voor het leven! Lieve Tanja (Tainka), "luctor et emergo", wijze uit het Oosten, begenadigd huisarts en bovenal goede vriendin. Binnenkort wereldproblemen oplossen in een kroegje in Luik? David, lieve bandiet en het voorbeeld van het gezegde "meervoud van lef is leven". Veel dank voor jouw inspirerende uitvluchten. Cha-Cha, you turned into a beloved friend with driving-license, husband of beautiful Lily and father of dragon-child Leo. You are one of the most brutally honest person I have known, able to use criticism as a motivational tool. Patrick, dankzij jouw branding skills is mijn CV nog nooit zo volledig geweest. Gini, wijs schoonzusje en goede vriendin. Bewonderingswaardig om jou zo te zien groeien! Niko en Katarina, passionate match! I love to spare my time with you. Ghans, ambitieus en doortastend, nu vader van

een tweeling. Vlek, binnenkort weer kokkels vangen op het Wad? Jessica, veel dank voor het doorlezen van dit proefschrift. Door jou staan alle puntjes op de i. Wouter, mijn Jozef in het kerstspel op de kleuterschool. Ik hoop nog vaak met jou en Irene van menig paasvuur te genieten.

Opa, de gedachten dat jij op jouw 87ste levensjaar bij de verdediging van dit proefschrift zult zijn, maakt mij heel gelukkig! Enny, dank voor jouw gezelligheid.

Lieve broertjes en zusjes, ik ben zo trots op jullie allemaal! De vele momenten die wij met elkaar hebben doorgebracht zijn van onkenbare waarde geweest voor mijn persoonlijke ontwikkeling en voor de geboorte van dit proefschrift. Anne, Fred, Pepijn, Kiki en Noortje, dank voor het kinderlijke geluk dat ik met jullie mag ervaren. Maartje, Gigi, de A is van aardig, de B is van blij, de C is van…jouw aanstekelijke enthousiasme helpen mij op die momenten dat ik het nodig heb. Pieter, grote stoere maar ook gevoelige broer, mag ik met jou zeilen op de Waddenzee? Jaap, wijze (levens)kunstenaar. Jij maakt het overal met iedereen gezellig. Ik heb zin in onze wereldreis, te beginnen in België. Inge, Utrecht is bevoorrecht met jouw aanstekelijke lach en bourgondische manier van leven.

Papa en mama, een hart dat geleerd heeft om te vertrouwen, kan gerust zijn. Met jullie onvoorwaardelijke steun, kan ik de wereld aan! Van hier tot aan de horizon en weer terug...

Guido, jouw onuitputtelijke liefde en geduld hebben ervoor gezorgd dat ik de tijd en de ruimte heb gehad om aan dit proefschrift te werken. Jij accepteert mij zoals ik ben, maar laat mij ook kritisch naar mezelf kijken. Ik hoop dat wij samen heel oud en rimpelig zullen worden.

…….. Nu, aan het einde van dit promotietraject, berust ik in de wetenschap dat er leven is na de catecholamine en de cytokine storm. De aanvankelijk sterk verhoogde geestelijke pre- en afterload is, door allen die ik in en buiten dit dankwoord genoemd heb, genormaliseerd. Na een jarenlange intensieve begeleiding door een zeer en hoog geleerd team is reverse remodeling opgetreden. Zodanig dat deze doctorandus nu in staat geacht moet worden zelfstandig wetenschappelijk door het leven te gaan.

Sjoukje Irene Lok
Utrecht, oktober 2013
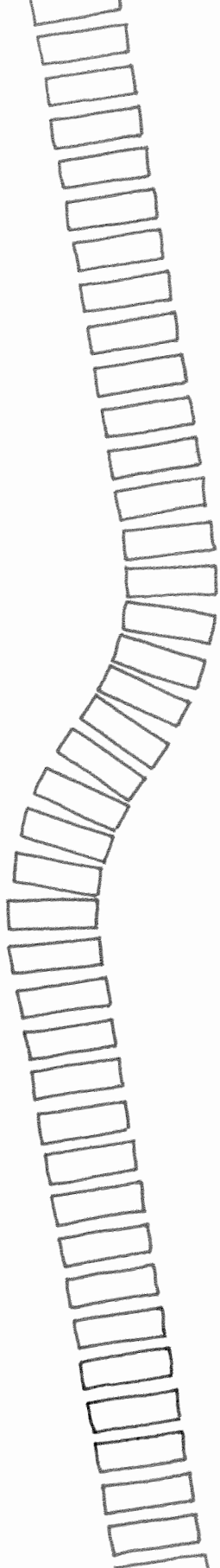
CURRICULUM VITAE

LIST OF PUBLICATIONS

Curriculum Vitae

Sjoukje Irene Lok was born on the 5th of January 1981 in the Dutch city of Groningen. She was born to Titia Y. Lok-Meijer and Dirk J.A. Lok, both medical professionals, as the eldest of 5. After completing her secondary education in 2000, she pursued her emerging passion for the medical sciences and enrolled in her degree studies at Maastricht University that same year. Having started her propaedeutic years with a focus on Health Science and Psychology, she proceeded to work on her Bachelor and Master of Science in Medicine to receive her Medical Degree in 2008. During her studies Sjoukje worked hard to obtain an international view on her profession with internships in the Community acquired Hospital, Pretoria, South Africa and Royal Brompton Hospital, London, UK; as well as scientific research projects in the Children's Hospital, Boston, USA. The common denominator during these years has been her interest and passion for the area of cardiology, resulting in the appointment in a Resident Cardiology role in 2008 at the University Medical Centre, Utrecht. After applying her knowledge and skills and gaining professional experience at the cardiology department for over one year, Sjoukje commenced her PhD program in 2009 on myocardial changes in patients with end-stage heart failure during continuous flow left ventricular assist device support. This was done under the supervision of prof. P.A.F.M. Doevendans, dr. N. de Jonge and dr. R.A. de Weger. Her research was successfully completed in October of 2012 at which point Sjoukje started with her official cardiology training. Currently, Sjoukje has been working at the department for internal medicine in the Meander Medisch Centrum, Amersfoort (dr. R. Fijnheer) for over a year. She is looking forward to the challenges and opportunities of the next steps in her training. From October 2014, she will attend cardiology training Meander MC (dr. P.J. Senden), followed by 3 years of cardiology training at the University Medical Centre, Utrecht (dr. J.H. Kirkels).

List of publications

Lok SI, Winkens B, Dimopoulos K, Fernandes S, Gatzoulis M, Landzberg M, Mulder B.
Recurrence of cerebrovascular events in young adults with a secundum atrial septal defect.
Int J Cardiol, 2010; 142:44-49.

Lok SI, Kirkels JH, Klöpping C, Doevendans PAF, de Jonge N.
Peripartum Cardiomyopathy: the need for a national database.
Neth Heart J, 2011; 19:126-133.

Lok SI, Doevendans PAF, Klöpping C, Kirkels JH, Lahpor JR, de Jonge N.
Peripartum cardiomyopathie bij jonge vrouwen.
Ned Tijdschr voor Geneeskd, 2011; 155:A2937.

Lok SI, Winkens B, Goldschmeding R, van Geffen AJ, Nous FM, van Kuik J, van der Weide
P, Klöpping C, Kirkels JH, Lahpor JR, Doevendans PA, de Jonge N, de Weger RA.
Circulating GDF-15 correlates with myocardial fibrosis in patients with end-stage dilated
cardiomyopathy and decreases rapidly after LVAD support.
Eur J Heart Fail, 2012; 14:1249-1256.

Lok SI, van Mil A, Bovenschen N, van der Weide P, van Kuik J, van Wichen D, Peeters T,
Siera E, Winkens B, Sluijter J, Doevendans P, da Costa Martins P, de Jonge N, de Weger RA.
Post-transcriptional regulation of α-1-antichymotrypsin by microRNA-137 in chronic
heart failure and mechanical support.
Circ Heart Fail, 2013; 6:853-861.

Lok SI, Schipper ME, De Jonge N, Lahpor JR.
Two young women with soft tissue tumours of the heart.
Eur J Cardiothorac Surg, 2013, epub ahead of print.

Lok SI*, Martina JR*, Hesselink T, Rodermans BF, Hulstein N, Winkens B, Klöpping C,
Kirkels JH, Doevendans PA, Ramjankhan F, de Weger RA, de Jonge N, Lahpor JR.
Single-centre experience of 85 patients with a continuous-flow left ventricular assist device:
clinical practice and outcome after extended support.
Eur J Cardiothorac Surg, 2013; 44:e233-238.

Pruijsten RV, **Lok SI**, Kirkels JH, Klöpping C, Lahpor JR, de Jonge N.
Functional and hemodynamic recovery after implantation of continuous-flow left ventricular assist devices in comparison with pulsatile left ventricular assist devices in patients with end-stage heart failure.
Eur J Heart Fail, 2012; 14:319-325.

Lok DJ, **Lok SI**, Bruggink-André de la Porte PW, Badings E, Lipsic E, van Wijngaarden J, de Boer RA, van Veldhuisen DJ, van der Meer P.
Galectin-3 is an independent marker for ventricular remodeling and mortality in patients with chronic heart failure.
Clin Res Cardiol, 2013; 102:103-110.

Lok DJ, Klip IT, **Lok SI**, Bruggink-André de la Porte PW, Badings E, van Wijngaarden J, Voors AA, de Boer RA, van Veldhuisen DJ, van der Meer P.
Incremental prognostic power of novel biomarkers (growth-differentiation factor-15, high-sensitivity C-reactive protein, galectin-3, and high-sensitivity troponin-T) in patients with advanced chronic heart failure.
Am J Cardiol, 2013; 112:831-837.

Leptidis S, El Azzouzi H, **Lok SI**, de Weger R, Olieslagers S, Kisters N, Silva GJ, Heymans S, Cuppen E, Berezikov E, De Windt LJ, da Costa Martins P.
A deep sequencing approach to uncover the miRNOME in the human heart.
PLoS One, 2013; 8; e57800.

Book chapters
Schipper MEI, **Lok SI**, Dullens H, van Kuik J, Gmelig-Meyling FHJ, Lahpor J, Vos MA, van der Laarse A, Jonge N, van Oosterhout MFM, de Weger RA.
Altered expression of mRNA and miRNA during mechanical support of the failing human heart.
Shuhaiber J (Ed.), Ventricular Assist Devices. ISBN: 978-953-307-164-0, InTech, DOI: 10.5772/15981

* Authors contributed equally